# Mechanisms regulating desmoglein clustering and hyper-adhesion of desmosomes

**Dissertation**
der Fakultät für Biologie
der Ludwig-Maximilians-Universität München
zur Erlangung des Doktorgrades


vorgelegt von

**Michael Tobias Fuchs**

München 2021

# Mechanisms regulating desmoglein clustering and hyper-adhesion of desmosomes

Dissertation

der Fakultät für Biologie

der Ludwig-Maximilians-Universität München

vorgelegt von

Michael Tobias Fuchs

München, 16.12.2021

Diese Dissertation wurde angefertigt
unter der Leitung von Prof. Dr. Heinrich Leonhardt
an der Fakultät für Biologie
der Ludwig-Maximilians-Universität München

| | |
|---|---|
| Erstgutachter/in: | Prof. Dr. Heinrich Leonhardt |
| Zweitgutachter/in: | Prof. Dr. Anja Horn-Bochtler |
| Tag der Abgabe: | 16.12.2021 |
| Tag der mündlichen Prüfung: | 09.06.2022 |

**Erklärung**

Ich versichere hiermit an Eides statt, dass die vorgelegte Dissertation von mir selbstständig und ohne unerlaubte Hilfsmittel angefertigt worden ist.
Die vorliegende Dissertation wurde weder ganz noch teilweise bei einer anderen Prüfungskommission vorgelegt.
Ich habe noch zu keinem früheren Zeitpunkt versucht, eine Dissertation einzureichen oder an einer Doktorprüfung teilzunehmen.

München, den 16.12.2021

Michael Fuchs

_____

(Michael Fuchs)

# Table of contents

# List of figures

# Summary

Desmosomes provide strong intercellular adhesion and therefore are essential in tissues exposed to constant mechanical stress, e.g. the epidermis or the heart. The molecular composition of desmosomes consists of several protein families, including intercellular adhesion molecules and plaque proteins. Desmosomal cadherins represent the adhesion molecules and are a group of proteins comprising four desmogleins (Dsg1-4) and three desmocollins (Dsc1-3) isoforms. These are transmembrane proteins which interact in a $Ca^{2+}$-dependent homophilic or heterophilic manner, thereby mediating strong intercellular adhesion with their neighboring cell counterparts. Within the desmosome, plaque proteins serve as linkers of desmosomal cadherins to the intermediate filament cytoskeleton. The plaque proteins consist of armadillo family proteins, plakoglobin (PG) and plakophilins (Pkps), and desmoplakin (DP), a protein of the plakin family. Pkps act as scaffolds in order to mediate adhesion and signaling and further regulate desmosomal turnover and assembly. They exist in three different isoforms (Pkp1-3) which show a tissue-specific expression. Further, Pkps show a wide ranging role in the cell-biological context and their physiological significance is evident in diseases, e.g. mutations in Pkp1 lead to ectodermal dysplasia skin fragility syndrome.
However, their role in regulating Dsg binding properties as well as Dsg clustering is not yet elucidated. Murine keratinocytes lacking either Pkp1 or Pkp3 were compared to wild type (wt) cells to characterize the role of Pkp1 and Pkp3 in the regulation of Dsg1- and Dsg3-binding properties and contribution to Dsg3 clustering. Dsg1 and Dsg3 are of particular interest since they are the main targets of autoantibodies in the autoimmune skin blistering disease pemphigus vulgaris (PV).

In the first part of the thesis, the roles of Pkp1 and Pkp3 in desmoglein clustering and adhesion were investigated. Characterization of Pkp1- or 3-deficient cell lines revealed reduced cell cohesion and especially in Pkp1-deficient cells loss of intercellular adhesion

is strong. Force mapping measurements, performed with atomic force microscopy (AFM), revealed reduced binding frequency of Dsg1 and Dsg3 at the cell borders and displayed low membrane availability of Dsg1 and Dsg3 in Pkp1- or Pkp3-deficient cell lines. This indicates that both proteins are important for proper membrane availability of desmogleins. The single molecule-binding properties of the remaining membrane-bound desmogleins showed Pkp-dependent changes. However, because their numbers were low, presumably these altered binding properties of the remaining cadherins have no strong effect on overall adhesion. Extracellular crosslinking revealed that Pkp1 but not Pkp3 is required for Dsg3 clustering. Overexpression of Dsg3 rescued the reduced number of Dsg3 clusters in Pkp3- but not in Pkp1-deficient cells, as shown by AFM and stimulated emission depletion (STED) microscopy experiments. This demonstrates that Pkp1 and Pkp3 regulate the membrane availability of Dsgs. Furthermore, these data demonstrate that Pkp1 but not Pkp3 is required for the clustering of Dsg3. This novel function of Pkp1 appears to be essential for proper intercellular adhesion.

In the second part of the thesis, regulation of desmosomal hyper-adhesion was studied. An interesting property of desmosomes is their ability to occur in two adhesive states, a weaker and a stronger one. Desmosomes in the stronger adhesive state become independent from extracellular $Ca^{2+}$ and are called hyper-adhesive. However, the roles of Pkps and Dsgs in desmosomal hyper-adhesion is not fully elucidated yet. To address this unsolved issue, the aforementioned cell culture model, a murine keratinocyte Dsg3 knockout cell line and an *ex-vivo* skin model were used. Murine keratinocytes acquire the hyper-adhesive state 72 hours after exposure to high $Ca^{2+}$, whereas Pkp- and Dsg3-deficient cell lines fail to reach this state during this time line. AFM force mappings revealed that the hyper-adhesive state correlates with increased Dsg3 single molecule binding strength and prolonged interaction lifetime. Both parameters were unchanged in the Pkp-deficient cells. In parallel, during differentiation, i.e. during the acquisition of hyper-adhesion, the Dsg3 clusters become $Ca^{2+}$-independent. In contrast, deficiency of Pkp1 prevented $Ca^{2+}$-independency of Dsg3 clusters whereas lack of Pkp3 led to a reduced amount of $Ca^{2+}$-independent Dsg3 clusters. Interestingly, Dsg1 clusters remained the same during the investigated time period. In accordance, Dsg1 single molecule binding properties were not altered. This shows that acquisition of hyper-adhesion may not be a state acquired by the entire desmosome but rather reveals an isoform-dependent regulation by Pkps. $Ca^{2+}$ chelation of *ex-vivo* human skin samples showed further isoform-specific differences in membrane localization between

desmosomal cadherins. Immunostaining for Dsg3 at the cell membrane appeared to be more resistant to $Ca^{2+}$ chelation compared to Dsg1 staining. This demonstrates that desmosomal cadherins have different roles in the acquisition of hyper-adhesion and that Pkp1-mediated clustering of desmogleins is required for the acquisition of the hyper-adhesive state of desmosomes.

In summary, this project revealed that Pkp1 and Pkp3 are important for membrane availability of desmogleins. However, for Pkp3 this phenotype is differentiation-dependent and decreases over time. Pkp1, in contrast to Pkp3, plays a crucial role in the clustering of desmogleins. This Pkp1-mediated clustering contributes to acquisition of hyper-adhesion and correlates with altered single molecule binding properties such as binding strength and interaction-lifetime of Dsg3 when becoming hyper-adhesive. Thus, development of the hyper-adhesive state is paralleled by alterations of binding properties of specific Dsg isoforms rather than by the entire desmosome.

In a side-project, keratin-dependent regulation of desmoglein-binding was characterized. Keratin filament detachment from the desmosomal plaque occurs as one of the pathomechanism of PV. We found that p38 mitogen-activated protein kinases (p38MAPK) signaling is regulated by keratins. Moreover, this signaling is essential for the regulation of cell adhesion and involves both keratin-dependent and -independent mechanisms. Using fluorescence recovery after photobleaching (FRAP) experiments it was observed that desmosomal cadherin uncoupling from the cytoskeleton resulted in higher Dsg3 mobility in the plasma membrane.

The studies presented demonstrate that Pkp1-mediated regulation of desmosomal clustering is important for desmosomal adhesion and contributes to hyper-adhesion of desmosomes.

# Chapter 1

# Introduction

## 1.1 Human skin

### 1.1.1 Structure and function

The human skin consists of three layers, namely the epidermis, dermis and subcutis. The subcutis loosely connects the skin with the underlying tissue, and is responsible for the different degrees of mobility of the skin. It consists mainly of loose connective and fatty tissue. The dermis is composed of connective tissue which supports the epidermis and connects it to the lower subcutis. Primarily, it is in charge of the mechanical stability of the skin. Further, it contains lympathic and blood vessels as well as nerves. The outermost layer of the skin is the epidermis, which is discussed in more detail in the following part. The functions of the skin are manifold and range from protection against mechanical, thermal or chemical stress, registration of pressure, touch, pain and temperature to thermal isolation, energy storage and protection against dehydration [1] [2].

### 1.1.2 The epidermis

Being hardly thicker than a piece of paper, the epidermis is the outermost layer of the skin. The mature epidermis, which mainly consists of keratinocytes, has a multilayered and stratified structure which is subjected to homeostatic regulation [3]. Hence, it renews itself every 28 days due to the proliferating keratinocytes. Those are connected with each other via intercellular junctions (explained in more detail in part 1.2) and are further the prevailing cell type [4] [5]. Keratinocytes synthesize keratin filaments among other proteins, which are the main structural protein of the epidermis [6]. Other cellular components of the epidermis

are melanocytes, Langerhans cells and Merkel cells. Furthermore, there are also so-called skin appendages such as hairs, glands and nails [1] [2]. Due to differentiation and maturation, keratinocyte morphology as well as the protein expression pattern change as they are shifted upwards across the epidermis. Therefore, the epidermis can be subdivided into different layers (Figure 1.1 A) [7]. The basal layer, *stratum basale*, is connected via hemidesmosomes and focal adhesion contacts to the basal lamina and consists of stem cells whose progeny differentiate and move towards the upper layers. The *stratum spinosum* is the next layer in which the different cell layers are interconnected via desmosomes. The nomenclature resulted due to an artifact in the fixation of the tissue for histological analysis. The cells shrink due to fixation and dehydration of water, but are still connected by desmosomes and their incoming keratin filaments. This leads to their spinous appearance and the naming of the cell layer. Next layer is the *stratum granulosum* which contains flattened cells. In this state, the cells start to lose their cell nucleus and organelles. Further keratohyalin granules are expressed which are a sign for the beginning cornification. Cornification is a specific form of differentiation and programmed cell death in epidermal keratinocytes. Within this process, intermediate filaments start to fill out the cell interior. Additionally, crosslinkage of proteins in the cell periphery forms the cornified envelope. This is orchestrated by precisely timed expression of specific genes [8]. The most apical layer is the *stratum corneum*, which is the result of the cornification process. It consists of multiple layers of flattened, cornified cells without a cell nucleus or organelles. Degradation of intercellular linkages between the cornified cells leads to a separation of the cells from each other [8]. Here the keratinocytes eventually end up as lifeless scales and detach from the skin surface [4] [9].

## 1.2 Intercellular junctions of the epidermis

Intercellular junctions are responsible for adhesion and communication between cells. Beside that, they are able to form barriers between tissues as well as between tissues and the environment. Four different types of intercellular junctions are required to fulfill the manifold tasks of the epidermis. First, there are tight junctions (TJs) which are needed to seal the intercellular space and prevent leakage. The second group ensures the communication between cells. This is done via a protein complex called gap junctions. Mechanical coupling and adhesion between cells is carried out by the third and fourth type of intercellular junctions, namely by adherens junctions (AJs) and desmosomes. The principal molecular composition of intercellular junction complexes is preserved throughout all types. There

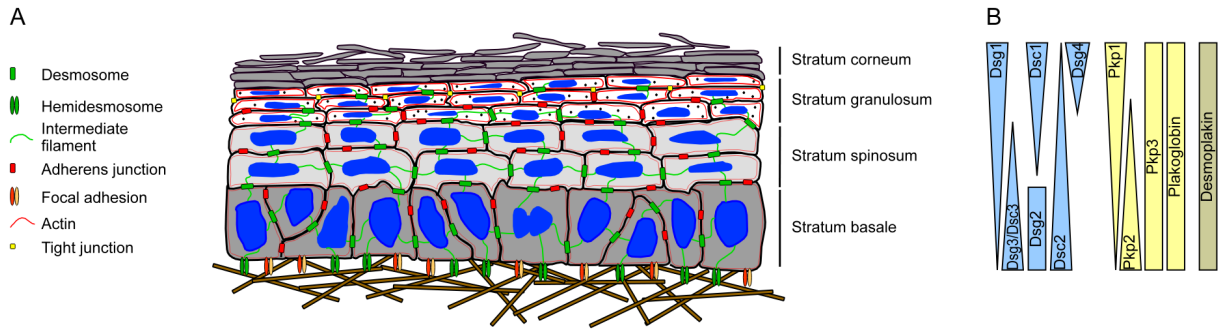


Figure 1.1: **A**: Layers of the epidermis and their sub-cellular structures as well as intercellular junctions consisting of: Desmosomes, adherens junctions, tight junctions and gap junctions (the latter two are not shown). Further, the cell-matrix contacts consist of hemidesmosomes and focal adhesions. **B**: Desmosomal proteins are not equally distributed along the multiple layers, some of them rather show a differentiation-dependent expression pattern.

are transmembrane proteins and plaque proteins, the latter connecting those to the cytoskeleton of the cell [7] [10]. The following section introduces the four different components of intercellular junctions in more detail.

The main function of TJs is to prevent leakage of molecules across the epithelium. They seal the gap between adjacent cells. TJs create a continuous strand around the cells [11]. In addition to its barrier-forming function, TJs also act as a fence to maintain cell polarity by preventing diffusion of apical and basolateral membrane components. Taking the epidermis as an example, the sealing strand is only present in the second layer of the stratum granulosum [12]. However, sealing is not complete. Some ions or small molecules are able to diffuse through the epithelial cells, a process known as paracellular transport. Depending on the tissue, the paracellular transport shows specific differences which are maintained by the molecular composition of the TJs [11]. Tissue-dependent regulation of paracellular transport is of high physiological importance. For example, the skin needs to prevent the uptake of pathogens and other harmful substances or vice versa the loss of water. In contrast, the epithelial in the intestine needs to absorb water, electrolytes or other macromolecules to fulfill its nutritive function [13]. The molecular composition of TJ consists of transmembrane components as well as of plaque proteins. The transmembrane proteins are comprised of many constituents, however the following three subfamilies are the most frequent ones. First there are claudins, of which 24 different isoforms exist. Those are essential for TJ formation. Further relevant transmembrane proteins are the MARVEL

domain proteins, which are occludin, relevant for junctional permeability and tricellulin, which is responsible for sealing adjacent cells at tricellular contacts. The third part of the constituents are junctional adhesion molecules (JAMs)-A, B and C. This constituent is a member of the immunoglobulin-G family which is essential in barrier formation as well as in regulating signal complex assembly [14] [15] [16] [17]. These transmembrane proteins are bound, organized and anchored to the actin cytoskeleton on their cytoplasmic side via scaffolding proteins, namely zona occludens (ZO)-1, 2 and 3 proteins. E.g. the ZO1 protein is expressed in epithelial and endothelial cells and contains three PDZ domains at the N-terminal site. Those PDZ domains are followed by a SH3 domain and a GUK domain. The PDZ domain is able to interact directly with claudin and JAMs. The GUK domain associates with occludin, while the SH3 domain connects with actin and thus establishes a direct link to the cytoskeleton [18]. In the epidermis, TJs structures are particularly found in the *stratum granulosum*. There they function as an indispensable barrier in order to prevent inside-out leakage. TJs in the epidermis comprise of multiple members of the claudin family proteins such as claudin-1, claudin-4 and claudin-7, occludin, JAM-A and ZO-1 [19].

Gap junctions connect neighboring cells directly to each other by interconnecting both cells cytoplasms and thus enable cellular communication [20]. They are present in almost all animal tissues, demonstrating the importance of this protein complex for cell communication [20]. The channel of the gap junctions is formed by channel-forming proteins called connexins (Cxs) in vertebrates and innexins in non-vertebrates [20] [21]. A semichannel consists of six Cxs, which builds a so called connexon. Two opposing connexons from adjacent cells create one continuous channel, called a gap junction. About 20 Cxs have been found in the human genome [22]. The pore diameter of the gap junctions is 1.4 nm, hence passage of only small molecules e.g. inorganic ions, sugars, amino acids and signaling molecules as cyclic adenosine monophosphate (cAMP) are possible. Transport of macromolecules e.g. proteins or polysaccharides is not feasible. Further, also electric coupling via gap junctions is possible [23] [24]. This is an important cell feature, hence action potentials can spread easily through the tissue, e.g. simultaneous contraction of the heart muscle cells. In physiological conditions many of those gap junction channels are found in close proximity, forming so-called gap junction plaques [20]. Hence gap junctions can be built via different Cxs, this leads to tissue specific permeabilities [25]. Gap junctions are almost expressed in the complete epidermis but not in the *stratum corneum*. Different types of Cxs are found in

the corresponding layers of the epidermis. In the basal epidermal layer of adult mice, Cx43 and Cx40 are expressed while Cx43 and Cx31 are present in the spinous layer. Cx31 but not Cx43 is found in the granular layer [26]. In addition, a cell differentiation-dependent alteration in Cxs isoform expression, in keratinocytes, was observed [27]. Further, Cxs play a role in epidermal wound healing, hence different Cxs are expressed upon wounding [28].

AJs belong to the adhesion-mediating complexes between cells in multicellular organisms. Their main function is to resist external forces that would otherwise pull cells apart. Classical cadherins and nectins are their transmembrane proteins, which link the cytoskeletons of neighboring cells. The name cadherin refers to their dependency of $Ca^{2+}$, as without extracellular $Ca^{2+}$-ions, no adhesion between neighboring cells is possible [29]. There are over 20 different members of the classical cadherins, some of them are named after their tissue of main occurrence, e.g. E-cadherin (E-Cad) in epithelial, N-cadherin (N-Cad) in nerve cells or P-cadherin (P-Cad) in the placenta [11]. However, these members are not limited to this particular tissue. Adhesion between neighboring cells is accomplished with the extracellular domain of nectins and cadherins in a homophilic manner. The intracellular part of cadherins is bound to plaque proteins and thereby indirectly linked to the actin cytoskeleton [30]. These plaque proteins comprise $\alpha$-, $\beta$-, $\gamma$-catenin and p120-catenin. The cadherins directly interact with $\beta$-, $\gamma$-catenin or p120-catenin. The complex is connected to the actin cytoskeleton via $\alpha$-catenin, which interacts with $\beta$-catenin and therefore links the cadherin proteins to the actin cytoskeleton [31]. For nectins, the cytoplasmic tail binds to afadin, which in turn links the nectins to the actin cytoskeleton [32]. In contrast to cadherins-catenin-complex, the nectin-afadin complexes do not mediate strong adhesion, but is essential for AJs maturation and cell polarity [30] [32] [33]. Even though binding of classical cadherins has a low affinity, the presence of many bonds in parallel results in strong adhesion. AJs are vast complexes, existing of up to $10^5$ cadherin molecules [11].

Desmosomes belong together with the AJs to the adhesion complexes of the intercellular junctions. Both adhesive units share a quite similar basic structure. From an evolutionary point of view, desmosomes have appeared for the first time with the origin of vertebrates. Hence they can be considered as an updated version of AJs [34] [7]. Their molecular composition however is different, as they use desmosomal cadherins and plaque proteins linking the complex to intermediate filaments (IFs) instead of actin filaments. In principle, desmosomes can withstand higher external forces as AJs. One cause for this is because

of the different cytoskeleton binding partner. IFs can withstand higher mechanical forces compared to actin. That is one reason of the desmosome-IF complex's ability to withstand higher forces than the AJ-actin complex, an important difference between desmosomes and AJs [7] [35]. Another reason is that desmosomes can adopt a stronger adhesive state compared to AJs (see 1.3.4) [36]. Desmosomes are therefore very important in vertebrates, as they provide mechanical integrity. The relevance of this strong linkage can be seen in the case of some diseases, where the function of desmosomes or their adhesive mechanisms are compromised. Impairment of desmosomal function can be caused due to autoantibodies, genetic defects of desmosomal components or bacterial infections leading to cleavage of desmosomal cadherins [37] [38] [39]. Desmosomes are found in almost all vertebrate epithelial, especially in mechanically stressed tissue, e.g. skin and heart [40]. Hence, investigation of desmosomal cadherin binding properties is the main part of this thesis, the desmosome will be described in more detail in the next section (see 1.3).

## 1.3 Desmosomes

Desmosomes are especially found in tissues which are particularly exposed to mechanical stress. These include stratified epithelial, e.g. the human epidermis (Figure 1.1 and 1.2 A-B). Other examples are mucous membranes and the myocardium. In addition, desmosomes can also be found in simple epithelial and non-epithelial cells including meningeal cells of the arachnoidea and in the follicular dendritic cells of lymph follicles [38]. In polarized epithelial cells desmosomes are located below the TJ and AJ, when viewed from the apical to the basal side [41].

The molecular composition of desmosomes consists of three building blocks or protein families: The adhesion-mediating transmembrane desmosomal cadherin proteins, armadillo proteins which are part of the desmosomal plaque and plakin proteins. The function of which is to create a connection to the IFs within the desmosomal plaque (Figure 1.2 C). The desmosomal cadherins are a subgroup of the cadherin superfamily. They consist of four desmoglein (Dsg 1-4) and three desmocollin (Dsc1-3) isoforms. Desmosomal cadherins are $Ca^{2+}$-dependent adhesion proteins consisting of five extracellular domains (EC1-5), a transmembrane and a cytoplasmic domain. $Ca^{2+}$-ions are essential as they stabilize the EC-domains, an important requirement for intercellular adhesion. *Trans*-interactions with partner molecules from opposing cells were suggested to be performed by the EC1-domain

via a strand-swap mechanism, while *cis*- or lateral interactions are carried out by a different regime of the EC1-domain, allowing both interactions to occur simultaneously (see 1.5.2) [42]. Ultrastructure images (Figure 1.2 B) show that desmosomes consist of a highly ordered, dense electron structure, which is less than 1 $\mu$m in diameter. There is a symmetrical midline between opposing cells spanning the extracellular space. This dense midline is believed to be the result of a highly ordered arrangement of the extracellular domains of desmosomal cadherins [43] [44] [45]. Following this model, at this line, *trans*-interactions between the extracellular domains of desmosomal cadherins, located on opposite cells, take place. On both sides of the dense midline, the desmosomal plaques, which are associated with the IF network, are located. They are composed of an outer dense plaque (ODP) and an inner dense plaque (IDP). The IFs attach at the IDP [45]. The $Ca^{2+}$ concentration required to form desmosomes is between $1.2 - 1.8\ mM$ [46]. The cytoplasmic domain of the desmosomal cadherins contains binding sites for the plaque proteins PG and Pkps 1-3, which are members of the armadillo family and are part of the desmosomal plaque. Dscs appear in two different isoforms, with respect to their cytoplasmic domain, an “a”- and a “b”-form. The shorter “b”-form lacks binding sites for the plaque protein PG. Further functions of the two different splice isoforms are poorly understood [7]. PG mediates the main linkage between the cytoplasmic domain of the desmosomal cadherins to DP, a member of the plakin family. Pkps are interacting with all parts of the desmosomal plaque and contribute to plaque assembly. The association of PG, Pkp and DP forms the ODP. Beside the linkage of cadherins to DP, plaque proteins are also able to translocate to the cell’s nucleus, therefore creating a link between intercellular junction and regulating the gene expression [39]. The role of DP is to provide a linkage between PG and Pkps to the IF. The IDP is formed by the binding of DP to the IF [39].

The expression of the different desmosomal component isoforms is tissue- and differentiation-dependent [47]. Dsg2 and Dsc2 are found in all tissues containing desmosomes [48]. As an example, the human intestinal epithelium contains only Dsg2 and Dsc2 as desmosomal cadherin isoforms [49]. Desmosomes in cardiomyocytes consist only of DP, Pkp2, Dsg2, Dsc2 and PG, while the other desmosomal components are missing [50]. These are only expressed in stratified epithelium such as the epidermis [48]. There, all desmosomal cadherins are present and reveal a differentiation-specific expression pattern [49]. Dsg1 and Dsc1 are mainly expressed in the upper layers of the epidermis, in contrast to Dsg3 and Dsc3, which are found more in the basal layers (see Figure 1.1B) [38]. The specific distribution pattern

of desmosomal components has an essential role in the proper differentiation and function of the epithelium [51] [38]. This was demonstrated by artificially induced overexpression of Dsg3 in mouse suprabasal epidermis. Phenotypes showed an abnormal differentiation, hyperproliferation and perinatal lethality due to transepidermal loss of water [52]. In the adult human epidermis, however, the expression patterns of the different cadherins overlap [47] [53].

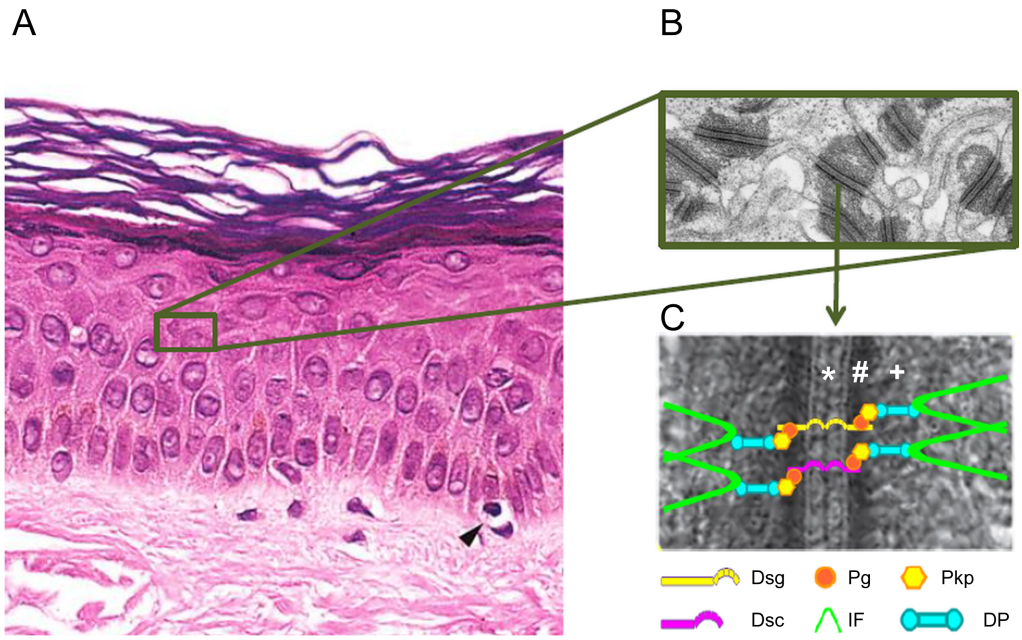


Figure 1.2: **A**: HE staining of a human skin section showing the different layers of the epidermis. **B**: Desmosomes appear as two opposing discs in an electron microscopy image. **C**: Ultrastructural image with superimposed schematic representation of a desmosome and its molecular components. Characters represent the following ultrastrucural regions: $*$ dense midline, # outer dense plaque (ODP), + inner dense plaque (IDP). Modified from (A) Welsch, Histologie, 2006 [2], (B) Radtke-Schuller and Bartels, 2012 [54] and (C) Wanzhong et al., 2003 [55].

### 1.3.1 Desmosomal cadherins

Desmosomal cadherins are also found outside of desmosomes on the cell surface of keratinocytes. There, they are not attached to the intermediate filaments and more soluble to detergents such as Triton-X-100 [56]. Outside of the desmosomal complex, they are then referred to as extradesmosomal cadherins. The latter do not only contribute to intercellular adhesion but rather act as adhesion receptors. In pemphigus, extradesmosomal Dsg3

molecules are the first molecules to be internalized. Due to this, desmosome assembly is perturbed, which leads to incomplete desmosomes and therefore compromised adhesion, a phenomenon described as non-assembly-disassembly hypothesis. This process occurs before the separation of desmosomes [57] [56].
Extradesmosomal cadherins serve as adhesion-dependent sensors, triggering intracellular signaling [58]. Supporting this hypothesis, stabilization of Dsg3 *trans*-interactions with peptides was carried out, leading to prevention of phosphorylation of p38MAPK after PV-IgG incubation [59]. Hence, activation of p38MAPK is a key aspect in the pathogenesis of pemphigus which supports a sensory role of extradesmosomal cadherins. Further, extradesmosomal Dsg3 is an upstream regulator of Rho GTPases, which are involved in the regulation of actin organization. This property is essential for cellular polarization, morphogenesis and tissue remodeling [60]. In line with this, stabilization of actin filaments inhibits PV-IgG-induced loss of intercellular adhesion. Taken together, extradesmosomal Dsg3 serves as a signal transducer involved in the regulation of adhesion [61].
As mentioned above, another property of extradesmosomal cadherins is their contribution to desmosome assembly. Interestingly, AJs and desmosomes do not independently mediate intercellular adhesion but are also interconnected and regulate each other. Complete AJs are required for desmosome formation [62] [63]. In this context, extradesmosomal Dsg3 is associated with E-Cad and sarcoma-associated kinase (Src) activation, which is important for desmosome assembly [60] [64] [65]. Activity of Src in combination with E-Cad is necessary for anchoring Dsg3 to the cytoskeleton. Further, Dsg3 regulates the activity of Src via forming a complex [65]. In summary, extradesmosomal desmogleins might act as primary signaling hubs which are important for the regulation of desmosomes, thus contributing to intercellular adhesion in an indirect fashion [39]. In addition to Dsg3, other desmosomal cadherins also occur outside of desmosomes. For example, Dsg1 and Dsg2 control epidermal growth factor receptor (EGFR) signaling, which regulates cell differentiation [66]. Moreover, Dsg2 interacts with caveolin-1, a property important for desmosome turnover [67] [68].

### 1.3.2 Plakophilins

Pkp1-3 belong to the armadillo-protein family [69]. The Pkp structure consist of a N-terminal head domain, which is between 246 and 348 amino acids long. In this section, the binding sites of the interacting binding partners are located. In the middle are the nine armadillo repeats. Between the fifth and sixth repeat a wedge is located, which leads to a bend in the protein structure [70]. The C-terminus domain is rather short (Figure 1.3)

[71]. Pkps localize to the desmosomal plaque where they interact with the cytosolic part of the desmosomal cadherins and DP, thereby supporting stable adhesion via cadherins. Similar to the desmosomal cadherins, Pkps have a tissue-dependent expression pattern. Further, in the human epidermis, Pkps also show a differentiation-dependent expression (Figure 1.1 B) [38]. Pkp1 is present in stratified epithelial where it is mainly expressed in the superficial layers. In contrast, Pkp2 is present in all simple and stratified epithelial and non-epithelial tissue such as the heart muscle. Pkp3 is expressed in simple and stratified epithelial and is abundant in the basal layers of the epidermis [69]. For Pkp1 and 2 two isoforms exist, a shorter "a" and a longer "b" form, while no further splice variant is known for Pkp3. The variation in length is due to an insertion of 21 amino acids of the third armadillo repeat for Pkp1 and 44 amino acids of the fourth armadillo repeat for Pkp2 [72] [73]. Besides their localization to the desmosomal plaque and their role to mediate linkage between DP and the desmosomal cadherins, Pkps fulfill other functions and are present outside of desmosomes as well. For instance, Pkp1a, Pkp2a and b are present in the cytoplasm and even localize to the nucleus. In contrast, Pkp1b appears to reside in the nucleus only [72] [73]. Resulting from that, the different distribution of the Pkp1 variants could explain various effects of the Pkp1 cellular functions. Nothing is so far known about the different functions of the Pkp2 splice variants [74] [75].

Pkps are also important for signal transduction. Their specific functions depend on the localization of the respective Pkps, as Pkp1-3 occurs in the cytoplasm, Pkp1-3 is present in the cell membrane and Pkp1 and Pkp2 are found in the nucleus [76]. A possible indication of the involvement of Pkps for signal transduction is that Pkp1 and Pkp3 occur in stress granules, which are aggregates of inactive translational complexes in the cytoplasm that are on hold due to cell stress [77]. In these stress granules, Pkp3 associates with RNA-binding proteins, indicating a function of Pkp3 for translation or RNA metabolism [77]. Other studies showed that Pkp1 and Pkp3 stimulate translation *in vitro* as well as in cells, via binding of the cap-binding complex [76]. Pkp2 in the cytoplasm is involved in signal transduction of the Wnt-pathway. There, it competes with E-Cad for binding to $\beta$-catenin and thus negatively regulates cell adhesion [78]. Regulation of Pkps during cell differentiation occurs via post-translational modification, mainly via its multiple phosphorylation sites or via palmitoylation [79] [80]. Pkp1 has an adhesive function in its unphosphorylated state, in contrast to its phosphorylated state. This change is mediated by insulin/IGF-1 signaling through the PI3K-AKT pathway. It follows a stabilization of the cytoplasmic

Pkp1 pool, which in turn increases translation rate and proliferation while cellular adhesion is decreased [81]. Palmitoylation describes a post-translational modification in which a 16-carbon fatty acid is attached to a specific cysteine residue. This process plays a role in several protein properties, including protein localization, activity, stability and to increase the probability of incorporation into the cell membrane [82]. For Pkps, palmitoylation is important for proper assembly and adhesion of desmosomes [80].

Although they fulfill different functions and reveal distinct localizations, all Pkps interact with desmosomal components and plaque proteins, which leads to a stabilization of intercellular adhesion and contributes to proper assembled desmosomes. Because of their various interaction partners, Pkps are regarded as scaffolding proteins, essential for desmosome assembly. Further, the respective Pkps show different functions with regard to cell adhesion, cytoskeleton interactions and signaling, which is explained for the individual isoforms in more detail in the following part.

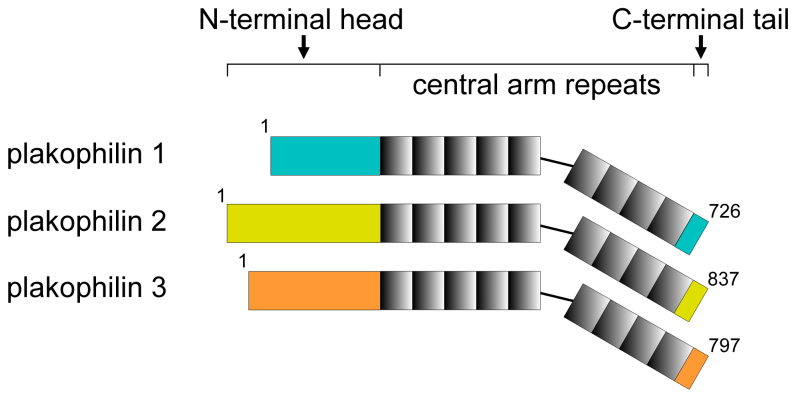


Figure 1.3: Structure of the plakophilin isoforms. The Pkp isoforms are composed of a N-terminus head domain, nine armadillo repeats with a characteristic bend between repeat five and six and a short C-terminus tail domain. The superscript numbers represent the amino acid residues.

Pkp1 interacts through its N-terminal head domain with DP and Dsg1 [83]. It further promotes the assembly and lateral clustering of DP [84]. Therefore, Pkp1 enhances the recruitment of desmosomal components to the plasma membrane, regulating desmosomal size. This leads to an indirect support of desmosomal mechanical stability [83] [74]. Further, Pkp1 can initiate the assembly of desmosomal components in a cell, even in the absence of classical cadherins. Classical cadherins however are required to form desmosomes between adjacent cells. Hence, Pkp1 is a key protein for DP clustering and is important for the

amount of desmosomal components [85]. According to that, Pkp1 seems to have an important role in promoting and stabilizing cell adhesion [74]. Due to the fact that Pkp1a is present at the desmosomes or at the nucleus and Pkp1b is only present in the cell nucleus it can be concluded that post-translational splicing is important for Pkp1 localization and therefore function. The generation of $Pkp1^{-/-}$ mice by Rietscher et al., showed the specific role of Pkp1 for a functional desmosome [86]. Mice lacking the Pkp1 gene were born with reduced weight but other than that appeared normal. However, their condition declined seriously and, without mechanical trauma, they developed fragile skin and lesions leading to death within 24 h. Desmosomes in the epidermis of $Pkp1^{-/-}$ mice were sparse and small. The observed phenotype revealed the importance of Pkp1 for desmosome function. Skin of $Pkp1^{-/-}$ mice was used to create spontaneously immortalized keratinocytes, which were used in this thesis (a kind gift from M. Hatzfeld) [86].

Pkp2 can interact with more desmosomal components compared to Pkp1 via its N-terminal head domain, namely with DP, Pg, Dsg1 and 2, Dsc1a and 2a [87]. Therefore, it can be speculated that Pkp2 has different functions compared to Pkp1 [78]. In cardiomyocytes, Pkp2 colocalizes with AJs, indicating that Pkp2 plays a role in forming some sort of mixed junctions [88]. Pkp2 colocalizes with DP in nonmembrane-bound precursors, which are transported to the membrane to regulate desmosome assembly [87]. Therefore, Pkp2 is required for DP accumulation in desmosomes of epithelial cells. Desmosome assembly requires Pkp2, which facilitates the association of protein kinase C (PKC) $\alpha$ to DP, and thereby weakens the interaction between DP and cytoplasmic IF. Unbound DP promotes desmosome assembly. Loss of Pkp2 inhibits the normal accumulation of DP at the cell membrane and, consequently, desmosome assembly [89]. Pkp2a and b can be localized at the cytoplasmic plaque of desmosomes as well as at the nucleus. Pkp2 was found to form a complex with RNA polymerase III [90]. This suggests that the amount of Pkp2 which exceeds the need for desmosome formation may be important in regulating growth control. The vital role of Pkp2 is shown in Pkp2 knockout mice, which display embryonic lethality during E10.5-E11. Hence, Pkp2 seems to be an essential factor for morphogenesis and an architectural component of the heart [91].

Pkp3 interacts with the highest number of proteins from the desmosome family, including PG, DP, Dsg1-3 and Dsc1a, 2a, 3a. The binding mechanism is via the N-terminal head domain. Furthermore, Pkp3 appears to contain two DP interaction sites. This feature

might be responsible for lateral DP-Pkp3 interactions, resulting in increased desmosome size and more keratin filaments anchoring points [92]. Consistent with this, Pkp3 knockdown experiments in human keratinocyte cell lines resulted in a decrease in desmosome size and reduced cell border staining of desmosomal proteins [93]. Pkp3 appears at the cell border even under low environmental $Ca^{2+}$ concentrations. Where it appears in a complex with E-Cad and PG. Therefore, it can be concluded that Pkp3 has an important role in the initiation of desmosome formation [93]. In agreement with this, overexpression of Pkp3 led to an increase in desmosome size and its stability, which was achieved via increased expression of Dsc2. This highlights the manifold capabilities of Pkp3 [94]. As for Pkp2, the role of Pkp3 is to provide a scaffold for desmosomal assembly [74]. Pkp3-null mice showed hair coat abnormalities and were susceptible for dermatitis. In the basal layer of the epidermis desmosome density was significantly altered [95]. Spontaneously immortalized keratinocytes from those Pkp3 knockout mice were used in this study [95].

### 1.3.3 Desmosome turnover

#### Desmosome assembly

Prior to the assembly of desmosomes, extracellular $Ca^{2+}$ as well as classical cadherins on the cell surface are required [96]. In a $Ca^{2+}$-dependent process, actin gets polymerized. This leads to the formation of filopodia which physically embed into neighboring cells forming transient contact points [97]. At the cellular contact sides, E-Cad clusters are formed leading to junctions, a process that depends on $\alpha$-catenin and VASP/Mena [98]. Those formed junctions mature into AJs. Afterwards, desmosomes are assembled at these intercellular contacts. Keratinocytes in a cell culture model showed desmosomal plaque formation with incoming cytokeratin filaments five minutes after being switched to high $Ca^{2+}$ medium, followed by the appearance of asymmetric desmosomes after ten minutes and symmetric desmosomes after one hour [99]. It is thought that Pkp3 is involved in desmosome formation, hence even under low $Ca^{2+}$ conditions Pkp3, E-Cad and PG are present at the cell borders. Due to the ability of PG to localize to desmosome as well as AJs, it plays a central role in the process of desmosome assembly [100]. In contrast, the localization of Pkp3 at the cell borders depends on the recruitment through PG and E-Cad [93]. Palmitoylation of Pkps is an important part of proper desmosome assembly. Mutation of a single cysteine residue prevents palmitoylation, which results in incorrect localization of desmosomal components [80]. Dscs are thought to be important for desmosome formation.

In Madin-Darby canine kidney II cells (MDCK), Dsc2 is the first desmosomal cadherin to appear at the cell surface within the first 30 min, followed by Dsg2 [101]. Further evidence for the role of Dscs in desmosome formation is provided by the N-terminal deleted Dsc3 in a human keratinocyte cell model. This mutation compromises the ability to form desmosomes, but mutant Dsc3 cadherins were able to bind $\beta$-catenin. This indicates that Dsc3 is able to interact with existing AJs via $\beta$-catenin, inducing desmosome formation [102].
Desmosomal components, after synthesis and post-translational modification, are transported to cellular contact sites by various mechanisms [103]. One is that cytoplasmic particles containing DP and Pkp2 are brought in an actin-dependent manner to the sites of desmosome formation. DP then first assembles in nascent junctions near the emerging desmosomes and is then gradually incorporated into the developing desmosomes [104]. For proper incorporation, Pkp2 is required to secure normal accumulation of DP in the desmosome. Afterwards Pkp2 recruits PKC$\alpha$ to DP. Due to PKC$\alpha$, DPs interactions with their cytoplasmic part and IF are weakened, leading to a better assembly of DP [89]. Apart from the function of Pkp2 regulating the DP-IF complex, it is also involved in another pathway. For a proper DP translocation towards emerging desmosomes, an organized actin cytoskeleton is necessary. Pkp2 modulates the actin cytoskeleton via RhoA, hence enabling desmosome assembly [105]. It can be concluded that at the plasma membrane Pkp2 acts as a scaffold for PKC$\alpha$ and RhoA and thus connecting those pathways. This supports DP phosphorylation and actin remodeling which is important for desmosome assembly [89] [105]. The carriage of the remaining desmosomal cadherins relays on a microtubule-dependent transport, mediated by distinct kinases [106].
Desmosomal cadherins in cooperation with PG and DP are already able to nucleate the desmosomal plaque [107]. So far, it is unclear whether the desmosomal cadherins are directly incorporated into the desmosome or not. For Dsg3 it is known that at first extradesmosomal clusters occur, which are then laterally incorporated into the desmosome [108]. Those extradesmosomal Dsg3 molecules are linked to actin. It seems that this state could represent a stopover towards desmosome formation [109]. In MDCK cells on a temporal level, first vesicles with the size of 60 nm, which mainly contain Dsc2, are brought to the cell membrane within the first 30 min. In a second step, vesicles with the size of 200 nm transport desmogleins, E-Cadherin, PG and $\beta$-catenin to the nucleation sites. Afterwards, plaque proteins are added. The whole process of desmosome assembly takes 2 h [101]. Once desmosomes have formed, they are stable and do not separate during mitosis. On the contrary, desmosomes are dynamic units able to adapt to external changes.

They are exposed to a high turnover with a half-life of roughly 30 min [110]. However, since the desmosomes are in a steady-state, this suggests that there is a freely diffusing pool of desmosomal components outside the desmosome, which represents a reservoir of desmosomes or an intermediate state [111].

#### Desmosome disassembly

Desmosomes are strong adhesive units, however their adhesive strength must be precisely controlled through assemble and disassemble dynamics. This is important to provide strong mechanical strength on the one side, but on the other side the cells must be able to undergo migration and rearrangement during wound healing. The degradation of desmosomes under non-pathological conditions is poorly studied. However, information about this process can be obtained from pemphigus autoantibody binding in model systems. Pemphigus antibodies bind to Dsg3 proteins and binding against extradesmosomal Dsg3 initiates raft-mediated Dsg3 endocytosis [112]. This leads to a lack of Dsg3 replenishment from the freely diffusing pool and subsequently to a reduction in Dsg3 level within the desmosome, ultimately leading to loss of desmosomal adhesion [113]. Furthermore, binding of pemphigus antibody to Dsg3 activates the signaling molecule p38MAPK. In the absence of pemphigus antibodies, p38MAPK is responsible for regulating the anchorage of the desmosomal plaque to the keratin filament cytoskeleton [114]. However, activation of p38MAPK leads to retraction of the keratin filament cytoskeleton followed by depletion of Dsgs, a phenomenon associated with loss of cell cohesion [111].

### 1.3.4 Concept of hyper-adhesion

One major difference between AJs and desmosomes is, that desmosomes can resist higher external forces. Intercellular adhesion complexes can be considered as a chain consisting of several subunits. Therefore, the rule applies that a chain is only as strong as its weakest link. This simple physical model can also be used for intercellular adhesion complexes. Hence, we have to consider the desmosome-IF complex as three components with individual linkages, namely the IF, the plaque proteins acting as the linkage point and the cadherins. Each connection needs to withstand the external tension force. The same amount of applied force is experienced by each individual part of the chain. Therefore, all linkages need to be equally strong, as the breakage threshold is defined by the weakest link. The desmosome-IF complex turns out to be more stress-resistant compared to the AJ-actin complex. As

mentioned above, IF can be stretched to a higher extend than actin [35]. This prevents the dissociation of tissue due to rupture of cells. The IFs are coupled to desmosomes via the plaque proteins, representing a linking point of the chain. Consequently, the desmosomal cadherins represent the next component of the chain, while desmosomal cadherin binding builds up the extracellular linkage. This bond connects the whole chain to the opposing complex of the neighboring cell. And it is this cadherin-cadherin-interaction that gives desmosomes their special property. Desmosomes appear in a weaker and a stronger adhesive state, the latter known as the hyper-adhesive state, in which desmosomes are independent of extracellular $Ca^{2+}$ [44] [50]. The stronger adhesive state of desmosomes is considered to be the normal state, which appears in most tissues constantly exposed to mechanical stress [115]. Hyper-adhesive desmosomes contain a dense midline [43]. In their weaker state, desmosomes are $Ca^{2+}$-dependent and are comparable to AJs in terms of force bearing. In the development of tissue it was found that desmosomes depend on $Ca^{2+}$ until embryonic day 12. After embryonic day 14, a dense midline was observed, suggesting that desmosomes are hyper-adhesive from this date onward [116]. Hyper-adhesive desmosomes have been found not only in the epidermis but also in numerous other tissues, e.g., the oesophagus, liver and cardiac muscle [115][117]. Moreover, hyper-adhesive desmosomes could also be detected in cell culture models, e.g., in the simple epithelial cell line MDCK and in cultured human keratinocytes (HaCaT) [36] [115]. Hyper-adhesive desmosomes are resistant to the chelation of $Ca^{2+}$. In case of $Ca^{2+}$ removal, they remain in their strong adhesive state, whereas $Ca^{2+}$-dependent desmosomes show a reduced level of adhesion.

The experimental way to test for hyper-adhesion in cell culture models underlies a simple protocol [115] [36]. However, it is important to consider that this approach is completely artificial as $Ca^{2+}$-depletion does not occur in a physiological setup. Normal cell culture media, as well as most body fluids, have a $Ca^{2+}$ concentration of $1-2\ mM$. To remove free $Ca^{2+}$ from the solution, the cells are exposed to ethylene glycol tetraacetic acid (EGTA), a specific $Ca^{2+}$ chelator [36]. Hyper-adhesive desmosomes remain in their strong adhesive state even after chelation of $Ca^{2+}$. In contrast, non-hyper-adhesive desmosomes and AJs lose their adhesive strength after $Ca^{2+}$-chelation. The withdrawal of $Ca^{2+}$ is a good and simple approach to identify the two different adhesive states of desmosomes. A concordantly performed dispase-based dissociation assay provides insights into overall intercellular adhesion [118]. A more concise approach is to investigate ultrastructural images. Here, it was proposed that $Ca^{2+}$-independent desmosomes show a dense midline whereas $Ca^{2+}$-dependent

desmosomes do not. Thus, this dense midline seems to be the ultrastructural correlate of a more precise arrangement of desmosomal cadherin [44].

Desmosomes are not locked in one adhesive state but are rather dynamic entities, which are able to change their adhesive properties. Transition between the two states was shown in the epidermis as well as in cell culture models [44] [115]. This ability is very important in order to adopt to various biological circumstances. Strong adhesion is required in intact tissue but in case of wounded tissue, cell migration is essential. This was proven in cell culture models as well as in the epidermis. It was shown that the transition between the normal $Ca^{2+}$-independent state to the weaker $Ca^{2+}$-dependent state underlies a couple of steps. At first, $PKC\alpha$ gets activated and translocates from the cytosol to the desmosomal plaque. There, $PKC\alpha$ activates DP leading to a rearrangement of the desmosomal plaque [115]. Following that altered desmosomal plaque composition might transmit signals to the EC-domains leading to a decrease of order [43]. In line with that, inhibition of $PKC\alpha$ supports the acquisition of the hyper-adhesive state.

On an ultrastructural level, hyper-adhesive desmosomes appear with an ordered and regular structure of their desmosomal cadherin EC-domains. Further, they show a prominent midline in ultrastructural images, which is not present in $Ca^{2+}$-dependent desmosomes [44] [119]. As stated before, the assembly of desmosomes depends on $Ca^{2+}$, followed by their ability to form *trans* binding [120] [121] [122]. It is therefore surprising how desmosomes can become independent of $Ca^{2+}$. A possible explanation may be the unique composition and structure of desmosomes. $Ca^{2+}$ may be locked within the arrangement of the EC-domains. Thereby the ions can not be removed by chelating agents. From classical cadherins it is known that *cis* binding takes place between the EC1-domain, which is involved in a swap-dimer formation (1.5.2), and the linker regions of the EC2- and EC3-domain of a neighboring cadherin molecules. The bound $Ca^{2+}$ ions are located between the EC2- and EC3-domain. Because of the high structural similarity between classical and desmosomal cadherins, Garrod suggested that *cis*-interactions between desmosomal cadherins trap the $Ca^{2+}$ and therefore lead to a resistance of $Ca^{2+}$ chelation [44]. Garrod et al. used the C-Cadherin structure in order to model the hyper-adhesive state [44][123]. Further, a $\beta - helix$ may be involved in this process, hence it covers one of the free $Ca^{2+}$ ions, therefore protecting it from extraction [50]. The transition to the weaker adhesive state requires disturbed order of the EC-domains, which is due to loss of *cis*-interactions. Importantly *trans*-interactions are still present,

since adhesion is not completely abrogated [45]. Therefore, the term $Ca^{2+}$-independent may be misleading. A better form to describe this state would be "$Ca^{2+}$ chelation resistance".

As mentioned at the beginning of the chapter, AJs remain $Ca^{2+}$-dependent and hence do not acquire a hyper-adhesive state. This is at first surprising because AJs also appear in clusters and classical and desmosomal cadherins show a high structural similarity. A difference between these two complexes is that classical cadherins do not arrange in highly ordered structures, whereas desmosomal cadherins do [43]. According to molecular dynamic simulations carried out in the presence of $Ca^{2+}$, a possible explanation for that difference could be due to different degrees in flexibility of the two cadherin families. These simulations took into account that the cadherins are partly membrane bound and attached to the cytoskeleton. Classical cadherin EC-domains are more rigid, and therefore unable to perform conformational changes that are needed for the adoption of an ordered arrangement. In contrast, desmosomal cadherin ectodomains show more flexibility and can therefore align in an ordered fashion, even with restriction of movement due to cytoskeleton anchorage. The lack of sequence conservation of two interdomain $Ca^{2+}$-binding sites is likely responsible for this higher flexibility [124]. To conclude, desmosomal cadherins cluster in an ordered arrangement due to higher flexibility of the EC-domains in contrast to classical cadherins [124].

Interestingly, increased expression of the plaque protein Pkp1 was shown to favor the transformation of $Ca^{2+}$-dependent to $Ca^{2+}$-independent desmosomes, in primary keratinocytes. This change in adhesive state is also protective against PV-IgG-induced effects [125]. Plaque proteins, especially Pkp1, are thus important for the development of the hyper-adhesive state.

To summarize, the main difference between the two adhesive states is the difference in degree of order of the extracellular domains and the resistance towards $Ca^{2+}$ chelation. The hyper-adhesive state refers to a higher ordered and stronger adhesive state. However, the mechanisms underlying the phenomenon of hyper-adhesion are hypothetical and further studies are required to elucidate the molecular basis and the regulation of $Ca^{2+}$-independency.

## 1.4 Desmosome-associated diseases

The importance of intact and appropriately regulated desmosomes are reflected by the pathogenesis of numerous diseases, where desmosomal adhesion is perturbed. This impairment can be due to autoantibodies, genetic defects or bacterial toxins. Alterations in protein expression of desmosomal cadherins have been found in various human carcinomas. However, mutations of the cadherins do not normally occur in these cases. The contribution of desmosomal cadherins to cancer is therefore not yet clear [38]. Various desmosomal components can be affected, leading to different diseases in distinct tissues. For example, mutations in Dsg2, Dsc2 and Pkp2 can cause arrhythmogenic right ventricular cardiomyopathy (ARVC) in cardiomyocytes, while impairment of desmosomal adhesion in the epidermis is accompanied in bullous diseases and skin fragility syndromes [126] [127].

In pemphigus, autoantibodies against Dsg1 and Dsg3 cause lesions in the skin and the mucous membranes [128]. Depending on the autoantibody profile and the resulting epidermal splitting, different forms of pemphigus are distinguished, namely pemphigus vulgaris (PV) and pemphigus foliaceus (PF), whereby PV is with 80-90 % of the cases much more common than PF [129] [38]. However, there is an endemic form of PF in South America, referred to as Fogo selvagem, which probably is transmitted via insect vectors [130]. PV-IgG antibodies cause blisters formation in the deep epidermis, whereas skin splitting in the granular layers of the epidermis is a hallmark of PF-IgG autoantibodies [131]. The two forms of pemphigus are characterized by different antibody profiles. People suffering from mucosal-dominant PV have autoantibodies against Dsg3, whereas patients with mucocutaneous PV develop autoantibodies against Dsg3 and Dsg1. In PF, patients have autoantibodies against Dsg1 but not to Dsg3 [38]. Pemphigus IgG also contains further antibodies directed against other keratinocyte antigens, such as Dsc1-3 or E-Cad. However, it has already been shown that these are not necessarily pathogenic. Whether and how these additional antibodies are involved in epidermal cleavage due to pemphigus has not yet been conclusively clarified [38]. Pathomechanistically, autoantibodies directed against the extracellular domains of Dsg1 and Dsg3 lead to a loss of intercellular adhesion of the epidermal keratinocytes, a process called acantholysis [132]. Histological hallmarks are depletion of Dsg1 and Dsg3 from the cell membranes and alterations of the keratin cytoskeleton [114]. The pathomechanism of this disease is however not fully understood. Nevertheless, two possible mechanisms are largely accepted, namely direct inhibition and cell signaling [39]. Direct inhibition is thought to occur when PV-IgG antibodies bind the

amino-terminal part of the EC1-domain, thereby interfering with the trans-interactions of desmosomal cadherin binding. This was observed for Dsg3 but not for homophilic Dsg1 indicating that the underlying mechanisms of PV and PF are different [133]. Direct inhibition in turn contributes to acantholysis [38]. However, it has been shown that direct inhibition alone is not sufficient to cause complete loss of cell cohesion. Rather, it was found that altered signaling events are crucial for the complete loss of intercellular adhesion [134]. Several altered signaling pathways in response to PV-IgG binding are involved in the pathogenesis of pemphigus [39]. Extradesmosomal Dsg3 mediate outside-in signaling, a function disturbed upon antibody binding [58]. In contrast, it was found that inhibition of several signaling pathways resulted in rescue of acantholysis after PV-IgG incubation [135]. Beyond that, keratins are involved in regulating several signaling pathways e.g., p38MAPK and PKC [114] [136]. Both signaling molecules also participate in the regulation of Dsg3 [137]. PV-IgG causes an increase in 1,4,5 trisphosphate and intracellular $Ca^{2+}$, both processes leading to activation of PKC [138]. It was shown that chelation of intracellular $Ca^{2+}$ blocked keratinocyte dissociation *in vitro* and inhibition of PKC stopped PV-IgG-induced acantholysis *in vivo* [139] [140]. This suggests the involvement of this signaling pathway. Other mechanisms have also been proposed for how PKC signaling contributes to PV acantholysis including phosphorylation of $\beta$-catenin in AJs [141]. In PV patients with skin lesions, p38MAPK is phosphorylated, which reflects its central role in pemphigus [142]. *In vivo* studies showed that not only p38MAPK but also its downstream target, heat shock protein (HSP) 27, are phosphorylated by binding PV-IgG or PF-IgG [142]. Studies with cultured human keratinocytes showed activation of p38MAPK and HSP 27 within 30 min after PV-IgG incubation [114]. In addition, pharmacological inhibition of p38MAPK inhibits blister formation by preventing keratinocyte dissociation, Rho inactivation, cytokeratin retraction, and actin cytoskeleton reorganization [114] [38]. Therefore, p38MAPK is most likely involved in the process leading to acantholysis but the exact mechanism is not yet elucidated. [38]. PV-IgG-induced loss of cell adhesion in keratinocytes can be prevented by overexpression of Pkp1. Increasing Pkp1 maintains Dsg3 proteins at cell-cell borders and inhibits ultrastructural desmosome changes [125]. This indicates that increased expression of a desmosomal component may be sufficient to prevent PV-IgG-induced pathogenic effects.

ARVC is a myocardial malfunction, which leads to loss of cardiomyocytes and their replacement by fatty tissue [143]. In patients with ARVC several mutations of desmosomal components such as Dsg2, Dsc2, DP and Pkp2 have been found [144] [145] [146]. This

genetic disorder can lead to sudden death in young patients [143].

Skin fragility-ectodermal dysplasia syndrome results from a functional knockout of the Pkp1 gene. Patients with this mutation suffer from cutaneous fragility, as well as congenital ectodermal dysplasia concerning skin, hair and nails [147]. Studies with mice showed that loss of Pkp1 leads to growth retardation and loss of desmosomal adhesion accompanied with smaller and fewer desmosomes [86].

## 1.5 Biophysical principles

This part is supposed to give a basic insight into the physical properties and models relevant to this thesis. Especially, atomic force microscopy (AFM) experiments are complex and require explanations regarding the details of their physical background. The following section explains at first the principle of AFM measurements, followed by the mechanisms of cadherin binding, which is essential for desmosome functionality. Subsequently, the approach of how single-molecule binding properties are determined with the AFM is explained. In the last part, the principal physics between receptor-ligand interactions will be outlined.

### 1.5.1 Atomic force microscopy

AFM is a non-optical microscopy technique. Its first application was to investigate the sample surface morphology. This is achieved through detection of distance-dependent interaction forces between the tip and the sample. Therefore, a small tip connected to a cantilever, which is basically a plate spring, is brought into contact with the surface. For feedback information a laser beam is focused on the back of the cantilever. The reflection of this laser is collected by a position-sensitive four-quadrant photodiode [148]. The measured deflection allows to measure small forces due to tip-surface interactions while scanning a sample (Figure 1.4 A). In this way, a three-dimensional image of the surface can be constructed. The AFM is operable in different modes; intermittent contact, non-contact mode and force modulation mode. These can be distinguished by the type of force acting between the tip and the surface. Basically, when two objects are brought together, they first sense the attractive van der Waals or capillary forces, followed by the repulsive forces due to overlapping electron orbitals (Figure 1.4 B). The non-contact mode works in the regime of the attractive force, the force modulation in the repulsive force range and the intermittent mode in between the two force areas. Those different modes of operation have

their own advantages and accordingly their own applications.

Besides measuring the topography of a surface, the AFM is often used for sensitive force measurements, which is referred to as force spectroscopy. For this purpose, the tip, which is coated with the molecule of interest, is moved back and forth in a vertical direction along the surface. The free end of the molecule can interact with binding partners from the substrate. In the case of an interaction, the bond molecules between the substrate and the tip are stretched. Deflection of the laser beam due to bending of the tip is registered on the detector. The obtained data contains information about the height position of the cantilever relative to its vertical deflection, which is proportional to the interaction force due to Hooks law [149]. The forces detectable by the AFM are in the range between 20 $pN$ and 10 $nN$ [150]. Because of the possibility to measure forces in this regime, the AFM is a suitable device to measure the interaction forces between two interacting partners or in this work proteins. Besides the AFM, there are also other techniques suitable to investigate single molecule interactions, e.g. optical tweezers, which are working in a lower force regime ($1 - 100$ $pN$) [150].

### 1.5.2 Cadherin-mediated adhesion mechanisms

This section describes the adhesive mechanism of classical cadherins. Following the observation that classical cadherins and desmosomal cadherins have a similar molecular composition with regard to their binding anchors and pockets, conclusions can be drawn on desmosomal cadherins, which are hard to investigate due to their low solubility. [40].

Cadherins contain several EC-domains. These are extremely important because adhesion between opposing cadherins occurs through these EC-sections. One EC-domain consists of seven antiparallel $\beta$-strands. Successive sections are arranged so that their N- and C-terminal-ends face each other (Figure 1.5A). This allows for consecutive assembly of multiple EC-domains. The number and arrangement of EC-domains classifies the subfamilies, e.g. both classical and desmosomal cadherins contain five EC-domains. Each EC-domain has conserved binding sites for $Ca^{2+}$ ions [42]. The name cadherin comes from its property to adhere in a $Ca^{2+}$-dependent manner. The individual EC-domains are stabilized by the binding of $Ca^{2+}$ ions. Three $Ca^{2+}$ ions bind to specific binding sites, which are located between two EC-domains, so that a total of twelve ions are required [42]. The dissociation constant of the $Ca^{2+}$ ions is lower than the extracellular $Ca^{2+}$ concentration

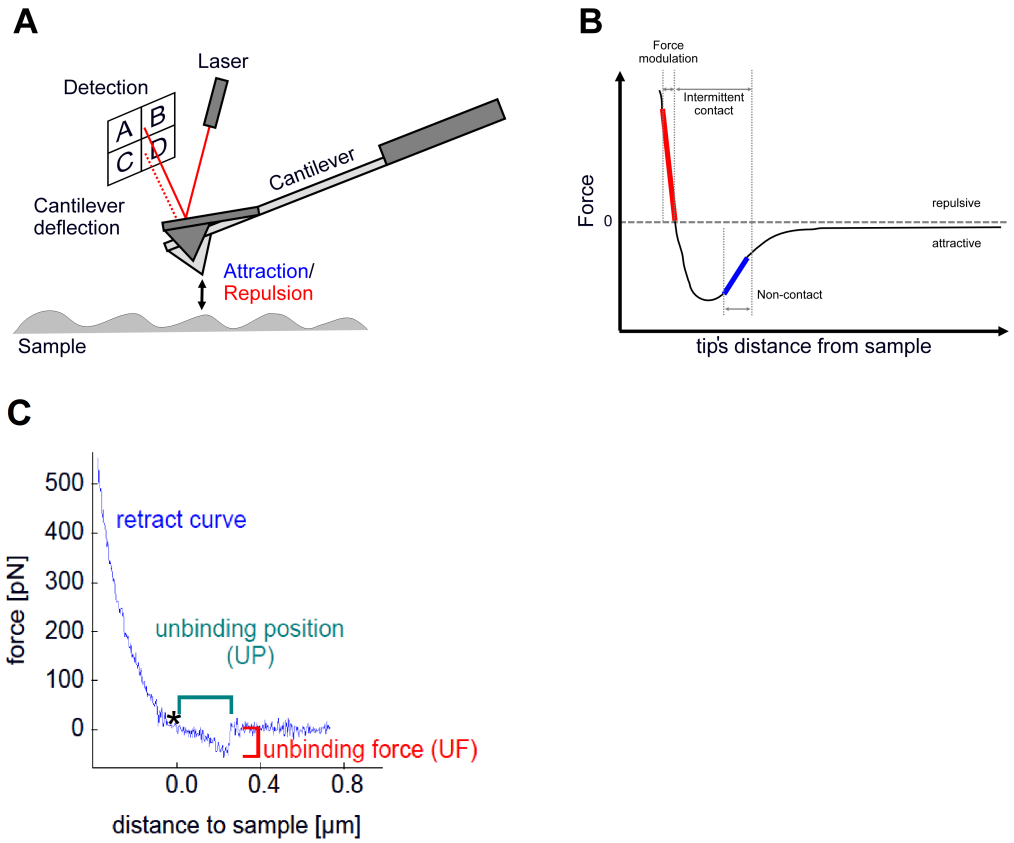


Figure 1.4: AFM working principle. **A**: Schematic setup of an AFM. A tip connected to a cantilever is repetitively approached to the sample's surface and retracted. A laser is focused on the back of the cantilever. Its reflection onto a photodetector is deflected by interaction of the tip with the surface. **B**: Attractive and repulsive forces on the tip as a function of distance. The different AFM operation modes are shown with regard to their sphere of action **C**: A force distance curve with an unbinding event. The unbinding force (UF) as well as the unbinding position (UP) are shown. The contact point, represented by the asterisk, describes the location of the first contact between the AFM tip and sample. (C) Modified from Fuchs et al., 2019 [151].

of the environment ($1\ mM$), so it can be assumed that the ectodomains are completely saturated under physiological conditions [152]. The binding of $Ca^{2+}$ ions leads to a certain rigidity of the EC-domains, which gives the extracellular part of the cadherin a specific curvature [122]. This geometrical shape is necessary for *trans*-binding because of spatial reasons [153].

The *trans*-dimerization occurs between the two most membrane distant EC1-domains

of opposing cadherins from facing cells. The bond cadherins form a bridge across the intermembrane gap. Dimerization is achieved with a "strand-swapped" conformation which is accomplished in a two step process. That involves the so called "X-dimer". The latter is a fast binding process and thought of as an intermediate state. The cadherins perform the swapped dimer state by exchanging the most N-terminal part of the $\beta$-A-strand, the A*-strand, between the two adhering EC1-domains of opposing cells (see Figure 1.5 A). The basis for this is the insertion of a conserved anchor residue on the A*-strand into a conserved hydrophobic acceptor pocket of the partner EC1-domain. The conserved anchor residue is the amino acid tryptophan at position 2 (at least for classical cadherins type I) [154]. Interestingly the swapping domain (A*-strand) can also be docked in its own hydrophobic pocket, what is then called "closed monomer" or in an identical pocket of the partner EC1-domain to form a "swapped dimer". Important for the swap dimer formation is an open state in which the hydrophobic anchor is undocked and freely floating (Figure 1.5 B-C) [42]. Worth mentioning is that the EC2-4-domains do not participate in strand swapping. A possible explanation could be their longer $\beta$-A-strand and the replacement of the hydrophobic conserved tryptophan at position 2 through phenylalanine [155]. However, this assumption is challenged by a recent study by Sikora et al. in which an atomic model of the desmosomal structure was constructed using cryo-electron tomography and molecular dynamics simulations, showing that the EC2-domain is also involved in *trans*-interactions [156].

The strand swapped dimers are formed through the so called "X-dimer" formation. In this state the cadherins are adjacent but no swap is performed. Here, the dimerization occurs between the EC1- and EC2-domain nearby the $Ca^{2+}$-binding region, however weaker than the swapped state [42]. Cadherins in this state have a lower activation energy needed for the strand swapping process, what underlines their role as an intermediate [157].

Another important way of binding is the lateral or *cis*-interaction. For type I cadherins conserved binding sites are present. Involved regions of binding are at the base of the EC1-domain and the other region at the apex of a parallel EC2-domain. Hence the conserved region for the *cis*-binding is on the opposite side of the *trans*-binding site, both interactions are possible at the same time. The function of the *cis*-binding is to laterally assemble the *trans*-bond cadherins into an ordered network of interacting cadherins, the latter of which is thought to be the basis of junctions [153] [42].

With respect to keratinocytes and desmosomal cadherins, some information on binding properties are known. In a cell-free setup, where AFM measurements are performed on functionalized mica sheets, homo- and heterophilic interactions of Dsgs and Dscs were found. Further, homophilic interactions of Dsg1, Dsg2, Dsg3 and Dsc3 were $Ca^{2+}$-dependent, as incubation with EGTA and specific antibodies decreased the binding frequency [158]. The $Ca^{2+}$-dependency of the Dsg1 homophilic interaction was investigated in more detail [159]. Half-optimal binding activity was identified for 0.8 $mM$ $Ca^{2+}$. This finding suggests that Dsg1 binding is most effective in the epidermal layers where an extracellular $Ca^{2+}$ concentration above 0.8 $mM$ occurs. AFM measurements performed with recombinant protein of the complete extracellular Dsg1 domain showed homophilic Dsg1 *trans*-interaction forces in the range of $37 - 68$ $pN$ (the force depends on the retrace velocity of the AFM tip, see chapter 1.5.4). Further, the lifetime of homophilic Dsg1 trans-interactions is 0.17 $s$ [159]. Binding strength of *trans* homophilic Dsg3 interactions was in the range of 50 $pN$ [160]. These values of homophilic desmosomal cadherin interactions are within the range of binding strengths for classical cadherins determined by the same method [161] [162]. Therefore, the molecular binding properties between desmosomal homophilic *trans*-interactions and classical cadherins are comparable and may be based on the same physical principles. By chemical crosslinking it was shown that the primary interaction of desmosomal cadherins in living keratinocytes are *trans*-homophilic interactions [163]. Measurements with Dsg3-coated tips on living keratinocytes also revealed primarily homophilic interactions [137]. However, heterophilic interactions between Dsg1 and Dsc3, Dsg2 and Dsg3, Dsg2 and Dsc1, Dsg2 and Dsc2 and even between Dsg2 and E-Cad were also found [164] [165] [166] [167] [168]. Interestingly, no interactions occurred between Dsg1 and Dsg3 [160].

### 1.5.3 AFM measurements on cells

First, the AFM was designed to obtain high resolution imaging. This is possible because AFM microscopy is not an imaging technique based on light. Thus, there is no diffraction limit and a resolution of $0.5 - 1$ $nm$ can be achieved [169]. Recently, the AFM has also been increasingly used to study biological samples [170]. This is done more often because no further fixation is required for cells that adhere to the surface. As a result measurements can be performed under almost physiological conditions (37°C and medium) [171]. Chemical coupling of recombinant adhesion molecules to the AFM tip enables force spectroscopy measurements between the molecule of interest and possible binding partners on the cell membrane [172]. Combining topography measurements with force spectroscopy enables the

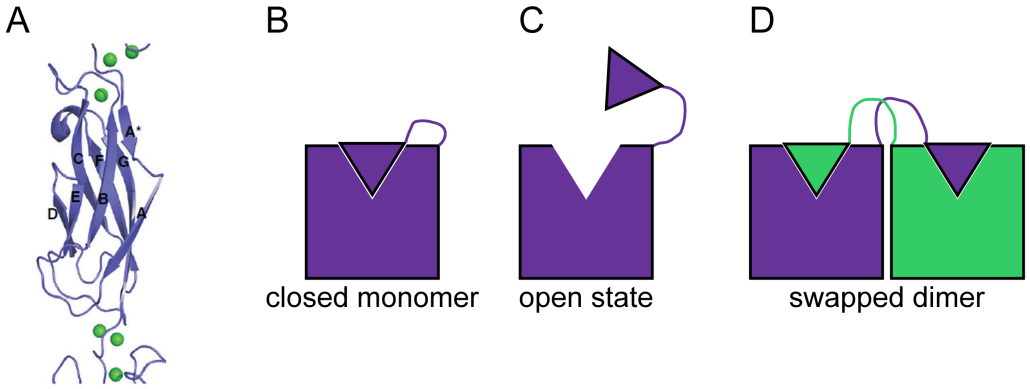


Figure 1.5: Schematic EC1-domain adhesion mechanism. A: Exemplary representation of a EC-domain showing the seven $\beta$-strands, while the A-strand is divided and also has a A*-strand. $Ca^{2+}$-ions are shown as green spheres. Modified from Brasch et al., 2012 [42]. B: In the closed monomer state the binding anchor, which symbolizes the A*-strand, is in its own pocket. C: The open state is an important intermediate state between closed monomer and swapped state. D: In the swapped dimer, the conserved anchors are bound in identical pockets of partner EC1-domains.

localization of binding events. For this purpose, the tip is periodically driven to the surface and retracted while scanning in parallel rows over a region of interest. This approach allows to obtain information about the topography of the cell, the localization of the binding partners and their frequency. Furthermore, information is gained about a number of biophysical properties of the single-molecule interactions, e.g. the binding strength which is referred to as unbinding force (UF), the quality of the cytoskeletal anchoring of the membrane protein (unbinding position or short UP) and the lifetime of the bond [158]. This information can be obtained with the help of a force distance curve (see Figure 1.4 C). As already explained, this is performed by approaching the surface with the tip, touching the surface in order to let biomolecules interact and retract the tip. The contact between tip and surface leads to a slight bending of the cantilever till a predefined setpoint. During this cycle, the position of the tip is monitored via the deflection of the laser. In case of an interaction, the cantilever gets bent towards the surface during retraction. As soon as the restoring spring force of the cantilever is greater than the binding force of the interaction, the cantilever jumps back to its neutral position. The amount of the interaction force corresponds to the difference between maximum deflection and neutral position of the cantilever, representing the UF. Another biophysical property gained from the force distance curve is the so-called unbinding position, which is the distance between the first contact of the tip and the rupture of the bond. The value of the unbinding position indicates an

indirect measure of the cytoskeletal anchorage with high values indicate a poor anchorage to the cytoskeleton [173].

### 1.5.4 Biophysical properties of receptor-ligand bonds

As mentioned in the previous section, many binding parameters between interacting molecules can be determined with the AFM technique. This part describes the physical principles behind the determination of these parameters and gives insight into the nature of these physical processes. Especially for the determination of the bond lifetime those considerations are indispensable.

A reversible reaction between two binding partners A and B, as occurs in the force measurements described above, can be written as follows [11].

$$A + B \underset{k_{off}}{\overset{k_{on}}{\rightleftharpoons}} AB \tag{1.1}$$

Here the molecules are present either in their bound complex AB or in their unbound state. The probability to find the molecules in their unbound state or the whole complex depends on the association rate constant $k_{on}$ $[1/Ms]$ and the dissociation rate constant $k_{off}$ $[1/s]$. The association rate $k_{on}$ gives information about how fast the binding occurs, depending on the concentration, while the $k_{off}$ rate says how fast the bound is released. These processes can be described by the differential equations.

$$\frac{d[A]}{dt} = \frac{d[B]}{dt} = -k_{on}[A][B] + k_{off}[AB] \tag{1.2}$$

$$\frac{d[AB]}{dt} = k_{on}[A][B] - k_{off}[AB] \tag{1.3}$$

For a steady state it is required that the amount of bound complex AB is constant over time.

$$\frac{d[AB]}{dt} \overset{!}{=} 0 \tag{1.4}$$

From that the dissociation constant $K_D$ can be derived, which gives information about the general affinity for the interaction.

$$K_D = \frac{k_{off}}{k_{on}} = \frac{[A][B]}{[AB]} \tag{1.5}$$

From equation 1.5 it can be seen that the dissociation constant $K_D$ is the fraction between the unbound molecules A and B and the product AB. Besides that it is the fraction between both kinetic rates [11].

The difference between bound and unbound states can also be illustrated using an potential landscape (Figure 1.6). Breakage of the bond complex occurs when the energy barrier $\Delta G_{off}$, consisting of the binding energy $\Delta G$ and the activation energy $\Delta G_{on}$, is overcome [174] [175].

$$\Delta G = \Delta G_{off} - \Delta G_{on} \tag{1.6}$$

The free energy $\Delta G$ without an external force and one mol of molecules is defined as:

$$\Delta G = \Delta H - T\Delta S = -N_A k_B T ln K_D \tag{1.7}$$

Here H describes the enthalpy, T the temperature and S the entropy of the system. $k_B$ is the Boltzmann constant. Equation 1.7 can be dissolved for the dissociation constant $K_D$

$$\frac{-\Delta G}{k_B T} = ln K_D \Rightarrow K_D = exp(-\Delta G / k_B T) \tag{1.8}$$

From equation 1.8 it can be seen that the dissociation constant depends on the energy barrier $\Delta G_{off}$ and on the thermal energy. Increasing temperature causes the bound complex to be raised more and more, which leads to a reduction of the energy barrier. Here the cause of dissociation is due to thermal energy fluctuations. For high temperatures (melting temperature) no bond is stable anymore. According to the Van't Hoff-Arrhenius equation the separation rate $k^0_{off}$ of a single bond is

$$k^0_{off} = \nu \cdot exp(\frac{-\Delta G_{off}}{k_B T}) \tag{1.9}$$

Here $\nu$ can be seen as an inertia-factor for the bond separation process. Using the AFM adds an external force F that changes the Van't Hoff-Arrhenius equation accordingly:

$$k_{off} = \nu \cdot exp(\frac{-\Delta G_{off} - F\Delta x}{k_B T}) = k^0_{off} exp(-F\Delta x / k_B T) \tag{1.10}$$

$k^0_{off}$ is the dissociation rate constant in case of no external force. The external force leads to a tilt in the energy landscape by the subtraction of $F \cdot \Delta x$. Here $\Delta x$ is the potential width. This means that the greater the force the greater the tilt and the more likely the

dissociation of the complex. According to Wieland et al., 2005 the maximum value of the force distribution F is related to $k^0_{off}$ and $\Delta x$ by the following formula. This is valid under the assumption of a bound state, which is confined by a single barrier [176]:

$$F(f) = \frac{k_B T}{\Delta x} ln(f \frac{\Delta x}{k_{off} k_B T}) \tag{1.11}$$

It can be seen that the measured force F depends logarithmically on the loading rate, which is given by $f = dF/dt$. Further, it also depends on thermal energy $k_B T$, a stochastic process that is additionally involved in bond separation. Due to that, the measured forces are distributed and the results therefore indicate the most probable force. From equation 1.11 it can be seen that the most probable force increases with the logarithm of the loading rate and decreases with the temperature (also seen in equation 1.7). This behavior can be illustrated by the following consideration. If the force is applied slowly (low loading rate), it is very likely that the bond ruptures due to thermal energy and the applied force is close to zero. If the force applied is fast, the probability of an unbinding due to thermal energy is less. Hence to separate the complex, a force strong enough to overcome the potential valley is needed. Therefore, higher forces are measured the faster the force is loaded to the bond. The concept of the most probable force can be summarized: It increases with the logarithm of the loading rate and decreases with the thermal energy. Therefore, when force measurements are conducted it is important to collect multiple measurements and determine the most probable force from the distribution of measured forces [177]. In order to obtain lifetime interactions about the bond it is necessary to perform multiple force measurements with increasing loading rates. Plotting the measured forces against the logarithmic loading rate results in a straight line. With the help of fitting methods the specific dissociation rate $k_{off}$ and the potential width $\Delta x$ of an interaction can be determined [175].

As seen from equation 1.11 the AFM is a tool to investigate the dissociation rate constant $k_{off}$ and the potential width $\Delta x$. With that the lifetime $\tau$ of a bond can indirectly be determined ($\tau = \frac{1}{k_{off}}$) [175].

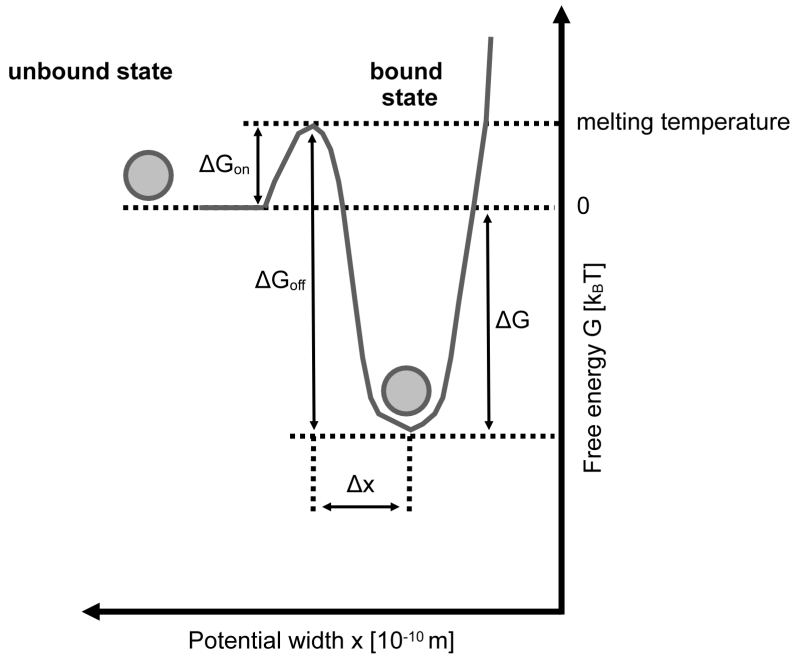


Figure 1.6: The sphere represents the bound or unbound complex according to the localization in the energy landscape. An activation energy $\Delta G_{on}$ is needed for bond formation. To unbind the complex the energy barrier $\Delta G_{off}$ needs to be overcome, which is composed of the Gibbs free energy $\Delta G$ and $\Delta G_{on}$.

## 1.6 Aim of this study

Desmosomes provide strong intercellular adhesion and are abundant in tissues exposed to mechanical stress, e.g. the epidermis or the heart. Autoantibodies against desmosomal components or genetic mutations lead to severe diseases such as pemphigus vulgaris in the epidermis or arrhythmogenic cardiomyopathy in cardiac myocytes. These desmosome-related diseases reveal the importance of an intact desmosome. On the ultrastructural level, desmosomes are composed of different protein families, including desmosomal cadherins, which provide strong intercellular adhesion via their extracellular domain. Another component is plaque proteins, which act as linkers for the desmosomal cadherins to the intermediate filament. Pkps are members of the plaque proteins, which function as scaffold proteins and are involved in regulating desmosomal turnover and many other cellular processes. However, their involvement in intercellular adhesion at the single molecule level was not fully elucidated. Further, the role of Pkps in the regulation of desmosomal cadherin binding properties and clustering remained unknown. A more detailed understanding of these is of

great clinical relevance.

Therefore, the first aim of this study was to elucidate the role of Pkps in desmosomal cadherin adhesion on a single molecule level. To this end, the focus was on keratinocytes which represent 90% of cells in the epidermis. The purpose was to investigate how altered Pkp expression affects the binding properties of desmosomal cadherins. Results of this study should provide new insights into the regulation of desmosomal cadherins. Therefore, atomic force microscopy was used in combination with biochemical approaches.

An outstanding characteristic of desmosomes is their ability to acquire two different adhesive states, a weaker and a stronger one. In which of the two states the desmosome is situated depends on the process of differentiation as well as on external environmental cues. Desmosomes in the stronger adhesive state are referred to as hyper-adhesive. Within this state, desmosomal cadherins become independent of extracellular $Ca^{2+}$. It is known that Pkps are involved in desmosomal hyper-adhesion. However, the molecular mechanisms underlying the acquisition of hyper-adhesion remains not fully elucidated. Hence, for the second part of this thesis, the aim was to determine the role of desmosomal cadherins and Pkps in acquisition of a hyper-adhesive state. As a working model murine keratinocytes lacking either Pkp1 or Pkp3 and *ex-vivo* human skin samples were used.

# Chapter 2

# Results

## 2.1 Plakophilin 1 but not plakophilin 3 regulates desmoglein clustering

Cellular and Molecular Life Sciences
https://doi.org/10.1007/s00018-019-03083-8



ORIGINAL ARTICLE

# Plakophilin 1 but not plakophilin 3 regulates desmoglein clustering

**Michael Fuchs[1] · Marco Foresti[1] · Mariya Y. Radeva[1] · Daniela Kugelmann[1] · Rene Keil[2] · Mechthild Hatzfeld[2] · Volker Spindler[3] · Jens Waschke[1] · Franziska Vielmuth[1]**

Received: 29 October 2018 / Revised: 15 February 2019 / Accepted: 25 March 2019


## Abstract

Plakophilins (Pkp) are desmosomal plaque proteins crucial for desmosomal adhesion and participate in the regulation of desmosomal turnover and signaling. However, direct evidence that Pkps regulate clustering and molecular binding properties of desmosomal cadherins is missing. Here, keratinocytes lacking either Pkp1 or 3 in comparison to wild type (wt) keratinocytes were characterized with regard to their desmoglein (Dsg) 1- and 3-binding properties and their capability to induce Dsg3 clustering. As revealed by atomic force microscopy (AFM), both Pkp-deficient keratinocyte cell lines showed reduced membrane availability and binding frequency of Dsg1 and 3 at cell borders. Extracellular crosslinking and AFM cluster mapping demonstrated that Pkp1 but not Pkp3 is required for Dsg3 clustering. Accordingly, Dsg3 overexpression reconstituted cluster formation in Pkp3- but not Pkp1-deficient keratinocytes as shown by AFM and STED experiments. Taken together, these data demonstrate that both Pkp1 and 3 regulate Dsg membrane availability, whereas Pkp1 but not Pkp3 is required for Dsg3 clustering.

**Keywords** Desmosome · Cell adhesion · Desmosomal clustering · Atomic force microscopy · STED

## Abbreviations

| | |
|---|---|
| AFM | Atomic force microscopy |
| ARVC | Arrhythmogenic cardiomyopathy |
| DP | Desmoplakin |
| Dsc | Desmocollin |
| Dsg | Desmoglein |
| EC | Extracellular domains |
| FRAP | Fluorescence recovery after photobleaching |
| HaCaT | Cultured human keratinocytes |
| IF | Intermediate filament |
| MAPK | Mitogen-activated protein kinase |
| MKZ | Murine keratinocytes |
| PEG | Polyethylenglycol |
| Pg | Plakoglobin |
| Pkp | Plakophilins |
| PV | Pemphigus vulgaris |
| QI | Quantitative imaging |
| STED | Stimulated emission depletion |
| Sulfo-EGS | Ethylene glycolbis (sulfosuccinimidylsuccinate) |
| UFs | Unbinding forces |
| UP | Unbinding position |
| wt | Wild type |

**Electronic supplementary material** The online version of this article (https://doi.org/10.1007/s00018-019-03083-8) contains supplementary material, which is available to authorized users.

Michael Fuchs, Marco Foresti, Jens Waschke and Franziska Vielmuth contributed equally.

✉ Jens Waschke
Jens.Waschke@med.uni-muenchen.de

✉ Franziska Vielmuth
Franziska.Vielmuth@med.uni-muenchen.de

[1] Faculty of Medicine, Institute of Anatomy, Ludwig-Maximilians-Universität Munich, Pettenkoferstr. 11, 80336 Munich, Germany

[2] Division of Pathobiochemistry, Institute of Molecular Medicine, Martin-Luther-University Halle-Wittenberg, Halle, Germany

[3] Department of Biomedicine, University of Basel, Basel, Switzerland

## Introduction

Desmosomes are cell–cell contacts crucial for proper intercellular adhesion. They are indispensable for the integrity of tissues which are exposed to repetitive mechanical stress, such as the heart or the epidermis [1]. Importance of desmosomal adhesion is reflected by severe diseases occurring

Published online: 04 April 2019

when cell cohesion is compromised, e.g., through autoantibodies in pemphigus vulgaris (PV) or genetic mutation in arrhythmogenic cardiomyopathy (ARVC) [2, 3] and skin fragility syndrome [4]. On the molecular level, desmosomes are composed of three major protein families: desmosomal cadherins, comprising three desmocollin (Dsc1-3) and four desmoglein (Dsg1-4) isoforms, which maintain intercellular adhesion via their extracellular domains in homo- and heterophilic $Ca^{2+}$-dependent manner [5–7]. Further, desmosomes consist of armadillo family proteins plakophilins (Pkp1-3) and plakoglobin (PG), and of desmoplakin (DP), the latter of which belongs to the family of plakin proteins. These proteins build up the desmosomal plaque, stabilize desmosomal cadherins and anchor them to the intermediate filament (IF) cytoskeleton [8–10].

Pkps, of which all three isoforms are expressed in a differentiation-dependent manner in keratinocytes, are important for desmosomal cadherin turnover [11, 12] and interact with various desmosomal proteins [13]. Different isoforms are involved in a broad range of signaling pathways and have in part opposing effects on the cellular processes [14]. For instance, loss of function of Pkp1 leads to ectodermal dysplasia-skin fragility syndrome [4, 15, 16]. In line with this, Pkp1 k.o. mice develop growth retardation, loss of desmosomal adhesion and impaired tight junction function [17], whereas Pkp3 k.o. mice reveal a mild phenotype with hair abnormalities and skin infections [18].

On a molecular level, studies using electron tomography and immune electron microscopy suggest that Pkps reveal a quasi-periodicity of approximately 7 nm in the desmosomal plaque neighboring intracellular domains of desmosomal cadherins [19], indicating that Pkps directly participate in the organization of the desmosomal plaque. In line with this, Pkps laterally cluster with desmoplakin to increase desmosome size [20–22]. Beside their structural function in desmosomes, Pkps regulate several signaling pathways [13, 14, 23, 24–26], which indicates specific roles for Pkps in the regulation of desmosomal adhesion. In line with this, Pkp3 is of importance for the formation of new desmosomes, whereas Pkp1 is involved in hyper-adhesion, a state in which desmosomes are insensitive to the reduction of extracellular $Ca^{2+}$ levels [14, 26, 27].

Changes in desmosomal organization and desmoglein clustering are present in various desmosomal diseases such as pemphigus and skin fragility syndrome [28–33]. Thus, it is possible that Pkps also differentially cluster desmosomal cadherins and via organizing the desmosomal plaque, this could be a critical mechanism for maintenance of proper intercellular adhesion. However, this has not been directly tested so far. Further, it remains unknown whether Pkps also participate in the regulation of desmosomal adhesion at the level of single-molecule binding properties. Since binding properties of desmosomal cadherins are affected by intracellular proteins such as keratins and various signaling pathways [34], we here investigated the role of Pkp 1 and 3 for Dsg binding and clustering. We focused on Dsg1 and 3, since the autoimmune blistering skin disease pemphigus shows that targeting Dsg1 and 3 interferes with stable tissue cohesion [35, 36].

## Materials and methods

### Cell culture, transfection and reagents

Wild type (wt) and Pkp1- or 3- (Pkp k.o.) deficient murine keratinocytes (MKZ) were isolated and maintained as described before and in Supplement Materials and Methods [14, 17]. Cells were used at 48 h after confluency and switching to high $Ca^{2+}$ conditions throughout all experiments. For some experiments, human keratinocyte cells (HaCaT) [37] were used (see Suppl. M&M). For Dsg3 overexpression, cells were grown to 70% confluency and subsequently transiently transfected with pEGFP-C1-Dsg3 (kindly provided by Dr. Yasushi Hanakawa, Ehime University School of Medicine, Japan) or pSNAPf-mDsg3-N (for cloning see Suppl. M&M) using Lipofectamine 3000 (Invitrogen, Carlsbad, USA). Change to high $Ca^{2+}$-containing media (1.2 mM) was carried out 24 h after transfection.

### Purification of recombinant Dsg1 and 3-Fc construct

Purification of recombinant human Dsg1 and 3-Fc proteins was carried out as described before [38, 39] and in Suppl. M&M.

### Atomic force microscopy (AFM)

Throughout all measurements, a NanoWizard® 3 AFM (JPK Instruments, Berlin, Germany) coupled with an inverted optical microscope (Carl Zeiss, Jena, Germany) was used, which enabled the selection of a scanning area by visualization of the cells through a 63 × objective. Recorded topographic images and adhesion measurements were performed according to the previously applied protocols [34, 40, 41]. Two different force spectroscopy-based imaging modes have been used, the quantitative imaging (QI) (setpoint: 0.5 nN, Z-length: 1500 nm, pulling speed: 50 µm/s) and the force mapping mode (setpoint: 0.5 nN, Z-length: 2000 nm, extend time: 0.2 ms, extend delay: 0.1 s). Recorded pixels contain the information of a single force–distance curve. For experiments, the D-Tip ($Si_3N_4$) of MLCT cantilevers (Bruker, Mannheim, Germany) with a nominal spring constant of 0.03 N/m and a tip radius of 20 nm was used. To detect specific single-molecule interactions, recombinant Dsg3- and Dsg1-Fc (concentration: 0.15 mg/ml) were utilized

for coating of the tips through a flexible heterobifunctional acetal-polyethylene glycol (PEG) linker (Gruber Lab, Institute of Biophysics, Linz, Austria) as described previously [42]. All experiments on MKZ cells were performed in full FAD medium supplemented with $Ca^{2+}$ at 1.2 mM concentration. Distribution ratio and stability coefficient were calculated as described before and in Suppl. Materials and Methods.

### Electrophoresis and Western blot analysis

Cells were lysed and Western blotting was conducted as shown previously and in Suppl. M&M [43]. For respective experiments, Triton X-100 fractionation or surface biotinylation was conducted.

### Chemical crosslinking

For investigation of protein oligomerization of desmosomal cadherins, the membrane-impermeable cross-linker ethylene glycolbis (sulfosuccinimidylsuccinate) (Sulfo-EGS) (Pierce Biotechnology, Rockford, USA) was used. The experimental procedure has been described before [7]. Briefly, Sulfo-EGS was added to cells 48 h after $Ca^{2+}$ switch at a concentration of 2 mM for 30 min at room temperature. TBS at a concentration of 50 mM was added to stop the reaction. Detection of crosslinked products was performed by Western blotting.

### Keratinocyte dissociation assay

To determine the adhesive strength of keratinocytes, dispase-based keratinocyte dissociation assays were performed as described previously [44].

### Immunostaining

For details regarding immunostaining please refer to Suppl. M&M.

### Stimulated emission depletion microscopy (STED)

Dsg3-snap transfected cells were labeled with SNAP-tag-kit® according to the manufacturer's protocol (New England Biolabs, Massachusetts, USA). Fixation and incubation with further antibodies were performed as described in Suppl. M&M. Recordings were made with the STED-Expert line setup from Abberior (Abberior Instruments GmbH, Göttingen, Germany).

### Data processing and statistics

Image processing was conducted with Photoline (Computerinsel, Bad Gögging, Germany) and Photoshop CS7 (Adobe, San José, USA). JPK data processing software (JPK Instruments) was used for AFM images and data analysis of force–distance curves. Further analysis of measured AFM data, such as, unbinding forces, peak fitting and step position was done with Origin Pro 2016, 93G (Northampton, MA, USA). Western blot bands were analyzed with ImageJ software (NIH, Bethesda, USA). Moreover, data were evaluated with Excel (Microsoft, Redmond, WA). The data of two groups were compared using two-tailed Student's *t* test. In case of more than two group comparisons, analysis of variance (one-way ANOVA) followed by Bonferroni post hoc test, was performed. The shown error bars represent standard error of the mean or the standard deviation as indicated. Statistical significance was assumed for $p$ values $< 0.05$.

## Results

### Intercellular adhesion depends on Pkp1 and Pkp3

Human keratinocytes (HaCaT) were used to delineate the expression patterns of Pkp1, 2 and 3 and their co-localization with Dsg3. As described earlier, HaCaT cells express all three Pkp isoforms [45]. In *xy*-plane, Dsg3 is distributed linearly along cell borders (Fig. 1a). Further, we observed punctate Dsg3 immunostaining on the cell surface of keratinocytes in the *xz*-plane, similar to that described before [34] (Fig. 1a). Staining of Pkp1, 2 and 3 showed that all isoforms localize along the cell boundaries and co-localize with Dsg3 at the cell border areas. Similar localization patterns were detected on the cell surface (Fig. 1a). Thus, we assumed that Pkps might regulate Dsg-binding properties at both localizations. To dissect the role of Pkps for desmoglein distribution and binding properties, we used murine keratinocytes lacking either Pkp1 or Pkp3, respectively [14, 17] (Figure S1a) and compared them to wt keratinocytes. Dispase-based keratinocyte dissociation assay revealed an increased number of fragments in Pkp3- and more drastically in Pkp1-deficient cells under untreated conditions, indicating that both Pkp isoforms contribute to intercellular adhesion, but Pkp1 is more important for strong cellular cohesion than Pkp3 (Fig. 1b). To investigate the effect of Pkp deficiency on expression and localization of Dsg3, proteins at the cell membrane were detected by cell surface biotinylation assays. Here, we observed a decreased total Dsg3 expression and a corresponding decrease in the biotinylated protein fraction, indicating that Pkp deficiency leads to loss of Dsg3 from the cell membrane (Fig. 1c). We further investigated the amount of Dsg3 in the cytoskeleton-unanchored (Triton X-soluble) and the cytoskeleton-anchored (Triton X-non-soluble) fraction, where we observed a drastic decrease of Dsg3 levels in both fractions from Pkp1-deficient cells, whereas Dsg3 levels were not altered in both fractions in Pkp3-deficient

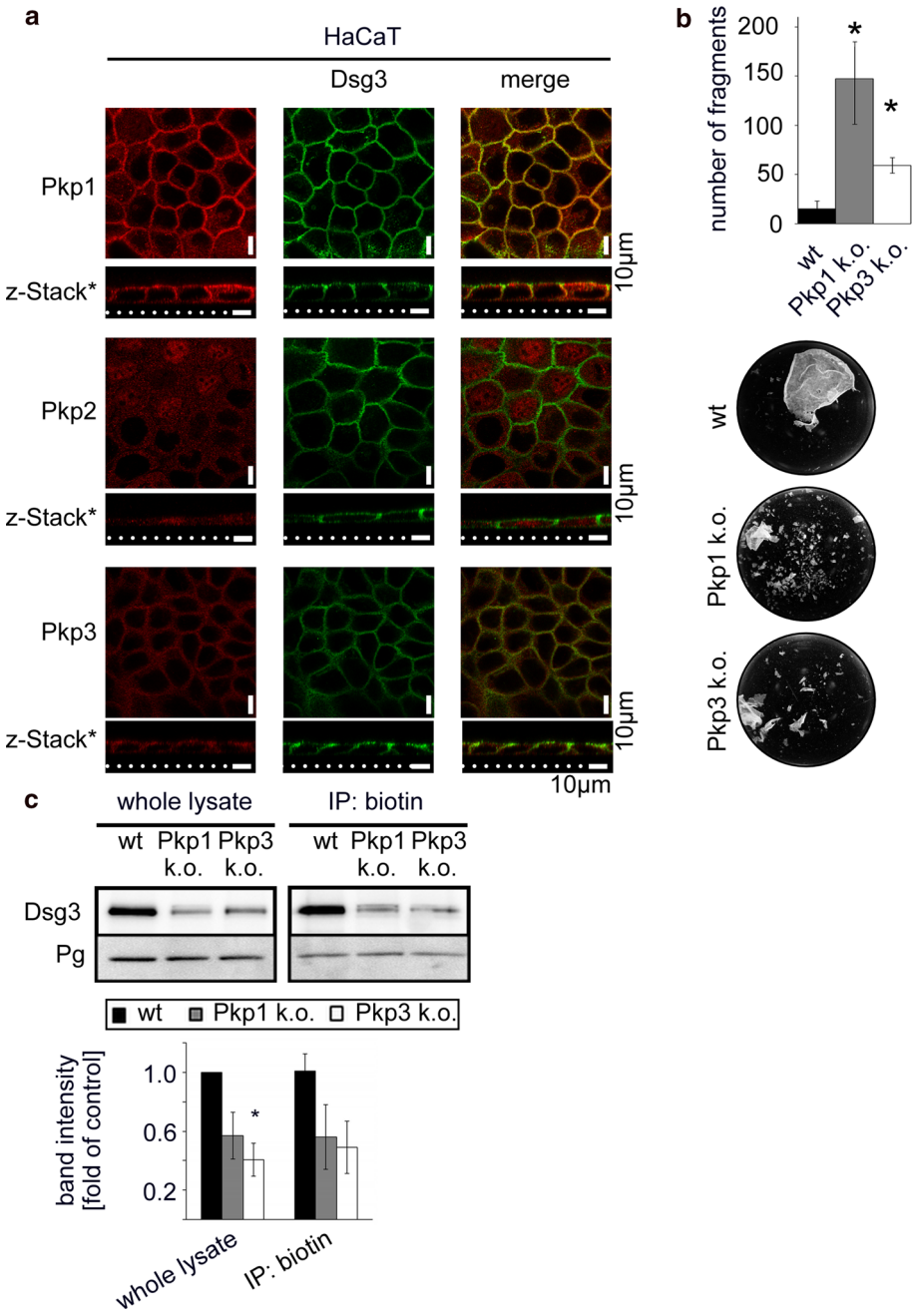


**Fig. 1** Intercellular adhesion is Pkp1- and 3-dependent. **a** HaCaT cells were stained with Dsg3 and Pkp1, 2 or 3-antibodies, respectively. Dsg3 colocalizes with Pkps both at the cell borders and on the cell surface. **b** Dissociation assay in murine keratinocytes show reduced intercellular adhesion in cells lacking Pkp1 or 3, indicated by increased fragmentation. $^*p < 0.05$ vs. wt control. Error bars show mean ± SEM ($n = 4$). **c** Biotinylation assay and quantification of MKZ cells reveal reduced Dsg3 expression and membrane levels in Pkp1- and Pkp3-deficient cells. $^*p < 0.05$ vs to wt. Error bars indicate mean ± SEM ($n = 4$)

keratinocytes (Figure S1b, c). Interestingly, Dsc1, 2 and 3 expression was not altered in Pkp1- and 3-deficient keratinocytes (Figure S1d, e) indicating that Pkps primarily regulate desmogleins. These data show that both Pkp1 and 3 control Dsg3 membrane availability, whereas Pkp1 is only required for cytoskeletal anchorage.

## Pkp loss reduces Dsg3 and Dsg1 interactions at cell borders

Although the impact of Pkps for intercellular adhesion has been described before [13, 14, 26], the underlying molecular mechanism is not yet known. Thus, we investigated the impact of Pkps for Dsg3-binding properties using atomic force microscopy (AFM). To do so, AFM tips were functionalized with recombinant Dsg3 extracellular domains (EC) and respective cell lines were mapped to detect specific Dsg3 single-molecule interactions. In previous studies, we have shown that Dsg3 undergoes homophilic and heterophilic interactions both under cell-free conditions as well as on the surface of living keratinocytes [34, 38, 40, 41]. Specificity of Dsg3 interactions on murine keratinocytes was confirmed in previous studies using inhibitory aDsg3 antibodies [34]. Scanning electron microscopy and

AFM topography showed elevated cell borders with similar morphology in all cell lines investigated (Figure S2a, b). Small areas from AFM topography images were selected to record adhesion maps (Figure S2b, green rectangles) at cell borders (10 $\mu m^2$) and on the cell surface (10 $\mu m^2$ or 4 $\mu m^2$) above the nucleus. In adhesion maps, each pixel represents an approach and retrace cycle of the AFM cantilever, gray values represent the topography at the respective position and every blue dot depicts a Dsg3-binding event (Fig. 2a). At cell borders, reduction of Dsg3-binding frequency $\nu$ ($\nu$ = #binding events/total#pixels) to 52% and 29% of wt levels was significant in both Pkp1- and Pkp3-deficient cells, respectively. In Pkp3-deficient cells, Dsg3-binding frequency was also reduced to about 28% on the cell surface (Fig. 2a, b). These data were in line with the results from the biotinylation assay (Fig. 1c) and suggest that Pkps are crucial for proper membrane availability of Dsg3-binding partners. Next, we evaluated more closely the distribution ratio between Dsg3-binding events on cell junctions (as indicated within the red dotted lines) and the junctional area in close proximity (Fig. 2a, c). No changes were observed in Pkp1- and Pkp3-deficient cells compared to wt cells indicating that junctional and peri-junctional Dsg3 availability was reduced to a similar extent as membrane availability in the peri-junctional compartment.

Furthermore, we investigated the strength of the single-molecule interactions, the so-called unbinding forces (UFs), of the remaining Dsg3-binding events (Fig. 2d and Figure S2c). For both areas, a significant reduction of UFs in cells lacking Pkp1 (42.8 pN at cell borders and 45.3 pN on the cell

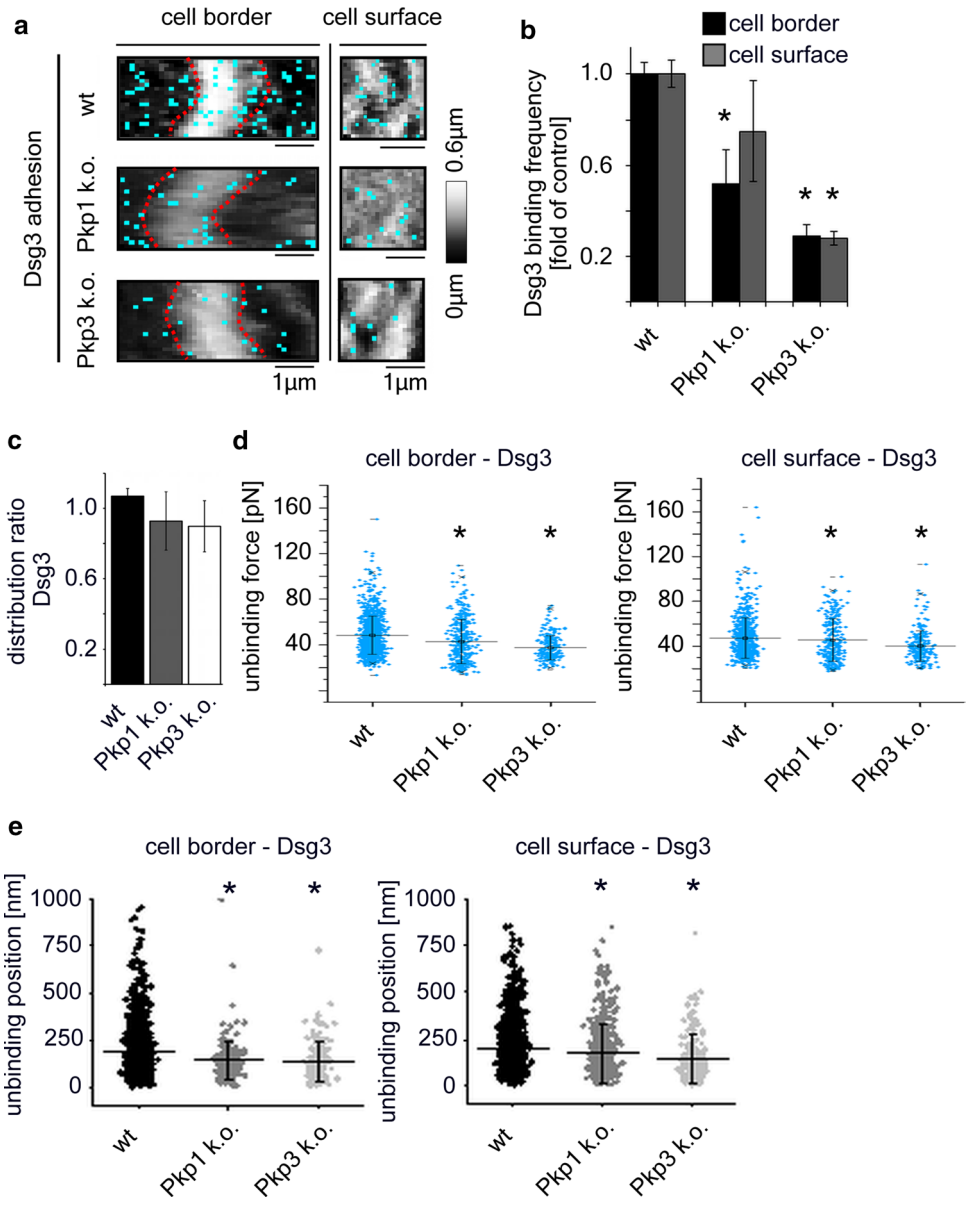


**Fig. 2** Pkp1- and 3-deficiency reduces Dsg3 single-molecule interactions at cell borders. **a** AFM adhesion maps, with each pixel displaying a force–distance curve, gray background colors show topography of cell borders and blue dots indicate Dsg3-binding events. Cell borders are marked by red dotted lines. **b** Dsg3-binding frequency is significantly reduced at cell borders and on cell surface of Pkp3-deficient cells as well as at cell borders in Pkp1-deficient keratinocytes. **c** Dsg3 distribution ratio between junctional and peri-junctional compartments shows no changes in Pkp-deficient keratinocytes. *$p < 0.05$ vs. wt. Error bars show mean ± SEM. $n \geq 6$ cell borders with 1000 force–distance curves each. **d** Analysis of unbinding forces (UF) of remaining Dsg3 molecules shows reduced values for cells lacking either Pkp1 or 3. **e** Unbinding positions (UP) of remaining Dsg3 molecules are reduced in Pkp1- and Pkp3-deficient cells. **d/e** *$p < 0.05$ vs. wt. Error bars indicate mean ± SD

surface) or Pkp3 (37.5 pN at cell borders and 40.1 pN on the cell surface) was detected compared to wt cells (48.5 pN at cell borders and 47.2 pN on the cell surface) (Suppl. Table 1, Fig. 2d). We further analyzed the unbinding position (UP) of the remaining Dsg3 interactions (Figure S2c). This measure describes the distance from the contact point at which the bond ruptures. Higher UPs could be a possible indication of the so-called tethers [46] and the UP was supposed to be an indirect measure for cytoskeletal anchorage [47, 48]. UP values were significantly reduced in cells deficient for Pkp1 by about 25.6% at cell borders and 13.6% on the cell surface and by 28.3% at the cell borders and 27.9% on the cell surface in Pkp3-deficient keratinocytes when compared to controls (Fig. 2e and Suppl. Table 1). Taken together, these data indicate that Pkp1 and 3 are required to maintain the number of Dsg3-binding events at cell junctions. In contrast, the subpopulation of remaining Dsg3 molecules is small and suggests that altered binding properties of this subpopulation are less important for intercellular adhesion compared to the drastic reduction in binding frequency along cell borders.

As Dsg1 represents the other main antigen for autoantibodies in pemphigus [49] and Dsg1 expression pattern in human skin is different from the expression pattern of Dsg3 [1, 50], we further investigated the binding properties of Dsg1. For these experiments, AFM tips were coated with Dsg1-EC recombinant proteins. Specificity of Dsg1 interactions on murine keratinocytes was shown in previous studies using an inhibitory aDsg1 antibody [51]. Similar to the data obtained for Dsg3, in both Pkp1- and 3-deficient cell lines, a significant reduction in Dsg1-binding frequency was observed mainly at cell borders (Fig. 3a, b). Moreover, the distribution ratio of Dsg1-binding events between the

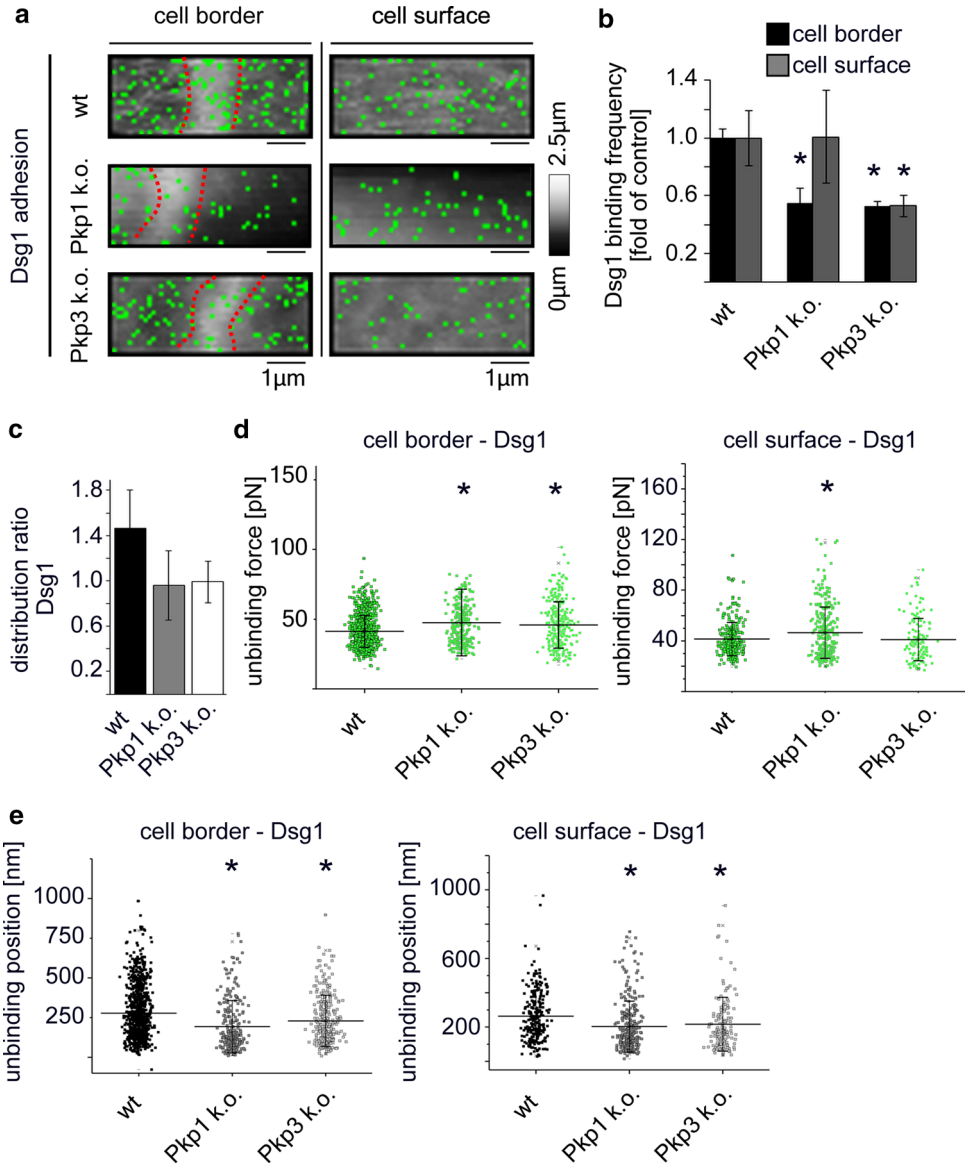


**Fig. 3** Pkp1- and 3-deficiency also reduces Dsg1 interactions at cell borders. **a** AFM adhesion maps for Dsg1 as described above. 2. **b** Dsg1-binding frequency is significantly reduced in Pkp-deficient cells at cell borders. **c** Distribution ratio for Dsg1 between junctional and peri-junctional compartment is not significantly altered in Pkp-deficient keratinocytes. $*p < 0.05$ vs. wt at respective localization, error bars indicate mean ± SEM. $n = 6$ cell borders with 1000 force–distance curves each. **d** Analysis of UF showed increased forces in binding strength for Pkp1 and 3 k.o. cells. $N = 6$ for independent measurements with 1000 force–distance curves each. $*p < 0.05$ vs. wt. **e** For Pkp1 and 3 k.o. cells the UP are shorter for both compared to wt. $*p < 0.05$ vs. wt

junctional and peri-junctional compartment was not significantly altered neither in Pkp1- and nor in Pkp3-deficient cells (Fig. 3c). In Pkp1- and Pkp3-deficient keratinocytes, the remaining Dsg1-binding events displayed slightly higher unbinding forces at cell borders and for Pkp1-deficient keratinocytes also on the surface when compared to wt cells (Fig. 3d and Suppl. Table 1), whereas UPs were reduced for Dsg1 in Pkp-deficient cell lines similar to Dsg3 as outlined above (Fig. 3e and Suppl. Table 1). These data indicate that both Pkp 1 and 3 are critical for the maintenance of Dsg1 and 3 availability at cell borders.

## Pkp deficiency does not alter p38MAPK signaling

So far, AFM experiments delineate that Dsg1 and 3 junctional availability is dependent on Pkps, therefore we next investigated the mechanisms underlying this phenomenon. As signaling pathways such as p38MAPK are central for the regulation of desmosomal adhesion and also modulate Dsg-binding properties [34, 51, 52], we further tested whether modulation of p38MAPK affects intercellular adhesion in the respective cell lines. Dispase-based dissociation assay using anisomycin for 1 h to activate p38MAPK showed compromised intercellular adhesion in wt- and Pkp-deficient keratinocytes. The effect was significant for wt- and Pkp3-deficient cells but not for Pkp1-deficient cells, most likely because in the latter adhesion was severely compromised under resting conditions as shown above (Fig. 4a, compare to Fig. 1b). Accordingly, Western blot analysis showed unaltered p38MAPK activity in all cell lines. This was not only true under resting conditions but also after anisomycin treatment (Fig. 4b). Hence, this signaling pathway seems not to be relevant for Pkp-dependent loss of cell cohesion.

## Pkp1 but not Pkp3 regulates Dsg3 clustering

Membrane-impermeable crosslinking was used to investigate Dsg3 oligomerization as an indirect indicator for Dsg3 clustering. Interestingly, Dsg3 oligomers were significantly reduced in Pkp1-deficient cells and also diminished in Pkp3-deficient cells (Fig. 4c, d). To investigate whether this is an effect specific for desmosomal cadherins, we checked for oligomers of the classical cadherin E-Cad. However, no significant difference between the cell lines was observed (Fig. 4c, d), underlining that Pkp-dependent oligomerization is specific for desmosomal cadherins. These results give a first hint that Pkp-dependent clustering may account for the observed differences in overall cell cohesion between Pkp1- and Pkp3-deficient cells as revealed by dispase-based assay.

To confirm the above results and correlate them with AFM experiments, we performed repetitive AFM scans of the same region to detect Dsg3 clusters at cell borders of the respective keratinocytes. To do so, the size of connected bond positions in these AFM measurements was determined (Fig. 4e, f, see Suppl. Materials and Methods). Interestingly, cluster size was reduced in both Pkp1- and Pkp3-deficient keratinocytes when compared to wt (Fig. 4e, f) which would be in line with impaired oligomerization and thus this provides a further approach to investigate Dsg clustering in living keratinocytes. Next, we tested whether there is a link between the amount of clustered proteins and their mobility. As molecule mobility seems to negatively correlate with strong intercellular adhesion [34], this could serve as a further explanation for impaired intercellular adhesion in Pkp-deficient keratinocytes. Therefore, we analyzed repetitive AFM experiments with respect to stable molecule clusters as described before [34]. AFM mobility measurements show higher mobility of the Dsg3 molecules as indicated by a significantly lower stability coefficient in Pkp1-deficient and a slight but not significantly reduced stability coefficient in Pkp3-deficient keratinocytes (Fig. 4g, h), indicating that Pkp1 is primarily required for Dsg3 clustering and immobilization. This reflects differential roles of Pkp1 and Pkp3 in promoting proper intercellular adhesion.

## Dsg3 clustering can be rescued by overexpression of Dsg3-GFP in Pkp3- but not in Pkp1-deficient keratinocytes

Pkp-deficient cells show reduced levels of Dsg3 (see Fig. 1c, Suppl. Figure 1b and c). Therefore, we asked whether impaired clustering and higher mobility may be due to reduced junctional availability of Dsg3 molecules or whether they are a direct result of Pkp deficiency. To address this, we overexpressed Dsg3 in all cell lines and performed AFM adhesion measurement according to Fig. 2 (Suppl. Figure 3a, b). Dsg3-binding frequency at cell borders was slightly higher after Dsg3 overexpression in wt cells but not in Pkp1- or Pkp3-deficient cells (Fig. 5a), suggesting that in the absence of Pkps, no additional Dsg3 molecules were incorporated in areas accessible for the AFM. In accordance, we observed no significant changes in the unbinding forces after Dsg3 overexpression in Pkp1- and Pkp3-deficient cell lines, i.e., unbinding forces of th remaining Dsg3 molecules remained slightly but significantly lower when compared to wt cells (Fig. 5b). Interestingly, the unbinding position dropped significantly in wt keratinocytes suggesting that overexpression of Dsg3 molecules enhanced its anchorage to the cytoskeleton [53]. This was accompanied by enhanced Dsg3 clustering indicating that in wt, molecule availability at the cell membrane correlates with molecule clustering (Fig. 5c). We further checked for the clustering size by performing repetitive Dsg3 AFM experiments at defined cell border areas. After Dsg3 overexpression the cluster size increased in wt- and Pkp3-deficient keratinocytes but not in Pkp1-deficient keratinocytes (Fig. 5d, e compared to

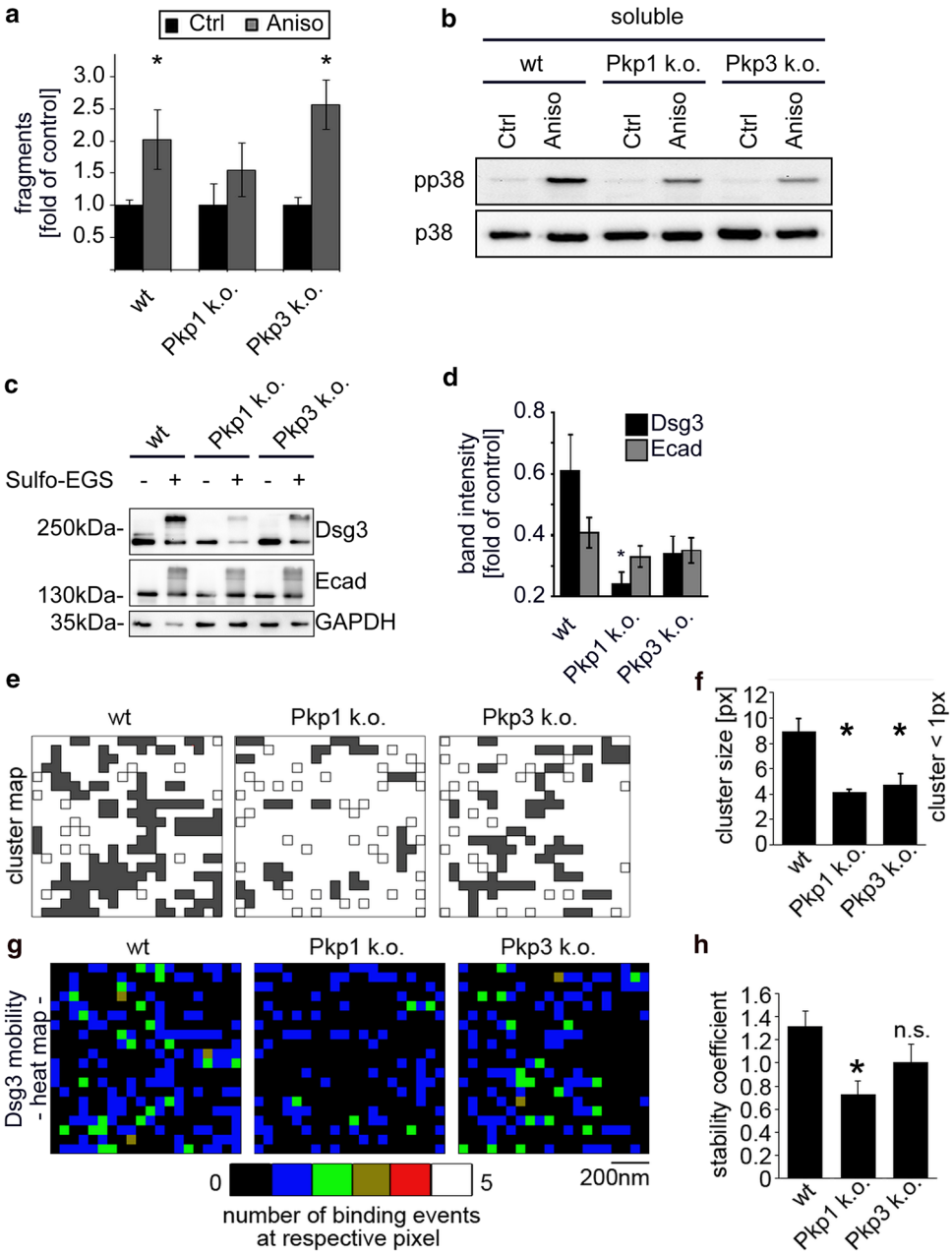


**Fig. 4** Dsg3 clustering is altered in Pkp-deficient keratinocytes. **a** p38MAPK activation using anisomycin (Aniso) reduced intercellular adhesion in all cell lines. $*p < 0.05$ vs. control (Ctrl). Error bars indicate mean ± SEM ($n \geq 4$). **b** Basal activity and anisomycin-induced activation of p38MAPK were similar in wt and Pkp-deficient cells. $n = 5$. **c** Membrane-impermeable crosslinking with sulfo-EGS significantly showed reduced numbers of Dsg3 oligomers in Pkp1-deficient cells whereas effect was minor in cells lacking Pkp3. **d** Densitometric quantification of Dsg3 and Ecad bands shows the ratio of crosslinked proteins to total protein. $N = 5$ and $*p < 0.05$ vs. wt. **e**, **f** Dsg3 clusters from AFM measurements show impaired cluster size in Pkp1- and Pkp3-deficient cells. **g** Mobility heat map shows color-coded maps of five successively scanned AFM adhesion maps (area = 1 µm$^2$, 20 × 20 pixels). **h** Quantification of g, by determining the stability coefficient which was reduced in Pkp1-deficient cells only (see Suppl. M&M). $N = 8$, $*p < 0.05$, error bars show ± SEM

Fig. 4e, f). Here, Pkp3-deficient cells reached cluster sizes similar to untransfected wt, whereas cluster sizes in Pkp1 k.o. cells remained comparable to its non-transfected control (Fig. 5d, e compared to Fig. 4e, f), indicating that Dsg3 overexpression restored Dsg3 clustering in Pkp3-, but not in Pkp1-deficient keratinocytes. Similarly, in FRAP experiments using Dsg3-GFP, Dsg3 mobility was increased in Pkp1-deficient cells but not in Pkp3-deficient keratinocytes (Suppl. Figure 3c, d). To further check the morphology of Dsg3 clusters, we performed STED microscopy imaging. To do so, cells were transfected with Dsg3-snap and labeled using SNAP®-Cell 647-SiR. Both wt- and Pkp3-deficient keratinocytes displayed dense clusters along cell borders and rounded clusters on the cell surface (Fig. 5f), which in size were comparable to Dsg3 clusters as measured by AFM. In contrast, molecule clusters were reduced in number and seemed irregular in shape in Pkp1-deficient cells, thus confirming disturbed Dsg3 clustering in Pkp1-deficient cells. Moreover, at cell borders, Dsg3 staining was stronger and broader in wt cells compared to both Pkp-deficient cell lines which is in line with the observation that Dsg3 overexpression did not rescue Dsg3-binding frequency at cell junctions in AFM (Fig. 5f, compared to Fig. 5a).

Taken together, these data demonstrate that restoration of Dsg3 levels is sufficient to rescue Dsg3 clustering in

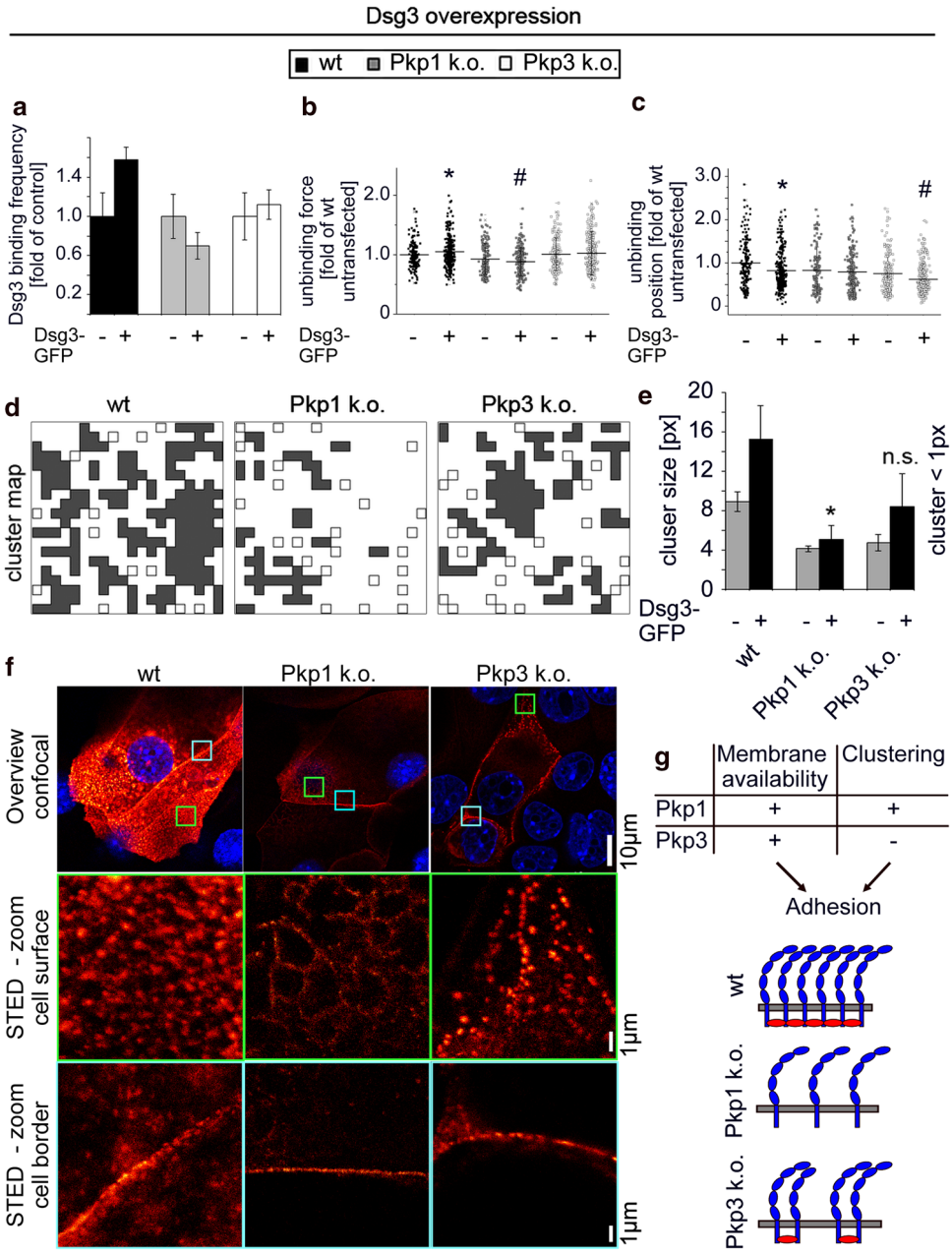


**Fig. 5** Dsg3 clustering can be rescued by Dsg3 overexpression in Pkp3- but not in Pkp1-deficient cells. **a** Dsg3-binding frequency was slightly increased in wt but not in Pkp1- and Pkp3-deficient keratinocytes when Dsg3-GFP was overexpressed. **b** Unbinding forces (UF) of remaining Dsg3 molecules were not significantly altered by Dsg3 overexpression in Pkp1- and Pkp3 k.o. cells. **c** Unbinding positions (UP) were significantly reduced in wt keratinocytes following Dsg3 overexpression. **a**–**c** $N=6$ cell borders with 1000 force–distance curves each, $*p<0.05$ vs. not Dsg3-overexpressed cells, $\#<0.05$ vs. wt Dsg3-overexpressed cells. **d**, **e** Dsg3 cluster sizes as evaluated by AFM after Dsg3 overexpression cells shows significantly reduced cluster size in Pkp1- but not in Pkp3-deficient cells. $N=6$, $*p<0.05$, error bars show ± SEM. **f** STED microscopy images to visualize Dsg3 clusters stained with SNAP®-Cell 647-SiR and DAPI. **g** A schematic summary of the mechanisms by which Pkp1 and Pkp3 control adhesion on the level of Dsg3 binding (Dsg3 in blue; Pkp1 in red)

Pkp3-deficient but not in Pkp1-deficient cells, indicating that Pkp1 in contrast to Pkp3 drives Dsg clustering.

## Discussion

In the present study, we demonstrate for the first time that Pkps regulate clustering of desmosomal cadherins in keratinocytes in an isoform-specific manner. Both Pkp1 and Pkp3 are required for junctional membrane availability of desmosomal cadherins Dsg1 and 3 (Fig. 5g). In contrast, Dsg3 clustering, as shown here by AFM and STED imaging, is a specific function of Pkp1 which correlates with the more pronounced adhesion defect in keratinocytes lacking Pkp1 compared to cells deficient for Pkp3 (Fig. 5g).

### Plakophilins regulate junctional membrane availability of desmogleins

It is known that Pkps participate in desmosome formation, where they act as scaffolds and are important for cellular signaling [9, 54]. Although Pkps share some functions, they display distinct roles in regulating intercellular adhesion. For instance, loss of Pkp1 has dramatic effects on the size and number of desmosomes [17] and mutations in Pkp1 lead to skin fragility syndrome in which the epidermal cohesion is

severely impaired [4, 15, 16]. In contrast, Pkp3 loss reveals a much milder phenotype [13, 18] but is associated with tumor formation and metastasis [55]. In accordance, although cells lacking either Pkp1 or Pkp3 display impaired cellular cohesion, Pkp1 is much more important for stable cohesion than Pkp3 [14].

Binding properties of adhesion molecules can be investigated on a single-molecule level using AFM [5, 56, 57]. Using this technique, we have previously shown that, Dsg1- and 3-binding properties are not uniformly distributed in keratinocytes and intracellular molecules such as keratins are involved in regulating the binding properties of desmogleins [34, 51]. The data presented show that frequencies of Dsg1- and Dsg3-binding events were drastically reduced to about 30% of wt levels in Pkp1- and Pkp3-deficient keratinocytes which was accompanied by less Dsg3 available at the cell membrane. As membrane availability of desmosomal cadherins was shown to correlate with firm intercellular adhesion [31, 58], these data indicate that Pkp1 and Pkp3 stabilize desmosomal adhesion by maintaining junctional membrane availability of desmogleins (Fig. 5g). This is in line with former studies providing evidence that desmosomal cadherin levels depend on Pkp1 [14, 15, 59]. Interestingly, binding properties of remaining binding events in Pkp1- and 3-deficient keratinocytes show weaker single-molecule interactions and a reduced unbinding position. Thus, it could be speculated that Pkps regulate especially the membrane availability of a desmoglein pool serving as desmosomal precursors, which is in line with the former studies showing that Pkp1 and 3 are crucial for desmosome assembly [11, 12, 14, 60, 61].

Reduced binding frequency and impaired intercellular adhesion were also observed in keratin-deficient keratinocytes for Dsg1 [51]. In contrast, Dsg3 was upregulated in keratin-deficient keratinocytes, which appears to be an insufficient rescue mechanism depending on PKC signaling [34]. Interestingly, this mechanism seems to be missing in Pkp1- and 3-deficient keratinocytes underlining their importance for PKC-dependent signaling [14, 62].

Since keratins also regulate p38MAPK activity, which is important for loss of cell adhesion in pemphigus, and regulates desmosome number and size [34, 35, 63], we studied whether altered p38MAPK signaling may account for impaired binding in keratinocytes deficient for Pkp1 and 3. Interestingly, activation of p38MAPK was not altered in Pkp-deficient keratinocytes and direct activation of p38MAPK was effective in further reducing cell cohesion. This indicates that loss of cell cohesion induced by loss of Pkp1 and Pkp3 is not p38MAPK dependent. Moreover, the data show that p38MAPK is not generally and unspecifically activated whenever desmosomal adhesion is impaired. This is in agreement with a previous study where loss of cell cohesion caused by siRNA-mediated depletion of plakoglobin but not of desmoplakin was paralleled by p38MAPK activation [64].

## Dsg clustering is regulated by Pkp1 and maybe crucial for proper desmosomal adhesion

It is well established that adhesion molecules are densely packed at cell contact areas. This is important for proper intercellular adhesion, because the force exerted on the cell is portioned to multiple binding sites [65]. Further, as lifetimes of desmogleins are short [5], it is conceivable that strong intercellular adhesion is dependent on proper cluster formation [65]. These clusters are well characterized for classical cadherins in adherens junctions but were also suggested to be present for desmosomal cadherin [66, 67]. As already described, Pkp1 plays a role in the clustering of Dsg3 with desmoplakin [26]. Here, we observed by AFM, STED and crosslinking that clustering of Dsg3 was strictly dependent on Pkp1. In contrast, in cells lacking Pkp3, these effects were less pronounced and significant only for a reduced cluster size.

This clustering function of desmosomal cadherins may be important for proper intercellular cohesion. This is indicated by a previous study which demonstrated homophilic interaction of desmogleins in living keratinocytes and oligomerization to correlate with strong intercellular adhesion [7]. Further, NMR, high-resolution fluorescence microscopy and electron microscopy studies provide models for the organization of the desmosomal plaque, revealing a localization of Pkps at the membrane-facing side of the outer dense desmosomal plaque neighboring desmogleins and thereby suggest interdependence of the order of intra- and extracellular parts of the desmosome [19, 28, 68, 69]. Thus, it is conceivable that Pkp isoforms contribute to cell adhesion by both maintaining junctional availability of desmogleins as well as by regulating clustering of desmogleins, the latter of which is a function specific for Pkp1 but not Pkp3 (Fig. 5g).

To exclude that changes in clustering are a result of impaired membrane availability in Pkp-deficient cell lines, we overexpressed Dsg3, which increased cluster sizes in AFM experiments and restored cluster formation and size in Pkp3-deficient keratinocytes, whereas no effect was observed in Pkp1-deficient cells. In line with this, FRAP experiments revealed that Dsg3 mobility in the membrane depends on Pkp1 but not on Pkp3, which is consistent with previous studies showing that molecule mobility is inversely proportional to intercellular adhesion [34]. These data demonstrate that Pkp1 is critical for Dsg3 clustering whereas Pkp3 is not, at least as long as junctional Dsg3 availability is sufficient (Fig. 5g). The data can explain the profound difference in overall cell cohesion for cell lines lacking Pkp1 and Pkp3 as detected by dissociation assays.

Taken together, the data provided show a new isoform-specific function of Pkp1 and Pkp3 in the regulation of desmosomal adhesion.

**Acknowledgements** We thank Andrea Wehmeyer and Sabine Mühlsimer for excellent technical assistance and JPK instruments and Sunil Yeruva for constructive technical and scientific discussion. The project is funded by Else-Kröner-Fresenius-Stiftung 2016_AW157 to FV and JW and DFG SPP1782 to JW.

**Author contributions** MFu, MF, MR, DK: methodology, data acquisition and analysis; FV and JW: funding acquisition, conceptualization and supervision; MFu, FV, JW: writing and editing, RK, MH, VS: methodology, review.

## Compliance with ethical standards

**Conflict of interest** The authors state that there was no conflict of interest.

## References

1. Delva E, Tucker KD, Kowalczyk AP (2009) The desmosome. Cold Spring Harb Perspect Biol 1:a002543
2. Spindler V, Waschke J (2014) Desmosomal cadherins and signaling: lessons from autoimmune disease. Cell Commun Adhes 21:8
3. Delmar M, McKenna WJ (2010) The cardiac desmosome and arrhythmogenic cardiomyopathies from gene to disease. Circ Res 107:15
4. McGrath JA, Mellerio JE (2010) Ectodermal dysplasia-skin fragility syndrome. Dermatol Clin 28(1):125–129
5. Vielmuth F, Spindler V, Waschke J (2018) Atomic force microscopy provides new mechanistic insights into the pathogenesis of pemphigus. Front Immunol 9:8
6. Harrison OJ et al (2016) Structural basis of adhesive binding by desmocollins and desmogleins. Proc Natl Acad Sci USA 113(26):6
7. Nie Z et al (2011) Membrane-impermeable Cross-linking provides evidence for homophilic, isoform-specific binding of desmosomal cadherins in epithelial cells. J Biol Chem 286(3):11
8. Hobbs R, Green K (2011) Desmoplakin regulates desmosome hyperadhesion. J Investig Dermatol 132:482
9. Waschke J (2008) The desmosome and pemphigus. Histochem Cell Biol 130:21–54
10. Waschke J, Spindler V (2014) Desmosomes and extradesmosomal adhesive signaling contacts in pemphigus. Med Res Rev 34:1127–1145
11. Bass-Zubeck AE et al (2009) Plakophilins: multifunctional scaffolds for adhesion and signaling. Curr Opin Cell Biol 21:708–716
12. Nekrasova O, Green KJ (2013) Desmosome assembly and dynamics. Trends Cell Biol 23(11):10
13. Hatzfeld M, Wolf A, Keil R (2014) Plakophilins in desmosomal adhesion and signaling. Cell Commun Adhes 21:708–716
14. Keil R, Rietscher K, Hatzfeld M (2016) Antagonistic regulation of intercellular cohesion by plakophilins 1 and 3. J Invest Dermatol 136(10):2022–2029. https://doi.org/10.1016/j.jid.2016.05.124
15. McGrath JA et al (1997) Mutations in the plakophilin 1 gene result in ectodermal dysplasia/skin fragility syndrome. Nat Genet 17(2):240–244
16. Boyce AE et al (2012) Ectodermal dysplasia-skin fragility syndrome due to a new homozygous internal deletion mutation in the PKP1 gene. Aust J Dermatol 53(1):61–65
17. Rietscher K et al (2016) Growth retardation, loss of desmosomal adhesion and impaired tight junction function identify a unique role of plakophilin 1 in vivo. J Invest Dermatol 136(7):1471–1478. https://doi.org/10.1016/j.jid.2016.03.021
18. Sklyarova T et al (2008) Plakophilin-3-deficient mice develop hair coat abnormalities and are prone to cutaneous inflammation. J Invest Dermatol 128(6):1375–1385
19. Al-Amoudi A et al (2011) The three-dimensional molecular structure of the desmosomal plaque. Proc Natl Acad Sci USA 108(16):6
20. Kowalczyk AP et al (1999) The head domain of plakophilin-1 binds to desmoplakin and enhances its recruitment to desmosomes: implications for cutaneous disease. J Biol Chem 274(26):5
21. Bonné S et al (2003) Defining desmosomal plakophilin-3 interactions. J Cell Biol 161(2):14
22. Hatzfeld M et al (2000) The function of plakophilin 1 in desmosome assembly and actin filament organization. J Cell Biol 149(1):209–222
23. Fischer-Kešo R et al (2014) Plakophilins 1 and 3 bind to FXR1 and thereby influence the mRNA stability of desmosomal proteins. Mol Cell Biol 34(23):13
24. Lee P et al (2017) Phosphorylation of Pkp1 by RIPK4 regulates epidermal differentiation and skin tumorigenesis. EMBO J 13:1963–1980
25. Neuber S et al (2010) The desmosomal plaque proteins of the plakophilin family. Dermatol Res Pract 2010:11
26. Tucker KD, Stahley S, Kowalczyk AP (2014) Plakophilin-1 protects keratinocytes from pemphigus vulgaris IgG by forming calcium-independent desmosomes. J Investig Dermatol 134:11
27. Garrod D, Tabernero L (2014) Hyper-adhesion: a unique property of desmosomes. Cell Commun Adhes. 21:8
28. Stahley SN et al (2016) Super-resolution microscopy reveals altered desmosomal protein organization in tissue from patients with pemphigus vulgaris. J Invest Dermatol 136(1):59–66
29. Winik BC et al (2009) Acantholytic ectodermal dysplasia: clinicopathological study of a new desmosomal disorder. Br J Dermatol 160(4):868–874
30. Diercks GF, Pas HH, Jonkman MF (2009) The ultrastructure of acantholysis in pemphigus vulgaris. Br J Dermatol 160(2):460–461
31. Oktarina DA et al (2011) IgG-induced clustering of desmogleins 1 and 3 in skin of patients with pemphigus fits with the desmoglein nonassembly depletion hypothesis. Br J Dermatol 165(3):552–562
32. van der Wier G et al (2014) Smaller desmosomes are seen in the skin of pemphigus patients with anti-desmoglein 1 antibodies but not in patients with anti-desmoglein 3 antibodies. J Invest Dermatol 134(8):2287–2290
33. Sokol E et al (2015) Large-scale electron microscopy maps of patient skin and mucosa provide insight into pathogenesis of blistering diseases. J Invest Dermatol 135(7):1763–1770
34. Vielmuth F et al (2018) Keratins regulate the adhesive properties of desmosomal cadherins through signaling. J Investig Dermatol 138:11
35. Spindler V et al (2018) Mechanisms causing loss of keratinocyte cohesion in pemphigus. J Invest Dermatol 138(1):6
36. Kasperkiewicz M et al (2017) Pemphigus. Nat Rev Dis Prim 3:17026
37. Boukamp P et al (1988) Normal keratinization in a spontaneously immortalized aneuploid human keratinocyte cell line. J Cell Biol 106(3):11
38. Heupel WM et al (2008) Pemphigus vulgaris IgG directly inhibit desmoglein 3-mediated transinteraction. J Immunol 181(3):10
39. Waschke J et al (2005) Pemphigus foliaceus IgG causes dissociation of desmoglein 1-containing junctions without blocking desmoglein 1 transinteraction. J Clin Invest 115(11):3157–3165

40. Vielmuth F et al (2015) Atomic force microscopy identifies regions of distinct desmoglein 3 adhesive properties on living keratinocytes. Nanomed Nanotechnol Biol Med 11(3):10
41. Vielmuth F, Waschke J, Spindler V (2015) Loss of desmoglein binding is not sufficient for keratinocyte dissociation in pemphigus. J Investig Dermatol 135(12):10
42. Ebner A et al (2007) A new, simple method for linking of antibodies to atomic force microscopy tips. Bioconj Chem 18(4):9
43. Hartlieb E et al (2013) Desmoglein 2 is less important than desmoglein 3 for keratinocyte cohesion. PLoS One 8(1):12
44. Spindler V et al (2013) Peptide-mediated desmoglein 3 crosslinking prevents pemphigus vulgaris autoantibody-induced skin blistering. J Clin Investig 123(2):12
45. Kowalczyk AP, Green KJ (2015) Structure, function and regulation of desmosomes. Prog Mol Biol Transl 116:23
46. Waugh R, Hochmuth R (1987) Mechanical equilibrium of thick, hollow, liquid membrane cylinders. Biophys J 52(3):10
47. Schmitz J, Benoit M, Gottschalk KE (2008) The viscoelasticity of membrane tethers and its importance for cell adhesion. Biophys J 95:12
48. Sariisik E et al (2015) Decoding cytoskeleton-anchored and non-anchored receptors from single-cell adhesion force data. Biophys J 109(7):4
49. Stanley JR, Amagai M (2006) Pemphigus, bullous impetigo, and the staphylococcal scalded-skin syndrome. N Engl J Med 355(17):10
50. Spindler V, Waschke J (2018) Pemphigus—a disease of desmosome dysfunction caused by multiple mechanisms. Front Immunol 9:136
51. Vielmuth F et al (2018) Keratins regulate p38MAPK-dependent desmoglein binding properties in pemphigus. Front Immunol. 9:528
52. Berkowitz P et al (2006) p38MAPK inhibition prevents disease in pemphigus vulgaris mice. Proc Natl Acad Sci USA 103:34
53. Sariisik E et al (2015) Decoding cytoskeleton-anchored and non-anchored receptors from single-cell adhesion force data. Biophys J 109(7):1330–1333
54. Hatzfeld M (2007) Plakophilins: Multifunctional proteins or just regulators of desmosomal adhesion? BBA Mol Cell Res 1773(1):9
55. Basu S et al (2018) Plakophilin3 loss leads to an increase in lipocalin2 expression, which is required for tumour formation. Exp Cell Res. 369:251–265
56. Muller DJ (2008) AFM: a nanotool in membrane biology. Biochemistry 47:13
57. Zlatanova J, Lindsya SM, Sanford HL (2000) Single molecule force spectroscopy in biology using the atomic force microscope. Prog Biophys Mol Biol 74:25
58. Cirillo N et al (2006) Serum from pemphigus vulgaris reduces desmoglein 3 half-life and perturbs its de novo assembly to desmosomal sites in cultured keratinocytes. FEBS Lett 580(13):3276–3281
59. South AP et al (2003) Lack of plakophilin 1 increases keratinocyte migration and reduces desmosome stability. J Cell Sci 116:12
60. Gurjar M et al (2017) Plakophilin3 increases desmosome assembly, size and stability by increasing expression of desmocollin2. Biochem Biophys Res Commun 495:768–774
61. Todorovic V et al (2014) Plakophilin 3 mediates Rap1-dependent desmosome assembly and adherens junction maturation. Mol Biol Cell 25(23):15
62. Tucker DK, Stahley SN, Kowalczyk AP (2014) Plakophilin-1 protects keratinocytes from pemphigus vulgaris IgG by forming calcium-independent desmosomes. J Invest Dermatol 134(4):1033–1043
63. Egu DT et al (2017) Inhibition of p38MAPK signalling prevents epidermal blistering and alterations of desmosome structure induced by pemphigus autoantibodies in human epidermis. Br J Dermatol. 177(6):1612–1618
64. Spindler V et al (2014) Plakoglobin but not desmoplakin regulates keratinocyte cohesion via modulation of p38MAPK signaling. J Invest Dermatol 134(6):10
65. Kusumi A, Suzuki K, Koyasako K (1999) Mobility and cytoskeletal interactions of cell adhesion receptors. Curr Opin Cell Biol 11(5):8
66. Truong Quang BA et al (2013) Principles of E-cadherin supramolecular organization in vivo. Curr Biol 23(22):11
67. Wu Y, Kanchanawong P, Zaidel-Bar R (2015) Actin-delimited adhesion-independent clustering of E-cadherin forms the nanoscale building blocks of adherens junctions. Dev Cell 32(2):6
68. Owen GR, Stokes DL (2010) Exploring the nature of desmosomal cadherin associations in 3D. Dermatol Res Pract 2010:930401
69. Stahley SN et al (2016) Molecular organization of the desmosome as revealed by direct stochastic optical reconstruction microscopy. J Cell Sci 129(15):2897–2904

**Supplementary Information**

**Supplementary Tables**

Table1: Unbinding forces (UF) and unbinding positions (UP) of the conducted AFM adhesion experiments.

| | Cell Border | | | Cell Surface | | |
|---|---|---|---|---|---|---|
| | wt | Pkp1 k.o. | Pkp3 k.o. | wt | Pkp1 k.o. | Pkp3 k.o. |
| UF Dsg3 [pN] | 48.5 ± 0.5 | 42.8 ± 1.0 | 37.59 ± 0.7 | 47.2 ± 0.7 | 45.3 ± 1.2 | 40.1 ± 0.9 |
| UF Dsg1 [pN] | 41.3 ± 0.4 | 47.50 ± 1.5 | 45.9 ± 1.0 | 41.5 ± 0.8 | 46.50 ± 1.2 | 41.1 ± 1.4 |
| UP Dsg3 [nm] | 190.1 ± 5.4 | 141.4 ± 8.2 | 136.2 ± 8.4 | 195.8 ± 4.8 | 169.2 ± 7.3 | 141.1 ± 10.1 |
| UP Dsg1 [nm] | 278.10 ± 5.8 | 193.4 ± 10.4 | 229.4 ± 9.5 | 263.3 ± 9.6 | 202.9 ± 8.6 | 216.5 ± 13.1 |

Mean ± SEM

**Supplementary Figure Legends**

**Supplementary Figure 1: Western blot and Triton protein extraction in Pkp1- and Pkp3-deficient keratinocytes.**

a: Representative Western blot analysis confirmed the complete knock out of Pkp1 or 3 in keratinocyte cell lines. As a loading control $\alpha$-Tubulin was used. b/c: in Pkp1- but not in Pkp3-deficient cells levels of Dsg3 in the Triton X-100 soluble as well as in the non-soluble fraction were decreased. Quantification of Dsg3 band intensity in Triton X-100 soluble and non-soluble fractions. N=4 and * $p < 0.05$ vs. wt, # $p < 0.05$ vs Pkp1 k.o. Error bars show $\pm$ SEM. d: Expression levels of Dsc1,2 or 3 were not altered in Pkp1- or 3-deficient keratinocytes in both Triton X-100 soluble and non-soluble fraction. e: Quantification of Dsc1, 2 and 3 band intensity in the Triton X-100 non-soluble fraction. N=5, error bars show ± SEM.

**Supplementary Figure 2: Exemplary AFM force curve and topography overview images**

a: Raster electron microscopy imaging of keratinocyte cell lines. Cells lacking Pkp1 or 3 show similar morphology with elevated cell borders. b: AFM topography imaging shows similar topography and elevated cell borders for all three cell lines. Green rectangles ($A=10\mu m^2$) show areas for adhesion maps. c: Representative retraction curve of a coated AFM tip with a binding event. The unbinding position (UP) represents the distance from tip contact point to protein-protein rupture whereas the unbinding force (UF) is defined as the delta of the distance between the positions of tip in contact with the cell surface to the position on which the bond ruptures.

**Supplementary Figure 3: AFM and FRAP measurements with Dsg3-overexpressing cells**

a: Cells transfected with Dsg3-GFP were first imaged using an epifluorescence lamp. Topographic imaging was carried out with AFM operating in QI-mode along the transfected cells. Fluorescence and topographic images were merged showing that transfected cell borders can be well localized in AFM topography images. b: AFM adhesion maps on Dsg3 overexpressing cells in which each pixel represents a force-distance curve. Dsg3 binding events are indicated by blue pixels. Grey background colors show the topography of cells. c: FRAP experiments with keratinocytes transfected with Dsg3-GFP. Kymographs visualize the Dsg3 recovery after photobleaching. d: Quantification of the immobile fraction reveals that Dsg3 is more mobile in the Pkp1- but not in Pkp3-deficient cells compared to wt cells. N=5 and * $p < 0.05$ vs. wt, error bars represent $\pm$ SEM.

**Supplementary Material and Methods**

**Cell culture, transfection and reagents**

Murine keratinocytes were grown on collagen I-coated culture dishes (rat tail; BD Bioscience, New Jersey, US) in complete FAD media (ThermoFisher Scientific, Germany) (0.05mM $CaCl_2$). After reaching confluency, cells were switched to high $Ca^{2+}$ concentrations (1.2mM) to induce differentiation. Cells were used for experiments 48h after switching throughout all experiments. For some experiments human keratinocyte cells (HaCaT) (Boukamp et al., 1988) were used. These cells were maintained in Dulbecco´s modified Eagle´s medium (DMEM) (Life Technologies; Carlsbad; CA; USA), supplemented with 10% fetal calf serum (Biochrom, Berlin, Germany), 50units/ml penicillin (AppliChem, Darmstadt, Germany), 50µg/ml streptomycin (AppliChem) and 1.8mM $Ca^{2+}$. For fluorescence recovery after photobleaching (FRAP) experiments, cells were grown to 70% confluency and subsequently

transient transfected with pEGFP-C1-Dsg3 (kindly provided by Dr. Yasushi Hanakawa, Ehime University School of Medicine, Japan) using Lipofectamine 3000 (Invitrogen, Carlsbad, USA) according to manufacturers´ protocol. Change to high $Ca^{2+}$ containing media (1.2mM) was carried out 24h after transfection and experiments were conducted 48h afterwards.

Human keratinocytes (HaCaT) cells were maintained in Dulbecco´s modified Eagle´s medium (DMEM) (Life Technologies; Carlsbad; CA; USA), supplemented with 10% fetal calf serum (Biochrom, Berlin, Germany), 50units/ml penicillin (AppliChem, Darmstadt, Germany), 50µg/ml streptomycin (AppliChem) and 1.8mM $Ca^{2+}$.

**Cloning**

By polymerase chain reaction, a mouse Dsg3 cDNA was amplified using gene specific primers. The resulted amplicon was introduced into a pSNAPf vector (New England Biolabs, Massachusetts, USA) with/utulizing unique restrictions sites (NheI and AscI). The constructed plasmid encoded a mouse Dsg3 protein coupled with N-terminal SNAP tag.

**Purification of recombinant Dsg-Fc constructs**

Purification of recombinant Dsg-Fc proteins was carried out as described before (Heupel et al., 2008).Briefly, Dsg1- and Dsg3-Fc constructs used here, which contain the entire extracellular domain of the corresponding Dsg isoform, were expressed stably in Chinese hamster ovarian cells (CHO cells). Those were cultured to confluency after transfection. Afterwards supernatant was collected and recombinant proteins were isolated utilizing protein-A-agarose affinity chromatography (Life Technologies). To verify purity and specificity, Coomassie staining and western blotting with anti Dsg1 monoclonal antibodies (mAb) (p124, Progen, Heidelberg, Germany) and anti Dsg3-mAb (clone5G11; Life Technologies) were performed.

**Calculation of distribution ratio, stability coefficient and cluster size**

Distribution ratio was calculated according the following formula: $distribution\,ratio = \frac{\nu_{cell\,border}}{\nu_{perijunctional\,area}}$. Where $\nu_{cell\,border}$ is the binding frequency at the cell border and $\nu_{cell\,surface}$ is the binding frequency at the surrounding cell surface.

For AFM mobility measurements, the same area (1 µm$^2$, 20x20 pixels) was scanned five times in a row. Adhesion maps were merged and according to n-times binding at one position, color-coded. The stability coefficient s was calculated according to the following formula:

$$s = \frac{5 \cdot n_5 + 4 \cdot n_4 + 3 \cdot n_3 + 2 \cdot n_2}{\bar{\nu}}$$

Where $n_i$ describes the number of pixels in i consecutive scans and $\bar{\nu}$ is the average binding frequency.

For calculation of cluster sizes repetitive AFM scans from mobility measurements were converted in black-white with every encolored pixel (containing ≥1 binding event) in black and every negative pixel in white. Pixels that were completely surrounded by positive pixels (containing ≥1 binding event) were classified as included in the respective cluster and therefore also colored black. Two or more contiguous pixels were ascertained to be clustered and numbers of pixels in each cluster were determined. Average of respective cluster size was analyzed.

**Electrophoresis and Western blot analysis**

Confluent cells were lysed in SDS – lysis buffer (containing 25mM HEPES, 2mMol EDTA, 25mM NaF and 1% sodiumdodecylsulfate, pH 7.4). Protein concentrations were adapted using a BCA protein assay kit (Pierce/Thermo Fisher Scientific, Waltham, USA) according to the manufacturer´s protocol. Western blotting was conducted as shown previously (Hartlieb et

al., 2013). As primary antibodies Pkp1 mAb (Progen, Heidelberg, Germany), Pkp 2 mAb (Progen), Pkp 3 mAb (Life Technologies, Carlsbad, California), Dsg3 pAb (Biozol, Eching, Germany), phospho-p38 mAb (Cell Signaling, Leiden, Netherlands), p38 MAPK mAb (Cell Signaling), Desmoplakin pAb (Santa Cruz, Dallas, TX, USA), GAPDH mAb (AviaSysBio, San Diego, CA, US), α-Tubulin mAb (Abcam, Cambridge, UK) were used. Utilized secondary antibodies were HRP-coupled goat anti rabbit Ab or goat anti mouse Ab (Dianova, Hamburg, Germany).

**Triton X-100 protein fractionation**

Experiments were performed according to a well-established protocol (Hartlieb et al., 2013). In short, cells were incubated with Triton X buffer (0.5% Triton X-100, 50mM MES, 25 mM EGTA, 5mM $MgCl_2$, protease inhibitors), collected and whole lysates were separated into a Triton – soluble (non-cytoskeletal, supernatant) and a Triton – insoluble (cytoskeletal, pellet) fraction via centrifugation at 10,000 rpm for 5min.

**Cell surface biotinylation**

Biotinylation assays were performed as described before (Vielmuth et al., 2015b). Briefly, cells were incubated on ice for 1h using 0.25mM membrane – impermeable EZ-Link Sulfo-NHS-Biotin (Thermo Scientific, Waltham, USA). Precipitation was done with NeutrAvidin-(HighCapacity)-agarose (Thermo Fisher Scientific).

**Immunostaining**

For immunofluorescence HaCaT and MKZ cells were fixed using 2% and 4% respectively paraformaldehyde and permeabilized with 1% Triton X-100.
The following antibodies were used as primary antibodies: Dsg3 pAb (Biozol, Eching,

Germany), Pkp1 mAb (Santa Cruz, Dallas, TX, USA), Pkp2 pAb (Santa Cruz, Dallas, TX, USA) and Pkp3 mAb (Progen, Heidelberg, Germany). As secondary antibodies Cy-labelled goat-anit-mouse and –rabbit secondary antibodies (Dianova, Hamburg, Germany) were used. Images were taken using a Leica SP5 confocal microscopy with a 63x NA 1.4 PL APO objective controlled by LAS AF software (Leica, Mannheim, Germany).

**Stimulated emission depletion microscopy (STED)**

Transfection of the cells was done as described before. The pSNAPf-mDsg3-N transfected cells were labeled with SNAP-tag-kit® according to manufacturer protocol (New England Biolabs, Massachusetts, USA). Labeling-Stock solution was prepared right before the experiment and incubation was carried out at a labeling concentration of 3µM for 15 min. After three washing steps with complete FAD media (ThermoFisher Scientific, Germany) (1.2mM $CaCl_2$) cells were immunostained (please refer to immunstaining-section). Recordings were made with the Expert line setup from Abberior (Abberior Instruments GmbH, Göttingen, Germany). Fluorescent dyes used was SNAP®-Cell 647-SiR (purchased from Abberior). The STED effect was attained with a 775 nm pulsed laser at a 10% laser power and a gating value of 800ps. Nuclei were stained using DAPI (Sigma-Aldrich) which was added for 10min while secondary antibody incubation at a concentration of 250ng/ml.

**Fluorescence Recovery after Photobleaching (FRAP)**

For all FRAP experiments MKZ cells were seeded in µ-Slide 8 well imaging Chambers (Ibidi, Martinsried, Germany) and Dsg3 was overexpressed by transient transfection. Experiments were carried out on a Leica SP5 confocal microscope with a 63x NA 1.4 PL APO objective at 37°C and 5% $CO_2$ with the FRAP wizard software (Leica) as described before (Rotzer et al., 2014). After defining a region of interest the Dsg3 signal between two adjacent cells was bleached using an Argon laser ($\lambda = 488nm$) at 100% transmission. Fluorescence recovery

was recorded over time for 3 minutes and intensity values were analyzed. Immobile Fraction values have been determined via the FRAP wizard.

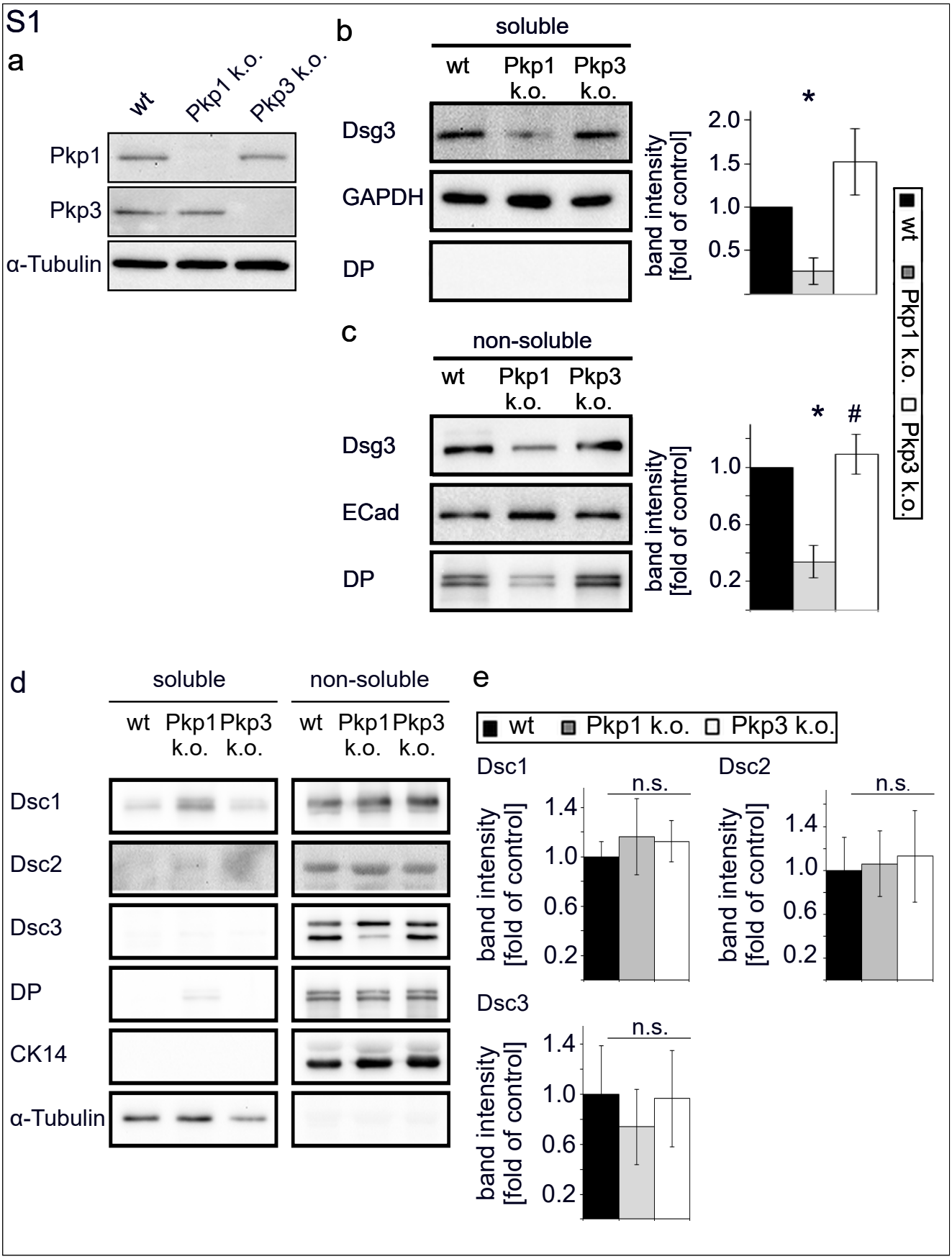
S1
a
wt
Pkp1 k.o.
Pkp3 k.o.
Pkp1
Pkp3
α-Tubulin
b
soluble
wt
Pkp1 k.o.
Pkp3 k.o.
Dsg3
GAPDH
DP
band intensity [fold of control]
2.0
1.5
1.0
0.5
*
wt
Pkp1 k.o.
Pkp3 k.o.
c
non-soluble
wt
Pkp1 k.o.
Pkp3 k.o.
Dsg3
ECad
DP
band intensity [fold of control]
1.0
0.6
0.2
*
#
d
soluble
non-soluble
wt
Pkp1 k.o.
Pkp3 k.o.
Dsc1
Dsc2
Dsc3
DP
CK14
α-Tubulin
e
wt
Pkp1 k.o.
Pkp3 k.o.
Dsc1
Dsc2
Dsc3
band intensity [fold of control]
1.4
1.0
0.6
0.2
n.s.

S2

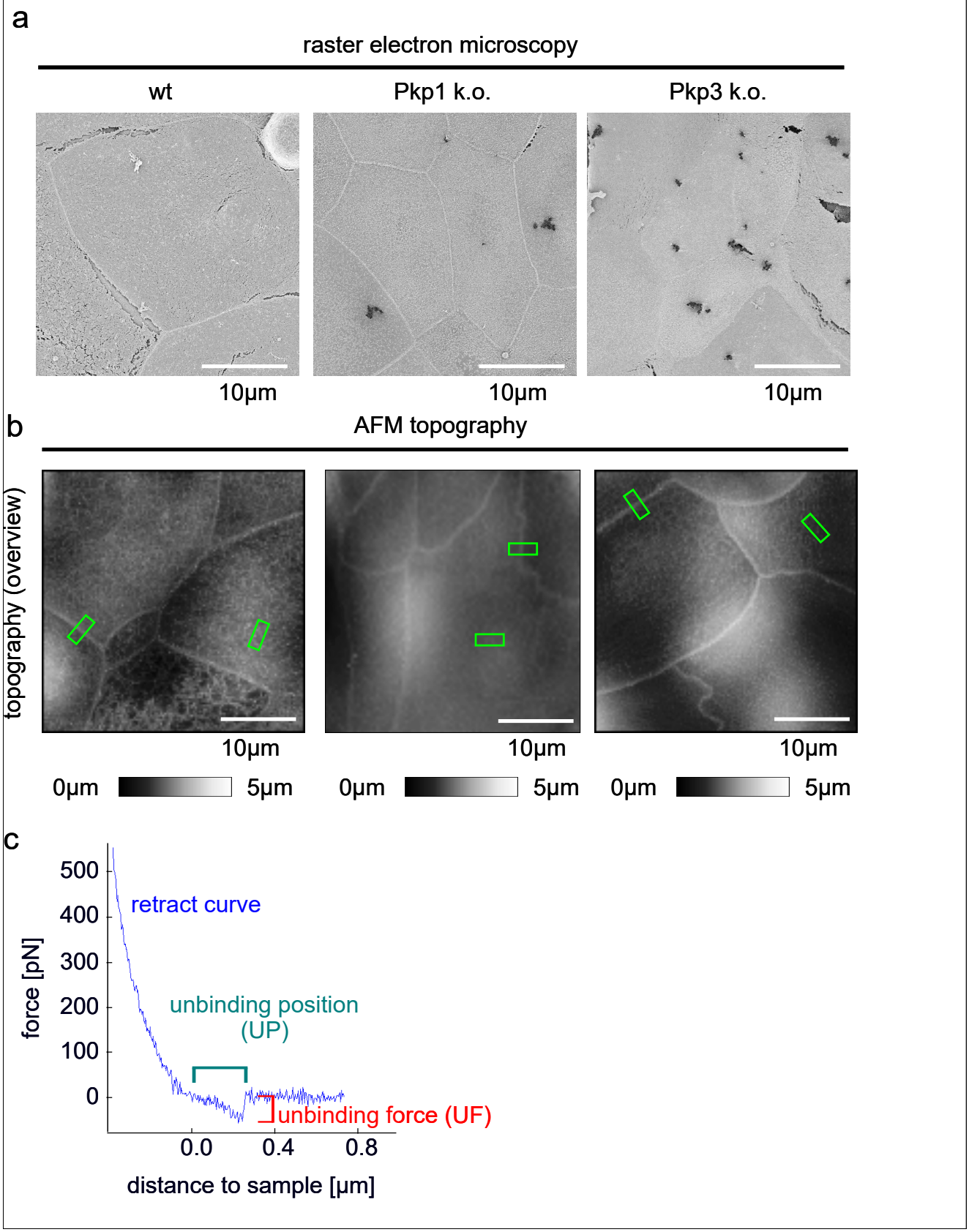
a
raster electron microscopy
wt
Pkp1 k.o.
Pkp3 k.o.
10µm
10µm
10µm
b
AFM topography
topography (overview)
10µm
10µm
10µm
0µm
5µm
0µm
5µm
0µm
5µm
c
force [pN]
500
400
300
200
100
0
retract curve
unbinding position
(UP)
unbinding force (UF)
0.0
0.4
0.8
distance to sample [µm]

S3

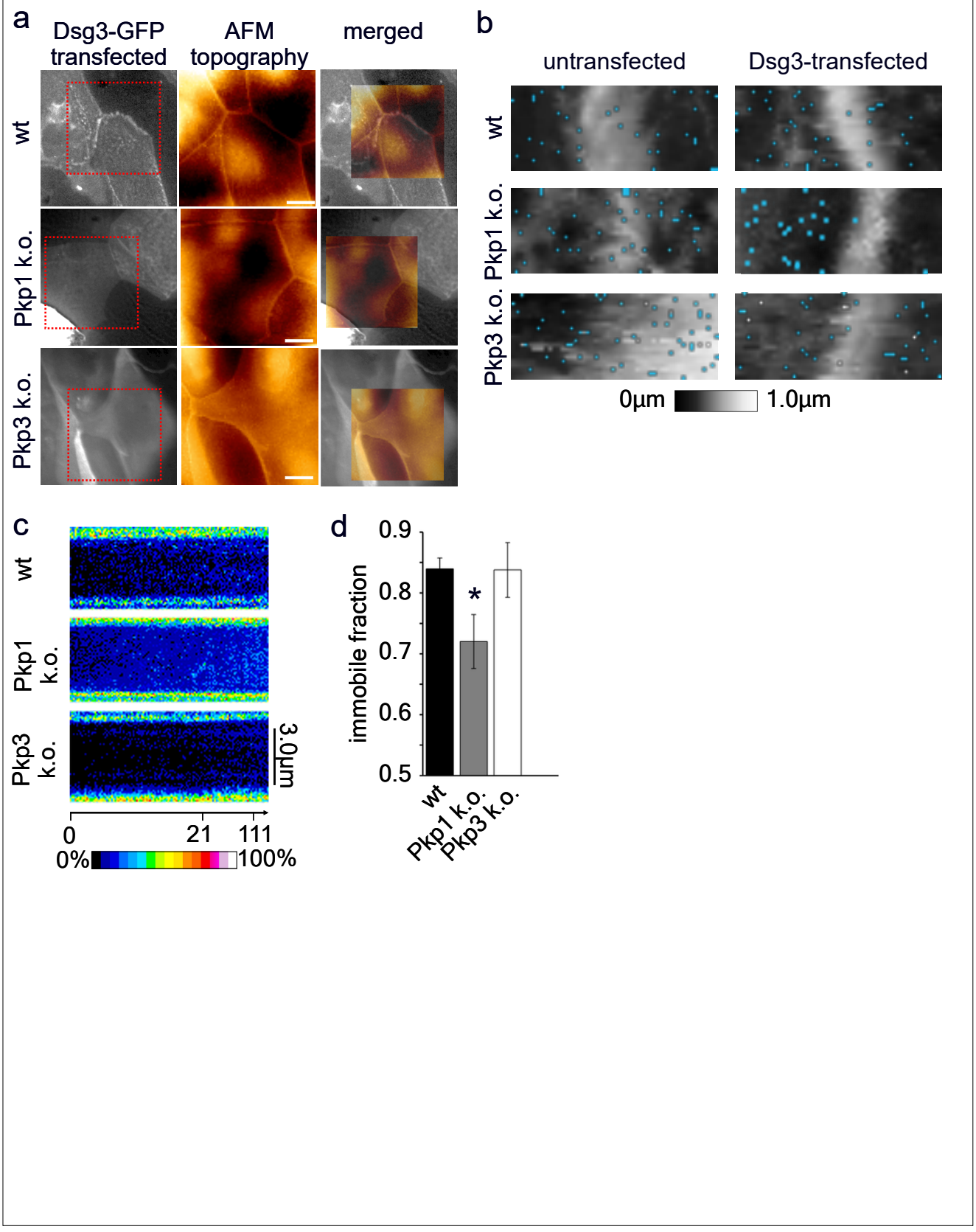
a
Dsg3-GFP transfected
AFM topography
merged
wt
Pkp1 k.o.
Pkp3 k.o.
b
untransfected
Dsg3-transfected
wt
Pkp1 k.o.
Pkp3 k.o.
0µm
1.0µm
c
wt
Pkp1 k.o.
Pkp3 k.o.
3.0µm
0
21
111
0%
100%
d
immobile fraction
0.9
0.8
0.7
0.6
0.5
*
wt
Pkp1 k.o.
Pkp3 k.o.

## 2.2 Desmosomal Hyperadhesion Is Accompanied with Enhanced Binding Strength of Desmoglein 3 Molecules

Biophysical Journal
Article

Biophysical Society

# Desmosomal Hyperadhesion Is Accompanied with Enhanced Binding Strength of Desmoglein 3 Molecules

Michael Fuchs,[1] Anna Magdalena Sigmund,[1] Jens Waschke,[1] and Franziska Vielmuth[1,*]
[1]Institute of Anatomy, Faculty of Medicine, Ludwig-Maximilians-Universität Munich, Munich, Germany

ABSTRACT Intercellular adhesion of keratinocytes depends critically on desmosomes that, during maturation, acquire a hyperadhesive and thus $Ca^{2+}$ independent state. Here, we investigated the roles of desmoglein (Dsg) 3 and plakophilins (Pkps) in hyperadhesion. Atomic force microscopy single molecule force mappings revealed increased Dsg3 molecules but not Dsg1 molecules binding strength in murine keratinocytes. However, keratinocytes lacking Dsg3 or Pkp1 or 3 revealed reduced $Ca^{2+}$ independency. In addition, Pkp1- or 3-deficient keratinocytes did not exhibit changes in Dsg3 binding on the molecular level. Further, wild-type keratinocytes showed increased levels of Dsg3 oligomers during acquisition of hyperadhesion, and Pkp1 deficiency abolished the formation of $Ca^{2+}$ independent Dsg3 oligomers. In concordance, immunostaining for Dsg1 but not for Dsg3 was reduced after 24 h of $Ca^{2+}$ chelation in an ex vivo human skin model, suggesting that desmosomal cadherins may have different roles during acquisition of hyperadhesion. Taken together, these data indicate that hyperadhesion may not be a state acquired by entire desmosomes but rather is paralleled by enhanced binding of specific Dsg isoforms such as Dsg3, a process for which plaque proteins including Pkp 1 and 3 are required as well.

SIGNIFICANCE Desmosomes provide adhesive strength to tissues constantly exposed to mechanical stress. They consist of different protein families, including desmosomal cadherins, which maintain strong interaction with their extracellular domains, and plaque proteins, among them plakophilins. Plakophilins are involved in desmosomal turnover and hyperadhesion, a state at which desmosomal cadherins become independent of extracellular $Ca^{2+}$. However, the molecular mechanisms underlying hyperadhesion are not yet fully elucidated. In this study, the authors show that hyperadhesion may not be a state acquired by entire desmosomes. The data indicate that it is rather paralleled by alterations of specific desmosomal cadherin binding properties, such as changes in clustering and single molecules binding strength. These changes also require the plaque proteins plakophilin 1 and 3.

## INTRODUCTION

Tissues such as the myocardium or the epidermis experience constantly mechanical pressure and shear stress (1–3). Desmosomes are crucial to withstand this mechanical stress by the maintenance of strong intercellular adhesion. The importance of desmosomes is reflected by diseases targeting desmosomal proteins such as pemphigus, in which cell cohesion is impaired by autoantibodies against the desmosomal cadherins desmoglein (Dsg) 1 and 3 (4,5), or ectodermal dysplasia skin fragility syndrome caused by mutations affecting the desmosomal plaque protein plakophilin (Pkp) 1 (6,7). On a molecular level, desmosomes consist of desmosomal cadherins that maintain intercellular adhesion via their extracellular domains in a $Ca^{2+}$ dependent, both homo- and heterophilic manner (8–10). Via the plaque proteins plakoglobin, Pkps, and desmoplakin, demosomes are linked to the intermediate filament cytoskeleton (2,11–13).

An outstanding characteristic of desmosomes is their ability to acquire two different adhesive states in adaptation to differentiation-dependent and environmental cues (14,15). In their weaker state, which is present during junctional assembly and wound healing, desmosomes are $Ca^{2+}$ dependent. In contrast, they acquire a strong and $Ca^{2+}$-independent state during maturation, which was

*Submitted April 24, 2020, and accepted for publication September 8, 2020.*
*Correspondence: franziska.vielmuth@med.uni-muenchen.de
Editor: Jason Swedlow.
https://doi.org/10.1016/j.bpj.2020.09.008

referred to as hyperadhesive (14,15). Importantly, cells are able to dynamically change from one state to the other and thus adapt quickly to changing environmental conditions, a fact that contributes to the importance of desmosomes in the maintenance of tissue integrity. Mechanistically, Garrod and Kimura suggested a model for desmosomal hyperadhesion, in which they propose that *cis* interactions of neighboring desmosomal cadherins capture $Ca^{2+}$ ions between their extracellular domains and thus drive $Ca^{2+}$ insensitivity (14,16). Further, regulation of hyperadhesion involves activity of protein kinase C-$\alpha$ and proper localization of Pkps (17), the latter of which also play a role in desmoglein clustering and desmosomal cadherin binding properties (18). Desmosomal hyperadhesion has so far been described as a characteristic that whole desmosomes acquire during their maturation, although the molecular mechanisms involved have not been elucidated. Challenging this hypothesis, desmosomal cadherins include four desmoglein (Dsg 1–4) and three desmocollin (Dsc 1–3) isoforms that show a tissue- and differentiation-specific expression (3,12). Interestingly, various isoform-specific functions of desmosomal cadherins have been reported, such as their respective involvement into signaling pathways and occurrence during morphogenesis (13,19–21). In accordance, we recently showed that Dsg1 and 3 binding properties and their regulation in keratinocytes are different (22,23). Thus, we here performed atomic force microscopy (AFM) on murine keratinocytes and chemical cross-linking experiments. We found different characteristics of Dsg1 and Dsg3 molecular binding properties during maturation, correlating with acquisition of hyperadhesion, which was paralleled with altered immunostaining characteristics of Dsg3 compared to Dsg1 in an ex vivo hyperadhesion model in human epidermis. These data indicate that $Ca^{2+}$ independency in keratinocytes is paralleled by the modulation of binding of specific desmoglein isoforms such as Dsg3 on the molecular level.

## MATERIALS AND METHODS

For detailed protocols regarding cell culture, immunostaining, and further experiments, please refer to Supporting Materials and Methods.

### Hyperadhesion keratinocyte dissociation assay

Dispase assays were performed as described before (17). Cell monolayers were detached from the well bottom by a mixture of Dispase II (Sigma-Aldrich) and 1% collagenase I (Thermo Fisher Scientific). When monolayers were floating, enzymes were removed and substituted by complete FAD media without phenol red (0.05 mM $CaCl_2$). EGTA at a concentration of 5 mM was added for 90 min at 37°C and 5% $CO_2$. Afterwards, cell monolayers were exposed to a defined shear stress by pipetting with a 1 mL electrical pipette. Using a binocular microscope (Leica Microsystems, Mannheim, Germany), pictures were taken from resulting fragments. Counting of these fragments was done in ImageJ (National Institutes of Health, Bethesda, MD) using the analyze tool Analyze Particles. The fragment number represents an inverse measure for intercellular adhesion.

### Purification of recombinant Dsg1- and 3-Fc construct

Recombinant human Dsg1- and 3-Fc proteins were purified as already described (24,25). In short, Dsg1- and Dsg3-Fc constructs contain the full extracellular domain of the corresponding Dsg isoform. Constructs were expressed in Chinese hamster ovarian cells. Isolation of recombinant proteins from the supernatants was performed using protein-A agarose affinity chromatography (Life Technologies, Carlsbad, CA).

### AFM

For all measurements in this study, a NanoWizard 3 AFM (Bruker Nano, Berlin, Germany) connected to an inverted optical microscope (Carl Zeiss, Jena, Germany) was used. Cells were visualized through a 63× objective, which further allowed the selection of a scanning area. Topographic images as well as adhesion measurements were performed according to existing protocols (10,26). For quantitative imaging, we applied the following parameters: setpoint, 0.5 nN; Z-length, 2000 nm; and pulling speed, 50 $\mu$m/s; and for force mapping mode, the subsequent values were applied: setpoint, 0.5 nN; Z-length, 2000 nm; extend time, 0.2 ms; and delay in extended position (resting contact time), 0.1 s. In case of multievent binding during a retract cycle, we used for statistical analysis only the final unbinding event that led to the return of the cantilever to its neutral and undeflected position (27). Bar diagrams of the unbinding forces show the mean value of all median values of the cell borders. Lifetime of the bonds were determined by increasing the pulling speed stepwise from 1 to 20 $\mu$m/s. For analysis, unbinding force and loading rate values were determined by using the origins extreme fit distribution. Data points were fitted to a modified Bells equation as already done (10,28,29). For all experiments, we used the D-Tip ($Si_3N_4$) of MLCT cantilevers (Bruker, Mannheim, Germany), which have a tip radius of 20 nm and a nominal spring constant of 0.03 N/m. Functionalization of the tips to detect specific single molecule interactions was done via coating of the tips with a flexible heterobifunctional acetal-polyethylene glycol linker (Gruber Lab, Institute of Biophysics, Linz, Austria; BroadPharm, San Diego, CA for lifetime and energy barrier measurements) as stated elsewhere (30,31). Measurements were performed on MKZ cells in full FAD medium containing 1.2 mM $Ca^{2+}$.

### Cross-linking, electrophoresis, and Western blot analysis

Membrane-impermeable cross-linking was performed as described elsewhere (9,18,32) and in Supporting Materials and Methods.

### Tissue culture and human ex vivo hyperadhesion model

Biopsies of healthy human skin samples were performed as previously described (33). A written agreement for the use of research samples was obtained from all body donors as a part of the body donor program from the Institute of Anatomy and Cell Biology of the Ludwig-Maximilians-Universität München (München, Germany).

### Data processing and statistics

For used software and applied statistics, please refer to the Supporting Materials and Methods.

## RESULTS

### Dsg3 single molecule binding is enhanced during acquisition of hyperadhesion

Keratinocytes in cell culture acquire a hyperadhesive state at a distinct time point of maturation (16). Thus, we investigated the time course during which murine keratinocytes become $Ca^{2+}$ independent and thus hyperadhesive. Hyperadhesion keratinocytes dissociation assays in wild-type (wt) keratinocytes showed a significant decrease in fragmentation from 24 to 72 h in high $Ca^{2+}$ medium, suggesting that wt cells become hyperadhesive after 72 h differentiation (Fig. 1, *A* and *B*). Next, we performed hyperadhesion keratinocyte dissociation assays at the same time points in Pkp-deficient keratinocytes as former studies showed that Pkps regulate Dsg3 binding properties (18), and Pkp1 is involved in desmosomal hyperadhesion (17). In contrast to wt keratinocytes, Pkp1- and 3-deficient keratinocytes failed to achieve $Ca^{2+}$ independency after 72 h in high $Ca^{2+}$ medium (Fig. 1, *A* and *B*), indicating that Pkps are required for desmosomal hyperadhesion. Underlining these data, immunostaining for Dsg3 and actin after EGTA incubation shows that Pkp1 and 3 both contribute to a proper localization of Dsg3 (Fig. S1, *A–C*).

We then applied AFM force measurements to investigate whether transition from the weak $Ca^{2+}$ dependent state (24 h in high $Ca^{2+}$ medium) to the strong hyperadhesive state (72 h in high $Ca^{2+}$ medium) is accompanied by changes in desmosomal cadherin binding properties. Thus, we analyzed the single molecule binding properties of Dsg1 and Dsg3 as two representatives of the desmosomal cadherin family crucial for desmosomal adhesion in the epidermis as revealed by pemphigus disease in which they are targeted by autoantibodies (34). AFM tips were functionalized with recombinant Dsg3-Fc or Dsg1-Fc comprising the whole extracellular domains of the respective protein, and cells were examined after 24 and 72 h in high $Ca^{2+}$ medium. Specificity of Dsg3 and Dsg1 interactions on murine keratinocytes was previously shown using inhibitory aDsg3 and aDsg1 antibodies (22,23).

AFM topography images showed no difference in cell morphology between different time points or several cell lines. All murine keratinocytes showed elevated cell borders (Fig. 1 *C*). We chose small areas along cell borders ($5 \times 2$ $\mu$m) from AFM topography images and recorded adhesion maps (shown by *blue rectangles*). Every pixel represents an approach/retrace cycle of the AFM cantilever ran in force mapping mode. Gray value of pixels represent the topography at this respective position, whereas blue pixels depict a specific binding event.

For Dsg3, binding frequency was similar between 24 and 72 h in wt cell lines. Interestingly, binding frequency was reduced during the same time period in Pkp-deficient keratinocytes (Fig. 1 *D*), underlining their contribution to membrane availability of Dsg3 (18). Next, we evaluated the distribution ratio between Dsg3 binding events located at cell junctions and at nonjunctional areas. Here, we only observed a significant alteration for Pkp3-deficient cells comparing 24 and 72 h, but the same trend was observed for wt cell line (Fig. 1 *E*). Furthermore, we investigated the strength of Dsg3 single molecule interactions, referred to as unbinding force (UF). Importantly, the UF of wt cells significantly increased by 20% after 72 h in high $Ca^{2+}$ medium compared to 24 h. In contrast, in Pkp1 and 3 knockout (k.o.) cells, UF was not significantly altered after differentiation (Fig. 1 *F*). Thus, Dsg3 molecules UFs in wt and Pkp-deficient keratinocytes clearly correlated with their ability to acquire a hyperadhesive state. This reflects a, to our knowledge, unreported phenomenon in which desmosomal hyperadhesion correlates with binding properties of a specific desmosomal cadherin. To characterize the measured bonds in more detail, we determined the bond lifetime for Dsg3 interactions. We therefore performed adhesion measurements at different pulling speeds ranging from 1 to 20 $\mu$m/s in wt murine keratinocytes. UF increased with increasing pulling speed at both time points, indicating that Dsg3 interactions in wt keratinocytes show a catch-bond behavior as reported earlier (10,23,35). Determination of bond lifetime for Dsg3 interactions was done by plotting the UF against the loading rate of the respective bond and fitting the values against a modified Bells equation (Fig. S2, *A* and *B*; (28,29)). Dsg3 bond lifetime for wt keratinocytes was increased from 1.38 to 3.52 s after 24 and 72 h, respectively (Fig. 1 *G*) and thus might be another correlate of desmosomal hyperadhesion. Interestingly, the unbinding position that was reported to be a measure for cytoskeletal anchorage (36) was not changed for wt cells comparing 24 and 72 h (Fig. S2 *C*), suggesting that cytoskeletal anchorage is not altered upon acquisition of hyperadhesion. Taken together, these results demonstrate increased UF and elongated bond lifetime of Dsg3 during acquisition of hyperadhesion in keratinocytes.

### Dsg1 binding properties do not change during acquisition of hyperadhesion

In addition, we investigated the single molecule binding properties of the other main pemphigus antigen Dsg1. Comparable to Dsg3 measurements, yellow rectangles in the topography images show the adhesion maps ($5$ $\mu$m $\times$ $2$ $\mu$m) and yellow dots mark specific binding events (Fig. 2 *A*). We observed a trend to decreased binding frequencies in all cell lines during differentiation, which was only significant in Pkp3-deficient keratinocytes (Fig. 2 *B*). The distribution ratio of Dsg1 binding events between 24 and 72 h was not changed in all cell lines (Fig. 2 *C*). Interestingly, Dsg1 single molecule UF was neither significantly altered

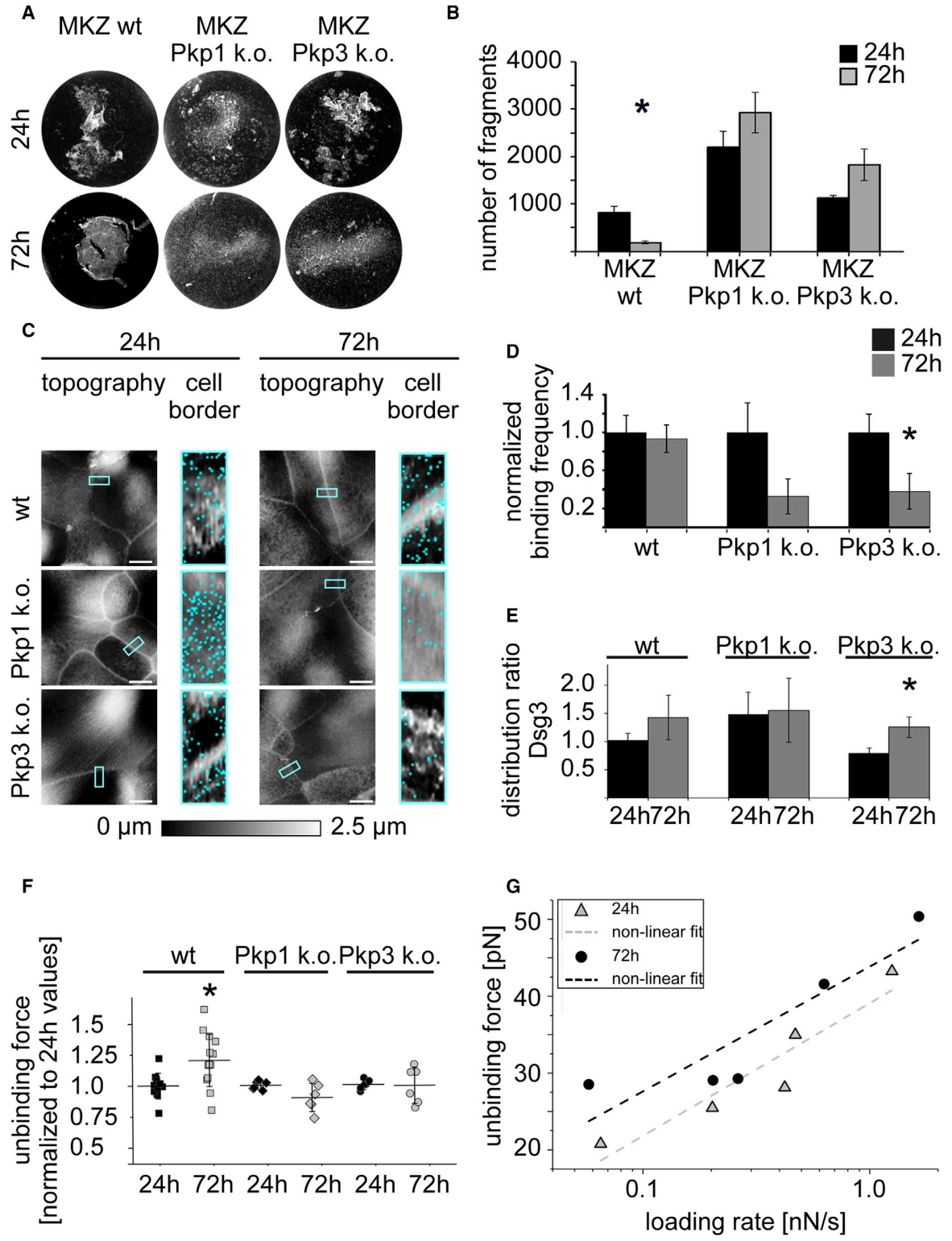


FIGURE 1 Dsg3 unbinding forces are increased in hyperadhesive wt keratinocytes. (*A*) Hyperadhesion dissociation assays in wt and Pkp1- and Pkp3-deficient murine keratinocytes are shown. Fragmentation after $Ca^{2+}$ chelation after 72 h compared to 24 h in high $Ca^{2+}$ medium was reduced for wt but not for Pkp-deficient keratinocytes, indicating that wt cells acquired a hyperadhesive state after 72 h differentiation. (*B*) Shown is quantification of dissociation assays ($n \geq 3$, $*p < 0.05$ vs. 24 h). (*C*) AFM topography images show similar cell morphologies in wt, Pkp1 k.o., and Pkp3 k.o. cells after 24 and 72 h in high $Ca^{2+}$ medium. Blue rectangles indicate areas of adhesion maps at cell borders, and blue dot represents one Dsg3 binding event. Scale bars, 10 $\mu$m. (*D*) Binding frequency is reduced in Pkp1- and significantly in Pkp3-deficient cells after 72 h of $Ca^{2+}$ presence but not in wt. The binding frequency was normalized to the corresponding

*(legend continued on next page)*

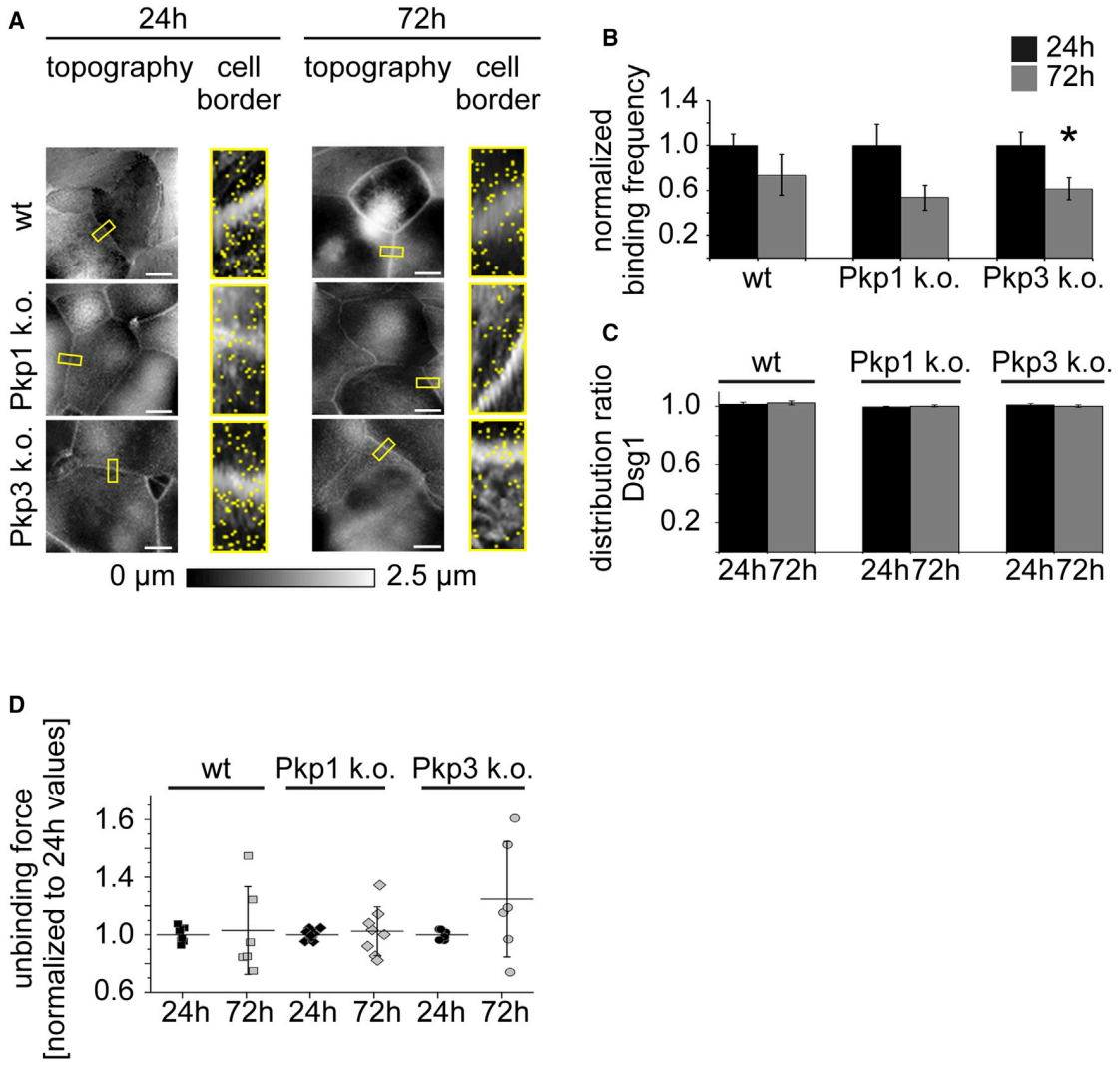


FIGURE 2 Binding properties of Dsg1 remain unchanged when keratinocytes become hyperadhesive. (*A*) All cell lines reveal similar cell morphology after 24 and 72 h in high $Ca^{2+}$ medium as shown by AFM topography images. Yellow rectangles indicate areas of adhesion maps at cell borders, and every yellow dot describes one Dsg1 binding event. Scale bars, 10 $\mu$m. (*B*) Binding frequency is significantly reduced in Pkp3-deficient cells after 72 h of $Ca^{2+}$ presence only. The binding frequency was normalized to the corresponding 24 h values. (*C*) Distribution ratio between junctional and perijunctional compartment is not altered between 24 and 72 h of maintenance in high $Ca^{2+}$ medium. (*D*) Dsg1 single molecule unbinding strength is not significantly changed in all cell lines after 72 h in high $Ca^{2+}$ medium. UF was calculated using the mean of single medians. (*B–D*) $n = 3$ with two cell borders/experiment and 1000 force curves per measured cell border; error bars represent standard error of the mean (*$p < 0.05$ vs 24 h).

after 72 h in high $Ca^{2+}$ medium in wt nor in Pkp-deficient keratinocytes when compared to 24 h (Fig. 2 *D*), indicating that Dsg1 shows another differentiation-dependent behavior during the acquisition of hyperadhesion then Dsg3. According to Dsg3 interactions, the unbinding position was not significantly altered between both time points in wt (Fig. S2 *B*). Taken together, these data show that contribution of single molecule binding properties to desmosomal hyperadhesion differs between Dsg1 and Dsg3 in this specific time interval.

## Desmosomal hyperadhesion correlates with increased Dsg3 clustering

Clustering of desmosomal molecules was suggested to be one mechanism underlying desmosomal hyperadhesion

24 h values. (*E*) Dsg3 distribution ratio between junctional and perijunctional compartments shows significant differences for Pkp3-deficient cells between both time points but not for wt and Pkp1 k.o. cells. (*F*) Dsg3 single molecule UF is increased in wt cells after 72 h of $Ca^{2+}$ compared to 24 h. In contrast, Pkp1 and Pkp3 k.o. cells lack an increase in Dsg3 UF. UF was calculated using the mean of single medians. (*D–F*) $n \geq 3$ with two cell borders/experiment and 1000 force curves per measured cell border; error bars represent standard error (*$p < 0.05$ vs 24 h). (*G*) Fitting of peaks of UF versus peaks of loading rates shows a linear increase with logarithm after 24 and 72 h in high $Ca^{2+}$ medium. $n = 8$ with two cell borders/experiment and 100 force curves per measured cell border.

(37). This is conclusive with regards to densely packed desmosomes in the epidermis (3,38,39). Desmosomal clustering can be studied indirectly by membrane-impermeable cross-linking, which demonstrates Dsg oligomerization (9,18). Thus, we checked for $Ca^{2+}$-insensitive Dsg oligomers after 24 and 72 h in high $Ca^{2+}$ medium by treatment with 5 mM EGTA for 90 min. In wt murine keratinocytes, the amount of $Ca^{2+}$ independent Dsg3 oligomers was significantly increased from 24 to 72 h (Fig. 3, *A* and *B*), suggesting that Dsg3 oligomers contribute to hyperadhesion. Interestingly, this increase occurs in parallel with an increased UF and an elongated bond lifetime of Dsg3 during the acquisition of hyperadhesion. These data indicate that Dsg3 contributes to desmosomal hyperadhesion not only via changing its single molecule binding properties but also by increased occurrence of $Ca^{2+}$ independent oligomers.

Recent results showed that Pkp1 is important for clustering of Dsg3 (18), Thus, we next investigated the effect of Pkp deficiency on $Ca^{2+}$ dependent Dsg3 oligomerization. In Pkp1-deficient keratinocytes, the amount of Dsg3 oligomers was drastically reduced compared to wt without EGTA treatment at both time points. Furthermore, as shown by oligomerization ratio, $Ca^{2+}$-insensitive Dsg3 oligomers do not significantly increase in Pkp1-deficient keratinocytes after 72 h (Fig. 3, *A* and *B*). These data indicate that Pkp1 deficiency diminishes the acquisition of hyperadhesion by changes in Dsg3 oligomerization and thus underline the importance of both Pkp1 presence and Dsg3 oligomerization for desmosomal hyperadhesion.

In contrast, $Ca^{2+}$ independent Dsg3 oligomers were reduced in Pkp3 k.o. cells after 24 h but increased from 24 to 72 h. Even though the increase was to a minor extent compared with wt cells, this result shows that Pkp3 is less relevant for desmosomal cadherin oligomerization (Fig. 3, *A* and *B*). Taken together, these findings suggest that Pkp1 but not Pkp3 contributes to desmosomal hyperadhesion via clustering of Dsg3.

We further checked for other desmosomal cadherins regarding their $Ca^{2+}$ independent oligomerization. The amount of Dsg1 oligomers was minor for all cell lines at both time points compared with Dsg3 (Fig. 3 *C*). However, there were at least some $Ca^{2+}$ independent Dsg1 oligomers in all cell lines at both time points (Fig. 3 *D*). In addition, the amount was not altered during differentiation, which is in concordance to unchanged Dsg1 single molecule binding properties shown above (Fig. 2, *C* and *D*). Interestingly, Pkp1-deficient cells almost completely lost their Dsg1 expression after 72 h, whereas Dsg1 expression was drastically increased in the wt cell line, indicating that Pkp1 is important for proper expression of Dsg1 during differentiation.

Hyperadhesion was referred to be a special feature of desmosomes and thus should not be present for classical cadherins in adherens junctions (16). Thus, we evaluated the occurrence of $Ca^{2+}$-insensitive oligomers of the classical cadherin E-cadherin (E-Cad). Accordingly, treatment with EGTA led to a complete disappearance of E-Cad oligomers in all cell lines, showing that E-Cad remains $Ca^{2+}$ dependent during maturation (Figs. 3 *E* and S3 *A*) and confirming that hyperadhesion is a specific feature of desmosomes. To further underline the $Ca^{2+}$ dependency of E-Cad, we did a comparison between EGTA-treated and control oligomer bands (Fig. S3 *A*).

These results demonstrate different Dsg1 and Dsg3 clustering during differentiation and thus underline the different contribution of desmosomal cadherin isoforms in the acquisition of hyperadhesion.

## Ex vivo models reveal distinct $Ca^{2+}$ dependency of Dsg1 and 3 immunostaining characteristics

Previous studies proposed that all desmosomes in mature epidermis are hyperadhesive and thus $Ca^{2+}$ independent regardless of their composition (15,16,40). With regards to the observed differences for Dsg1 and 3 during differentiation, we tested the $Ca^{2+}$ dependency of several desmosomal cadherin isoforms in a human ex vivo model. To do so, human skin samples from body donors were incubated with the $Ca^{2+}$ chelator EGTA for 1.5 or 24 h, respectively. Subsequently, skin sections were stained for Dsg1 or Dsg3. Viability of the tissue was confirmed in previous studies (33).

According to previous results, Dsg1 and 3 showed different expression gradients in human epidermis with Dsg1 being predominant in superficial epidermis, whereas Dsg3 is more abundant in the basal epidermal layers (Fig. 4, *A* and *B*). EGTA treatment for 1.5 h had no effect on Dsg1 and 3 expression along keratinocyte cell membranes in human epidermis (Fig. 4, *A*, *B*, and *E*). In contrast, EGTA incubation for 24 h led to a fragmentation, reduction, and confinement to small dots of Dsg1 staining throughout all epidermal layers (Fig. 4, *C* and *F*). On the contrary, Dsg3 staining was not altered after 24 h of EGTA treatment (Fig. 4, *D* and *F*). These results argue for a distinct behavior of desmosomal cadherins in human epidermis in which Dsg3 is largely $Ca^{2+}$ independent, whereas Dsg1 remains at least in part $Ca^{2+}$ dependent. Taken together, these data suggest a stronger $Ca^{2+}$ independency of Dsg3 immunostaining compared to Dsg1 in the human epidermis.

To test whether Dsc show different $Ca^{2+}$ dependent immunostaining as well, we stained the human epidermis for Dsc1 and Dsc3 after 1.5 and 24 h of EGTA incubation. Interestingly, Dsc1 showed no overall reduction in staining after 1.5 but a significant change after 24 h EGTA treatment. Further, staining along cell borders after 24 h of EGTA treatment was broadened and showed a partly cytosolic pattern. These data, similarly to Dsg1, indicate that Dsc1 is at least in part $Ca^{2+}$ dependent. In contrast, Dsc3 staining showed

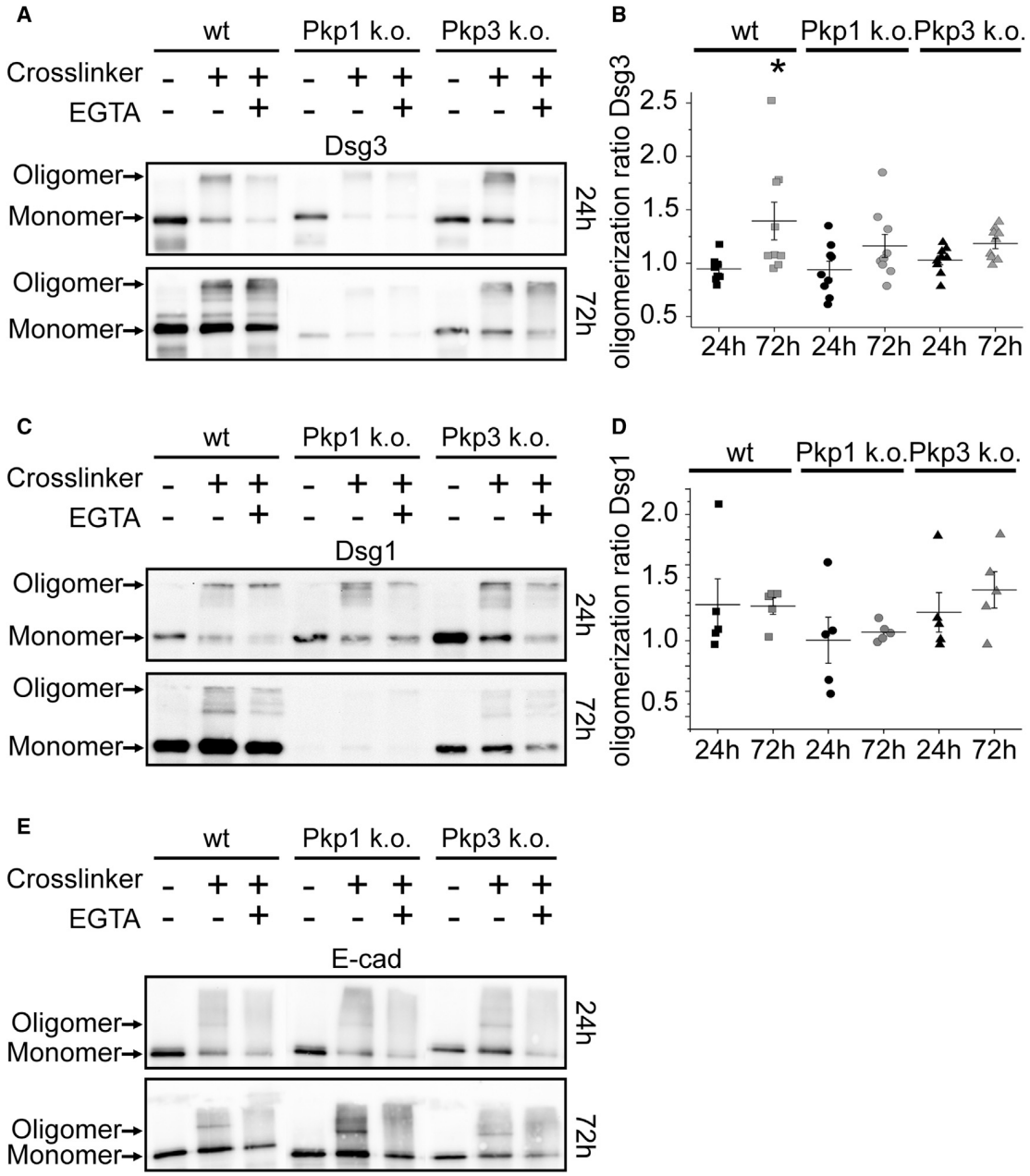


FIGURE 3 Pkp1-dependent Dsg3 oligomerization correlates with the development of a hyperadhesive state in murine keratinocytes. Cells were treated with EGTA (5 mM for 90 min at 37°C) after 24 or 72 h in high $Ca^{2+}$ medium followed by chemical cross-linking with ethylene glycol bis(sulfosuccinimidyl succinate). Cell lysates were prepared after standard protocol. (*A*) Wt and Pkp3-deficient keratinocytes show increased $Ca^{2+}$ independent Dsg3 oligomers after 72 h compared to 24 h in high $Ca^{2+}$ medium. In contrast, almost no $Ca^{2+}$ independent Dsg3 oligomers develop in Pkp1-deficient keratinocytes. (*B*) Ratio of oligomerization reveals a significantly increased number of $Ca^{2+}$ independent Dsg3 oligomers after 72 h compared to 24 h in wt keratinocytes. Error bars represent standard error of the mean ($n = 9$, $*p < 0.05$ vs. 24 h). (*C*) The extent of $Ca^{2+}$ independent Dsg1 oligomers was smaller in all cell lines after 24 h as well as after 72 h in high $Ca^{2+}$ medium, although total protein amount was drastically increased after 72 h in wt keratinocytes. (*D*) Ratio of oligomerization reveals no significantly increased number of $Ca^{2+}$ independent Dsg1 oligomers after 72 h compared to 24 h in all cell lines. Error bars represent standard error of the mean ($n = 5$). (*E*) Western blot shows that E-Cad oligomers are $Ca^{2+}$ dependent after both 24 and 72 h maintenance in high $Ca^{2+}$ medium. All Western blots are representative of $n = 5$.

no overall reduction after 1.5 or 24 h EGTA incubation. Thus, Dsc3 and Dsg3 reveal similarity in their $Ca^{2+}$ independency (Fig. S3, *B–G*). To exclude that these results are caused by shedding of desmosomal cadherins or changes in antibody epitope binding by EGTA treatment, we performed all experiments with a second set of primary antibodies (Table S1). These experiments confirmed the results shown above (Fig. S4, *A–D*).

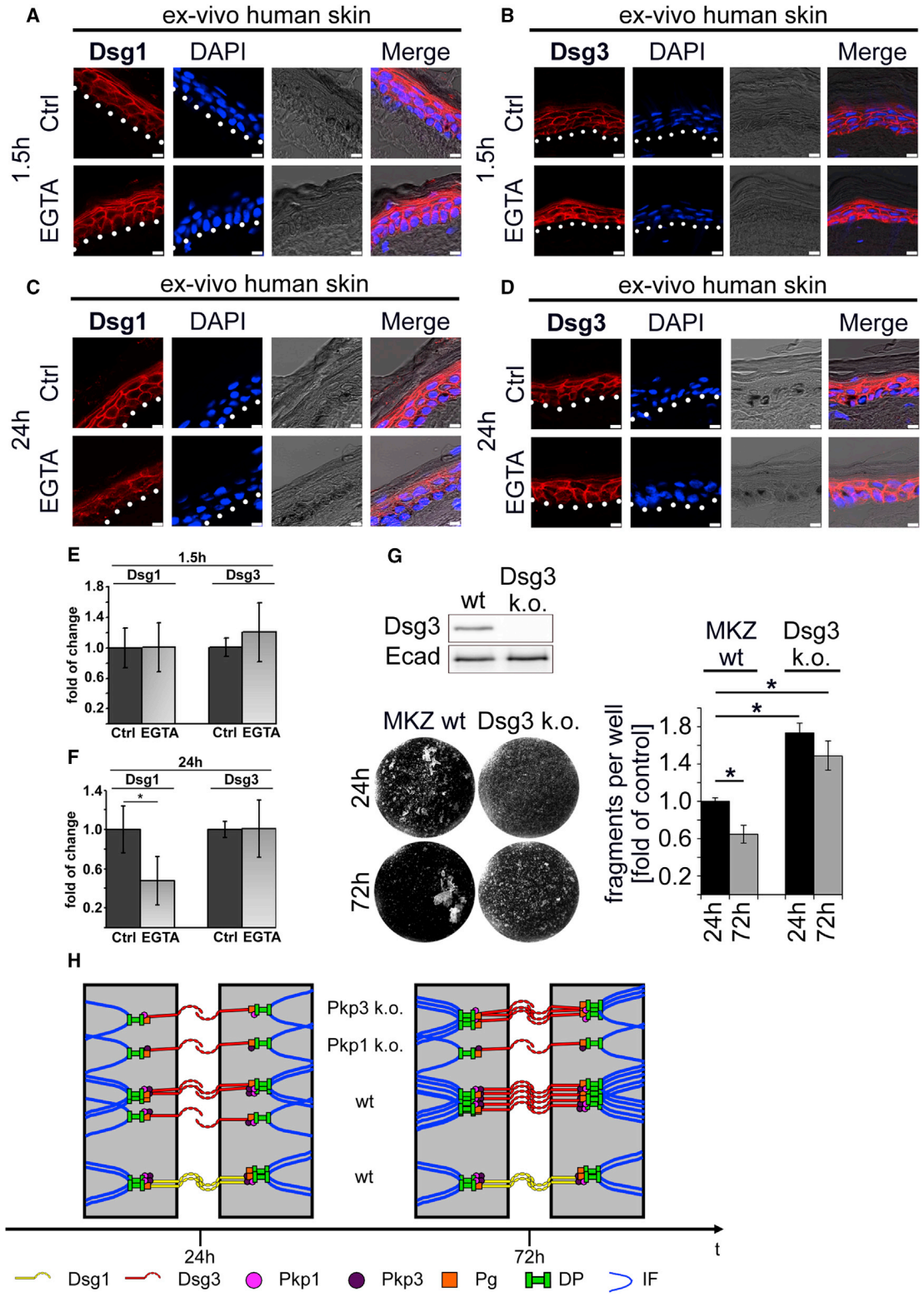


FIGURE 4 Dsg3 is hyperadhesive in human epidermis. (*A* and *B*) 1.5 h of EGTA incubation showed no alterations of Dsg1 and Dsg3 staining in human ex vivo skin samples. (*C*) Treatment of EGTA for 24 h led to a fragmentation of Dsg1 throughout all human epidermal layers. Dsg1 staining is drastically reduced and confined to small dots at cell membranes. (*D*) In contrast to Dsg1, Dsg3 staining in human epidermis is not altered after 24 h of EGTA treatment. (*A–D*) Scale bars, 7.5 $\mu$m. (*E* and *F*) Quantification of Dsg1 and Dsg3 staining after 1.5 and 24 h of EGTA incubation shows a significant decrease for Dsg1 staining after 24 h between control and EGTA treatment, whereas 1.5 h EGTA treatment led to no change. $n \geq 4$ different body donors; error bars represent

*(legend continued on next page)*

### Keratinocytes lacking Dsg3 fail to become hyperadhesive

To investigate the influence of a specific desmosomal cadherin isoform for desmosomal hyperadhesion, we conducted hyperadhesion keratinocyte dissociation assays in murine keratinocytes lacking Dsg3 (Fig. 4 *G*). According to our previous results, Dsg3-deficient keratinocytes in contrast to wt cells failed to acquire a hyperadhesive and thus $Ca^{2+}$ independent state during the given differentiation time period (Fig. 4 *G*). This shows the importance of Dsg3 for desmosomal hyperadhesion.

Taken together, the data show that different desmosomal cadherin isoforms contribute to desmosomal hyperadhesion by distinct mechanisms. Our experiments demonstrate for the first time, to our knowledge, that acquisition of desmosomal hyperadhesion correlates with alterations in clustering as well as single molecule binding properties of specific desmosomal cadherins such as Dsg3.

## DISCUSSION

### Dsg3 single molecule binding properties provide insights into molecular mechanisms contributing to the acquisition of hyperadhesion

Hyperadhesion is a cell-cell adhesion concept that refers to the strong adhesive state of desmosomes (14,15). In mature epidermis, most desmosomes were characterized as hyperadhesive, which seem to be crucial for strong cell cohesion and to withstand mechanical shear stress (14,37). In contrast, desmosomes were described to be in a weaker and $Ca^{2+}$ dependent state during assembly and wound healing (40). Thus, desmosomes switch between the two adhesive states. Apart from tissue (41), also, desmosomes in cell culture models can acquire the hyperadhesive state during maturation (42,43). In pemphigus vulgaris, a blistering skin disease in which autoantibodies against Dsg1 and 3 affect cell cohesion, experiments with hyperadhesive keratinocytes showed less disturbance of intercellular contacts and internalization of the adhesion molecules (44). Hence, hyperadhesion is a very important property of keratinocytes, for example to reduce susceptibility for diseases. In cell culture models, chelation of $Ca^{2+}$ ions provides an approach to investigate $Ca^{2+}$ independency of desmosomes. In our model, murine keratinocytes acquire a hyperadhesive state within 72 h in high $Ca^{2+}$ medium. Mechanistically, hyperadhesion was attributed to organized desmosomal cadherins, which capture $Ca^{2+}$ ions via *cis* binding between their extracellular domains (14,15). However, the contribution of certain desmosomal cadherins remains unclear.

Because hyperadhesion is thought to be a strong adhesive state, we performed AFM experiments investigating single molecule binding properties of desmosomal cadherins (10,45–47). Here, we measured single molecule interactions of Dsg1 and 3 under nonhyperadhesive and hyperadhesive conditions in murine keratinocytes. Binding properties for Dsg3 were drastically altered when cells reached a hyperadhesive state, whereas no changes were observed for Dsg1. Interestingly, different regulations of Dsg1 and 3 binding properties were determined before (23). The frequencies of Dsg1 and 3 interactions were slightly reduced for wt and Pkp1 k.o. cells between 24 and 72 h in high $Ca^{2+}$ medium and dropped significantly in Pkp3 k.o. cells. Those results confirm former results that Pkp3 is relevant for desmosome assembly during maturation (17,48,49). Therefore, Pkp3 may contribute to desmosomal hyperadhesion via this mechanism, whereas Pkp1 may primarily control clustering of Dsg3. Interestingly, we found that unbinding forces of Dsg3 interactions increased from 24 to 72 h in high $Ca^{2+}$ medium for wt but not for Pkp-deficient keratinocytes, whereas Dsg1 unbinding forces showed no significant alterations for all cell lines at both time points. Higher unbinding forces of Dsg3 interactions were shown to correlate with the strengthening of overall intercellular adhesion and thus fit to the acquirement of a hyperadhesive state (10,23). Changes in Dsg3 unbinding forces may also be due to participation of more Dsg3 molecules as we use Fc-tagged Dsg3 extracellular domains to functionalize AFM cantilevers. This would be in line with increased clustering of Dsg3 after 72 h in high $Ca^{2+}$ medium and thus an enhanced possibility of multiple bindings because of a higher Dsg3 molecule density. However, former data on cadherin-mediated adhesion indicate that multiple molecules participating in a certain unbinding event cause unbinding forces that are multiples of the single molecule unbinding strength (35,50). In contrast, UF only increased by 20% in our data, suggesting changes in the single molecule binding to be more likely.

Furthermore, acquisition of the hyperadhesive state seems to have an isoform-specific timeline. For Dsg3 but not for Dsg1, we found changes in its single molecules properties between 24 and 72 h. Nevertheless, data using Dsg2 k.o. cells argue for a contribution of all desmosomal cadherins to desmosomal hyperadhesion. Thus, it can be speculated that Dsg1 binding properties may change during another time period in the differentiation process. An explanation for this observation could be found in the epidermis

the SD (*$p < 0.05$ versus respective control). (*G*) Representative Western blot confirms complete k.o. of Dsg3 in murine keratinocyte cell lines. After 72 h in high $Ca^{2+}$ medium, cells lacking Dsg3 fail to become hyperadhesive as shown by the high degree of fragmentation compared to wt cells after 72 h in high $Ca^{2+}$ medium. $n = 3$ ($p < 0.05$ vs. wt 24 h). (*H*) Mechanistic model of the experimental findings is shown. Dsg1 clusters remain unaltered for wt cells under nonhyperadhesive and hyperadhesive conditions, whereas Dsg3 clusters are increased and UF is enhanced. In Pkp3-deficient cells, Dsg3 is still able to cluster, even though the UF remains unchanged. In contrast, Pkp1 deficiency abrogates proper clustering of Dsg3.

where Dsg1 is more prominent in the superficial layers. Therefore, Dsg1 properties may change late during differentiation. Further studies are necessary for a deeper understanding of this process.

Dsg3 interactions behave like catch bonds at both adhesive states, which fits former studies (10,51). However, Dsg3 bond lifetime was prolonged when cells become hyperadhesive. Bond lifetime at 24 h in high $Ca^{2+}$ medium was similar as shown before for desmosomal cadherins, whereas the lifetime increased during 72 h in high $Ca^{2+}$ medium and reaches levels known for classical cadherins (10,35,52). Interestingly, Dsg3 molecules unbinding forces are also increased during this time period, suggesting that altered forces and bond lifetimes may be interdependent (53). Moreover, the data indicate that changes in single molecules binding properties of Dsg3 contribute to desmosomal hyperadhesion.

### Desmosomal clustering correlates with hyperadhesion and is mediated by Pkp1

Previous studies showed the importance of Pkps for desmosomal hyperadhesion as well as for clustering of desmosomal cadherins (17,18,54). Further, desmosomes require organized desmosomal proteins to become hyperadhesive (14). As previously shown, clustering of Dsg3 is mediated by Pkp1 but not Pkp3. Here, we observed that $Ca^{2+}$ independent Dsg3 oligomers correlate with desmosomal hyperadhesion and require Pkp 1. In contrast, Dsg1 demonstrated a minor extent of $Ca^{2+}$ independent oligomers. However, this reduced amount of $Ca^{2+}$ independent oligomers remained unchanged after 24 and 72 h in wt murine keratinocytes. This finding supports the AFM data, in which no differences in single molecule binding properties of Dsg1 were observed during this time frame. Hence, we propose that oligomerization of desmosomal proteins is a correlate of desmosomal hyperadhesion, which occurs for desmosomal cadherins during different time intervals.

### Specific desmosomal cadherins show different $Ca^{2+}$ dependencies in human epidermis

Finally, we show that Dsg1 immunostaining is less resistant to $Ca^{2+}$ chelation compared to Dsg3 in human epidermis by the usage of ex vivo models and application of EGTA. The fact that Dsg3 distribution patterns as revealed by immunostaining are resistant to $Ca^{2+}$ chelation whereas Dsg1 staining properties are not indicates a further isoform specificity of desmosomal cadherins in the desmosome. This is in line with former studies providing evidence for different functions of desmosomal cadherin isoforms (19–21,32). Further desmosomal cadherins are differentially expressed throughout the epidermis (3,39,55). Thus, it is conclusive that they engage different functions during tissue maturation and hyperadhesion.

## CONCLUSION

In this study, we investigated the acquisition of hyperadhesion in murine keratinocytes and the $Ca^{2+}$ dependency of desmosomal cadherins in human epidermis by AFM, biochemical cross-linking, and immunostaining experiments. Our data show a, to our knowledge, unreported phenomenon that during acquisition of desmosomal hyperadhesion, desmosomal cadherins undergo an isoform-specific process and thus contribute to desmosomal hyperadhesion via several mechanisms, including desmosomal clustering and increased molecules binding strength. Further, the acquisition of this state depends on Pkps. We demonstrate that desmosomal cadherin clustering, which requires Pkp1, correlates with hyperadhesion. On a single molecule level, we detected an increase in the Dsg3 molecules unbinding force and interaction lifetime as a correlate for desmosomal hyperadhesion. Taken together, the data suggest that desmosomal hyperadhesion is paralleled by alterations of specific desmosomal cadherin binding properties such as changes in clustering and molecules binding strength (Fig. 4 *H*).

## SUPPORTING MATERIAL

Supporting Material can be found online at https://doi.org/10.1016/j.bpj.2020.09.008.

## AUTHOR CONTRIBUTIONS

M.F. conducted experiments, acquired data, and analyzed data. M.F. and A.S. determined methodology. F.V. and J.W. designed research studies. M.F., F.V., and J.W. wrote the manuscript.

## ACKNOWLEDGMENTS

We thank Andrea Wehmeyer, Nadine Albrecht, Sabine Mühlsimer, and Martina Hitzenbichler for excellent technical assistance and JPK Instruments for constructive discussion. We thank Mechthild Hatzfeld and Rene Keil for providing the MKZ cell lines.

The project is funded by Else Kröner-Fresenius-Stiftung 2016_AW157 to F.V. and J.W., Deutsche Forschungsgemeinschaft VI 921/2-1 to F.V., and Deutsche Forschungsgemeinschaft WA2474/10-2 to J.W.

## REFERENCES

1. Price, A. J., A.-L. Cost, …, C. Grashoff. 2018. Mechanical loading of desmosomes depends on the magnitude and orientation of external stress. *Nat. Commun.* 9:5284.
2. Hatzfeld, M., R. Keil, and T. M. Magin. 2017. Desmosomes and intermediate filaments: their consequences for tissue mechanics. *Cold Spring Harb. Perspect. Biol.* 9:a029157.
3. Delva, E., D. K. Tucker, and A. P. Kowalczyk. 2009. The desmosome. *Cold Spring Harb. Perspect. Biol.* 1:a002543.
4. Spindler, V., and J. Waschke. 2018. Pemphigus—a disease of desmosome dysfunction caused by multiple mechanisms. *Front. Immunol.* 9:136.

5. Pollmann, R., T. Schmidt, …, M. Hertl. 2018. Pemphigus: a comprehensive review on pathogenesis, clinical presentation and novel therapeutic approaches. *Clin. Rev. Allergy Immunol.* 54:1–25.
6. McGrath, J. A., J. R. McMillan, …, R. A. Eady. 1997. Mutations in the plakophilin 1 gene result in ectodermal dysplasia/skin fragility syndrome. *Nat. Genet.* 17:240–244.
7. Winik, B. C., R. A. Asial, …, M. C. Boente. 2009. Acantholytic ectodermal dysplasia: clinicopathological study of a new desmosomal disorder. *Br. J. Dermatol.* 160:868–874.
8. Harrison, O. J., J. Brasch, …, L. Shapiro. 2016. Structural basis of adhesive binding by desmocollins and desmogleins. *Proc. Natl. Acad. Sci. USA.* 113:7160–7165.
9. Nie, Z., A. Merritt, …, D. Garrod. 2011. Membrane-impermeable cross-linking provides evidence for homophilic, isoform-specific binding of desmosomal cadherins in epithelial cells. *J. Biol. Chem.* 286:2143–2154.
10. Vielmuth, F., V. Spindler, and J. Waschke. 2018. Atomic force microscopy provides new mechanistic insights into the pathogenesis of pemphigus. *Front. Immunol.* 9:485.
11. Hobbs, R. P., and K. J. Green. 2012. Desmoplakin regulates desmosome hyperadhesion. *J. Invest. Dermatol.* 132:482–485.
12. Waschke, J. 2008. The desmosome and pemphigus. *Histochem. Cell Biol.* 130:21–54.
13. Waschke, J., and V. Spindler. 2014. Desmosomes and extradesmosomal adhesive signaling contacts in pemphigus. *Med. Res. Rev.* 34:1127–1145.
14. Garrod, D., and T. E. Kimura. 2008. Hyper-adhesion: a new concept in cell-cell adhesion. *Biochem. Soc. Trans.* 36:195–201.
15. Garrod, D. R., M. Y. Berika, …, L. Tabernero. 2005. Hyper-adhesion in desmosomes: its regulation in wound healing and possible relationship to cadherin crystal structure. *J. Cell Sci.* 118:5743–5754.
16. Garrod, D., and L. Tabernero. 2014. Hyper-adhesion: a unique property of desmosomes. *Cell Commun. Adhes.* 21:249–256.
17. Keil, R., K. Rietscher, and M. Hatzfeld. 2016. Antagonistic regulation of intercellular cohesion by plakophilins 1 and 3. *J. Invest. Dermatol.* 136:2022–2029.
18. Fuchs, M., M. Foresti, …, F. Vielmuth. 2019. Plakophilin 1 but not plakophilin 3 regulates desmoglein clustering. *Cell. Mol. Life Sci.* 76:3465–3476.
19. Walter, E., F. Vielmuth, …, J. Waschke. 2019. Role of Dsg1- and Dsg3-mediated signaling in pemphigus autoantibody-induced loss of keratinocyte cohesion. *Front. Immunol.* 10:1128.
20. Valenzuela-Iglesias, A., H. E. Burks, …, K. J. Green. 2019. Desmoglein 1 regulates invadopodia by suppressing EGFR/Erk signaling in an erbin-dependent manner. *Mol. Cancer Res.* 17:1195–1206.
21. Waschke, J. 2019. Desmogleins as signaling hubs regulating cell cohesion and tissue/organ function in skin and heart - EFEM lecture 2018. *Ann. Anat.* 226:96–100.
22. Vielmuth, F., E. Walter, …, J. Waschke. 2018. Keratins regulate p38MAPK-dependent desmoglein binding properties in pemphigus. *Front. Immunol.* 9:528.
23. Vielmuth, F., M. T. Wanuske, …, V. Spindler. 2018. Keratins regulate the adhesive properties of desmosomal cadherins through signaling. *J. Invest. Dermatol.* 138:121–131.
24. Heupel, W. M., D. Zillikens, …, J. Waschke. 2008. Pemphigus vulgaris IgG directly inhibit desmoglein 3-mediated transinteraction. *J. Immunol.* 181:1825–1834.
25. Waschke, J., P. Bruggeman, …, D. Drenckhahn. 2005. Pemphigus foliaceus IgG causes dissociation of desmoglein 1-containing junctions without blocking desmoglein 1 transinteraction. *J. Clin. Invest.* 115:3157–3165.
26. Vielmuth, F., E. Hartlieb, …, V. Spindler. 2015. Atomic force microscopy identifies regions of distinct desmoglein 3 adhesive properties on living keratinocytes. *Nanomedicine (Lond.).* 11:511–520.
27. Baumgartner, W., P. Hinterdorfer, and H. Schindler. 2000. Data analysis of interaction forces measured with the atomic force microscope. *Ultramicroscopy.* 82:85–95.
28. Bell, G. I. 1978. Models for the specific adhesion of cells to cells. *Science.* 200:618–627.
29. Wieland, J. A., A. A. Gewirth, and D. E. Leckband. 2005. Single molecule adhesion measurements reveal two homophilic neural cell adhesion molecule bonds with mechanically distinct properties. *J. Biol. Chem.* 280:41037–41046.
30. Ebner, A., L. Wildling, …, H. J. Gruber. 2007. A new, simple method for linking of antibodies to atomic force microscopy tips. *Bioconjug. Chem.* 18:1176–1184.
31. Wildling, L., B. Unterauer, …, H. J. Gruber. 2011. Linking of sensor molecules with amino groups to amino-functionalized AFM tips. *Bioconjug. Chem.* 22:1239–1248.
32. Hartlieb, E., B. Kempf, …, J. Waschke. 2013. Desmoglein 2 is less important than desmoglein 3 for keratinocyte cohesion. *PLoS One.* 8:e53739.
33. Egu, D. T., E. Walter, …, J. Waschke. 2017. Inhibition of p38MAPK signalling prevents epidermal blistering and alterations of desmosome structure induced by pemphigus autoantibodies in human epidermis. *Br. J. Dermatol.* 177:1612–1618.
34. Schmidt, E., M. Kasperkiewicz, and P. Joly. 2019. Pemphigus. *Lancet.* 394:882–894.
35. Baumgartner, W., P. Hinterdorfer, …, D. Drenckhahn. 2000. Cadherin interaction probed by atomic force microscopy. *Proc. Natl. Acad. Sci. USA.* 97:4005–4010.
36. Sariisik, E., C. Popov, …, M. Benoit. 2015. Decoding cytoskeleton-anchored and non-anchored receptors from single-cell adhesion force data. *Biophys. J.* 109:1330–1333.
37. Kimura, T. E., A. J. Merritt, …, D. R. Garrod. 2012. Desmosomal adhesiveness is developmentally regulated in the mouse embryo and modulated during trophectoderm migration. *Dev. Biol.* 369:286–297.
38. Kowalczyk, A. P., and K. J. Green. 2013. Structure, function, and regulation of desmosomes. *Prog. Mol. Biol. Transl. Sci.* 116:95–118.
39. Green, K. J., A. Jaiganesh, and J. A. Broussard. 2019. Desmosomes: essential contributors to an integrated intercellular junction network. *F1000Res.* 8:F1000 Faculty Rev-2150.
40. Wallis, S., S. Lloyd, …, D. Garrod. 2000. The alpha isoform of protein kinase C is involved in signaling the response of desmosomes to wounding in cultured epithelial cells. *Mol. Biol. Cell.* 11:1077–1092.
41. Borysenko, J. Z., and J. P. Revel. 1973. Experimental manipulation of desmosome structure. *Am. J. Anat.* 137:403–421.
42. Kimura, T. E., A. J. Merritt, and D. R. Garrod. 2007. Calcium-independent desmosomes of keratinocytes are hyper-adhesive. *J. Invest. Dermatol.* 127:775–781.
43. Mattey, D. L., and D. R. Garrod. 1986. Splitting and internalization of the desmosomes of cultured kidney epithelial cells by reduction in calcium concentration. *J. Cell Sci.* 85:113–124.
44. Cirillo, N., A. Lanza, and S. S. Prime. 2010. Induction of hyper-adhesion attenuates autoimmune-induced keratinocyte cell-cell detachment and processing of adhesion molecules via mechanisms that involve PKC. *Exp. Cell Res.* 316:580–592.
45. Zlatanova, J., S. M. Lindsay, and S. H. Leuba. 2000. Single molecule force spectroscopy in biology using the atomic force microscope. *Prog. Biophys. Mol. Biol.* 74:37–61.
46. Panorchan, P., M. S. Thompson, …, D. Wirtz. 2006. Single-molecule analysis of cadherin-mediated cell-cell adhesion. *J. Cell Sci.* 119:66–74.
47. Muller, D. J. 2008. AFM: a nanotool in membrane biology. *Biochemistry.* 47:7986–7998.
48. Bass-Zubek, A. E., L. M. Godsel, …, K. J. Green. 2009. Plakophilins: multifunctional scaffolds for adhesion and signaling. *Curr. Opin. Cell Biol.* 21:708–716.

49. Nekrasova, O., and K. J. Green. 2013. Desmosome assembly and dynamics. *Trends Cell Biol.* 23:537–546.

50. Waschke, J., C. Menendez-Castro, …, W. Baumgartner. 2007. Imaging and force spectroscopy on desmoglein 1 using atomic force microscopy reveal multivalent Ca(2+)-dependent, low-affinity trans-interaction. *J. Membr. Biol.* 216:83–92.

51. Rakshit, S., Y. Zhang, …, S. Sivasankar. 2012. Ideal, catch, and slip bonds in cadherin adhesion. *Proc. Natl. Acad. Sci. USA.* 109:18815–18820.

52. Baumgartner, W., N. Golenhofen, …, D. Drenckhahn. 2003. Ca2+ dependency of N-cadherin function probed by laser tweezer and atomic force microscopy. *J. Neurosci.* 23:11008–11014.

53. Rakshit, S., and S. Sivasankar. 2014. Biomechanics of cell adhesion: how force regulates the lifetime of adhesive bonds at the single molecule level. *Phys. Chem. Chem. Phys.* 16:2211–2223.

54. Tucker, D. K., S. N. Stahley, and A. P. Kowalczyk. 2014. Plakophilin-1 protects keratinocytes from pemphigus vulgaris IgG by forming calcium-independent desmosomes. *J. Invest. Dermatol.* 134:1033–1043.

55. Johnson, J. L., N. A. Najor, and K. J. Green. 2014. Desmosomes: regulators of cellular signaling and adhesion in epidermal health and disease. *Cold Spring Harb. Perspect. Med.* 4:a015297.

**Biophysical Journal, Volume *119***

## Supplemental Information

# Desmosomal Hyperadhesion Is Accompanied with Enhanced Binding Strength of Desmoglein 3 Molecules

**Michael Fuchs, Anna Magdalena Sigmund, Jens Waschke, and Franziska Vielmuth**

## Results

### Cells lacking Pkp1 or 3 have reduced levels of Dsg3 after EGTA treatment

We investigated the expression and distribution of Dsg3 and actin using immunostainings. Interestingly, in wt murine keratinocytes Dsg3 and actin staining showed gaps (indicated by white arrows) when cells were treated with EGTA after 24 h in high $Ca^{2+}$-medium. After 72 h in high $Ca^{2+}$ we found that Dsg3 and actin are properly located at the cell membrane and observed no gaps even after EGTA treatment in wt. However, Dsg3 staining was slightly reduced (Figure S1A). In contrast, Pkp1-deficient cells revealed a drastic phenotype with gaps after EGTA treatment at 24 h and 72 h of differentiation with reduced levels of Dsg3 at the cell membranes (Figure S1B) resembling the results from dissociation assays. Pkp3-deficient cells showed no reduced intensity of Dsg3 at the cell membrane after EGTA treatment at both time points (Figure S1C) but a more blurred distribution along the cell membrane. This is in line with their diminished ability to acquire hyper-adhesion in dissociation assays. The results suggest that Pkp1 and 3 both are important for hyper-adhesion in murine keratinocytes by contributing to a proper localization of Dsg3.

## Materials and Methods

### Tissue culture and human *ex-vivo* hyper-adhesion model

A small piece of skin from the shoulder area, < 24 h post mortem, was taken from each body donor and cut into equal pieces (1 cm × 1 cm). The age of the body donors ranged from 74 to 95 years. The samples were incubated in Dulbecco modified Eagle medium (DMEM) with 5 mM of ethylene glycol tetraacetic acid (EGTA) for 1.5 h or 24 h respectively at 37°C and 5% $CO_2$. Skin samples were afterwards embedded in TissueTec (Leica Biosystems, Nussloch,

Germany) and cut into 7 µm thick slices using a cryostat microtome (CryoStar$^{TM}$ NX70, Thermo Scientific$^{TM}$, Waltham, Massachusetts, USA).

## Cell culture

Wild type (wt) and Pkp1- or 3- (Pkp k.o.) deficient murine keratinocytes (MKZ) were isolated and immortalized as described before (kindly provided by Prof. Dr. Hatzfeld, University of Halle (Saale)) [1, 2]. A stable Dsg3 k.o. cell line of mouse epidermal keratinocytes (MKZ) was generated by spontaneous immortalization from Dsg3$^{-/-}$ and $^{+/+}$ C57BL/6J mice. Epidermis was gained from neonatal mice by overnight incubation of the skin with dispase II (Sigma-Aldrich, Munich, Germany). Epidermal cells were physically washed out after treatment for 1 h with accutase (Sigma-Aldrich, Munich, Germany) and seeded in Dulbecco's modified Eagle's medium (DMEM) (Life Technologies; Carlsbad; CA; USA) supplemented with 10 % Chelex-treated fetal calf serum (Biochrom, Berlin, Germany), 50 units/ml penicillin (AppliChem, Darmstadt, Germany), 50 µg/ml streptomycin (AppliChem), 1 mM sodium pyruvate, 0.18 mM adenine, 0.5 µg/ml hydrocortison, 5 µg/ml insulin, 100 pM cholera toxin (all 5 from Sigma-Aldrich, Munich, Germany), 10 ng/ml epidermal growth factor (Life Technologies; Carlsbad; CA; USA) and 2 mM GlutaMAX (Life Technologies; Carlsbad; CA; USA) on collagen I (rat tail; BD Bioscience, New Jersey, US) coated T25 culture flasks and maintained at 35°C and 5 % $CO_2$. After passaging for 10-15 times keratinocytes immortalized spontaneously while other epidermal cells died. For all experiments with MKZ, cells were switch to high $Ca^{2+}$ (1.2 mM) containing medium after reaching confluency and grown for 24 h or 72 h, respectively, before experiments were conducted.

## Immunostaining

Immunofluorescence of skin sections was done as described elsewhere [3]. Briefly summarized, skin sections were fixed with 4% formaldehyde, permeabilized with 1% Triton

X-100 and incubated with primary antibodies. For human skin samples two different primary antibodies were used (Table S1).. As secondary antibodies Cy-labelled goat-anti-mouse and –rabbit secondary antibodies (Dianova, Hamburg, Germany) were used, respectively. Further DAPI (Roche, Mannheim, Germany) was used to visualize the cells nuclei. Quantification was done with ImageJ Software using the selection brush tool. The raw integrated density was measured along all cell membranes and then divided by the measured area. Murine keratinocytes were fixed, 24 h or 72 h after $Ca^{2+}$ switch respectively, in pure ethanol for 30 min on ice followed by three min aceton at room temperature. Primary antibodies were Desmoglein 3 pAb (Biozol Diagnostica, Eching, Germany), Alexa 488-phalloidin (Dianova, Hamburg, Germany) and DAPI. Images were taken with a Leica SP5 confocal microscope using a 63x NA 1.4 PL APO objective controlled by LAS AF software (Leica, Mannheim, Germany).

| Antibody against: | In Figure 4, S3 and S4 | Figure S4 |
|---|---|---|
| Dsg1 | Desmoglein 1-P124 mAb (Progen Biotechnik GmbH, Heidelberg, Germany) | A9812 pAb (Abclonal Technology, USA) |
| Dsg3 | Desmoglein 3 pAb, E-AB-62720 (Biomol GmbH, Hamburg, Germany) | 5G11 mAb (Invitrogen, USA) |
| Dsc1 | Desmocollin 1 pAb (1), abx176152 (Abbexa, Cambridge, United Kingdom) | L15, sc-18115, pAb (2), (Santa Cruz, Dallas, TX, USA) |
| Dsc3 | Desmocollin 3 mAb (Progen Biotechnik GmbH, Heidelberg, Germany) | Abx334157 pAb, (Abbexa, Cambridge, United Kingdom) |

Table S1: Used primary antibodies for human skin samples.

## Crosslinking, Electrophoresis and Western blot analysis

After washing with PBS cells were lysed with SDS-lysis buffer (25 mmol/l HEPES, 25 mmol/l NaF and 1% SDS, pH 7.4) followed by sonication on ice. The amount of protein was determined with the Pierce$^{TM}$ BCA Protein Assay Kit (Thermo Fisher, USA). Western blotting was implemented following established protocols [4].

The membrane-impermeable cross-linker ethylene glycolbis (sulfosuccinimidylsuccinate) (Sulfo-EGS) (Pierce Biotechnology, Rockford, USA) was used for detection of oligomerization of desmosomal cadherins. The experimental approach followed a well-established protocol [5, 6]. In brief, cells were subjected to respective experimental conditions, washed three times with cold PBS and Sulfo-EGS was added to the cells at a concentration of 2 mM for 30 min at room temperature. In order to stop the reaction, TBS was added at a concentration of 50 mM and incubated for 15 min. Western blotting to detect crosslinked proteins was performed following a standard protocol. For quantification, the raw integrated density of the oligomer band was first divided by the band of oligomer plus monomer. Afterwards the EGTA-treated column was divided by the non-EGTA treated column to obtain the oligomerization ratio.

## Data processing and Statistics

For image processing Photoline software (Computerinsel, Bad Gögging, Germany) was applied. AFM images and data analysis of measured force-distance curves were processed with JPK data processing software (Bruker Nano GmbH, Berlin, Germany). Further AFM parameters were determined with Origin Pro 2016, 93G (Northampton, MA, USA). For densitometric measurements ImageJ software (NIH, Bethesda, USA) was used. Other data shown in this study were evaluated and depicted with Excel (Microsoft, Redmond, WA, USA).

For statistical significance in case of two groups we applied two-tailed Student´s t test. For multiple groups analysis of variance (one-way ANOVA) followed by Bonferroni post hoc test was done. Error bars are standard error of the mean or standard deviation as indicated. Significance was assumed at a p-value $< 0.05$.

## Supporting References


1. Keil, R., K. Rietscher, and M. Hatzfeld, *Antagonistic Regulation of Intercellular Cohesion by Plakophilins 1 and 3.* Journal of Investigative Dermatology, 2016. **136**: p. 8.
2. Rietscher, K., A. Wolf, G. Hause, A. Rother, R. Keil, T.M. Magin, M. Glass, C.M. Niessen, and M. Hatzfeld, *Growth Retardation, Loss of Desmosomal Adhesion, and Impaired Tight Junction Function Identify a Unique Role of Plakophilin 1 In Vivo.* Journal of Investigative Dermatology, 2016. **136**(7): p. 8.
3. Egu, D.T., E. Walter, V. Spindler, and J. Waschke, *Inhibition of p38MAPK signalling prevents epidermal blistering and alterations of desmosome structure induced by pemphigus autoantibodies in human epidermis.* British Journal of Dermatology, 2017. **177**(6).
4. Hartlieb, E., B. Kempf, M. Partilla, B. Vigh, V. Spindler, and J. Waschke, *Desmoglein 2 Is Less Important than Desmoglein 3 for Keratinocyte Cohesion.* PLoS ONE, 2013. **8**(1): p. 12.
5. Nie, Z., A. Merritt, M. Rouhi-Parkouhi, L. Tabernero, and D. Garrod, *Membrane-impermeable Cross-linking Provides Evidence for Homophilic, Isoform-specific Binding of Desmosomal Cadherins in Epithelial Cells.* JOURNAL OF BIOLOGICAL CHEMISTRY, 2011. **286**(3): p. 11.
6. Fuchs, M., M. Foresti, M.Y. Radeva, D. Kugelmann, R. Keil, M. Hatzfeld, V. Spindler, J. Waschke, and F. Vielmuth, *Plakophilin 1 but not plakophilin 3 regulates desmoglein clustering.* Cellular and Molecular Life Sciences, 2019.

**Figures:**

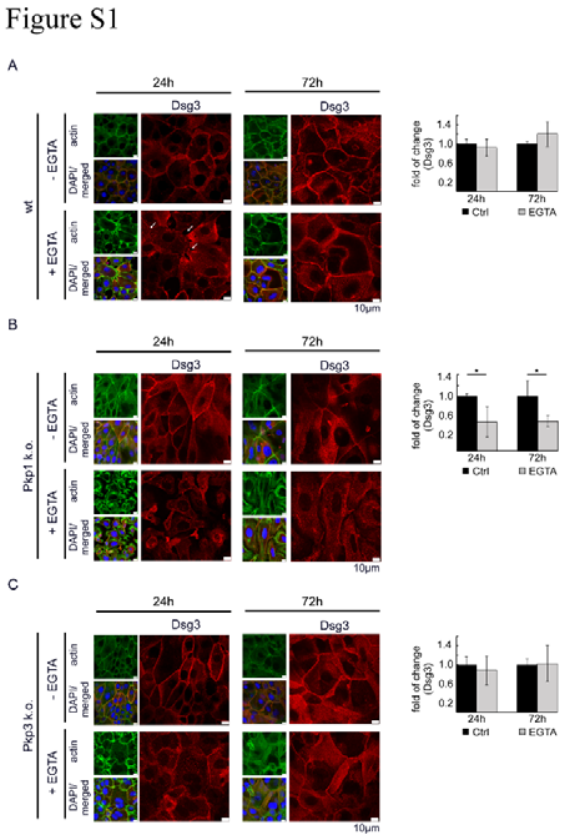


**Figure S1**: Reduced levels of Dsg3 after EGTA treatment for Pkp1 or 3 lacking cells.

**A**/**B**/**C**: Murine keratinocytes were maintained for 24 h or 72 h in high $Ca^{2+}$ medium and were subsequently subjected to $Ca^{2+}$ chelation with EGTA for 90 min. Immunostaining for Dsg3 and actin revealed disturbed membrane localization after 24 h in high $Ca^{2+}$ medium as well as gap formation between the cells (white arrows). In contrast, membrane staining was preserved after $Ca^{2+}$ chelation in wt and Pkp3-deficient but not in Pkp1-deficient keratinocytes after 72h in high $Ca^{2+}$ medium. DAPI was used to stain cell nuclei. Pictures show representatives of $n \geq 3$. Scale bar = 10 µm. *$p<0.05$ vs. corresponding control, error bars represent standard deviation.

Figure S2

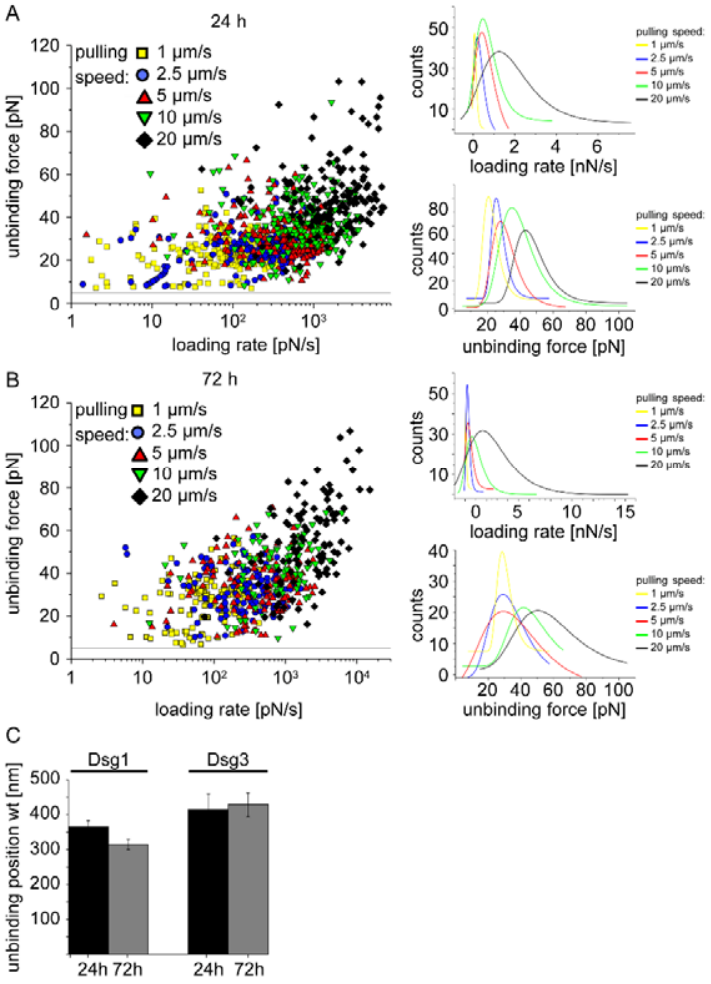


**Figure S2: A-B:** UF plotted against logarithmic loading rate with respect to their pulling speed after 24 h and 72h in high Ca2+ medium, shows an increase of UF and loading rate for higher pulling forces. Grey line indicates 5 pN threshold level, values below that line were excluded from analysis. On the right side the distribution of the loading rates and unbinding forces of the increasing pulling speeds is shown. n=8 with 2 cell borders/experiment. **C:** Unbinding position of Dsg1 and 3 coated tips comparing 24 h and 72 h in high Ca2+ medium shows no significant alterations. For Dsg1 n=4 and for Dsg3 n=6 were used for analysis, error bars represent error of the mean.

Figure S3

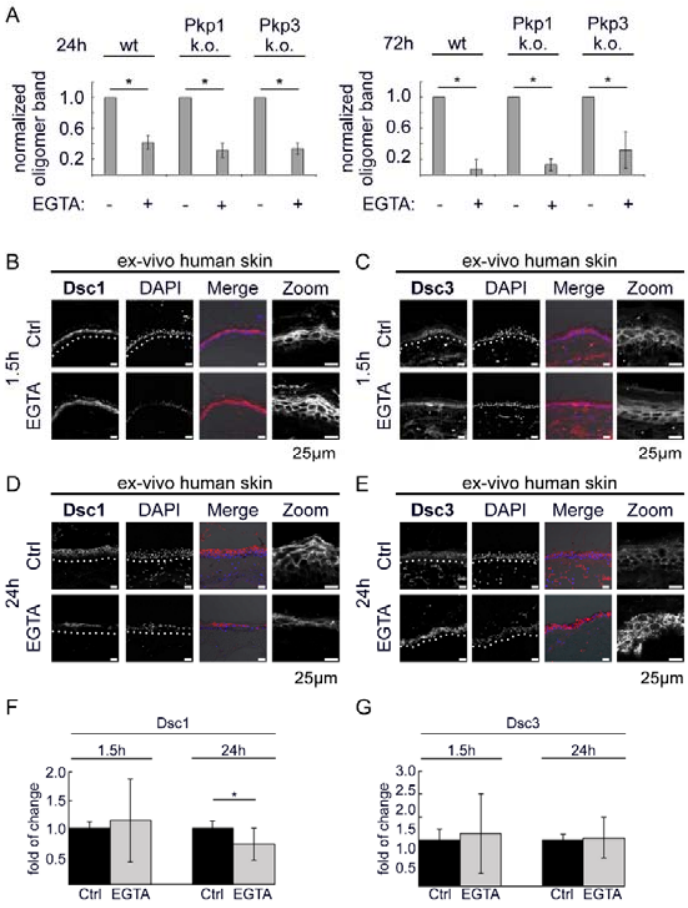


**Figure S3**: A: Quantification of oligomer band density of ECad shows significant decrease after EGTA treatment for all cell lines after 24h and 72h in high $Ca^{2+}$ medium. n≥4, *p<0.05 vs. corresponding control, error bars represent standard deviation. B-**G:** Immunostaining for Dsc1 and 3 of human epidermis after 1.5h or 24h of EGTA incubation reveals reduced and fragmentated levels of Dsc1 but not Dsc3 staining. n≥3, *p<0.05 vs respective control, error bars represent standard deviation.

Figure S4

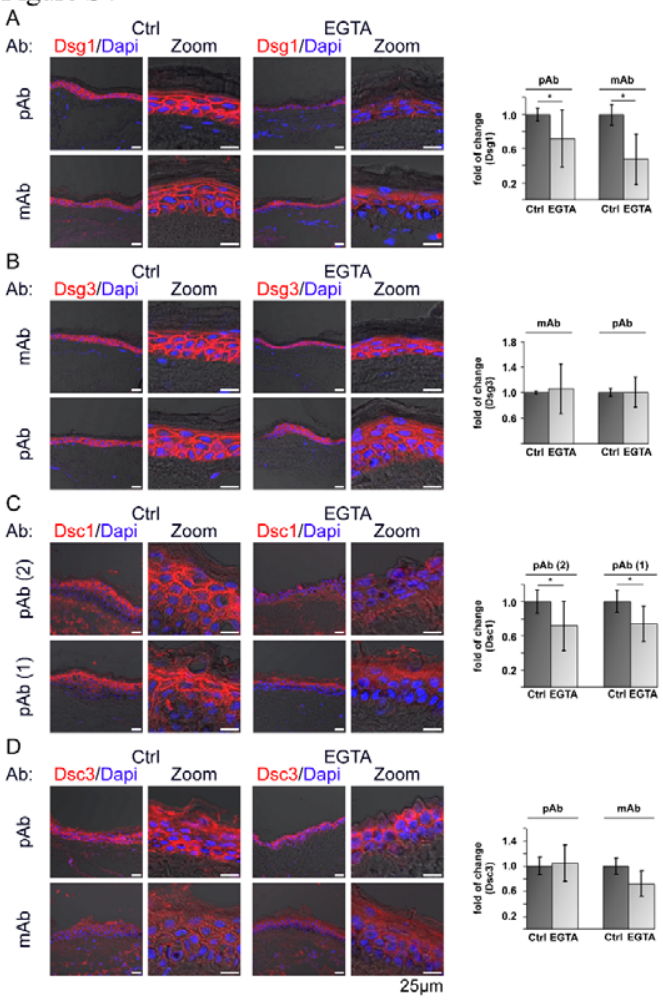


**Figure S4**: Immunostaining of respective desmosomal cadherins in human epidermis after 24h of EGTA treatment using two sets of primary antibodies. **A:** For Dsg1 both antibodies show a significant reduced membrane staining and protein amount after 24h EGTA treatment. **B:** Dsg3 immunostaining with two different primary antibodies show little alterations after 24h EGTA incubation. **C:** Significantly reduced membrane staining of Dsc1 after EGTA treatment is shown for both primary antibodies. **D:** For Dsc3 staining no difference can be found for the used primary antibodies. **A-D:** n=4, *p<0.05 vs corresponding control, error bars represent standard deviation.

## 2.3 Keratins Regulate p38MAPK-Dependent Desmoglein Binding Properties in Pemphigus

frontiers in Immunology

ORIGINAL RESEARCH
published: 19 March 2018
doi: 10.3389/fimmu.2018.00528

# Keratins Regulate p38MAPK-Dependent Desmoglein Binding Properties in Pemphigus

*Franziska Vielmuth[1], Elias Walter[1], Michael Fuchs[1], Mariya Y. Radeva[1], Fanny Buechau[2], Thomas M. Magin[2], Volker Spindler[1] and Jens Waschke[1]**

[1] Faculty of Medicine, Institute of Anatomy, Ludwig-Maximilians-Universität München, Munich, Germany, [2] Division of Cell and Developmental Biology, Institute of Biology, Sächsische Inkubator für Klinische Translation (SIKT), University of Leipzig, Leipzig, Germany

Keratins are crucial for the anchorage of desmosomes. Severe alterations of keratin organization and detachment of filaments from the desmosomal plaque occur in the autoimmune dermatoses pemphigus vulgaris and pemphigus foliaceus (PF), which are mainly caused by autoantibodies against desmoglein (Dsg) 1 and 3. Keratin alterations are a structural hallmark in pemphigus pathogenesis and correlate with loss of intercellular adhesion. However, the significance for autoantibody-induced loss of intercellular adhesion is largely unknown. In wild-type (wt) murine keratinocytes, pemphigus autoantibodies induced keratin filament retraction. Under the same conditions, we used murine keratinocytes lacking all keratin filaments (KtyII k.o.) as a model system to dissect the role of keratins in pemphigus. KtyII k.o. cells show compromised intercellular adhesion without antibody (Ab) treatment, which was not impaired further by pathogenic pemphigus autoantibodies. Nevertheless, direct activation of p38MAPK *via* anisomycin further decreased intercellular adhesion indicating that cell cohesion was not completely abrogated in the absence of keratins. Direct inhibition of Dsg3, but not of Dsg1, interaction *via* pathogenic autoantibodies as revealed by atomic force microscopy was detectable in both cell lines demonstrating that keratins are not required for this phenomenon. However, PF-IgG shifted Dsg1-binding events from cell borders toward the free cell surface in wt cells. This led to a distribution pattern of Dsg1-binding events similar to KtyII k.o. cells under resting conditions. In keratin-deficient keratinocytes, PF-IgG impaired Dsg1-binding strength, which was not different from wt cells under resting conditions. In addition, pathogenic autoantibodies were capable of activating p38MAPK in both KtyII wt and k.o. cells, the latter of which already displayed robust p38MAPK activation under resting conditions. Since inhibition of p38MAPK blocked autoantibody-induced loss of intercellular adhesion in wt cells and restored baseline cell cohesion in keratin-deficient cells, we conclude that p38MAPK signaling is (i) critical for regulation of cell adhesion, (ii) regulated by keratins, and (iii) targets both keratin-dependent and -independent mechanisms.

**Keywords: desmosome, keratin, desmoglein, atomic force microscopy, p38MAPK**

OPEN ACCESS

***Edited by:***
*Ralf J. Ludwig, University of Lübeck, Germany*

***Reviewed by:***
*Marcel F. Jonkman, University Medical Center Groningen, Netherlands*
*Giovanni Di Zenzo, Istituto Dermopatico dell'Immacolata (IRCCS), Italy*

****Correspondence:***
*Jens Waschke*
*jens.waschke@med.uni-muenchen.de*

***Specialty section:***
*This article was submitted to Immunological Tolerance and Regulation, a section of the journal Frontiers in Immunology*

***Received:*** *30 November 2017*
***Accepted:*** *28 February 2018*
***Published:*** *19 March 2018*

***Citation:***
*Vielmuth F, Walter E, Fuchs M, Radeva MY, Buechau F, Magin TM, Spindler V and Waschke J (2018) Keratins Regulate p38MAPK-Dependent Desmoglein Binding Properties in Pemphigus. Front. Immunol. 9:528. doi: 10.3389/fimmu.2018.00528*

**Abbreviations:** AFM, atomic force microscopy; Dsg, desmoglein; EC, extracellular domain, PF, pemphigus foliaceus; PV, pemphigus vulgaris; NGS, normal goat serum; BSA, bovine serum albumin; PEG, polyethylenglycol; QI, quantitative imaging; FM, force mapping; FRAP, fluorescence recovery after photobleaching.

## INTRODUCTION

Desmosomes are highly organized protein complexes required for proper intercellular adhesion especially in tissues which are constantly exposed to mechanical stress, such as the heart and the epidermis. They are composed of desmosomal cadherins which maintain the strong intercellular adhesion with their extracellular domains (EC), thus bridging the intercellular cleft, and plaque proteins connecting the desmosomal cadherins to the intermediate filament cytoskeleton (1–3).

Pemphigus is a life-threatening autoimmune dermatosis in which autoantibodies directed against the desmosomal cadherins desmoglein (Dsg) 1 and 3 lead to a flaccid blistering of the skin and mucous membranes (4, 5). On a morphological level, blistering occurs by separation of epidermal layers either suprabasal in pemphigus vulgaris (PV) or superficially in pemphigus foliaceus (PF) which represent the two main clinical manifestations of the disease (6). In PF, blisters are restricted to the skin and only Dsg1 autoantibodies occur. By contrast, in PV erosions additionally affect mucous membranes especially of the oral cavity. Blisters in PV are primarily caused by autoantibodies against both, Dsg1 and 3 (7). Thus, autoantibody profiles largely correlate with the clinical phenotype, a phenomenon which was proposed to be explained at least in part by autoantibody-specific cellular signaling patterns (8). In addition to signaling pathways which apparently are crucial for pemphigus pathogenesis (7, 9) direct inhibition of Dsg interactions by autoantibodies was described for Dsg3 but not for Dsg1 (10–12). Furthermore, the typical morphological hallmark of keratin filament retraction from cell borders is a common feature of all clinical phenotypes and can be detected in pemphigus models *in vitro* (13–16) as well as *ex vivo* and in patients' lesions (17–21). Keratins, the constituents of intermediate filaments in the epidermis, are crucial for proper desmosomal adhesion and retraction of the keratin cytoskeleton correlated with loss of intercellular adhesion induced by pemphigus autoantibodies (11, 22, 23). They, furthermore, account for the mechanical properties of keratinocytes (24) and are involved in the regulation of important signaling pathways for desmosomal adhesion, such as protein kinase C (PKC) and p38 mitogen-activated protein kinase (p38MAPK) both of which also regulate Dsg3-binding properties in a keratin-dependent fashion (22, 23, 25).

In these settings, the exact mechanism and contribution of alterations of the keratin cytoskeleton to loss of intercellular adhesion in pemphigus is not well characterized. Thus, we here use murine keratinocytes lacking all keratins to dissect the contribution of keratins in pemphigus pathogenesis. With this approach we demonstrate that keratins differentially regulate the binding properties of the two major antigens for autoantibodies in pemphigus, Dsg1 and 3. Moreover, we observed that p38MAPK underlies a keratin-mediated regulation, which is crucial for loss of intercellular adhesion in pemphigus.

## MATERIALS AND METHODS

### Cell Culture and Reagents

In this study, murine keratinocytes (KtyII) isolated from wild-type (KtyII wt) and keratin cluster II knockout (KtyII k.o.) were used. Cells were immortalized as described elsewhere in detail (22). Cells were grown in complete FAD media (0.05 mM $CaCl_2$) on collagen I-coated culture dishes (rat tail; BD). For all experiments, cells were grown to confluency before switching them to high $Ca^{2+}$ (1.2 mM) for 48 h to induce proper differentiation and usage for experiments. For fluorescence recovery after photobleaching (FRAP) experiments, cells were transient transfected at 70% confluency with pEGFP-C1-*Dsg3* (kindly provided by Dr. Yasushi Hanakawa, Ehime University School of Medicine, Japan) using Lipofectamine 3000 (Invitrogen, Carlsbad, CA, USA) according to manufacturers' protocol. 24 h after transfection, cells were switched to high $Ca^{2+}$ (1.2 mM) and grown for further 48 h before the experiments. Activity of p38MAPK was modulated using either p38 inhibitors SB202190 (Merck, Darmstadt, Germany) and SB203580 (Sigma Aldrich, Munich, Germany) (both 30 μM) or p38 activator anisomycin (60 μM) (Sigma Aldrich, Munich, Germany).

### Purification of Recombinant Dsg Fc Constructs

Dsg1- and Dsg3-Fc constructs containing the full extracellular domain of the respective Dsg were stably expressed in Chinese hamster ovary cells (CHO-cells). Purification was performed as described elsewhere in detail (10). Briefly, transfected CHO-cells were grown to confluence, supernatants were collected and recombinant proteins were isolated using Protein A Agarose (Life Technologies). To test purity and specificity Coomassie staining and Western blotting using anti Dsg1-monoclonal antibody (mAb) (p124, Progen, Heidelberg, Germany) and anti Dsg3-mAb (clone5G11; Life Technologies) which both detect the extracellular domain of the respective Dsg were conducted (data not shown).

### Purification of Patients IgG Fractions and Antibodies (Abs)

Serum of PV patients was provided by Enno Schmidt (Department of Dermatology, University of Lübeck). Sera were used with informed and written consent and under approval of the local ethic committee (number: AZ12-178). All patients had an active disease at the time of collection including lesions of the skin and the mucous membranes. ELISA scores are given in **Table 1**.

Purification of IgG fraction from pemphigus patients (PV-IgG) or healthy volunteer (control-IgG) was conducted as described elsewhere (10, 12, 26) using Protein A Agarose (Life Technologies). The pathogenic monoclonal Dsg3 Ab, AK23 (Biozol, Eching, Germany) was used at a concentration of 75 μg/ml.

**TABLE 1** | ELISA score of pemphigus vulgaris (PV)-IgG fraction.

| | Dsg1 | Dsg3 |
|---|---|---|
| PV1-IgG | 1,207 | 3,906 |
| PV2-IgG | 212.27 | 181.440 |
| Pemphigus foliaceus (PF)-IgG | 215.34 | 8.2[a] |

[a]*Beneath relevant threshold.*

## Immunostaining

Murine keratinocytes were used 48 h after $Ca^{2+}$ switch and 72 h after transfection for the FRAP and respective immunofluorescence experiments. Cells were fixed with freshly prepared 4% paraformaldehyde for 20 min, permeabilized with 1% Triton X-100 for 10 min and blocked with 10% normal goat serum/1% bovine serum albumin. Cytokeratin 14 mAb (LL002, Abcam, Cambridge, UK) was used as primary Ab. As secondary Ab Cy3-labeled goat anti-mouse Ab was used (Dianova, Hamburg, Germany). Furthermore, Alexa 488-phalloidin (Invitrogen, Carlsbad, CA, USA) and DAPI (Roche, Mannheim, Germany) were used to visualize the actin cytoskeleton and the nuclei respectively. Images were recorded using a Leica SP5 confocal microscopy with a 63× NA 1.4 PL APO objective controlled by LAS AF software (Leica, Mannheim, Germany). For some experiments, *z*-stacks were recorded, and pictures represent maximum intensity projections. For quantification of keratin retraction keratin 14 fluorescence intensity was measured at small areas in close proximity to the cell border and above the nucleus, and a ratio was calculated to quantify keratin filament retraction (Figure S1A in Supplementary Material).

## Dispase-Based Keratinocytes Dissociation Assay

For dissociation assay, cells were grown in high $Ca^{2+}$ medium for 48 h after confluence. Dispase assay was conducted as described in detail before (25, 27). Briefly, cells exposed to different conditions were removed from well bottom using a mixture of Dispase II (Sigma Aldrich) and 1% collagenase I (Thermo Fisher Scientific). After application of defined shear stress by pipetting the monolayers with a 1 ml pipette the resulting fragments were counted. The latter represent an inverse measure for intercellular adhesion.

## Biotinylation Assay and Western Blotting

Cell surface biotinylation was conducted as described before (11, 25). In brief, cell monolayers were incubated with 0.25 mM of membrane-impermeable EZ-Link Sulfo-NHS-Biotin (Thermo Fisher Scientific, Waltham, MA, USA) on ice and rinsed in ice-cold PBS containing 100 mM glycin. Cells were lysed in PIPES buffer (50 mM NaCl, 10 mM PIPES, 3 mM $MgCl_2$, 1% Triton X-100, protease inhibitors) and centrifuged. Supernatants were collected, and pull-down of biotinylated molecules was carried out using NeutrAvidin (HighCapacity)-agarose (Thermo Fisher Scientific). Precipitated molecules were suspended in 3× Laemmli buffer with 50 mM dithiothreitol (AppliChem) and subjected to Western blotting.

For whole cell lysates SDS buffer (25 mmol/l HEPES, 2 mmol EDTA, 25 mmol/l NaF and 1% sodiumdodecylsulfate, and pH 7.4) was used. Western blotting was performed according to standard protocol (27).

## Fluorescence Recovery After Photobleaching

For all FRAP experiments, KtyII cells were seeded in 8-well imaging chambers (Ibidi, Martinsried, Germany). Cells were transfected with pEGFP-C1-Dsg3 as described in cell culture section. FRAP experiments were conducted with the FRAP wizard software on a Leica SP5 confocal microscopy with a 63× NA 1.4 PL APO objective at 37°C as described before (25, 28). The Dsg3-GFP signal was bleached at cell border areas of two adjacent cells with the 488 nm line of an Argon laser at 100% transmission. Fluorescence recovery was monitored during the following 3 min and fluorescence intensities were analyzed. The immobile fraction was determined using the FRAP wizard.

## Atomic Force Microscopy (AFM) Measurements

A NanoWizard® 3 AFM (JPK Instruments, Berlin, Germany) mounted on an inverted optical microscope (Carl Zeiss, Jena, Germany) was used throughout all experiments. The setup was described in detail before and allows the selection of the scanning areas by usage of an optical image acquired with a 63× objective (11, 25, 29). All measurements were accomplished at 37°C in cell culture medium containing 1.2 mM $Ca^{2+}$.

For all experiments pyramidal-shaped D-Tips of $Si_3N_4$ MLCT cantilevers (Bruker, Mannheim, Germany) with a nominal spring constant of 0.03 N/m and tip radius of 20 nm were functionalized with Dsg1- or 3-Fc constructs as described before (30). Briefly, a flexible heterobifunctional acetal-polyethylenglycol (synthetized by the Hermann Gruber Lab, Institute of Biophysics, Linz, Austria) was interspaced between the tip and the purified Fc construct whose concentration was adjusted to 0.15 mg/ml. For measurements on living murine keratinocytes a protocol which was recently developed in our group (29) was used. AFM was run in quantitative imaging (QI) mode for overview images or force mapping (FM) mode for measurement and characterization of Dsg binding properties. For the latter mode, a force map consisted of 1,200 pixels with each pixel representing one force–distance cycle that covered an area of 6 µm × 2 µm along cell borders or 4 µm × 2 µm above the nucleus. Settings of the respective modes can be found in **Table 2**.

Resulting force–distance curves were analyzed with regard to topography and adhesive properties of specific surface molecules (31).

For Ab experiments, the respective Abs were incubated solely on the cell to avoid binding to the scanning tip. After the incubation period, cells were extensively washed to remove unbound Abs and reprobed by AFM. For characterization of molecule distribution at the cell border areas a distribution coefficient was calculated as described before (32). Briefly, a ratio of number of binding events per area along the elevated cell borders (Figure S1B in Supplementary Material, green area) and in the surrounding cell surface (Figure S1B in Supplementary Material, red area) was

**TABLE 2** | Atomic force microscopy settings.

| Settings | Quantitative imaging mode | Force mapping mode |
|---|---|---|
| Setpoint | 0.5 nN | 0.5 nN |
| *Z*-length | 1.5 µm | 1.5 µm |
| Pulling speed | 50 µm/s | 10 µm/s |
| Resting contact time | – | 0.1 s |

calculated, in which values higher than 1 demonstrate increased localization of molecules along the cell borders.

## Data Analysis and Statistics

For image processing, Adobe Photoshop CS5 (Adobe, Dublin, Ireland) was used. AFM images and data analysis of force–distance curves were done on JPK Data Processing Software (JPK Instruments). For further calculation of the analyzed AFM data with regard to unbinding forces, peak fitting, and step position Origin Pro 2016, 93G (Northampton, MA, USA) was used. In addition, Origin was utilized for comparison of data values with a paired Student's *t*-test (two sample groups) or one-way analysis of variance following Bonferroni correction (more than two groups), respectively. Error bars given in the figures are mean ± SD for all diagrams depicting unbinding forces ± SEM for all other experiments. Significance was presumed at a $p$-value $< 0.05$.

# RESULTS

## Keratin Deficiency Reduces Effect of Pathogenic Autoantibodies on Intercellular Adhesion

Keratin alterations are morphological hallmarks of pemphigus and correlate with loss of intercellular adhesion in human keratinocytes (11). Wild-type murine keratinocytes (KtyII wt) were used to test whether pathogenic autoantibodies are able to induce comparable changes of the keratin cytoskeleton in murine cells. Keratinocytes were treated either with control-IgG of healthy volunteers or with pathogenic autoantibodies for 24 h and subjected to immunostaining for keratin14 or keratinocyte dissociation assay, respectively (**Figures 1A,B**). We used AK23, a pathogenic monoclonal Ab derived from a PV mouse model, which is specific for Dsg3 (33), PF-IgG containing Ab against Dsg1 as well as PV-IgG with Abs against Dsg1 and 3 (**Table 1**). In control-IgG treated cells, the keratin cytoskeleton formed a dense network throughout the cells which is composed of delicate fibers and covers the cell periphery (**Figure 1A**). Actin was labeled to delineate the cell periphery and DAPI was included to stain nuclei (**Figure 1A**). By contrast, after treatment with all pathogenic autoantibodies keratin filament bundles were thicker and more irregular throughout and were retracted from some segments of cell borders (**Figure 1A**, arrows). Keratin retraction was quantified as described in materials and methods. In control-IgG treated cells, the coefficient was around 1 indicating a homogeneous distribution of the keratin network throughout the whole cell. The coefficient was significantly reduced after treatment with all pathogenic autoantibodies indicating a reduced fluorescent signal at cell border areas and thus confirms the occurrence of keratin retraction (**Figure 1B**).

To further dissect the role of keratins for loss of intercellular adhesion in pemphigus, KtyII k.o. cells were compared with wt monolayers in dissociation assays (Figure S1C in Supplementary Material). Under control conditions and after incubation with control-IgG, KtyII k.o. cells showed a significantly impaired intercellular adhesion compared with wt similar as shown before (22, 23, 25) (**Figure 1C**). Interestingly, treatment with AK23, PV-IgG or PF-IgG did not further compromise intercellular adhesion in KtyII k.o. cells whereas a significant reduction in wt cells was observed (**Figure 1C**). Given that anisomycin-mediated activation of p38MAPK as shown below (**Figure 4B**) was efficient to strongly reduce adhesion in keratin-deficient cells, these data indicate that keratins are important for the loss of intercellular adhesion in pemphigus.

## Keratins Differentially Regulate Dsg-Binding Properties

Keratin filament alterations in response to autoantibodies were accompanied by depletion of Dsg3 from the cell membrane (8, 11). In a recent study, it was shown that keratins regulate Dsg3-binding properties through signaling (25). Thus, we next studied distribution, binding frequency, and binding strength of Dsg1 and Dsg3 by AFM in parallel. Dsgs can interact homo- and heterophilic (34–36). However, in our last studies by comparing parallel experiments under cell-free conditions and on living keratinocytes as well as by using isoform-specific inhibitory Abs, we predominantly detected homophilic interactions (25, 29, 32). A modified cantilever holder setup allowed the measurement at the same area with scanning tips functionalized with Dsg1 or Dsg3, respectively. First, topography overview images spanning an area of 50 µm × 30 µm were performed using QI mode (**Figures 1D,E**). In both cell lines, cell surfaces exhibited a reticular structure, and cell borders could be identified clearly by an elevated region (25) (**Figures 1D,E**, red arrows). Defined areas along cell borders were chosen for adhesion measurements (**Figures 1D,E**, red rectangles) and probed using FM mode with a pulling speed of 10 µm/s and a resting contact time of 0,1 s. Same areas along the cell border were chosen with both cantilevers after respective overview imaging to compare Dsg1 and 3 localization. In adhesion panels, each blue and green pixel represents a specific binding event of Dsg3 and Dsg1, respectively (**Figures 1D–F**). Evaluation of binding frequencies revealed a higher binding frequency for Dsg3 in keratin-deficient keratinocytes (**Figures 1D,G**) whereas the Dsg1-binding frequency was significantly reduced (**Figures 1E,H**). By contrast, binding forces of Dsg3 were reduced in KtyII k.o. cells as shown previously (25) (**Figures 1D,G**) whereas no difference in binding strength was observed for Dsg1 (**Figures 1E,H**). Finally, we analyzed the distribution of binding events using a distribution coefficient (see Material and Methods; Figure S1B in Supplementary Material) in which values >1 indicated higher binding frequency along the cell border. In accordance with former studies, Dsg3 shows a uniform distribution in both cell lines (25, 29) (**Figures 1D,F,G**). However, Dsg1-binding events were localized along cell borders (**Figures 1E,F,H**) in wt cells, whereas distribution was uniform in KtyII k.o. cells (**Figures 1E,F,H**) suggesting that keratins are important for proper localization of Dsg1 at cell junctions. Moreover, keratins differentially modulate Dsg binding properties.

## Direct Inhibition of Dsg3 Single Molecule Interactions Occurs in Keratin-Deficient Keratinocytes

Direct inhibition of Dsg3 interactions is a well-characterized phenomenon in pemphigus which occurs fast after binding of

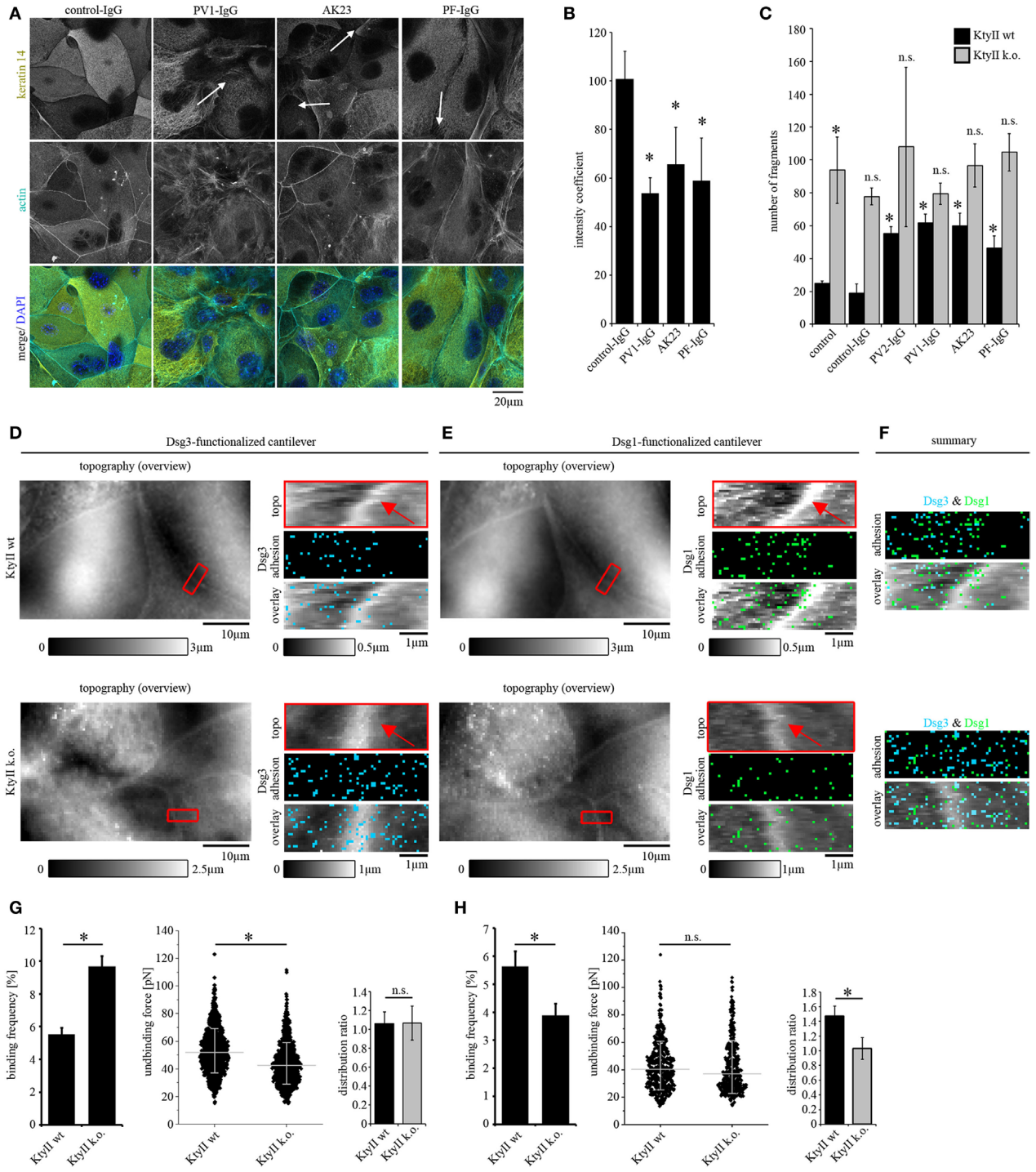


**FIGURE 1** | Keratin retraction in murine keratinocytes and regulation of desmoglein binding properties through keratins. **(A)** Immunostaining of wild-type murine keratinocytes (KtyII wt) using keratin 14 monoclonal antibody and Alexa488-phalloidin for actin staining. Control-IgG treated keratinocytes show a dense keratin network throughout the whole cell whereas keratin filament retraction (arrows) and formation of thick filament bundles were detectable after treatment with pemphigus vulgaris (PV)-IgG, pemphigus foliaceus (PF)-IgG, and AK23. Pictures are representatives of $n > 4$. **(B)** Quantification of keratin retraction using an intensity coefficient confirms occurrence of keratin retraction in all autoantibody treated conditions. **(C)** Dissociation assay of KtyII wt and k.o. keratinocytes reveals that keratin-deficient keratinocytes show impaired intercellular adhesion. Treatment with pathogenic autoantibodies (PF-IgG, PV1- and PV2-IgG, and AK23) reduced intercellular adhesion in wild-type (wt) but not in KtyII k.o. cells. $n = 5$, $^*p > 0.05$ vs. wt control and wt control-IgG. **(D,E)** Atomic force microscopy adhesion measurements using Dsg3-Fc- or Dsg1-Fc-functionalized cantilevers on the same scanning area. In adhesion panels, each blue or green pixel represents a specific Dsg3- or Dsg1-binding event, respectively. **(F)** Merged panels of adhesion measurements reveal distinct clustering of Dsg1- and 3-binding events. **(G,H)** Analysis of binding frequency and unbinding forces of Dsg1 and 3 interactions. $n = 6$ from ≥3 independent coating procedures, 1,200 force–distance curves/adhesion maps ($^*p < 0.05$).

pathogenic autoantibodies but alone is not sufficient to cause complete loss of cell cohesion (5, 11, 26). To investigate the role of keratins for direct inhibition, we treated both cell lines with AK23 which is directed against the extracellular domain (EC) 1 of Dsg3 and was reported to interfere with Dsg3 interaction under cell-free conditions as well as in living keratinocytes (10, 11, 36). To avoid Ab binding to the AFM cantilever, AK23 was incubated on cells for 1 h in absence of cantilevers, washed extensively after incubation with fresh media to remove unbound Abs, and cells were reprobed. Doing so, small areas along the cell borders were chosen and measured before and after AK23 incubation. AK23 reduced Dsg3-binding frequency in both cell lines to a comparable extent suggesting that loss of keratins do not effect autoantibody-induced direct inhibition of Dsg3 interaction (**Figures 2A,B**). In line with this, distribution of the remaining binding events was not changed (**Figures 2A,B**).

## Keratin Deficiency Accelerates Depletion of Dsg3

Next, we investigated depletion of Dsg3 which accompanied loss of intercellular adhesion and was linked to several signaling pathways such as p38MAPK in models of pemphigus (19, 37). As reported previously, keratin-deficient keratinocytes reveal a higher expression level of Dsg3 (25) (**Figure 2C**). Cells were treated with PV-IgG for 1 h and subjected to a surface

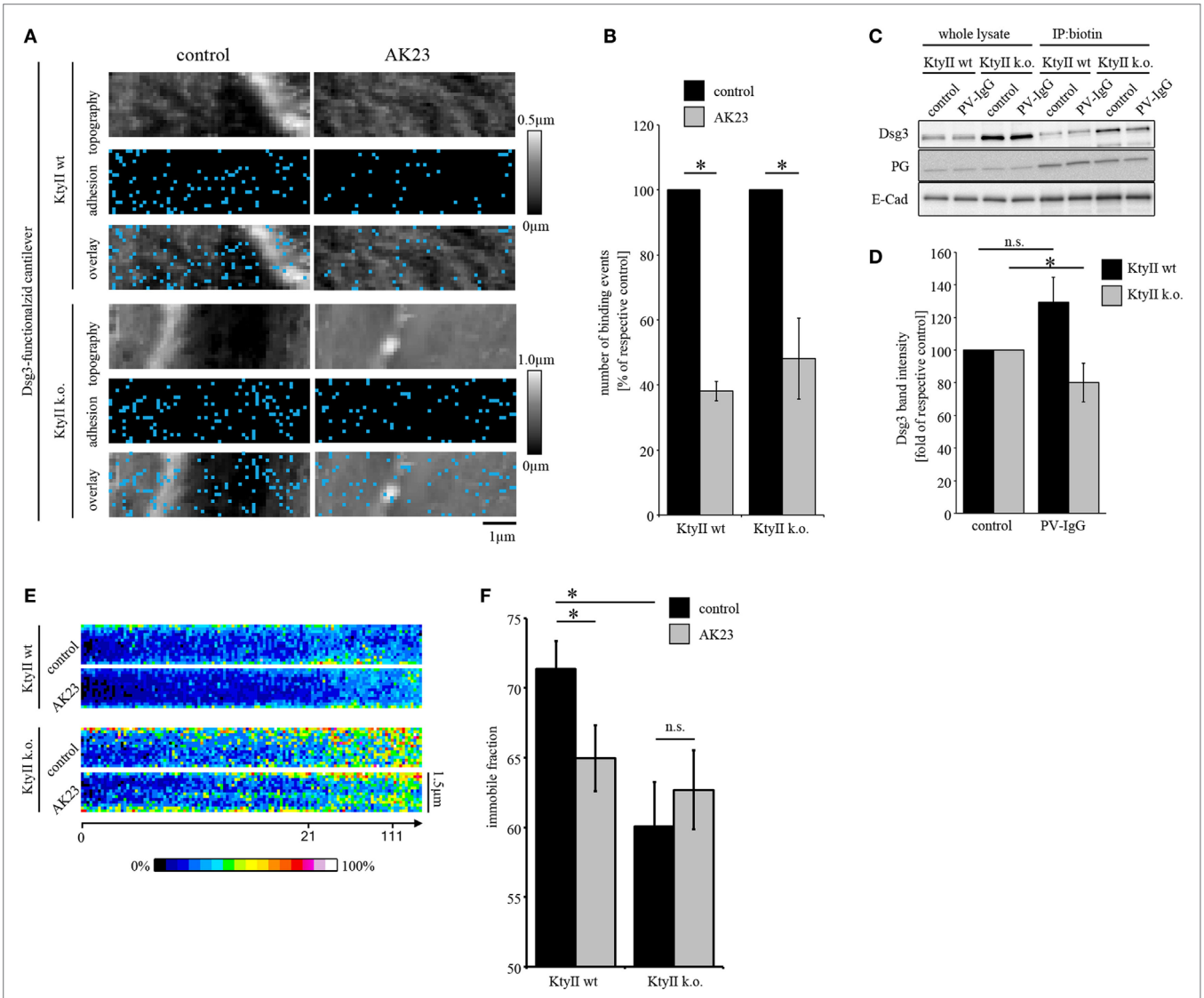


**FIGURE 2** | Keratin-deficiency accelerates depletion of Dsg3. **(A,B)** Dsg3 adhesion measurements on KtyII wt and k.o. cells using AK23. Treatment of KtyII wt and k.o. cells with AK23 for 1 h reduced Dsg3 binding to comparable extent. $n = 6$ from ≥3 independent coating procedures, 1,200 force–distance curves/adhesion maps (*$p < 0.05$). **(C,D)** Cell surface biotinylation delineates depletion of Dsg3 in keratin-deficient keratinocytes after 1 h of pemphigus vulgaris (PV) 1-IgG treatment but not in wild-type keratinocytes. Representative of $n = 5$, *$p < 0.05$ vs. respective control. **(E)** Kymographs of fluorescence recovery after photobleaching experiments using Dsg3-eGFP-transfected KtyII wt and k.o. keratinocytes. **(F)** Immobile fractions of Dsg3-eGFP in KtyII wt and k.o. cells under basal conditions and after incubation with AK23 incubation for 1 h; $n = 7$, 5 cell borders/experiment; *$p < 0.05$.

biotinylation assay. In whole cell lysates, no reduction of Dsg3 levels was detectable in both cell lines (**Figure 2C**). However, in the surface membrane pool harvested *via* immunoprecipitation of biotin PV-IgG induced a significant depletion of Dsg3 in KtyII k.o. cells but not wt monolayers after 1 h of incubation (**Figures 2C,D**) indicating that the turnover of Dsgs is altered in keratin-deficient keratinocytes. This may be explained by enhanced mobility of Dsg3 when keratins are missing (25). Thus, we performed FRAP experiments on Dsg3-pEGFP-transfected KtyII cells using AK23. Indeed, KtyII k.o. cells revealed a reduced immobile fraction indicating higher mobility of Dsg3 molecules under basal conditions (**Figures 2E,F**). However, incubation of AK23 enhanced Dsg3 mobility in wt cells only suggesting that higher mobility resulted from keratin uncoupling (**Figures 2E,F**).

## PF-IgG and PV-IgG Cause Redistribution of Dsg1-Binding Events and Subsequently Reduce Dsg1-Binding Strength

Under cell-free conditions, direct inhibition of Dsg interaction was observed for Dsg3 but not for Dsg1 (8, 10, 12). To test whether direct inhibition of Dsg1 occurs on living keratinocytes, we performed AFM adhesion measurements using PF-IgG. Small areas along cell borders and on the cell surface above the nucleus (Figure S2A in Supplementary Material) were chosen and probed in FM mode.

As outlined earlier, under control conditions Dsg1-binding events exhibited clusters along the cell borders in wt cells and uniform distribution in KtyII k.o. cells. In line with this, less Dsg1-binding events were detected on the cell surface of wt cells

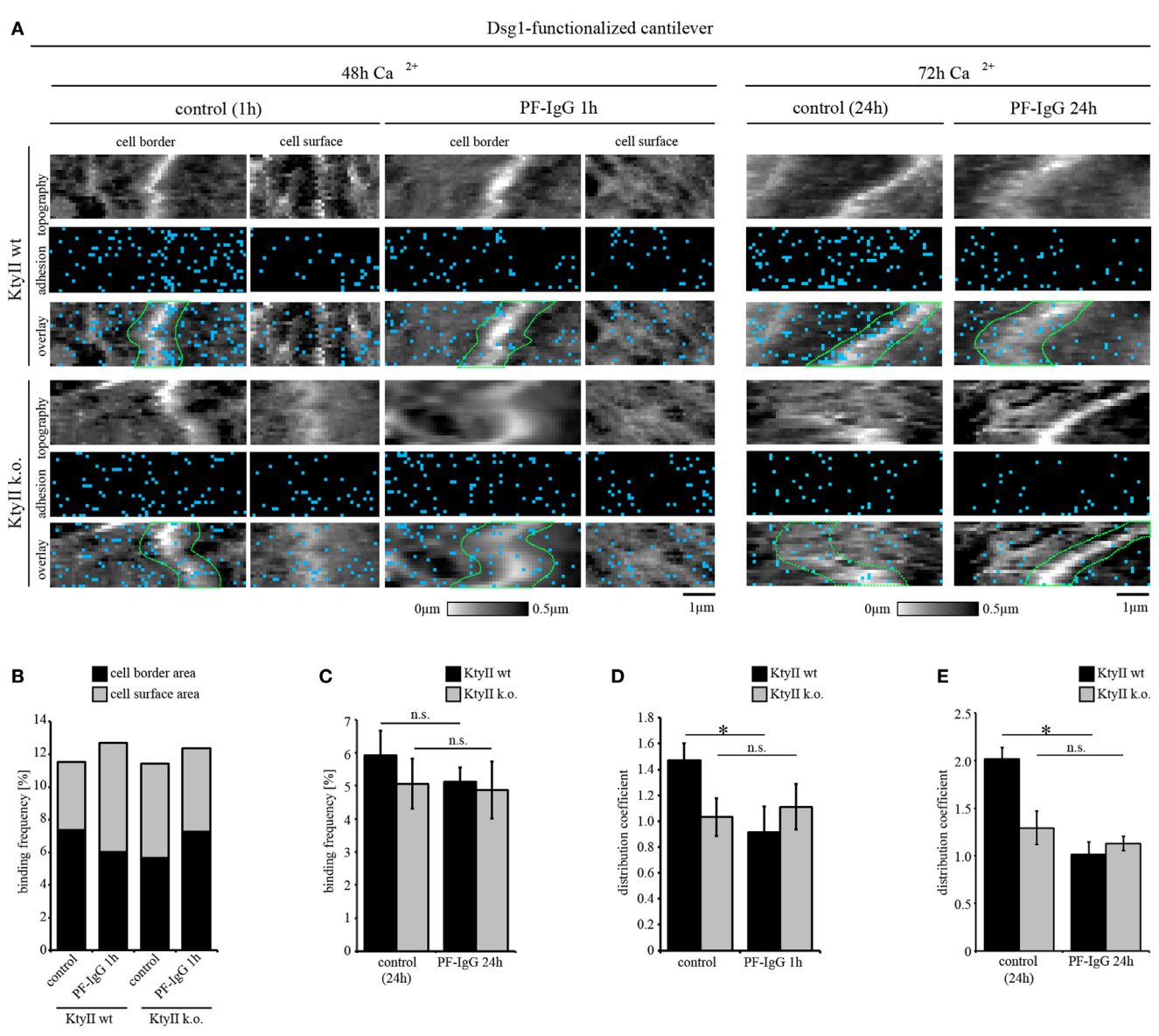


**FIGURE 3** | Continued

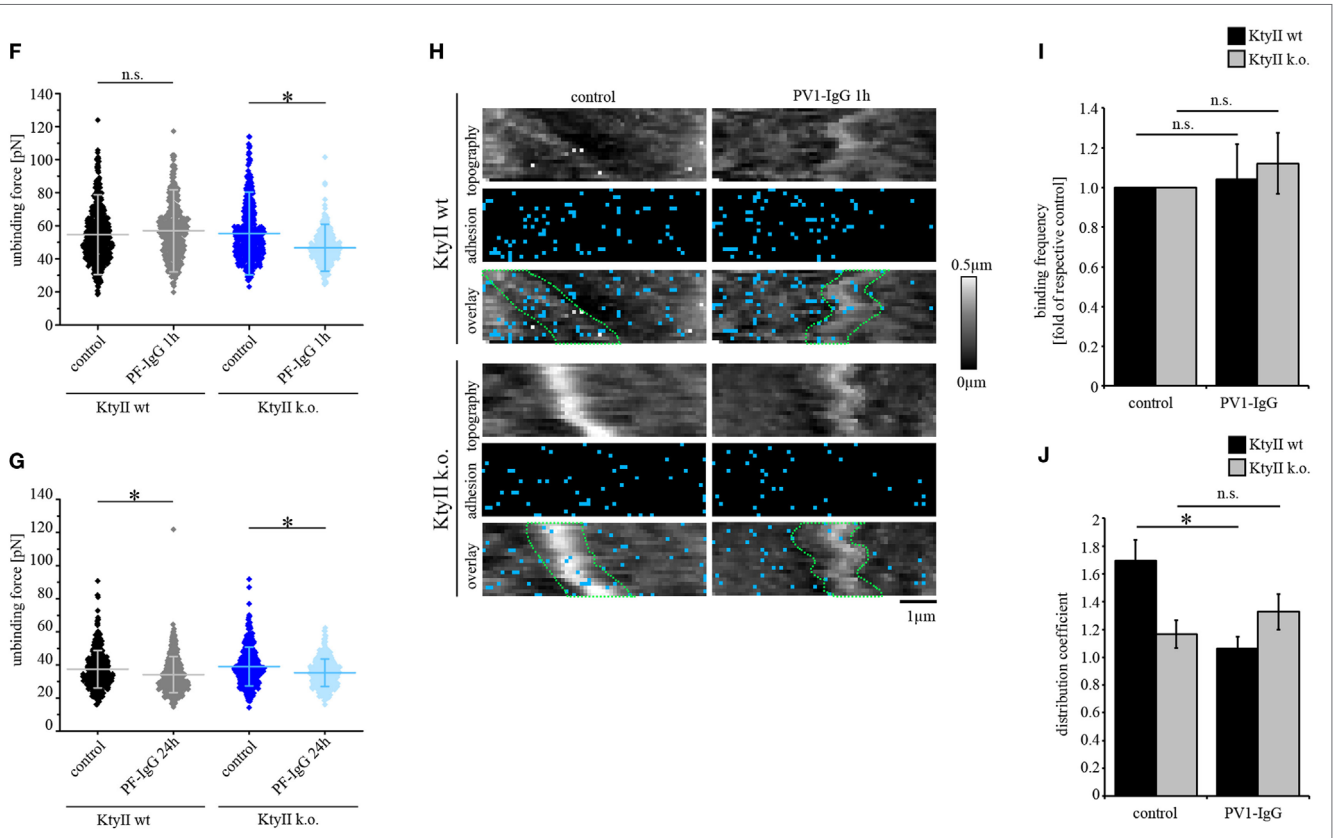


**FIGURE 3** | aDsg1 antibodies (Abs) causes a keratin-dependent redistribution of Dsg1. **(A)** Atomic force microscopy (AFM) adhesion measurements using Dsg1-Fc-functionalized tips at small areas along cell borders and on the cell surface above the nucleus. Pemphigus foliaceus (PF)-IgG for 1 h and 24 h induced redistribution of Dsg1 from cell junctions in wild type. **(B)** Dsg1-binding frequencies under control condition and after 1 h of PF-IgG treatment show no direct inhibition of binding events. **(C)** 24 h of PF-IgG treatment slightly reduced Dsg1-binding frequency in KtyII wt and k.o. cells. **(D,E)** Distribution coefficient of Dsg1-binding events under control conditions and after 1 and 24 h of PF-IgG incubation. $n = 4$ from 3 independent coating procedures, 1,200 force–distance curves/adhesion map (*$p < 0.05$). **(F,G)** Unbinding forces of Dsg1-binding events under control conditions and after 1 or 24 h of PF-IgG incubation. $n = 4$ from 3 independent coating procedures, 1,200 force–distance curves/adhesion map (*$p < 0.05$). **(H)** AFM adhesion measurements using Dsg1-Fc functionalized tips in KtyII wt and k.o. cells under control conditions or after incubation with pemphigus vulgaris (PV) 1-IgG containing aDsg1 Abs for 1 h. **(I)** Dsg1-binding frequency did not change after 1 h of PV-IgG treatment in both cell lines. **(J)** Distribution of Dsg1-binding events was altered in KtyII wt but not in KtyII k.o. cells after PV1-IgG treatment. $n = 4$ from 3 independent coating procedures, 1,200 force–distance curves/adhesion map (*$p < 0.05$).

compared with cell borders whereas no difference in binding frequency was observed in KtyII k.o. (**Figures 3A,B**; Figure S2B in Supplementary Material). Interestingly, the sum of binding frequencies along cell borders and on the cell surface was similar in both lines (**Figures 3A,B**), indicating that attachment to desmosomes is crucial for the localization of Dsg1 at cell borders. To test the specificity of Dsg1-binding events, we used a monoclonal aDsg1, which was capable of blocking homophilic interactions under cell-free conditions (25, 36). Incubation of the Ab for 1 h on the cells in the absence of cantilevers revealed a significant reduction of binding frequency in both cell lines indicating that we measured specific Dsg1 interactions (Figures S2C,D in Supplementary Material).

Next, we tested whether PF-IgG can induce direct inhibition of Dsg1 binding. Interestingly, PF-IgG did not reduce Dsg1-binding frequency in both cell lines but led to a redistribution of Dsg1-binding events from cell borders in wt cells (**Figure 3A**, cell borders surrounded by dashed green lines, **Figures 3B,D**) as reflected by the distribution coefficient (**Figure 3D**). However, no shift was observed in keratin-deficient keratinocytes where Dsg1 was less localized at cell borders under resting conditions (**Figures 3A,B,D**) suggesting that keratin uncoupling may account for this phenomenon. By contrast, after PF-IgG treatment for 1 h Dsg1-binding strength was reduced in KtyII k.o. cells only (**Figure 3F**). Thus, we assumed a cascade in which redistribution of Dsg1-binding events occurs first, followed by a reduction of Dsg1-binding strength, both of which may contribute to loss of intercellular adhesion. To test this, we incubated wt and k.o. cells with PF-IgG for 24 h. Importantly, 72 h after $Ca^{2+}$-induction, we observed binding properties of Dsg1 similar to that after 48 h (**Figure 3A**). Incubation with PF-IgG for 24 h did not significantly alter Dsg1-binding frequency (**Figure 3C**). In agreement with the alterations described above, less Dsg1-binding events localized to cell borders after 24 h of PF-IgG treatment in wt cells (**Figure 3E**). By contrast, binding forces were reduced in both cell lines after 24 h of PF-IgG treatment (**Figure 3G**) indicating that relocalization of Dsg1 preceded alterations in Dsg1 adhesive strength.

We confirmed these results for aDsg1 Abs with PV-IgG in Dsg1 adhesion measurements. Similar to PF-IgG, incubation with PV-IgG for 1 h led to no reduction in binding frequency in both lines whereas a redistribution of Dsg1-binding events was present in wt cells only (**Figures 3H–J**). Thus, the distribution coefficient of Dsg1-binding events was comparable in wt and k.o. cells after treatment with both PF- and PV-IgG (**Figures 3D,E,J**).

## p38MAPK Activation Induces Keratin Filament Retraction and Leads to Redistribution of Dsg1- and Dsg3-Binding Events

Activation of p38MAPK is a central signaling mechanism induced by pemphigus autoantibody binding and correlates with both, loss of intercellular adhesion and keratin filament retraction (13, 38, 39). Furthermore, inhibition of p38MAPK is capable of restoring intercellular adhesion and keratin filament alterations even under conditions in which direct inhibition of Dsg3 binding is present (11, 38). Furthermore, p38MAPK inhibition prevented Dsg3-binding force reduction in keratin-deficient keratinocytes which show an activation of p38MAPK already under basal conditions (25). Thus, we aimed to investigate how activation of p38MAPK affects Dsg binding properties. Since autoantibodies targeting Dsg3 induce direct inhibition and therefore do not allow characterization of binding properties by autoantibodies (8, 40), we followed a pharmacological approach more specific for p38MAPK and used anisomycin for 1 h to activate p38MAPK similar to previous studies (26). Anisomycin activated p38MAPK after 1 h of incubation both in KtyII k.o. and wt cells which was reduced by the p38MAPK

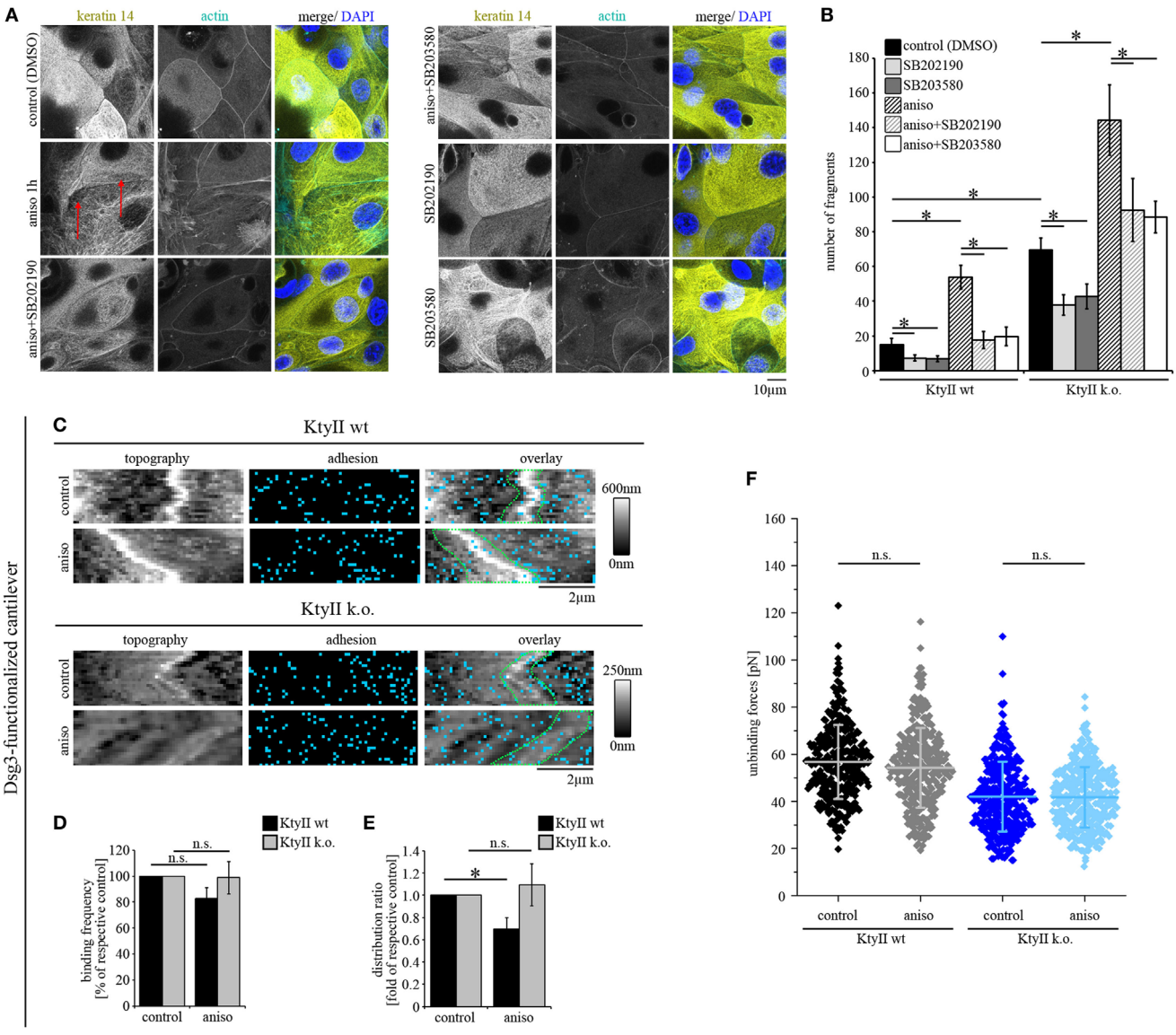


**FIGURE 4** | Continued

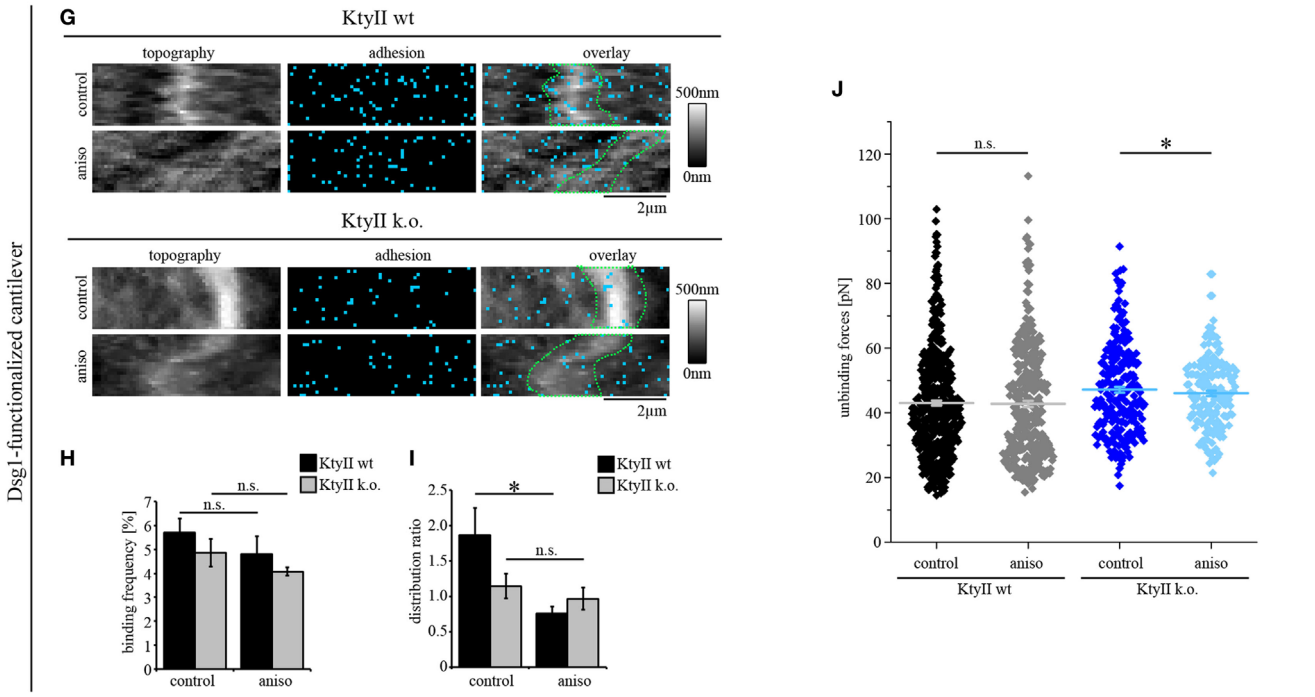


**FIGURE 4** | p38MAPK activation induces redistribution of Dsg1- and Dsg3-binding events. **(A)** Immunostaining of keratin 14 and Alexa488-phalloidin staining of actin in KtyII wt after anisomycin treatment for 1 h revealed keratin filament retraction (red arrows), which was blocked by p38MAPK inhibitors SB202190 and SB203580 when preincubated for 1 h. Representative images from $n = 4$. **(B)** Dissociation assay after treatment with anisomycin alone or after preincubation with SB202190 or SB203580 in keratin-deficient keratinocytes compared with wild-type (wt) ($n > 4$, $^*p < 0.05$). **(C–E)** Dsg3 adhesion measurements show no change in binding frequency after anisomycin treatment but reveal a redistribution of binding events away from cell borders in KtyII wt but not in KtyII k.o. cells. **(F)** Unbinding forces of Dsg3 adhesion measurements were not significantly altered in both cell lines. $n = 4$ from 3 independent coating procedures, 1,200 force–distance curves/adhesion map ($^*p < 0.05$). **(G–I)** Dsg1 adhesion measurements revealed redistribution of binding events away from cell borders in KtyII wt but not in KtyII k.o. cells. **(J)** Unbinding forces of Dsg1 adhesion measurements were not significantly altered in wt but reduced in KtyII k.o. cells. $n = 4$ from 3 independent coating procedures, 1,200 force–distance curves/adhesion map ($^*p < 0.05$).

inhibitors SB202190 and SB203580 as revealed by Western blotting (Figure S3A in Supplementary Material). First, we performed immunostaining against keratin 14 to study anisomycin-mediated alterations of keratin filaments in wt cells (**Figure 4A**). Anisomycin induced keratin filament retraction and reorganization of filaments toward thick bundles similar as described earlier for experiments with pathogenic autoantibodies (**Figure 4A**, arrows, compare with **Figure 1**). To confirm that the alterations were induced by anisomycin *via* activation of p38MAPK, we used the p38MAPK inhibitors SB202190 and SB203580, which alone had no effect on the morphology of keratin filaments. Nevertheless, both inhibitors abrogated anisomycin-induced keratin filament alterations (**Figure 4A**). Next, we tested whether effects of p38MAPK on intercellular adhesion is dependent on keratin filaments using a dissociation assay. Interestingly, anisomycin induced a drastic loss of intercellular adhesion in both KtyII wt and k.o. cells (**Figure 4B**; Figure S3B in Supplementary Material), which was blocked by co-incubation with p38MAPK inhibitors SB202190 and SB203580. Interestingly, both inhibitors improved basal cell adhesion in wt and keratin-deficient keratinocytes (**Figure 4B**; Figure S3B in Supplementary Material).

Next, we performed AFM adhesion measurements for Dsg3 and Dsg1 to characterize the effects of p38MAPK activation on Dsg binding properties. Under control conditions Dsg3-binding events were distributed uniformly over the cell surface (**Figure 4C**). After incubation with anisomycin for 1 h, the overall binding frequency was not changed in both cell lines (**Figures 4C,D**), but the distribution of Dsg3 was altered in KtyII wt cells and the distribution coefficient indicated less binding events along cell borders (**Figures 4C,E**). By contrast, distribution was not changed in KtyII k.o. cells (**Figures 4C,E**). Moreover, aniosomycin did not affect Dsg3 unbinding force (**Figure 4F**). Next, we performed Dsg1 adhesion measurements. Activation of p38MAPK using anisomycin for 1 h led to a redistribution of Dsg1-binding events from the cell borders only in wt keratinocytes (**Figures 4G–I**). Furthermore, binding strength of Dsg1 interactions were slightly reduced in KtyII k.o., but not in wt cell after activation of p38MAPK using anisomycin (**Figure 4J**). Taken together these data indicate that p38MAPK regulates organization of Dsg binding events.

## Effect of p38MAPK on Loss of Intercellular Adhesion Caused by Autoantibodies and Keratin Deficiency

Keratin-deficient keratinocytes show a robust activation of p38MAPK under untreated conditions (**Figure 5A**), which accounts for impaired Dsg3-binding forces on single molecule

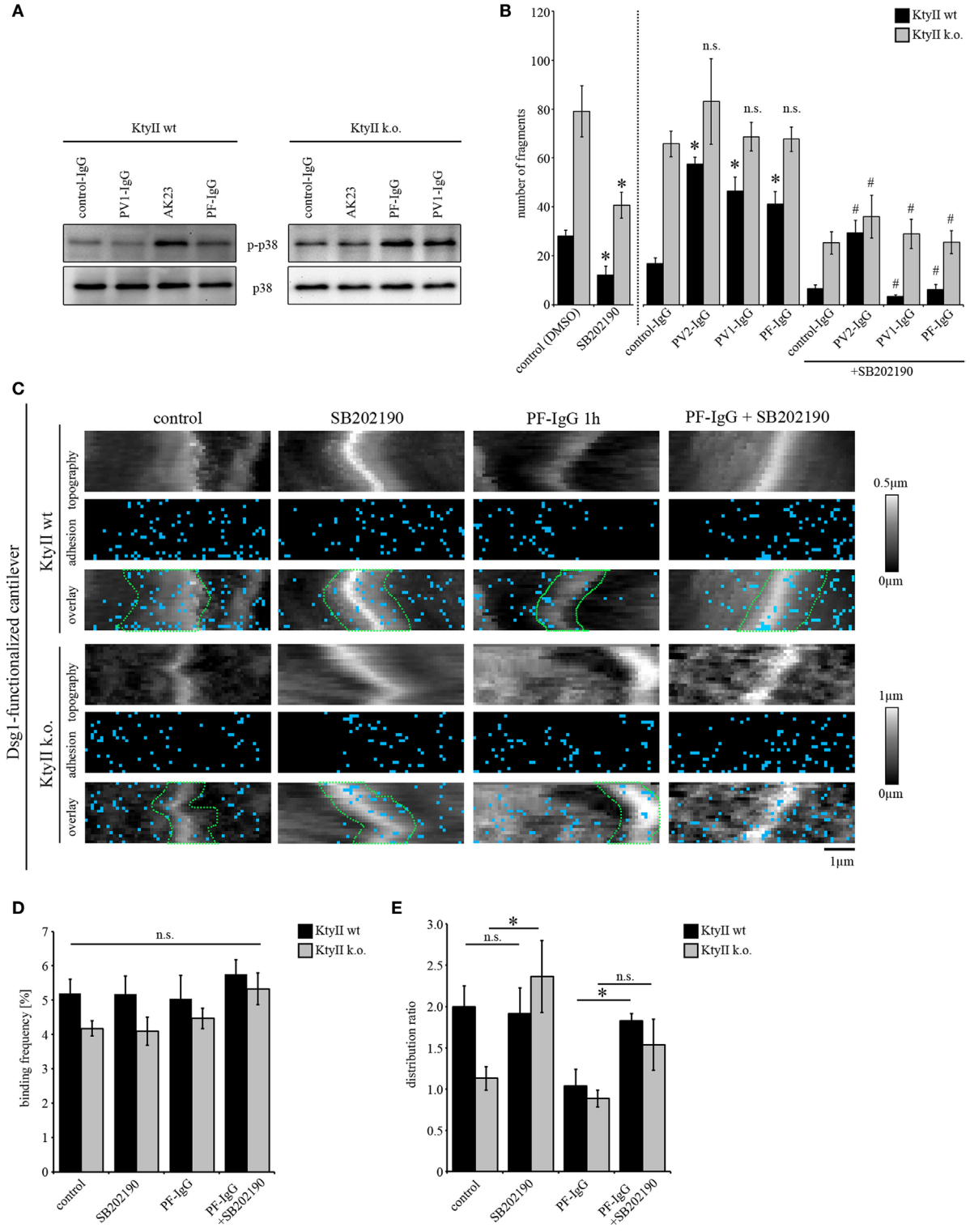


**FIGURE 5** | p38MAPK inhibition restores loss of intercellular adhesion caused by autoantibodies and keratin deficiency. **(A)** Western blot showing activation of p38MAPK after treatment with AK23, pemphigus vulgaris (PV) 1-IgG and pemphigus foliaceus (PF)-IgG for 1 h. Representative of $n > 4$. **(B)** Dissociation assay of KtyII wt and k.o. cells after incubation with pathogenic autoantibodies alone or in combination with SB202190 for 24 h ($n > 5$). $^{*}p < 0.05$ vs. respective control (control panel for SB202190-treated cells and control-IgG for conditions treated with pathogenic autoantibodies); $^{\#}p < 0.05$ vs. respective condition treated with pathogenic autoantibodies alone. **(C–E)** Dsg1 adhesion measurements reveal a redistribution of binding events away from cell borders in KtyII wt but not in KtyII k.o. cells after 1 h PF-IgG. SB202190 preincubation for 1 h blocked PF-IgG-induced redistribution in KtyII wt cells and alone caused redistribution of Dsg1-binding events to cell borders in k.o. cells. Binding frequencies were not altered in all conditions. $n = 3$ from 3 independent coating procedures, 1,200 force–distance curves/adhesion map ($^{*}p < 0.05$).

level (25). On the other hand, pemphigus autoantibodies were not effective to induce additional loss of cell cohesion in KtyII k.o. cells. Thus, we investigated whether autoantibody-induced p38MAPK activation is dependent on expression of keratins. Interestingly, all autoantibodies induced an activation of p38MAPK after 1 h of incubation (**Figure 5A**) in both KtyII wt and k.o. cell lines indicating that mechanisms leading to an activation of p38MAPK after autoantibody binding are still present in keratin-deficient keratinocytes (**Figure 4A**). Thus, we wondered whether inhibition of p38MAPK would restore intercellular adhesion after autoantibody treatment in both cell lines. As efficiency of p38MAPK inhibition was similar for both inhibitors SB202190 and SB203580, we used SB202190 only for the further experiments (**Figure 5B**). As shown above, all Ab fractions caused loss of intercellular adhesion in KtyII wt but not in KtyII k.o. cells after 24 h of incubation (**Figure 5B**). SB202190 in KtyII wt cells blocked loss of cohesion after autoantibody treatment and in addition restored intercellular adhesion in keratin-deficient keratinocytes to levels of wt cells (**Figure 5B**).

Next, we probed the effect of p38MAPK inhibition on Dsg binding properties after autoantibody incubation by AFM. Since Dsg3-binding events cannot be characterized because of autoantibody-mediated direct inhibition (11) we here focused on Dsg1-binding properties. For AFM experiments, cells were treated either with SB202190 or PF-IgG alone or in a combination using a preincubation of SB202190 for 1 h followed by addition of PF-IgG for another 1 h. After treatment cells were extensively washed and reprobed using a cantilever functionalized with Dsg1. Again, PF-IgG alone caused redistribution of Dsg1-binding events away from the cell borders as outlined above whereas no change was observed in KtyII k.o. cells (**Figure 5C**). SB202190 alone did not change distribution or number of Dsg1-binding events in wt keratinocytes, but led to redistribution toward the cell borders in k.o. cells (**Figures 5C–E**). Furthermore, SB202190 abolished PF-IgG-induced redistribution in wt cells indicating that p38MAPK signaling participates in the relocalization of Dsg1 from cell junctions in pemphigus (**Figures 5C–E**). Taken together, the last set of data supports the notion that loss of cell cohesion caused by both autoantibodies and, keratin deficiency is mediated or at least modulated by p38MAPK and that relocalization of Dsg1 may be a primary mechanism to destabilize keratinocyte cohesion. Moreover, together with experiments using anisomycin described earlier, the data suggest that the targets of p38MAPK autoantibodies are to some extent not dependent on expression of keratins.

## DISCUSSION

Taken together, the data presented demonstrate that keratins differentially regulate the binding properties of Dsg1 and 3, the two major antigens of pemphigus. Moreover, we observed that direct inhibition of Dsg3 but not of Dsg1-binding occurs on living keratinocytes treated with PV-IgG and PF-IgG. We found that p38MAPK signaling is crucial for loss of cell cohesion in response to both pemphigus autoantibodies as well as keratin deficiency. Importantly, PV-IgG and PF-IgG as well as direct p38MAPK activation induced redistribution of Dsg1-binding events away from cell borders in wt keratinocytes resulting in a Dsg1 distribution pattern similar to keratin-deficient keratinocytes. No temporal sequence and thus no causative relation between keratin retraction and Dsg redistribution as the underlying mechanism for loss of intercellular adhesion are provided by the data of the study. However, the data demonstrate that keratin deficiency induces activation of p38MAPK and that p38MAPK regulates Dsg distribution. This indicates that keratin uncoupling may account for loss of cell cohesion by redistribution of Dsg1. Thus, we propose the concept that as least in part loss of intercellular adhesion in pemphigus is mediated by keratin-dependent regulation of binding properties and distribution of desmosomal cadherins *via* p38MAPK.

### Keratins Regulate Distribution and Binding Properties of Pemphigus Antigens Dsg1 and 3

Keratin filaments are crucial for mechanical properties and stability of keratinocytes (24, 41–43). Furthermore, they influence the turnover of desmosomal components (44) such as DP (45) and plakophilins (46, 47) and regulate desmosomal adhesion through signaling (22, 23, 48). Moreover, keratin filament retraction is a morphological hallmark in pemphigus pathogenesis and correlates with loss of intercellular adhesion, depletion of Dsgs from the cell membrane and is interconnected with several signaling pathways known to be crucial for pemphigus such as PKC and p38MAPK (11, 15, 25). Until now, no temporal sequence could be delineated for Dsg internalization and keratin retraction. Some studies indicate that keratin retraction does only occur when desmosomes are lost (17) whereas other studies implicate that Dsgs internalization and uncoupling from keratins are temporally closely related (Schlögl et al., this issue) or show that Dsgs which are not coupled to keratins get rapidly internalized after autoantibody treatment (49).

In the study presented here we show that keratins regulate the binding properties of Dsg1 and Dsg3, which are the major antigens in pemphigus (7, 50), and propose a new concept how keratins could directly influence desmosomal adhesion. It is conceivable that keratins by anchoring the desmosomal plaque modulate the binding properties of desmosomal cadherins which may account for the observation that retraction of keratin filaments from the desmosomal plaque after treatment with autoantibodies similar to deficiency of keratins impairs intercellular adhesion (13, 15, 22, 26). In line with this, it was reported that increased DP association to keratins strengthened intercellular adhesion and reduced autoantibody induces loss of intercellular adhesion in a pemphigus model (14, 45). With this respect, we observed the effect of keratins on desmosomal cadherin binding properties is different for Dsg isoforms. More Dsg3-binding events occurred in keratin-deficient keratinocytes whereas less interactions were detectable for Dsg1. For Dsg3, enhanced Dsg3 expression may reflect an insufficient compensatory mechanism because mRNA levels were elevated in keratin-deficient keratinocytes (25). Furthermore, it appears that keratins are not crucial for proper localization of Dsg3 at cell junctions (**Figure 2C**). By contrast, keratin expression was

crucial for proper localization of Dsg1 to cell junctions. As known for other desmosomal cadherins this may be explained by posttranslational modifications such as phosphorylation and palmitoylation leading to altered expression or membrane localization of the respective isoform (51, 52). However, also alterations in desmosomal turnover could account for this phenomenon (9, 23, 44). Interestingly, in pemphigus patients smaller desmosomes were reported for aDsg1 but not for aDsg3 antibodies, fitting to the observation that keratins differentially regulate Dsg distribution and binding properties (53). In addition, adhesive strength of Dsg3 but not of Dsg1 binding was altered by absence of keratins (**Figure 3**). Thus, additionally to reduced Dsg3-binding forces keratin-dependent clustering of Dsg1 may also be crucial for strong intercellular adhesion which is well established for classical cadherins (54, 55). Changes in binding forces maybe caused by missing anchorage of the molecules or by conformational changes induced by loss of keratin coupling (42, 56) or induced by signal pathways such as p38MAPK which were shown to restore Dsg3-binding force in keratin-deficient keratinocytes (25). Finally, Dsg3 depletion was accelerated in keratin-deficient keratinocytes, which could be caused by a higher molecule mobility found when keratins are missing. Beginning of depletion of Dsg3 molecules was not detectable before 1 h after incubation with PV-IgG in wt keratinocytes which is contradictory to other studies where depletion was already detectable after 30 min of autoantibody incubation (57, 58). However, these differences in our opinion can be explained by different model systems, methodical approach and several PV-IgG fractions used in the respective studies (51, 59–61). Changes in molecule mobility may depend on PKC signaling (22, 23, 25) and be accompanied with changes in clustering of the desmosomal molecules. Thus, clustering which conforms to the note that it is crucial for proper adhesive function (5, 62), could serve as an explanation for altered forces.

## Mechanisms of Loss of Intercellular Adhesion in PF

Direct inhibition of Dsg interaction was thought to be the primary mechanism for loss of intercellular adhesion in pemphigus because autoantibodies predominantly target the EC1 domain (63). Indeed, direct inhibition of Dsg3 binding has been shown to occur after incubation with AK23 or with PV-IgG both under cell-free conditions as well as on the surface of living keratinocytes (8, 10, 11, 64). However, no direct inhibition of Dsg1 interactions was observed for both PV-IgG and PF-IgG, at least under cell-free conditions (8, 10, 12). Rather, signaling mechanisms were found to be crucial for loss of intercellular adhesion in response to pemphigus autoantibodies both in PV and PF (4, 7). Since several signaling pathways were found to be activated after binding of autoantibodies against Dsg1 and 3 such as p38MAPK, Erk, and Src (8, 37, 65–68), the molecular mechanism how PF-IgG impairs Dsg1 binding is not elucidated yet.

In this study, we demonstrate that keratins are crucial for proper localization of Dsg1 at cell junctions. Furthermore, we observed that PF-IgG led to a redistribution of Dsg1-binding events from cell junctions thereby inducing a distribution pattern similar to Dsg1 distribution of keratin-deficient keratinocytes. Together with the finding that PF-IgG similar to PV-IgG did not further impair keratinocyte cohesion in keratin-deficient cells, this suggests that uncoupling of keratin filaments from the desmosomal plaque maybe the underlying mechanism for both redistribution of Dsg1 and loss of keratinocyte cohesion. This is in line with an altered clustering of Dsg1 in pemphigus patients' lesions which was described using electron microscopy (17, 20). Furthermore, we observed Dsg1-binding forces were reduced after 1 h of PF-IgG treatment in keratin-deficient keratinocytes but not in wt cells whereas forces were reduced in the wt monolayers after 24 h as well, suggesting that redistribution of Dsg1 may precede reduction of Dsg1-binding forces. Thus, a possible sequence of events after PF-IgG binding is conceivable in which Dsg1 redistribution caused by uncoupling from keratins and subsequently impaired Dsg1-binding forces may account for loss of intercellular adhesion. Similarly, a sequence of distinct phases has been shown for treatment with PV-IgG before (49, 69, 70). Here, depletion of non-desmosomal Dsg3 with the first 2 h was followed by rearrangement of desmosomal components into linear arrays aligned with keratin filaments between 2 and 6 h. From these arrays, desmosomal components including Dsg3 were internalized within 6–24 h, which was paralleled by disassembly of desmosomes. Furthermore, uncoupling and redistribution of Dsg3 may also be explained by the concept of Dsg non-assembly depletion hypothesis (20). Direct inhibition of Dsg3 binding occurring as fast as within 15 min (11) may facilitate depletion of both non-desmosomal as well desmosomal Dsg3. Because within the first hour of autoantibody incubation we observed redistribution of Dsg1 from cell junctions, the data of this study are in line with the hypothesis that Dsg1 after treatment with PF-IgG is affected in comparable manner, however, in absence of direct inhibition of Dsg1 interaction.

## Keratin-Dependent p38MAPK Signaling Contributes to Loss of Intercellular Adhesion in Pemphigus

Signaling pathways essentially contribute to the loss of intercellular adhesion in pemphigus (4, 7). As mentioned earlier, a broad spectrum of signaling mechanisms contribute to the loss of intercellular adhesion including PKC, Erk, Src, and p38MAPK (5). Especially, p38MAPK signaling is well characterized. Pemphigus autoantibodies induce activation of p38MAPK, and inhibition of this pathway is effective to inhibit both loss of intercellular adhesion and keratin filament alterations induced by pemphigus autoantibodies in cell culture (13, 38, 39, 71, 72). More recently, AK23- and PV-IgG-induced alterations of keratin insertion into desmosomes in human epidermis *ex vivo* as revealed by electron microscopy were shown to be dependent on p38MAPK (18). Furthermore, rapid disruption of the keratin cytoskeleton also induced p38MAPK activation whereas inhibition of p38MAPK abrogated pharmacological disruption of the keratin cytoskeleton (73–75) indicating that keratin reorganization and p38MAPK signaling are closely related.

Here, we observed that activation of p38MAPK both mediated by anisomycin as well as in response to pemphigus autoantibodies induced keratin filament retraction and led to a redistribution of

Dsg3-binding events away from the cell borders in wt but not in keratin-deficient keratinocytes. Similarly, pemphigus antibodies as well anisomycin activated p38MAPK in both wt and keratin-deficient cells, the latter of which displayed robust activation of p38MAPK under resting conditions (25). Interestingly, p38MAPK activation in response to AK23 and PV-IgG was stronger in keratin-deficient cells after 1 h when compared with wt cells. All these data indicate that keratins participate in the suppression of p38MAPK activity. By contrast, anisomycin was effective to further impair cell cohesion in keratin-deficient cells whereas AK23, PV-IgG, and PF-IgG were not. Since anisomycin-induced loss of cell adhesion was abrogated by two different inhibitors of p38MAPK, loss of adhesion appears not to be due to off-target effects. Rather, this discrepancy may be explained by the observation that anisomycin is stronger to activate p38MAPK compared with autoantibodies. Alternatively, it is possible that several p38MAPK pools are available in cells (76, 77) which when activated by anisomycin contribute to loss of cell cohesion, whereas p38MAPK activation in response to autoantibodies is restricted to the pool associated with desmosomal cadherins as shown for Dsg3 (26). Indeed, immunostaining revealed that in contrast to Src only a small portion of p38MAPK was confined to cell junctions (66). Nevertheless, inhibition of p38MAPK restored intercellular adhesion after pemphigus autoantibody treatment in wt and k.o. cells and rescued keratinocyte cohesion in keratin-deficient cells indicating that p38MAPK signaling is crucial for intercellular adhesion. This is in line with former studies which show that keratin filament alteration correlate with loss of intercellular adhesion in pemphigus (11, 13, 37). Moreover, these data demonstrate that the targets of p38MAPK are in part keratin dependent, as indicated by anisomycin-mediated keratin retraction which is similarly observed after treatment with autoantibodies. In addition, given the efficiency of p38MAPK inhibitors on cell cohesion in keratin-deficient cells, keratin-independent targets must also be involved. However, it has to be noted that no temporal sequence can be ascertained by the data provided. Taken together, the data show that p38MAPK activation in response to pemphigus autoantibodies is regulated *via* keratin filaments and is critical for loss of cell adhesion. This is at least in part mediated on the level of redistribution of Dsg1 and Dsg3 molecules from cell junctions.

## ETHICS STATEMENT

The human sera used in this study were collected and used in accordance with the recommendations of ethic committee of University of Lübeck, AZ 12-178. Name of the indicated project: Autoantikörperreaktivität und Pathophysiologie bei blasenbildenden Autoimmundermatosen (Pemphigoid und Pemphigus).

## AUTHOR CONTRIBUTIONS

FV, EW, MF, and MR performed experiments. FV, MR, and FB analyzed data. FV, TM, and VS discussed data and interpreted results. FV and JW designed the study and wrote the manuscript.

## ACKNOWLEDGMENTS

We thank Andrea Wehmeyer, Sabine Mühlsimer, Kilian Skowranek, and Linda Jakobi for excellent technical assistance, Enno Schmidt (Department of Dermatology, University of Lübeck) for providing patients sera, and JPK Instruments for helpful discussion on the AFM data.

## FUNDING

Supported by Friedrich-Baur-Stiftung 01/16 to FV and DFG SPP1782 and DFG FOR 2497 to JW.

## SUPPLEMENTARY MATERIAL

The Supplementary Material for this article can be found online at https://www.frontiersin.org/articles/10.3389/fimmu.2018.00528/full#supplementary-material.

**FIGURE S1** | Distribution coefficient to determine localization of desmoglein binding events. **(A)** For calculation of intensity coefficient areas in close proximity to the cell borders (red rectangle) and above the nuclei (green rectangle) were chosen, intensity was measured, and a coefficient was calculated in which values <1 indicate less keratin fluorescence signal at cell border areas, thus suggesting keratin retraction under these conditions. **(B)** For calculation of distribution coefficient, areas along the cell borders (green area) and on the cell surface (red area) were marked, and respective binding frequencies were defined by calculating a ratio of number of binding events per area. Distribution coefficient was calculated as a ratio from these. Binding frequencies in which values >1 announce increased clusters of the molecules along the cell borders. **(C)** Immunostaining of KtyII wt and KtyII k.o. cells show dense filamental structures throughout the whole cell in wild-type and confirm knockout in KtyII k.o. cells. Representative of $n = 4$.

**FIGURE S2** | Dsg1-binding events in KtyII wt and k.o. cells. **(A)** Topography overview images of KtyII wt and k.o. cells. Small areas along the cell borders (green rectangles, 6 μm × 2 μm) and cell surfaces above the nucleus (red rectangles, 4 μm × 2 μm) were chosen for adhesion mapping presented in **Figure 3**. **(B)** Dsg1-binding frequency in KtyII wt and k.o. cells at cell border and cell surface areas under control conditions and after treatment with pemphigus foliaceus (PF)-IgG for 1 h. $n = 3$ from 3 independent coating procedures, 1,200 force–distance curves/adhesion map (*$p < 0.05$). **(C,D)** Dsg1 adhesion measurements at cell borders in KtyII wt and k.o. cells under control conditions and after treatment with aDsg1 monoclonal antibody (mAb) (p124). $n = 3$ from 3 independent coating procedures, 1,200 force–distance curves/adhesion map (*$p < 0.05$). **(E)** Immunostaining of keratin 14 in KtyII wt after anisomycin treatment in higher magnification for 1 h revealed keratin filament retraction. Representative images from $n = 4$.

**FIGURE S3** | p38MAPK signaling is crucial for intercellular adhesion in KtyII wt and k.o. cells. **(A)** Western blot using SB202190 and SB203580 for 2 h to inhibit and anisomycin for 1 h to activate p38MAPK. KtyII k.o. cells show activation of p38MAPK under basal conditions compared with wild-type (wt) cells. Anisomycin drastically increased p38MAPK activation, which was partially blocked by SB202190 and SB203580. For co-incubation experiments, SB202190 and SB203580 were preincubated for 1 h before anisomycin was added for 1 h. **(B)** Pictures of dissociation assay from **Figure 4** confirmed impaired adhesion in keratin-deficient keratinocytes compared with wt. Activation of p38MAPK with anisomycin reduced intercellular adhesion whereas SB202190 or SB203580 improved intercellular adhesion in both cell lines ($n > 4$, *$p < 0.05$).

## REFERENCES


1. Delva E, Tucker DK, Kowalczyk AP. The desmosome. *Cold Spring Harb Perspect Biol* (2009) 1(2):a002543. doi:10.1101/cshperspect.a002543
2. Garrod DR, Merritt AJ, Nie Z. Desmosomal adhesion: structural basis, molecular mechanism and regulation (review). *Mol Membr Biol* (2002) 19(2):81–94. doi:10.1080/09687680210132476
3. Waschke J. The desmosome and pemphigus. *Histochem Cell Biol* (2008) 130(1):21–54. doi:10.1007/s00418-008-0420-0
4. Kitajima Y. New insights into desmosome regulation and pemphigus blistering as a desmosome-remodeling disease. *Kaohsiung J Med Sci* (2013) 29(1):1–13. doi:10.1016/j.kjms.2012.08.001
5. Waschke J, Spindler V. Desmosomes and extradesmosomal adhesive signaling contacts in pemphigus. *Med Res Rev* (2014) 34(6):1127–45. doi:10.1002/med.21310
6. Kneisel A, Hertl M. Autoimmune bullous skin diseases. Part 1: clinical manifestations. *J Dtsch Dermatol Ges* (2011) 9(10):844–56; quiz 57. doi:10.1111/j.1610-0387.2011.07793.x
7. Spindler V, Eming R, Schmidt E, Amagai M, Grando S, Jonkman MF, et al. Mechanisms causing loss of keratinocyte cohesion in pemphigus. *J Invest Dermatol* (2018) 138(1):32–7. doi:10.1016/j.jid.2017.06.022
8. Walter E, Vielmuth F, Rotkopf L, Sardy M, Horvath ON, Goebeler M, et al. Different signaling patterns contribute to loss of keratinocyte cohesion dependent on autoantibody profile in pemphigus. *Sci Rep* (2017) 7(1):3579. doi:10.1038/s41598-017-03697-7
9. Spindler V, Waschke J. Pemphigus—a disease of desmosome dysfunction caused by multiple mechanisms. *Front Immunol* (2018) 9:136. doi:10.3389/fimmu.2018.00136
10. Heupel WM, Zillikens D, Drenckhahn D, Waschke J. Pemphigus vulgaris IgG directly inhibit desmoglein 3-mediated transinteraction. *J Immunol* (2008) 181(3):1825–34. doi:10.4049/jimmunol.181.3.1825
11. Vielmuth F, Waschke J, Spindler V. Loss of desmoglein binding is not sufficient for keratinocyte dissociation in pemphigus. *J Invest Dermatol* (2015) 135(12):3068–77. doi:10.1038/jid.2015.324
12. Waschke J, Bruggeman P, Baumgartner W, Zillikens D, Drenckhahn D. Pemphigus foliaceus IgG causes dissociation of desmoglein 1-containing junctions without blocking desmoglein 1 transinteraction. *J Clin Invest* (2005) 115(11):3157–65. doi:10.1172/JCI23475
13. Berkowitz P, Hu P, Liu Z, Diaz LA, Enghild JJ, Chua MP, et al. Desmosome signaling. Inhibition of p38MAPK prevents pemphigus vulgaris IgG-induced cytoskeleton reorganization. *J Biol Chem* (2005) 280(25):23778–84. doi:10.1074/jbc.M501365200
14. Dehner C, Rotzer V, Waschke J, Spindler V. A desmoplakin point mutation with enhanced keratin association ameliorates pemphigus vulgaris autoantibody-mediated loss of cell cohesion. *Am J Pathol* (2014) 184(9):2528–36. doi:10.1016/j.ajpath.2014.05.016
15. Muller EJ, Hunziker T, Suter MM. Keratin intermediate filament retraction is linked to plakoglobin-dependent signaling in pemphigus vulgaris. *J Am Acad Dermatol* (2007) 56(5):890–1; author reply 1–2. doi:10.1016/j.jaad.2006.10.989
16. Caldelari R, de Bruin A, Baumann D, Suter MM, Bierkamp C, Balmer V, et al. A central role for the armadillo protein plakoglobin in the autoimmune disease pemphigus vulgaris. *J Cell Biol* (2001) 153(4):823–34. doi:10.1083/jcb.153.4.823
17. Sokol E, Kramer D, Diercks GFH, Kuipers J, Jonkman MF, Pas HH, et al. Large-scale electron microscopy maps of patient skin and mucosa provide insight into pathogenesis of blistering diseases. *J Invest Dermatol* (2015) 135(7):1763–70. doi:10.1038/jid.2015.109
18. Egu DT, Walter E, Spindler V, Waschke J. Inhibition of p38MAPK signaling prevents epidermal blistering and alterations of desmosome structure induced by pemphigus autoantibodies in human epidermis. *Br J Dermatol* (2017) 177(6):1612–8. doi:10.1111/bjd.15721
19. Spindler V, Endlich A, Hartlieb E, Vielmuth F, Schmidt E, Waschke J. The extent of desmoglein 3 depletion in pemphigus vulgaris is dependent on Ca(2+)-induced differentiation: a role in suprabasal epidermal skin splitting? *Am J Pathol* (2011) 179(4):1905–16. doi:10.1016/j.ajpath.2011.06.043
20. Oktarina DA, van der Wier G, Diercks GF, Jonkman MF, Pas HH. IgG-induced clustering of desmogleins 1 and 3 in skin of patients with pemphigus fits with the desmoglein nonassembly depletion hypothesis. *Br J Dermatol* (2011) 165(3):552–62. doi:10.1111/j.1365-2133.2011.10463.x
21. Wilgram GF, Caulfield JB, Lever WF. An electron microscopic study of acantholysis in pemphigus vulgaris. *J Invest Dermatol* (1961) 36:373–82. doi:10.1038/jid.1961.58
22. Kroger C, Loschke F, Schwarz N, Windoffer R, Leube RE, Magin TM. Keratins control intercellular adhesion involving PKC-alpha-mediated desmoplakin phosphorylation. *J Cell Biol* (2013) 201(5):681–92. doi:10.1083/jcb.201208162
23. Loschke F, Homberg M, Magin TM. Keratin isotypes control desmosome stability and dynamics through PKCalpha. *J Invest Dermatol* (2015) 136:202–13. doi:10.1038/jid.2015.403
24. Ramms L, Fabris G, Windoffer R, Schwarz N, Springer R, Zhou C, et al. Keratins as the main component for the mechanical integrity of keratinocytes. *Proc Natl Acad Sci U S A* (2013) 110(46):18513–8. doi:10.1073/pnas.1313491110
25. Vielmuth F, Wanuske MT, Radeva MY, Hiermaier M, Kugelmann D, Walter E, et al. Keratins regulate the adhesive properties of desmosomal cadherins through signaling. *J Invest Dermatol* (2018) 138(1):121–31. doi:10.1016/j.jid.2017.08.033
26. Spindler V, Rotzer V, Dehner C, Kempf B, Gliem M, Radeva M, et al. Peptide-mediated desmoglein 3 crosslinking prevents pemphigus vulgaris autoantibody-induced skin blistering. *J Clin Invest* (2013) 123(2):800–11. doi:10.1172/JCI60139
27. Hartlieb E, Kempf B, Partilla M, Vigh B, Spindler V, Waschke J. Desmoglein 2 is less important than desmoglein 3 for keratinocyte cohesion. *PLoS One* (2013) 8(1):e53739. doi:10.1371/journal.pone.0053739
28. Rotzer V, Breit A, Waschke J, Spindler V. Adducin is required for desmosomal cohesion in keratinocytes. *J Biol Chem* (2014) 289(21):14925–40. doi:10.1074/jbc.M113.527127
29. Vielmuth F, Hartlieb E, Kugelmann D, Waschke J, Spindler V. Atomic force microscopy identifies regions of distinct desmoglein 3 adhesive properties on living keratinocytes. *Nanomedicine* (2015) 11(3):511–20. doi:10.1016/j.nano.2014.10.006
30. Ebner A, Wildling L, Kamruzzahan AS, Rankl C, Wruss J, Hahn CD, et al. A new, simple method for linking of antibodies to atomic force microscopy tips. *Bioconjug Chem* (2007) 18(4):1176–84. doi:10.1021/bc070030s
31. Carvalho FA, Santos NC. Atomic force microscopy-based force spectroscopy – biological and biomedical applications. *IUBMB Life* (2012) 64(6):465–72. doi:10.1002/iub.1037
32. Schinner C, Vielmuth F, Rotzer V, Hiermaier M, Radeva MY, Co TK, et al. Adrenergic signaling strengthens cardiac myocyte cohesion. *Circ Res* (2017) 120(8):1305–17. doi:10.1161/CIRCRESAHA.116.309631
33. Tsunoda K, Ota T, Aoki M, Yamada T, Nagai T, Nakagawa T, et al. Induction of pemphigus phenotype by a mouse monoclonal antibody against the amino-terminal adhesive interface of desmoglein 3. *J Immunol* (2003) 170(4):2170–8. doi:10.4049/jimmunol.170.4.2170
34. Nie Z, Merritt A, Rouhi-Parkouhi M, Tabernero L, Garrod D. Membrane-impermeable cross-linking provides evidence for homophilic, isoform-specific binding of desmosomal cadherins in epithelial cells. *J Biol Chem* (2011) 286(3):2143–54. doi:10.1074/jbc.M110.192245
35. Harrison OJ, Brasch J, Lasso G, Katsamba PS, Ahlsen G, Honig B, et al. Structural basis of adhesive binding by desmocollins and desmogleins. *Proc Natl Acad Sci U S A* (2016) 113(26):7160–5. doi:10.1073/pnas.1606272113
36. Spindler V, Heupel WM, Efthymiadis A, Schmidt E, Eming R, Rankl C, et al. Desmocollin 3-mediated binding is crucial for keratinocyte cohesion and is impaired in pemphigus. *J Biol Chem* (2009) 284(44):30556–64. doi:10.1074/jbc.M109.024810
37. Jolly PS, Berkowitz P, Bektas M, Lee HE, Chua M, Diaz LA, et al. p38MAPK signaling and desmoglein-3 internalization are linked events in pemphigus acantholysis. *J Biol Chem* (2010) 285(12):8936–41. doi:10.1074/jbc.M109.087999
38. Berkowitz P, Chua M, Liu Z, Diaz LA, Rubenstein DS. Autoantibodies in the autoimmune disease pemphigus foliaceus induce blistering via p38 mitogen-activated protein kinase-dependent signaling in the skin. *Am J Pathol* (2008) 173(6):1628–36. doi:10.2353/ajpath.2008.080391
39. Berkowitz P, Diaz LA, Hall RP, Rubenstein DS. Induction of p38MAPK and HSP27 phosphorylation in pemphigus patient skin. *J Invest Dermatol* (2008) 128(3):738–40. doi:10.1038/sj.jid.5701080

40. Spindler V, Waschke J. Desmosomal cadherins and signaling: lessons from autoimmune disease. *Cell Commun Adhes* (2014) 21(1):77–84. doi:10.3109/15419061.2013.877000
41. Osmani N, Labouesse M. Remodeling of keratin-coupled cell adhesion complexes. *Curr Opin Cell Biol* (2014) 32C:30–8. doi:10.1016/j.ceb.2014.10.004
42. Loschke F, Seltmann K, Bouameur JE, Magin TM. Regulation of keratin network organization. *Curr Opin Cell Biol* (2015) 32:56–64. doi:10.1016/j.ceb.2014.12.006
43. Seltmann K, Fritsch AW, Kas JA, Magin TM. Keratins significantly contribute to cell stiffness and impact invasive behavior. *Proc Natl Acad Sci U S A* (2013) 110(46):18507–12. doi:10.1073/pnas.1310493110
44. Nekrasova O, Green KJ. Desmosome assembly and dynamics. *Trends Cell Biol* (2013) 23(11):537–46. doi:10.1016/j.tcb.2013.06.004
45. Godsel LM, Hsieh SN, Amargo EV, Bass AE, Pascoe-McGillicuddy LT, Huen AC, et al. Desmoplakin assembly dynamics in four dimensions: multiple phases differentially regulated by intermediate filaments and actin. *J Cell Biol* (2005) 171(6):1045–59. doi:10.1083/jcb.200510038
46. Olivry T, Linder KE, Wang P, Bizikova P, Bernstein JA, Dunston SM, et al. Deficient plakophilin-1 expression due to a mutation in PKP1 causes ectodermal dysplasia-skin fragility syndrome in Chesapeake Bay retriever dogs. *PLoS One* (2012) 7(2):e32072. doi:10.1371/journal.pone.0032072
47. McGrath JA, McMillan JR, Shemanko CS, Runswick SK, Leigh IM, Lane EB, et al. Mutations in the plakophilin 1 gene result in ectodermal dysplasia/skin fragility syndrome. *Nat Genet* (1997) 17(2):240–4. doi:10.1038/ng1097-240
48. Bar J, Kumar V, Roth W, Schwarz N, Richter M, Leube RE, et al. Skin fragility and impaired desmosomal adhesion in mice lacking all keratins. *J Invest Dermatol* (2014) 134(4):1012–22. doi:10.1038/jid.2013.416
49. Calkins CC, Setzer SV, Jennings JM, Summers S, Tsunoda K, Amagai M, et al. Desmoglein endocytosis and desmosome disassembly are coordinated responses to pemphigus autoantibodies. *J Biol Chem* (2006) 281(11):7623–34. doi:10.1074/jbc.M512447200
50. Kitajima Y. 150 anniversary series: desmosomes and autoimmune disease, perspective of dynamic desmosome remodeling and its impairments in pemphigus. *Cell Commun Adhes* (2014) 21(6):269–80. doi:10.3109/15419061.2014.943397
51. Aoyama Y, Owada MK, Kitajima Y. A pathogenic autoantibody, pemphigus vulgaris-IgG, induces phosphorylation of desmoglein 3, and its dissociation from plakoglobin in cultured keratinocytes. *Eur J Immunol* (1999) 29(7):2233–40. doi:10.1002/(SICI)1521-4141(199907)29:07<2233::AID-IMMU2233>3.0.CO;2-4
52. Roberts BJ, Johnson KE, McGuinn KP, Saowapa J, Svoboda RA, Mahoney MG, et al. Palmitoylation of plakophilin is required for desmosome assembly. *J Cell Sci* (2014) 127(Pt 17):3782–93. doi:10.1242/jcs.149849
53. van der Wier G, Pas HH, Kramer D, Diercks GFH, Jonkman MF. Smaller desmosomes are seen in the skin of pemphigus patients with anti-desmoglein 1 antibodies but not in patients with anti-desmoglein 3 antibodies. *J Invest Dermatol* (2014) 134(8):2287–90. doi:10.1038/jid.2014.140
54. Brasch J, Harrison OJ, Honig B, Shapiro L. Thinking outside the cell: how cadherins drive adhesion. *Trends Cell Biol* (2012) 22(6):299–310. doi:10.1016/j.tcb.2012.03.004
55. Yap AS, Brieher WM, Pruschy M, Gumbiner BM. Lateral clustering of the adhesive ectodomain: a fundamental determinant of cadherin function. *Curr Biol* (1997) 7(5):308–15. doi:10.1016/S0960-9822(06)00154-0
56. Homberg M, Magin TM. Beyond expectations: novel insights into epidermal keratin function and regulation. *Int Rev Cell Mol Biol* (2014) 311:265–306. doi:10.1016/B978-0-12-800179-0.00007-6
57. Aoyama Y, Kitajima Y. Pemphigus vulgaris-IgG causes a rapid depletion of desmoglein 3 (Dsg3) from the Triton X-100 soluble pools, leading to the formation of Dsg3-depleted desmosomes in a human squamous carcinoma cell line, DJM-1 cells. *J Invest Dermatol* (1999) 112(1):67–71. doi:10.1046/j.1523-1747.1999.00463.x
58. Sato M, Aoyama Y, Kitajima Y. Assembly pathway of desmoglein 3 to desmosomes and its perturbation by pemphigus vulgaris-IgG in cultured keratinocytes, as revealed by time-lapsed labeling immunoelectron microscopy. *Lab Invest* (2000) 80(10):1583–92. doi:10.1038/labinvest.3780168
59. Saleh MA, Hashimoto R, Kase Y, Amagai M, Yamagami J. Low pathogenicity of anti-desmoglein 3 immunoglobulin G autoantibodies contributes to the atypical clinical phenotypes in pemphigus. *J Dermatol* (2015) 42(7):685–9. doi:10.1111/1346-8138.12888
60. Lo AS, Mao X, Mukherjee EM, Ellebrecht CT, Yu X, Posner MR, et al. Pathogenicity and epitope characteristics do not differ in IgG subclass-switched anti-desmoglein 3 IgG1 and IgG4 autoantibodies in pemphigus vulgaris. *PLoS One* (2016) 11(6):e0156800. doi:10.1371/journal.pone.0156800
61. Ishii K, Amagai M. In vitro pathogenicity assay for anti-desmoglein autoantibodies in pemphigus. *Methods Mol Biol* (2013) 961:219–25. doi:10.1007/978-1-62703-227-8_13
62. Stahley SN, Warren MF, Feldman RJ, Swerlick RA, Mattheyses AL, Kowalczyk AP. Super-resolution microscopy reveals altered desmosomal protein organization in tissue from patients with pemphigus vulgaris. *J Invest Dermatol* (2016) 136(1):59–66. doi:10.1038/JID.2015.353
63. Amagai M, Ahmed AR, Kitajima Y, Bystryn JC, Milner Y, Gniadecki R, et al. Are desmoglein autoantibodies essential for the immunopathogenesis of pemphigus vulgaris, or just "witnesses of disease"? *Exp Dermatol* (2006) 15(10):815–31. doi:10.1111/j.1600-0625.2006.00499_1.x
64. Heupel WM, Muller T, Efthymiadis A, Schmidt E, Drenckhahn D, Waschke J. Peptides targeting the desmoglein 3 adhesive interface prevent autoantibody-induced acantholysis in pemphigus. *J Biol Chem* (2009) 284(13):8589–95. doi:10.1074/jbc.M808813200
65. Rotzer V, Hartlieb E, Winkler J, Walter E, Schlipp A, Sardy M, et al. Desmoglein 3-dependent signaling regulates keratinocyte migration and wound healing. *J Invest Dermatol* (2016) 136(1):301–10. doi:10.1038/jid.2015.380
66. Rotzer V, Hartlieb E, Vielmuth F, Gliem M, Spindler V, Waschke J. E-cadherin and Src associate with extradesmosomal Dsg3 and modulate desmosome assembly and adhesion. *Cell Mol Life Sci* (2015) 72(24):4885–97. doi:10.1007/s00018-015-1977-0
67. Chernyavsky AI, Arredondo J, Kitajima Y, Sato-Nagai M, Grando SA. Desmoglein versus non-desmoglein signaling in pemphigus acantholysis: characterization of novel signaling pathways downstream of pemphigus vulgaris antigens. *J Biol Chem* (2007) 282(18):13804–12. doi:10.1074/jbc.M611365200
68. Tsang SM, Liu L, Teh MT, Wheeler A, Grose R, Hart IR, et al. Desmoglein 3, via an interaction with E-cadherin, is associated with activation of Src. *PLoS One* (2010) 5(12):e14211. doi:10.1371/journal.pone.0014211
69. Jennings JM, Tucker DK, Kottke MD, Saito M, Delva E, Hanakawa Y, et al. Desmosome disassembly in response to pemphigus vulgaris IgG occurs in distinct phases and can be reversed by expression of exogenous Dsg3. *J Invest Dermatol* (2011) 131(3):706–18. doi:10.1038/jid.2010.389
70. Yamamoto Y, Aoyama Y, Shu E, Tsunoda K, Amagai M, Kitajima Y. Anti-desmoglein 3 (Dsg3) monoclonal antibodies deplete desmosomes of Dsg3 and differ in their Dsg3-depleting activities related to pathogenicity. *J Biol Chem* (2007) 282(24):17866–76. doi:10.1074/jbc.M607963200
71. Berkowitz P, Hu P, Warren S, Liu Z, Diaz LA, Rubenstein DS. p38MAPK inhibition prevents disease in pemphigus vulgaris mice. *Proc Natl Acad Sci U S A* (2006) 103(34):12855–60. doi:10.1073/pnas.0602973103
72. Bektas M, Jolly PS, Berkowitz P, Amagai M, Rubenstein DS. A pathophysiologic role for epidermal growth factor receptor in pemphigus acantholysis. *J Biol Chem* (2013) 288(13):9447–56. doi:10.1074/jbc.M112.438010
73. Strnad P, Windoffer R, Leube RE. Induction of rapid and reversible cytokeratin filament network remodeling by inhibition of tyrosine phosphatases. *J Cell Sci* (2002) 115(Pt 21):4133–48. doi:10.1242/jcs.00096
74. Strnad P, Windoffer R, Leube RE. Light-induced resistance of the keratin network to the filament-disrupting tyrosine phosphatase inhibitor orthovanadate. *J Invest Dermatol* (2003) 120(2):198–203. doi:10.1046/j.1523-1747.2003.12038.x
75. Woll S, Windoffer R, Leube RE. p38 MAPK-dependent shaping of the keratin cytoskeleton in cultured cells. *J Cell Biol* (2007) 177(5):795–807. doi:10.1083/jcb.200703174
76. Mavropoulos A, Orfanidou T, Liaskos C, Smyk DS, Billinis C, Blank M, et al. p38 mitogen-activated protein kinase (p38 MAPK)-mediated autoimmunity: lessons to learn from ANCA vasculitis and pemphigus vulgaris. *Autoimmun Rev* (2013) 12(5):580–90. doi:10.1016/j.autrev.2012.10.019

77. Mavropoulos A, Orfanidou T, Liaskos C, Smyk DS, Spyrou V, Sakkas LI, et al. p38 MAPK signaling in pemphigus: implications for skin autoimmunity. *Autoimmune Dis* (2013) 2013:728529. doi:10.1155/2013/728529

**Conflict of Interest Statement:** The authors declare that the research was conducted in the absence of any commercial or financial relationships that could be construed as a potential conflict of interest.

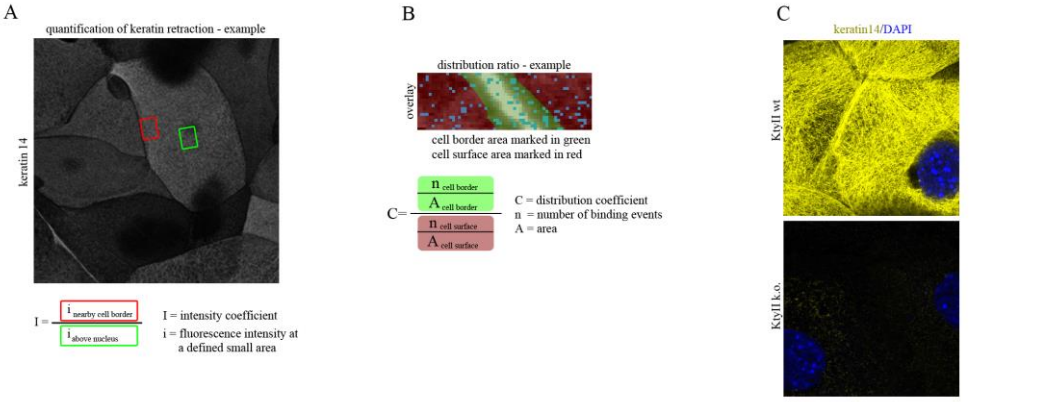


Supplemental Figure 1

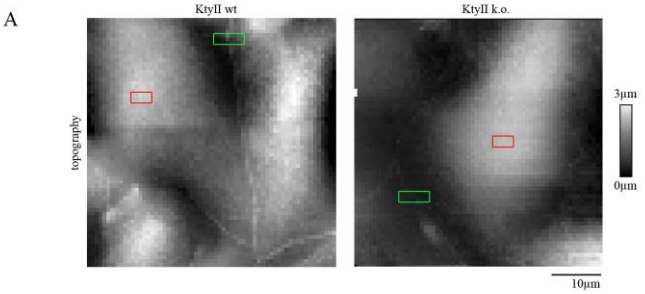


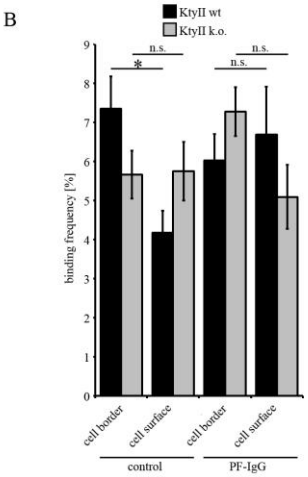


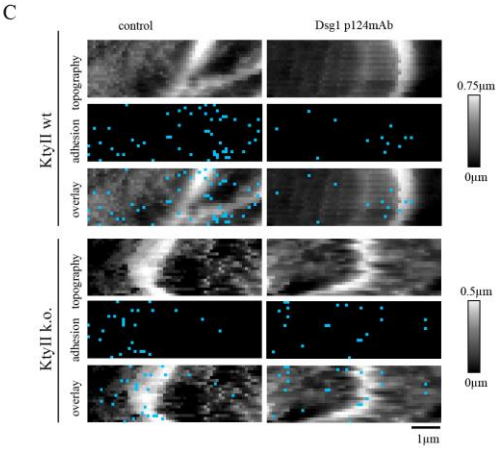


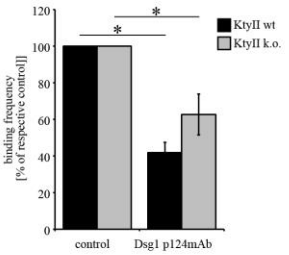


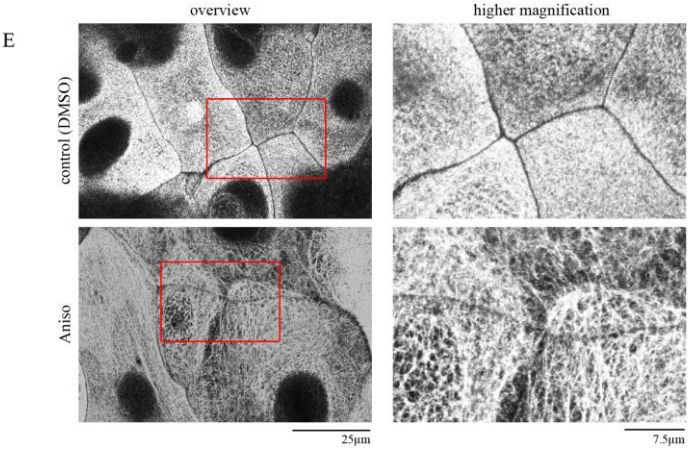


Supplemental Figure 2

A

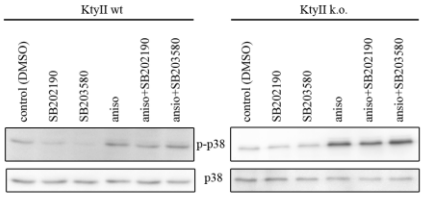


B

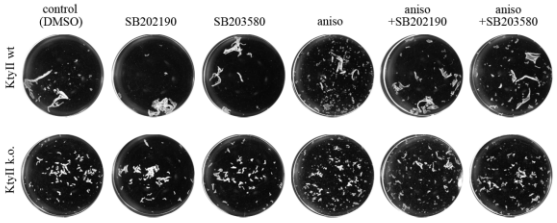


Supplemental Figure 3

# Chapter 3

# Discussion

The desmosomal plaque proteins, Pkps, are essential for desmosomal adhesion. Hence, they are involved in regulation of desmosomal turnover and signaling [74]. However, their role in the regulation of adhesive strength of desmosomes at the level of single molecule binding properties of desmosomal cadherins is unknown. Previous studies showed that single molecule binding properties of desmosomal cadherins rely on intracellular proteins, such as keratin as well as on signaling pathways [178]. For example, keratins control cell adhesion by regulating the binding properties of Dsg3. For this process, the keratin-dependent signaling pathways p38MAPK and PKC$\alpha$ seem to be crucial [137].

Previous studies reported that Pkp1 contributes to the organization of desmosomes by clustering of DP whereby it regulates desmosome size [84]. Thus, our studies aimed to investigate the Pkp-dependent clustering of different desmosomal cadherin isoforms. We observed that Pkp1 and Pkp3 are important for the membrane availability of Dsg1 and Dsg3, whereas Pkp1 only is involved in Dsg3 clustering. This property correlates with drastically decreased adhesion in Pkp1-deficient keratinocytes compared to the Pkp3-deficient cells [151]. The importance of this clustering is reflected during acquisition of desmosomal hyper-adhesion. Thus, in the follow-up project, we showed that $Ca^{2+}$-independent Dsg3 clusters are an indispensable contributor to desmosomal hyper-adhesion. Further, we found that the hyper-adhesive state of desmosomes correlates with increased single-molecule interaction forces and a prolonged lifetime of Dsg3. Interestingly, Dsg1 shows different properties with unchanged binding properties and clustering. Taken together, we concluded that desmosomal cadherins participate in acquisition of a hyper-adhesive state by different mechanisms and suggest that the different isoforms are not of equal importance in this

process.

## 3.1 A novel role for Pkp1 in desmosomal adhesion

Pkps act as scaffolds in the formation of desmosomes and therefore have a critical role in the assembly of desmosomes [74]. Although the three isoforms share high structural similarities, they fulfill a plethora of individual functions. For example, Pkp1 is involved in clustering of DP and therefore important for desmosome size [84]. Pkp2 is important for the assembly of desmosomes as it forms a complex with DP and PKC$\alpha$ which, triggered by cell-cell contact, translocates to the cell borders to nascent desmosomes [89]. Pkp3 was shown to be in a complex with E-Cad and Src and therefore critical for desmosome assembly [93]. Accordingly, genetic mutations that lead to a functional knockout of a respective Pkp isoform show different phenotypes. Pkp1 lead to skin fragility syndrome with severe impaired epidermal cohesion, whereas mutations in Pkp3 show a milder phenotype in mice, with hair coat abnormalities susceptible to skin inflammation [147] [179] [95]. However, loss of Pkp3 was suggested to be involved in cancer development [180]. Those phenotypes can also be found in mouse models lacking either Pkp1 or Pkp3. Pkp1-deficient mice had reduced weight but otherwise no notable changes. The skin looked intact at the macroscopic level. However, their condition changed rapidly within 24 hours, leading to death. During that time frame, the mice developed skin lesions caused by skin fragility without obvious mechanical trauma. At a histological level, these mice had altered desmosomes which were reduced in number and size [86]. In contrast to the Pkp1 knockout mice, Pkp3-deficient mice showed hair abnormalities but were viable. At birth, the skin of the mutant mice showed no visible changes. However, on the seventh postnatal day, when mouse skin develops hair growth, this process was delayed in Pkp3-null mice. Four-week-old Pkp3 mutant mice had a crinkled, thinner and duller coat, in contrast to wt mice. Ultrastructurally, no desmosomes were present at the basal layer of the outer root arch of the hair follicles [95].

Murine keratinocytes cultured in low $Ca^{2+}$-medium show high proliferation rates, but desmosomes are not present under these conditions. However, the addition of $Ca^{2+}$ to the medium starts terminal differentiation leading to cell-cell contacts, including the formation of desmosomes after 2 h [181]. The murine keratinocyte model system is a suitable approach because after global onset of differentiation all cells are in a comparable differentiation state. Murine keratinocytes express Pkp1 and Pkp3 to a comparable extent as human

keratinocytes, which makes it a good model system [179]. In this study, spontaneously immortalized keratinocytes from Pkp1 and Pkp3 knockout mice were used to investigate their role in regulating desmosomal cadherin binding properties [86] [95]. The Pkp1-deficient cells have reduced intercellular cohesion, consistent with the smaller number and reduced size of desmosomes in the Pkp1-null mice [86]. Pkp3 lacking cells show a delayed formation of desmosomes and AJs [179]. As various desmosomal cadherin isoforms exist, we focused on Dsg1 and Dsg3 as they are the major antigens in PV. Therefore several biophysical and biochemical approaches were used. At first it was shown by dispase dissociation assays that Pkp1- and Pkp3-deficient keratinocytes have reduced adhesion in contrast to wt cells. Comparable to the pathological phenotype, compromised adhesion is more pronounced in Pkp1 deficient cells than in cells lacking Pkp3.

### 3.1.1 Plakophilins 1 and 3 mediate junctional membrane availability of desmogleins

Previous studies in mice and cell culture models revealed reduced adhesion in Pkp3- and even more pronounced in Pkp1-deficient keratinocytes [179]. This represents the importance of both Pkp isoforms for cell adhesion. Further, the significant difference in intercellular adhesion in Pkp1- or Pkp3-deficient keratinocytes respectively shows that there are functional differences between the two isoforms [151].

Interestingly, AFM high resolution imaging revealed no significant morphological alterations between the different cell lines in terms of cell size, cell shape and composition of intercellular borders. Our results showed that both Pkp1 and 3 are important for the membrane availability of Dsg1 and Dsg3. Decreased membrane availability was previously shown to correlate with impaired intercellular adhesion [113]. This is consistent with the desmoglein non-assembly depletion hypothesis, which describes a possible mechanism of how PV-IgG causes acantholysis. Briefly, non-junctional Dsg3 targeted by PV-IgG is internalized, resulting in disturbed desmosome assembly due to Dsg3 missing desmosomes [57]. The reduced amount of junctional Dsg1 and Dsg3 might lead to formation of desmosomes depleted for those desmogleins. Compromised adhesion would follow due to incomplete desmosomes, which is in line with the nonassembly depletion hypothesis. Same applies for Dsg1, hence pemphigus inhibits the incorporation of extradesmosomal Dsg1 into the desmosome [113]. Taken together, compromised cohesion and decreased membrane availability of Dsg1 and 3, in Pkp-deficient keratinocytes reveal that Pkps stabilize desmosomal cadherins

at the membrane. This seems to be an important aspect for proper desmosomal adhesion. In accordance, it was shown that the expression of desmosomal cadherins is dependent on Pkp1 in terms of desmosome assembly [182]. Another study revealed that impaired intercellular adhesion and reduced AFM binding frequency correlate [178]. Interestingly, Triton x-100 experiments revealed no difference between wt and Pkp-deficient cells, with respect to the amount of soluble and insoluble fraction of Dsc1-3. This indicates, that the expression as well as the incorporation of different desmosomal cadherins into the desmosome are not necessarily dependent on Pkps. Former studies also showed that Pkp isoforms have specific functions for the expression of Dsgs, e.g. loss of Pkp2 reduces the expression of Dsg2 in cardiac myocytes [91]. Thus, it can be concluded that one specific role of Pkp1 and Pkp3 is to regulate the membrane availability and the stabilization of the desmosomal precursors Dsg1 and Dsg3, what leads to an increased intercellular adhesion.

For both knockout cell lines, the reduction in membrane availability of Dsg1 and Dsg3 is comparable but the dissociation assay revealed different degrees of impaired cellular cohesion. Therefore, reduced membrane availability alone does not fully explain the observed findings. In a previous study, it has been shown that knockout of desmosomal components can differentially alter the binding properties of desmosomal cadherins on a single molecule level. For example, complete knockout of all keratins (KtyII k.o.) resulted in an increase in Dsg3 binding frequency accompanied with reduced binding strength. In parallel, the binding frequency of Dsg1 was reduced while the binding force remains the same [178]. In this study, even though the binding frequency is compromised there are still remaining binding events. Application of a Dsg3-coated AFM tip revealed for those remaining membrane-localized Dsg3 molecules, that the parameters unbinding force as well as the unbinding position were reduced for both knockout cell lines. AFM experiments with Dsg1 molecules revealed a reduced binding frequency to a similar level as for Dsg3. The single molecule binding properties of the remaining Dsg1 molecules were also altered. The unbinding force was slightly increased for both knockout cell lines and the unbinding position was comparably reduced similar to Dsg3. For both interactions, the unbinding position is reduced for all knockout cell lines compared to wt. The parameter unbinding position is an indirect measure of correct cytoskeletal anchoring [173] [183]. Therefore, the improved cytoskeletal anchoring of the interaction partners in both knockout cell lines is surprising. This indicates that the remaining proteins are not anchored by Pkp1 or Pkp3 but by another mechanism. It was shown that the binding partners of Dsg3 from

human keratinocytes, which are deficient for DP, have a higher proportion of tether bonds [184]. This supports the role of DP in anchoring desmosomal components to the IF and strengthens the UP parameter as a readout of cytoskeletal anchorage of binding partners in AFM experiments. From this it could be concluded that a reduction in Dsg3 binding strength could be due to decreased membrane availability and thus lack of Dsg3 clusters. The lack of cluster formation could be responsible for essential conformational changes leading to altered binding properties [185]. The increase in Dsg1 binding strength may be due to unknown compensatory rescue mechanisms.
However, since the amount of remaining Dsg1 and Dsg3 molecules at the cell membrane is small compared to the level in the wt cells, it can be concluded that the observed altered binding properties may be less important for overall intercellular adhesion. Taken together, Pkp1 and Pkp3 are crucial for intercellular adhesion by maintaining Dsg1 and 3 at the cell membrane. They also reveal an affect on single molecule binding properties of desmogleins although this seems to be less important for cellular cohesion.

### 3.1.2 Pkp-deficiency does not activate p38MAPK signaling

In PV patients as well as in cultured cell lines exposed to PV-IgG, several signaling pathways are modulated. These include, among others, increase in intracellular $Ca^{2+}$ levels, activation and translocation of PKC, phosphorylation of Src and activation of p38MAPK [186] [187] [141] [136]. Activation of p38MAPK is followed by recruitment of multiple downstream targets including HSP27 [142]. Since inhibition of p38MAPK prevents the pathological phenotype in mice in response to PV-IgG, it can be concluded that p38MAPK is a critical contributor to PV pathogenesis [136] [39]. In principle, the role of p38MAPK is to regulate intermediate filament organization. The activation of p38MAPK therefore has implications on cell shape and flexibility [188]. Hence, p38MAPK gets activated upon PV-IgG binding. This activation leads to the retraction of keratin filaments, which is a hallmark of pemphigus pathogenesis. For PV-autoantibodies the main antigens are Dsg1 and Dsg3. PV-IgG binding leads to an internalization of Dsg3 and therefore to a reduction of membrane-bound Dsg3 [57]. Previous studies found compromised cellular cohesion upon deletion of structural components caused by activation of p38MAPK for example after deletion of type II keratins in murine keratinocytes. This showed that a significant increase in p38MAPK activation accompanied with decreased intercellular adhesion [189]. However, p38MAPK is not activated in Pkp-lacking cells. Therefore, the reduced cell cohesion due to the absence of Pkp1 or Pkp3 is not caused by activation of p38MAPK. From this it

can be concluded that p38MAPK is not necessarily activated when intercellular adhesion is impaired due to reduction of Dsg1 and 3 membrane levels. Rather more processes are involved in the pathomechanism of PV as described above. In accordance with this finding, it was shown that Pg, but not DP, regulates keratinocyte cohesion via p38MAPK signaling [190].

### 3.1.3 Pkp1 is crucial for Dsg clustering and necessary for desmosomal adhesion

Cluster formation of AJs is an important mechanism for cellular cohesion. This can be explained by the characteristics of single molecule interactions of cadherins where forces are relatively low and lifetimes are short, in the range of a few tenths of a second [158]. To overcome this problem, cadherins accumulate in clusters, within the aforementioned AJs, distributing the force acting on the cell to many binding sites. Another advantage of this accumulation is that opening *trans*-bonds are less relevant since they are balanced by the amount of simultaneously closing bonds [191]. Furthermore, it was shown that cluster formation is an important process in the maturation of adhesive contacts. The classical cadherin E-Cad accumulates in precursor clusters before being incorporated into AJs [192]. The same mechanism was also proposed for desmosomal cadherins [184]. It is known that Pkp1 is relevant for desmosomal size via clustering of DP. In this study, Dsg3 clusters were shown to be significantly reduced in Pkp1-deficient cells. These effects were less pronounced in Pkp3 knockout cells. Results were demonstrated by chemical cross-linking of membrane bound proteins and repeated AFM scans over predetermined cell-cell-contact area. AFM measurements showed smaller Dsg3 clusters for Pkp1- and Pkp3-deficient keratinocytes. Consistent with this, biochemical crosslinking showed a strong reduction of oligomerized Dsg3. The amounts of E-Cad clusters were not changed between cell lines, which indicates the specific role of Pkps for desmosomal cadherin clustering. Thus, clustered desmosomal cadherins appear to be essential for proper intercellular cohesion.

In concordance, it has already been shown that homophilic interactions of desmosomal cadherins and their oligomerization may be essential for the proper strength of desmosomes and thus for the maintenance of tissue integrity [163]. The molecular composition of the desmosomal plaque provides further insight into the role of Pkps in this context. In junctions the cytoplasmic surface, which appears as an irregular periodic lattice, links the extracellular part to the IF. The desmosomal plaque is a 3D cytoplasmic surface consisting

of an IDP and an ODP, which are two electron-dense surfaces. Here, the ODP is closer to the plasma membrane and consists of the Pkps and Pg. Furthermore, in this area the cytoplasmic part of the desmosomal cadherins are linked to DP, which in turn builds up the IDP with major parts of the molecule. The ultrastructural basis for desmosomal cadherin binding is a template consisting of the Pg and DP complex in which the cadherins cluster before forming *trans*-interactions with their extracellular part. The Pkps are located in between the PG-DP complex and the cadherins. Those reinforce the molecular assembly, hence they can interact with various desmosomal components. The fact that Pkps are located closer to the cell membrane, where they are adjacent to the cytosolic part of the desmosomal cadherins, indicates a mutual dependence between the intra- and extracellular parts of the desmosome [193]. Thus, it can be concluded that Pkp isoforms are important for cell adhesion by enabling and maintaining junctional availability of desmosomal cadherins. Furthermore, Pkp1-dependent regulation of cadherin clustering contributes to proper cell cohesion.

Our study showed that Dsg3 cluster size is smaller in Pkp-deficient cells. However, this could also be due to the reduced membrane availability of Dsg3 and thus be a simple matter of molecule quantity. Therefore, we overexpressed Dsg3 by transient transfection. This resulted in cluster restoration and an increase in cluster size for Pkp3-deficient but not for Pkp1-deficient cells as shown by AFM experiments and super-resolution microscopy (stimulated emission depletion microscopy (STED)). Those findings correlate with the enormous differences in cell cohesion between the different cell lines detected by dispase dissociation assays. Consistent with this, fluorescence recovery after photobleaching (FRAP) experiments showed an increased mobility for overexpressed Dsg3 molecules in the membrane of Pkp1- but not of Pkp3-deficient cells. Membrane mobility of desmosomal cadherins was shown to be negatively correlated with desmosome maturation state [194]. In addition, it was shown that molecule mobility may negatively correlate with strong intercellular adhesion. In a former study, keratin-deficient murine keratinocytes were compared to wt cells. The keratin-deficient cells showed drastic compromised intercellular adhesion and in parallel an increased Dsg3 mobility in the membrane [178]. This correlation has also been supported by other studies. In cultured human keratinocytes lacking DP, intercellular adhesion was impaired while transient transfected Dsg2-GFP showed increased mobility in the membrane [184]. Loss of the actin-binding protein $\alpha$-Adducin leads to decreased cellular cohesion accompanied with increased Dsg3-GFP mobility in the cell membrane

[195]. Incubation with AK23, a monoclonal antibody against Dsg3 derived from a PV mouse model, led to an increase of Dsg3 mobility in wt cells paralleled by a decrease in cellular cohesion [196]. Given the assumption that AK23 incubation results in decoupling of Dsg3 from the IF, this is in line with negative correlation of molecule mobility and intercellular adhesion [114] [178]. As an opposing mechanism, lateral- or cis-clustering of cadherins was shown to be essential for intercellular adhesion [197]. It was found that this essential lateral clustering of cadherins is goverend by their cytoplasmic tail and adhesion is modulated via the presence of clusters [198]. It was further shown that F-actin interacts with the cis-interface of cadherin clusters. This leads to increased assembly and stability of cadherin clustering [199]. Therefore, it can be concluded that cluster formation is an essential component for strong intercellular adhesion.
In our study it was shown that desmosomal cadherin clustering is essential for proper cellular cohesion and abolished cluster formation contributes to the observed differences in intercellular adhesion of Pkp1- and Pkp3-deficient keratinocytes. Worth mentioning, this effect is only present for desmosomal cadherins, whereas clustering of the classical cadherin E-Cad remained unaffected in Pkp-deficient keratinocytes.

To summarize, our study showed that Pkp1 and Pkp3 are both essential for membrane availability of Dsg3. Further, it provided a new isoform-specific function of Pkp1 in clustering of Dsg3. The importance of Dsg clustering for intercellular adhesion in keratinocytes has been demonstrated in this study (Figure 3.1) [151]. The significance of cadherin clustering for cellular cohesion has been shown previously in other studies and can be seen as the general basis of cell-cell-adhesion [198] [199]. With our study, we have added another component to the mechanism for desmosomal cadherin clustering.

## 3.2 Desmosomal hyper-adhesion depends on Dsg3 clusters and is correlated with increased single molecule binding strength of Dsg3

Our main finding in this study is that not all desmosomal cadherins are equally involved in the acquisition of the hyper-adhesive state. We showed that the binding strength and interaction lifetime of Dsg3 increases during cell differentiation, which is not the case for Dsg1. Furthermore, we found that the presence of $Ca^{2+}$-independent desmosomal cadherin

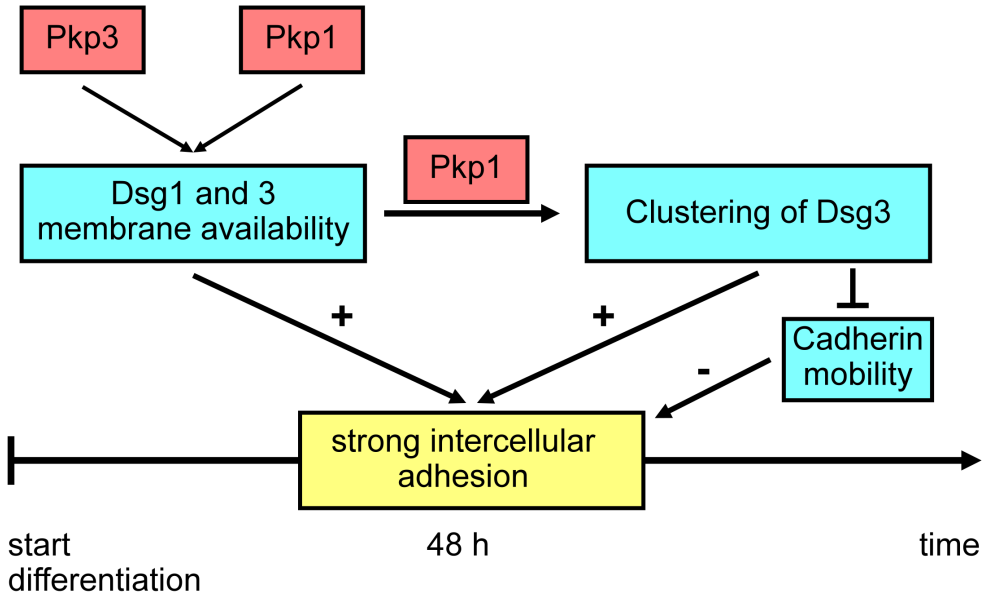


Figure 3.1: Regulation of desmosomal cadherin clustering in keratinocytes shows a Pkp isoform-specific manner. Both, Pkp1 and Pkp3 are important for junctional membrane availability of the desmosomal cadherins Dsg1 and Dsg3, thereby contributing to strong intercellular adhesion. Additionally, Pkp1 but not Pkp3 is required for clustering of membrane bound Dsg3 molecules, which is crucial for strong intercellular cohesion. Clustered desmosomal cadherins show lower mobility within the membrane.

clusters are a crucial contributor to hyper-adhesion. We showed that this property is mediated by the plaque protein Pkp1.

*PKCα* and Pkp1 are important for achieving the hyper-adhesive state [125] [182]. At the molecular level, the dense arrangement of desmosomal cadherins leads to a highly ordered state. In this state, the desmosomal cadherins are $Ca^{2+}$-independent [44] [116]. Here, we demonstrated that the dense arrangement is mediated by the plaque protein Pkp1. Until now, it was assumed that the entire desmosome becomes hyper-adhesive. However, our data shows for the first time that this is not necessarily the case. Rather, several cadherins could contribute differently. The assumption that ordered desmosomal cadherins are necessary for hyper-adhesion was challenged recently [194]. Here, using a genetically modified extracellular domain of Dsg3, it was shown that order in hyper-adhesive desmosomes is lost upon chelation of extracellular $Ca^{2+}$. However, it should be mentioned that this modified Dsg3 protein may not be comparable to the original Dsg3. Artificial modifications

of the cadherin could result in loss of basic protein properties. Therefore, we according to our data assume that the highly ordered state is a hallmark of hyper-adhesive desmosomes.

So far the underlying mechanism of how desmosomes acquire a hyper-adhesive state is not entirely clear. As mentioned, it is known that this process depends on $PKC\alpha$ and additionally overexpression of Pkp1 supports the development. However, how Pkp1 is involved in this process remains to be elucidated. Therefore, in this study, we wanted to understand how Pkps are involved in the acquisition of hyper-adhesion and investigated the contributions of different desmosomal cadherins during acquisition of hyper-adhesion.

### 3.2.1 Dsg3 binding properties contribute to hyper-adhesion

Murine keratinocyte wt cells developed resistance to $Ca^{2+}$ chelation after 72 h in high $Ca^{2+}$ medium. In contrast, 24 h in medium with a high $Ca^{2+}$ concentration resulted in $Ca^{2+}$-dependent desmosomes. Chelation of extracellular $Ca^{2+}$ led to internalization of Dsg3. Previous experiments with human keratinocytes and kidney cells showed that desmosomes become hyper-adhesive six days after reaching confluency. Important to note is that non-confluent cells did not become hyper-adhesive at any time [36] [115]. This shows that, depending on the tissue origin of the desmosomes, different time periods are needed to reach hyper-adhesion. Besides a certain differentiation time, switching desmosomes from a $Ca^{2+}$-dependent to the hyper-adhesive state can also be accomplished via pharmacological induction with the PKC inhibitor Gö6976. Inhibition of $PKC\alpha$ leads to hyper-adhesion of desmosomes in cultured epithelial cells and human keratinocytes, probably due to loss of DP phosphorylation [115] [36] [44]. Interestingly, cells with hyper-adhesive desmosomes exposed to PV-IgG showed minor loss of adhesion and less internalization of Dsg3, in contrast to non-hyper-adhesive cells [140]. In Pkp1- and Pkp3-deficient cells, there was a dramatic decrease in intercellular adhesion after $Ca^{2+}$ chelation, both after 24 h and 72 h in high $Ca^{2+}$ medium. Thus, murine wt keratinocytes reach a state resistant to $Ca^{2+}$-ion chelation 72 h after the onset of differentiation and are considered to be hyper-adhesive. In contrast, Pkp-deficient cells remain $Ca^{2+}$-dependent and lack hyper-adhesive properties of wt cells. Consequently, we concluded that both Pkp isoforms are important for the acquisition of desmosomal hyper-adhesion. This is in line with the already known role of Pkp1 but shows a new role of Pkp3 [125]. Failure of desmosomes becoming hyper-adhesive in Pkp3-deficient cells could be due to compromised membrane availability of desmosomal cadherins [151]. Interestingly, earlier results with the same cell line showed the opposite result for the

Pkp3-deficient cell line [179]. Keil et. al. found that Pkp1 but not Pkp3 is involved in the acquisition of the hyper-adhesive state. It is known that Pkp3 is important for the assembly of desmosomes [93]. Therefore, loss of Pkp3 could be responsible for impaired or delayed desmosome assembly. Since impaired desmosome formation was observed to reduce cellular cohesion, this could account for the failure to achieve the hyper-adhesive state [151]. From the second aspect, regarding the delayed desmosome assembly, it can be concluded that the desmosomes of Pkp3-deficient cells are not in the same differentiation state as in wt cells. The Pkp3-deficiency of the desmosomes is initially responsible for the later onset of differentiation, but eventually also become hyper-adhesive. Therefore, we think that the conflicting results could be due to different cell culture conditions. This is supported by the fact that in the earlier study murine keratinocytes were described not to express Pkp2, which is not the case under our cell culture conditions [179].

The hyper-adhesive state is considered to be the state of stronger cell cohesion. AFM experiments on keratinocytes using Dsg1- and Dsg3-coated tips showed strong differences in the single molecule binding properties between the hyper-adhesive and non hyper-adhesive state as well as for the two interaction partners. Acquisition of the hyper-adhesive state resulted in drastically altered binding properties of Dsg3, whereas no changes were observed for Dsg1. The frequency of binding for Dsg1 and 3 interactions was slightly but not significantly reduced for wt cells between the hyper-adhesive and non hyper-adhesive states. For Pkp1-lacking cells, the frequency was reduced between 24 h and 72 h in high $Ca^{2+}$ medium but not as drastically as for Pkp3 k.o.-cells. Reduced binding frequency may be due to lack of binding partners on the cell membrane. Previous studies demonstrated the importance of Pkp3 for desmosome assembly during maturation, where Pkp3 is in complex with E-cad and PG at the cell membrane even under low $Ca^{2+}$-conditions [93] [103]. Accordingly, insufficient assembly leads to reduced binding frequency with binding partners. The results shown here confirm this specific function of Pkp3. Impaired desmosome assembly explains the inability to reach the hyper-adhesive state. Pkp1 is important for desmosomal cadherin clustering, a required property for the establishment of proper adhesion between cadherins [198] [44]. Therefore, the absence of cadherin clusters lead to failure in acquisition of hyper-adhesive state [151] [200]. It is known from a previous study that strong intercellular adhesion correlates with higher unbinding forces of Dsg3 [137]. Consistent with that, Dsg3 unbinding forces were increased by about 20% when wt cells became hyper-adhesive. However, Dsg3 single molecule binding properties of Pkp1- or Pkp3-deficient cells were

unaltered between 24 h and 72 h in high $Ca^{2+}$ medium. This shows that both plaque proteins regulate the adhesive binding properties of Dsg3 in its respective adhesive states. Interestingly, the binding strength for the Dsg1 interaction was not altered between the two adhesive-states for all cell lines, indicating that these desmosomal cadherins contribute differently to the hyper-adhesive state. We did not observe alterations for Dsg1 and Dsg3 interactions regarding the unbinding position between both time points. Given that the unbinding position is a measure for the cytoskeletal anchorage, it can be concluded that the acquisition of the hyper-adhesive state does not change keratin or actin anchorage of Dsg1 and Dsg3 [183].

The development of hyper-adhesion is a differentiation-dependent process and thus time-dependent. As shown, the desmosomes of murine keratinocytes require 72 h in high $Ca^{2+}$ medium to become hyper-adhesive. Within this time interval the desmosomal cadherins Dsg1 and Dsg3 develop their hyper-adhesive properties unequally. While an increase in binding strength was observed for Dsg3, this was not the case for Dsg1. However, unpublished data from a HaCaT Dsg2 k.o. cell line suggest that some desmosomal cadherins are involved in the acquisition of hyper-adhesion, as even these Dsg2-deficient cells do not become hyper-adhesive even after 72 h of differentiation. Thus, it can be speculated that Dsg1 changes its binding properties later during the differentiation process. In line with this suggestion is the fact, that Dsg1 is mainly expressed in the apical layers of the epidermis, and thus later during the differentiation process of keratinocytes in the epidermis. However, it is also possible that the Dsg1 molecules contributing to hyper-adhesion are not accessible with the AFM technique used. The accessibility of Dsg3 might be different. For example, Dsg3 occurs predominantly in the basal layers, representing an earlier stadium of keratinocyte differentiation which might be more reflected by our cell culture model. Another explanation for the observed changes in Dsg3 but not in Dsg1 could be due to the desmosome assembly properties. It is known that Dsg3 clusters before being incorporated into desmosomes [124]. Therefore, along differentiation these lateral clusters may mature. This could lead to a higher ordered structure and due to conformational changes of the desmosomal cadherins to altered binding properties. So far it is not known if Dsg1 also clusters prior to desmosome incorporation. Nevertheless, Dsg1 also occurs outside of desmosomes and is therefore accessible with the AFM tip [67]. However, when Dsg1 molecules are incorporated directly into the desmosome, cluster-induced changes in binding properties may not be detectable. Therefore, no alterations in binding properties

due to cluster-induced conformational changes would be detectable with the AFM. However, additional experiments would be necessary to prove this assumption.

Duration of a receptor-ligand interaction, the so called lifetime, can be determined using a modified version of the Bells equation [177] [176]. The importance of temporally persistent interactions can be demonstrated in many biological processes, as a minimal amount of time is necessary for the functionality of many cellular processes. Receptor-ligand bonds which last too short can result in signaling cascades not being triggered [201]. For several adhesion molecules, including E-Cad, these receptor-ligand bonds have been shown to behave like catch bonds [202][203]. The peculiarity of these adhesive bonds is that they strengthen under mechanical force, in particular there is an extension of the lifetime with increasing force [204][203]. Therefore, interaction-lifetime is an important parameter, also in terms of cell adhesion. Previous studies showed that the interaction-lifetime of classical cadherins is in the range of one second [161] [162]. Similarly, in this study the determined lifetime of Dsg3 interactions for non hyper-adhesive desmosomes is about one second, which is in the range of classical cadherins. However, for hyper-adhesive desmosomes, the Dsg3 interaction lifetime was strongly increased. The ability to extend the interaction lifetime of cadherins within desmosomes reveals another difference between desmosomes and AJs. From these experiments it can be assumed that desmosomal cadherins in non-hyper-adhesive desmosomes resemble classical cadherins whereas desmosomal cadherins in hyper-adhesive desmosomes revealed improved properties in terms of adhesive strength and duration. It can be concluded that enhanced unbinding forces as well as the increased bond lifetimes are interdependent and correlate with the acquisition of the hyper-adhesive state.

Depletion of Dsg3 in murine keratinocytes leads to failure in the acquisition of $Ca^{2+}$-independency, even after 72 h of differentiation [118]. This result further underlines the role of Dsg3 for desmosomal hyper-adhesion. This could be reflected by different binding properties depending on the desmosomal adhesive state as discussed above or by Dsg3-clustering on the cell surface. Both aspects might be related. The role of Dsg3 for desmosome-mediated adhesion can be seen under pathological condition, in the autoimmune-disease pemphigus [38]. However, stabilization of the Dsg3-bonds via crosslinking with specifically-designed peptides inhibited loss of cell cohesion triggered by PV-IgG and AK23 in living mice and cell culture models. Therefore, preservation of Dsg3 binding properties is sufficient to prevent the pathomechanism of pemphigus. Other experiments showed that presence of

hyper-adhesive desmosomes also inhibited the pathological effects of PV-IgG [140]. Consequently stabilization of Dsg3 proteins via peptides and hyper-adhesive desmosomes are sufficient to prevent the loss of cell adhesion in PV. For further investigation on Dsg1 and its role in hyper-adhesion, a Dsg1-deficient cell line would be of great importance. However, from what we know there is no such model.

Dsg3-deficient mice appear normal at birth but after day 18 a phenotype similar to incubation with PV-IgG occurs [205]. Suprabasal acantholysis occurs, most prominent in oral and vaginal mucous membrane but also in the epidermis. However, $Dsg1^{-/-}$ mice develop a lethal pemphigus phenotype with impaired barrier function and lethal skin blistering [206]. These animal models indicate different roles of those two cadherins for maintenance of epidermal integrity. We conclude that Dsg3 compared to Dsg1 is less important for basal adhesion but rather for development of hyper-adhesive desmosomes.

### 3.2.2 Desmoglein clustering correlates with hyper-adhesion and is mediated via Pkp1

As already indicated by the dispase-based dissociation assays and AFM experiments, Pkps are critical for hyper-adhesion. This is consistent with another study showing that enhanced expression of Pkp1 protects keratinocytes from PV-IgG, via desmosomal hyper-adhesion [125]. In the previous section it was shown that Pkp1 has a specific function, namely the clustering of desmosomal cadherins (see 3.1.3) [151]. A basic requirement of hyper-adhesion is the presence of clustered and organized desmosomal cadherins within $Ca^{2+}$-independent desmosomes [44].

This study showed that the acquisition of $Ca^{2+}$-independent desmosomes is accompanied by and may be based on the formation of $Ca^{2+}$-independent Dsg3 clusters. The same method was used before to show that desmosomal cadherins undergo isoform-specific homophilic binding [163]. While Dsg3 clusters in wt keratinocytes are $Ca^{2+}$-dependent after 24 h in high $Ca^{2+}$ medium, 72 h differentiation results in $Ca^{2+}$ chelation-resistant Dsg3 clusters. The acquisition of these clusters are strictly dependent on Pkp1 but not on Pkp3. However, the amount of Dsg3-clusters in Pkp3-deficient cells is significantly lower than in the wt cells due to reduced membrane availability caused by Pkp3-loss. This is in line with the involvement of Pkp3 in desmosome assembly [151]. The acquisition of $Ca^{2+}$-independent Dsg1 clusters was also investigated in this study. However, the amount of $Ca^{2+}$-independent

Dsg1 clusters remains unchanged between cells whose desmosomes are either hyper-adhesive or not. In comparison to Dsg3 clusters the level of $Ca^{2+}$-independent Dsg1 clusters is clearly reduced. Therefore, it can be concluded that, at least in the observed time frame, the alterations of Dsg3 clusters are of greater relevance towards desmosomal hyper-adhesion. The unchanged proportion of $Ca^{2+}$-independent Dsg1 clusters is consistent with unaltered single molecule Dsg1 binding properties from the AFM experiments between hyper- and non hyper-adhesive-state. Since Dsg1 in the epidermis is primarily expressed in the more superficial layers, this reflects that Dsg1 appears predominantly in later stages of the keratinocytes differentiation [38]. Therefore, it is likely that the time interval studied does not reflect the main physiological expression pattern of Dsg1. Thus, the unchanged binding properties determined might not reflect physiological contributions of Dsg1 for hyper-adhesion. On the contrary, Dsg3 is predominantly expressed in the basal layers of the epidermis [38]. The alterations in $Ca^{2+}$-dependent clusters are in excellent agreement with these expression patterns. From the literature it is known that classical cadherin clusters do not become independent of $Ca^{2+}$ [43]. This fact was also shown in this study, hence no $Ca^{2+}$-independent E-Cad clusters were detected at either time point. This supports that the concept of hyper-adhesion only applies for desmosomes and not AJs. One crucial difference between desmosomes and AJs is that classical cadherins do not occur in a highly-ordered arrangement, which is apparently a key function. This may be caused by the fact that under physiological conditions desmosomal cadherins are more flexible compared to classical cadherins. Thus, desmosomal cadherins can, even in a tightly packed space and being half bond to the plaque proteins, assemble in an ordered array because of their increased flexibility [43].

The amount of Dsg3 clusters increases during differentiation. Therefore, it needs to be discussed whether the observed increase in Dsg3 binding strength might be due to multiple binding events. A rise in Dsg3 clusters would result in higher probability for multiple binding events. Even though this probability can not be ruled out, it is rather unlikely because multiple binding would result in measured forces which are multiples of a single molecule unbinding strength [159]. However, an increase of 20% was detected only which point towards altered adhesive properties of a single-molecule interaction.

### 3.2.3 $Ca^{2+}$-dependent membrane localization differs between desmosomal cadherin isoforms in human epidermis

As described above, desmosomal cadherins are differentially expressed in the epidermis. While Dsg3 is more strongly expressed in the basal layers, Dsg1 is more abundant in the apical layers [38]. Those different expression patterns of cadherins along keratinocyte differentiation are important for proper tissue function, as desmosomes are an important regulator for intercellular signaling. Forced expression in a specific layer led to changed proliferation and cell survival [7] [207]. Furthermore, previous work showed different adhesive contributions of desmosomal cadherins since Dsg3 was more important for cellular cohesion than Dsg2 [208]. This study provides another difference between Dsg1 and Dsg3 in human the epidermis from the *ex vivo* skin model. Immunostaining of $Ca^{2+}$-depleted skin sections for Dsg1 and Dsg3 showed that Dsg1 immunostaining is less resistant to $Ca^{2+}$ chelation compared to Dsg3. Apparently, desmosomal cadherins Dsg1 and Dsg3 may have different extracellular $Ca^{2+}$-dependency. This observation is in line with the previous experiments where differences between Dsg1 and Dsg3 were observed. The results are another indication that desmosomal cadherins have different functions and properties. Therefore, the contribution towards $Ca^{2+}$-independent desmosomes is provided by specific desmosomal cadherins. The unique role of Dsg3 towards hyper-adhesion was also shown in other studies. PKC$\alpha$ is a crucial signaling molecule, hence it is regulating the conversion between the two adhesive states [115]. Some keratin isoforms sequester PKC$\alpha$ in the cytoplasm, resulting in increased desmosome stability. In line with these results, it was found that in keratin-deficient cells PKC$\alpha$ is activated, which is paralleled by impaired cellular cohesion. Interestingly, inhibition of PKC$\alpha$ signaling led to a stabilization of Dsg3 at the cell membrane [137]. Those studies further underline the relevance of Dsg3 for hyper-adhesion. On the contrary, Dsg1 was shown to interact with Erbin, which in turn suppresses EGFR/Erk signaling and thereby keratinocyte proliferation [209].

In summary, murine keratinocytes become hyper-adhesive after 72 h in high $Ca^{2+}$ medium. We found isoform-specific differences regarding the contribution of the desmosomal cadherins. $Ca^{2+}$-independent Dsg3 clusters develop during acquisition of the desmosomal hyper-adhesion, whereas Dsg1 clusters exhibit no alterations during this time frame. The formation of $Ca^{2+}$-independent clusters is mediated via Pkp1. Additionally these clusters contain Dsg3 molecules which show increased binding strength and prolonged lifetime when becoming hyper-adhesive. Altered Dsg3 binding properties from $Ca^{2+}$-independent

clusters represent a new correlate in hyper-adhesion. Pkp3-deficient cells fail to acquire a hyper-adhesive state within the studied time-interval due to reduced desmosomal cadherin membrane availability (Figure 3.2). Further, the *ex-vivo* skin model revealed differences in the membrane localization between Dsg1 and Dsg3 following $Ca^{2+}$ chelation.

In conclusion, clustered $Ca^{2+}$-independent desmosomal cadherins with altered single molecule binding properties appear to be another correlate of hyper-adhesive desmosomes. The changes in binding properties might be due to conformational changes of the cadherins within the dense clusters. We identified Dsg3 as a major component for the acquisition of hyper-adhesion. From the expression patterns of the epidermis, a possible hypothesis might be that Dsg3 interaction provides the basis of desmosomal adhesion. Absence of Dsg3 might be compensated by Dsg2, as it was shown in keratinocytes [208]. This rescue mechanism might explain the mild phenotype of the Dsg3-deficient mice. In parallel to Dsg3-mediated foundation, additional desmosomal cadherins are expressed during the differentiation process, with various functions. This was proven by the *ex-vivo* skin model that revealed different properties of desmosomal cadherins from various layers. The role of Dsg1 regarding hyper-adhesion was not observed in this study, which may be due to the fact that later time points of differentiation were not considered. However, Dsg3 seems to be crucial for hyper-adhesion because Dsg3 k.o. cells did not become hyper-adhesive. Nevertheless, it is likely that most desmosomal components are necessary for the acquisition of this state. This can be concluded for keratinocytes from mice deficient for Pkp1, Pkp3 or Dsg3. Therefore, it is conceivable that only intact desmosomes can provide full intercellular cohesion and fully acquire the hyper-adhesive state. In this scenario, an important molecular mechanism for hyper-adhesion is Pkp1-mediated assembly of $Ca^{2+}$-independent Dsg3 clusters in desmosomes with increased single-molecule unbinding strength and prolonged interaction lifetime (Figure 3.2).

Taken together, the experiments described here contributed to a better understanding of the role of Pkps for desmosomal adhesion and hyper-adhesion and provide a mechanism how desmosomal cadherins adopt their binding properties during differentiation.

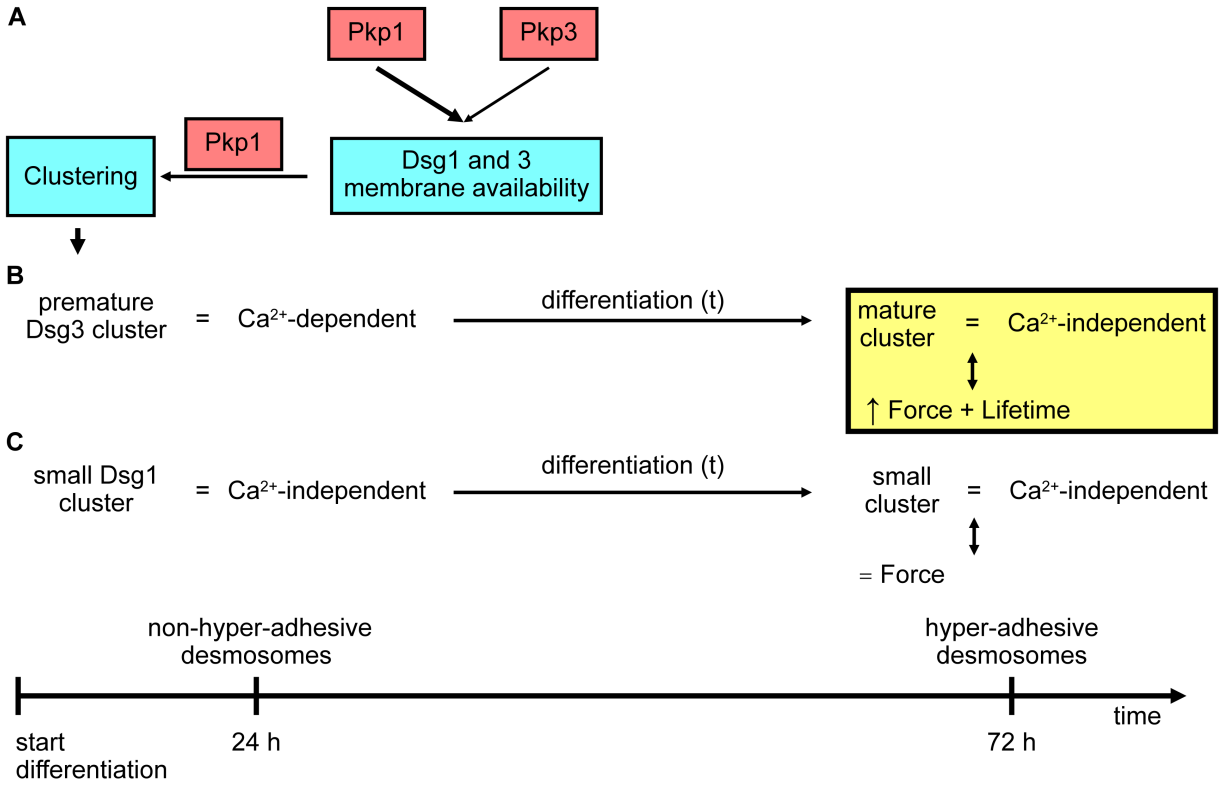


Figure 3.2: Schematic role of Pkps for hyper-adhesion through altered binding properties of desmosomal cadherins. **A**: Pkp1 and Pkp3 are important for junctional membrane availability of Dsg1 and Dsg3. However, this Pkp-subjected property has a time-dependency. Along differentiation Pkp3 becomes less relevant for desmosomal cadherin membrane availability, although a certain degree remains. For desmosomal cadherin clustering, Pkp1 has a unique role, different to Pkp3. **B**: Early time points in the differentiation process leads to premature Dsg3 cluster, which are $Ca^{2+}$-dependent, hence no hyper-adhesive desmosomes are present. During differentiation, mature Dsg3 cluster evolve, which are $Ca^{2+}$-independent and in parallel desmosomes become hyper-adhesive. Within the mature clusters, increased single molecule unbinding forces as well as prolonged lifetimes of Dsg3 interactions correlate with the formation of hyper-adhesive desmosomes (represented by arrow up). **C**: Early after onset of differentiation Dsg1 clusters are small, however $Ca^{2+}$-independent to a certain degree. During differentiation, Dsg1 clusters remain in their small size within the observed time frame. Consistent, no alterations regarding single molecule binding properties for Dsg1 were observed.

# Bibliography


[1] Luiz Carlos U Junqueira, Jose Carneiro, and Manfred Gratzl. *Histologie*, volume 6. Springer-Lehrbuch, Heidelberg, 2004.

[2] Ulrich Welsch and Wolfgang Kummer. *Lehrbuch Histologie*, volume 4. Urban and Fischer in Elsevier, 2014.

[3] Jean Kanitakis. Anatomy, histology and immunohistochemistry of normal human skin. *European Journal of Dermatology*, 12(4):390–401, 2002.

[4] Cory L Simpson, Dipal M Patel, and Kathleen J Green. Deconstructing the skin: cytoarchitectural determinants of epidermal morphogenesis. *Nature Reviews Molecular Cell Biology*, 12(9):565–580, 2011.

[5] Randall R Wickett and Marty O Visscher. Structure and function of the epidermal barrier. *American Journal of Infection Control*, 34(10):S98–S110, 2006.

[6] Peter M Steinert. Structure, function, and dynamics of keratin intermediate filaments. *Journal of Investigative Dermatology*, 100(6):729–734, 1993.

[7] Kathleen J Green, Avinash Jaiganesh, and Joshua A Broussard. Desmosomes: essential contributors to an integrated intercellular junction network. *F1000Research*, 8, 2019.

[8] Leopold Eckhart, Saskia Lippens, Erwin Tschachler, and Wim Declercq. Cell death by cornification. *Biochimica et Biophysica Acta (BBA)-Molecular Cell Research*, 1833(12):3471–3480, 2013.

[9] Elaine Fuchs and Srikala Raghavan. Getting under the skin of epidermal morphogenesis. *Nature Reviews Genetics*, 3(3):199–209, 2002.

[10] Qi Wei and Hayden Huang. Insights into the role of cell–cell junctions in physiology and disease. *International Review of Cell and Molecular Biology*, 306:187–221, 2013.

[11] Bruce Alberts, Alexander D Johnson, Julian Lewis, David Morgan, Martin Raff, Keith Roberts, and Peter Walter. *Molecular Biology of the Cell*, volume 6. Garland Science, New York, 2015.

[12] Kaelyn D Sumigray and Terry Lechler. Cell adhesion in epidermal development and barrier formation. *Current Topics in Developmental Biology*, 112:383–414, 2015.

[13] Johanna M Brandner and Jörg D Schulzke. Hereditary barrier-related diseases involving the tight junction: lessons from skin and intestine. *Cell and Tissue Research*, 360(3):723–748, 2015.

[14] James M Anderson and Christina M Van Itallie. Physiology and function of the tight junction. *Cold Spring Harbor Perspectives in Biology*, 1(2):a002584, 2009.

[15] Mitinori Saitou, Mikio Furuse, Hiroyuki Sasaki, Jorg-Dieter Schulzke, Michael Fromm, Hiroshi Takano, Tetsuo Noda, and Shoichiro Tsukita. Complex phenotype of mice lacking occludin, a component of tight junction strands. *Molecular Biology of the Cell*, 11(12):4131–4142, 2000.

[16] Junichi Ikenouchi, Mikio Furuse, Kyoko Furuse, Hiroyuki Sasaki, Sachiko Tsukita, and Shoichiro Tsukita. Tricellulin constitutes a novel barrier at tricellular contacts of epithelial cells. *The Journal of Cell Biology*, 171(6):939–945, 2005.

[17] David Vermette, Pamela Hu, Michael F Canarie, Melissa Funaro, Janis Glover, and Richard W Pierce. Tight junction structure, function, and assessment in the critically ill: a systematic review. *Intensive Care Medicine Experimental*, 6(1):1–18, 2018.

[18] Eveline E Schneeberger and Robert D Lynch. The tight junction: a multifunctional complex. *American Journal of Physiology-Cell Physiology*, 286(6):C1213–C1228, 2004.

[19] Johanna M Brandner. Tight junctions and tight junction proteins in mammalian epidermis. *European Journal of Pharmaceutics and Biopharmaceutics*, 72(2):289–294, 2009.

[20] Gülistan Meşe, Gabriele Richard, and Thomas W White. Gap junctions: basic structure and function. *Journal of Investigative Dermatology*, 127(11):2516–2524, 2007.

[21] Daniel A Goodenough. Bulk isolation of mouse hepatocyte gap junctions: Characterization of the principal protein, connexin. *The Journal of Cell Biology*, 61(2):557–563, 1974.

[22] Howard W Evans and Patricia EM Martin. Gap junctions: structure and function. *Molecular Membrane Biology*, 19(2):121–136, 2002.

[23] Yoshinobu Kanno and Werner R Loewenstein. Low-resistance coupling between gland cells. some observations on intercellular contact membranes and intercellular space. *Nature*, 201(4915):194–195, 1964.

[24] Theodore S Lawrence, William H Beers, and Norton B Gilula. Transmission of hormonal stimulation by cell-to-cell communication. *Nature*, 272(5653):501–506, 1978.

[25] Nalin M Kumar and Norton B Gilula. The gap junction communication channel. *Cell*, 84(3):381–388, 1996.

[26] Markus Kretz, Carsten Euwens, Sonja Hombach, Dominik Eckardt, Barbara Teubner, Otto Traub, Klaus Willecke, and Thomas Ott. Altered connexin expression and wound healing in the epidermis of connexin-deficient mice. *Journal of Cell Science*, 116(16):3443–3452, 2003.

[27] Janice L Brissette, Nalin M Kumar, Norton B Gilula, James E Hall, and Paolo G Dotto. Switch in gap junction protein expression is associated with selective changes in junctional permeability during keratinocyte differentiation. *Proceedings of the National Academy of Sciences*, 91(14):6453–6457, 1994.

[28] Claire A Scott, Daniel Tattersall, Edel A O'Toole, and David P Kelsell. Connexins in epidermal homeostasis and skin disease. *Biochimica et Biophysica Acta (BBA)-Biomembranes*, 1818(8):1952–1961, 2012.

[29] T Perez and W Nelson. Cadherin adhesion: mechanisms and molecular interactions. *Handbook of Experimental Pharmacology*, 165:3–21, 01 2004.

[30] Hannah K Campbell, Jessica L Maiers, and Kris A DeMali. Interplay between tight junctions & adherens junctions. *Experimental Cell Research*, 358(1):39–44, 2017.

[31] Hermann Aberle, Stefan Butz, Jörg Stappert, Helge Weissig, Rolf Kemler, and Heinz Hoschuetzky. Assembly of the cadherin-catenin complex in vitro with recombinant proteins. *Journal of Cell Science*, 107(12):3655–3663, 1994.

[32] Kenichi Takahashi, Hiroyuki Nakanishi, Masako Miyahara, Kenji Mandai, Keiko Satoh, Ayako Satoh, Hideo Nishioka, Junken Aoki, Akio Nomoto, Akira Mizoguchi, et al. Nectin/prr: an immunoglobulin-like cell adhesion molecule recruited to cadherin-based adherens junctions through interaction with afadin, a pdz domain–containing protein. *The Journal of Cell Biology*, 145(3):539–549, 1999.

[33] Kyoji Takekuni, Wataru Ikeda, Tsutomu Fujito, Koji Morimoto, Masakazu Takeuchi, Morito Monden, and Yoshimi Takai. Direct binding of cell polarity protein par-3 to cell-cell adhesion molecule nectin at neuroepithelial cells of developing mouse. *Journal of Biological Chemistry*, 278(8):5497–5500, 2003.

[34] Kathleen J Green, Spiro Getsios, Sergey Troyanovsky, and Lisa M Godsel. Intercellular junction assembly, dynamics, and homeostasis. *Cold Spring Harbor Perspectives in Biology*, 2(2):a000125, 2010.

[35] Elisabeth E Charrier and Paul A Janmey. Mechanical properties of intermediate filament proteins. *Methods in Enzymology*, 568:35–57, 2016.

[36] Tomomi E Kimura, Anita J Merritt, and David R Garrod. Calcium-independent desmosomes of keratinocytes are hyper-adhesive. *Journal of Investigative Dermatology*, 127(4):775–781, 2007.

[37] Masayuki Amagai and John R Stanley. Desmoglein as a target in skin disease and beyond. *Journal of Investigative Dermatology*, 132(3):776–784, 2012.

[38] Jens Waschke. The desmosome and pemphigus. *Histochemistry and Cell Biology*, 130(1):21–54, 2008.

[39] Jens Waschke and Volker Spindler. Desmosomes and extradesmosomal adhesive signaling contacts in pemphigus. *Medicinal Research Reviews*, 34(6):1127–1145, 2014.

[40] Helen A. Thomason, Anthea Scothern, Selina McHarg, and David R. Garrod. Desmosomes: adhesive strength and signalling in health and disease. *Biochemical Journal*, 429(3):419–433, 07 2010.

[41] Miguel A Garcia, W James Nelson, and Natalie Chavez. Cell–cell junctions organize structural and signaling networks. *Cold Spring Harbor Perspectives in Biology*, 10(4):a029181, 2018.

[42] Julia Brasch, Oliver J Harrison, Barry Honig, and Lawrence Shapiro. Thinking outside the cell: how cadherins drive adhesion. *Trends in Cell Biology*, 22(6):299–310, 2012.

[43] David R Garrod and Lydia Tabernero. Hyper-adhesion: a unique property of desmosomes. *Cell Communication & Adhesion*, 21(5):249–256, 2014.

[44] David R Garrod, Mohamed Y Berika, William F Bardsley, David Holmes, and Lydia Tabernero. Hyper-adhesion in desmosomes: its regulation in wound healing and possible relationship to cadherin crystal structure. *Journal of Cell Science*, 118(24):5743–5754, 2005.

[45] David R Garrod and Martyn Chidgey. Desmosome structure, composition and function. *Biochimica et Biophysica Acta (BBA)-Biomembranes*, 1778(3):572–587, 2008.

[46] Henry Hennings and Karen A Holbrook. Calcium regulation of cell-cell contact and differentiation of epidermal cells in culture: an ultrastructural study. *Experimental Cell Research*, 143(1):127–142, 1983.

[47] Jodi L Johnson, Nicole A Najor, and Kathleen J Green. Desmosomes: regulators of cellular signaling and adhesion in epidermal health and disease. *Cold Spring Harbor Perspectives in Medicine*, 4(11):a015297, 2014.

[48] Emmanuella Delva, Dana K Tucker, and Andrew P Kowalczyk. The desmosome. *Cold Spring Harbor Perspectives in Biology*, 1(2):a002543, 2009.

[49] Bastian Holthöfer, Reinhard Windoffer, Sergey Troyanovsky, and Rudolf E Leube. Structure and function of desmosomes. *International Review of Cytology*, 264:65–163, 2007.

[50] David R Garrod and Tomomi E Kimura. Hyper-adhesion: a new concept in cell–cell adhesion. *Biochemical Society Transactions*, 36(2):195–201, 2008.

[51] Kathleen J Green and Cory L Simpson. Desmosomes: new perspectives on a classic. *Journal of Investigative Dermatology*, 127(11):2499–2515, 2007.

[52] Peter M Elias, Norihisa Matsuyoshi, Hong Wu, Chenyan Lin, Zhi Hong Wang, Barbara E Brown, and John R Stanley. Desmoglein isoform distribution affects stratum corneum structure and function. *The Journal of Cell Biology*, 153(2):243–250, 2001.

[53] Volker Spindler, Detlev Drenckhahn, Detlef Zillikens, and Jens Waschke. Pemphigus IgG causes skin splitting in the presence of both desmoglein 1 and desmoglein 3. *The American Journal of Pathology*, 171(3):906–916, 2007.

[54] Susanne Radtke-Schuller and Helmut Bartels. Online-atlas histologie. `https://www.mhh.de/fileadmin/mhh/funktionelle-angewandte-anatomie/2_Zellverbindungen_01.pdf`, 2012. "Accessed: 22-08-2022.

[55] Wanzhong He, Pamela Cowin, and David L Stokes. Untangling desmosomal knots with electron tomography. *Science*, 302(5642):109–113, 2003.

[56] Yurni Aoyama and Yasuo Kitajima. Pemphigus vulgaris-IgG causes a rapid depletion of desmoglein 3 (dsg3) from the triton x-100 soluble pools, leading to the formation of dsg3-depleted desmosomes in a human squamous carcinoma cell line, djm-1 cells. *Journal of Investigative Dermatology*, 112(1):67–71, 1999.

[57] Miki Sato, Yumi Aoyama, and Yasuo Kitajima. Assembly pathway of desmoglein 3 to desmosomes and its perturbation by pemphigus vulgaris-IgG in cultured keratinocytes, as revealed by time-lapsed labeling immunoelectron microscopy. *Laboratory Investigation*, 80(10):1583–1592, 2000.

[58] Eliane J Müller, Lina Williamson, Carine Kolly, and Maja M Suter. Outside-in signaling through integrins and cadherins: a central mechanism to control epidermal growth and differentiation? *Journal of Investigative Dermatology*, 128(3):501–516, 2008.

[59] Volker Spindler, Vera Rötzer, Carina Dehner, Bettina Kempf, Martin Gliem, Mariya Radeva, Eva Hartlieb, Gregory S Harms, Enno Schmidt, Jens Waschke, et al. Peptide-mediated desmoglein 3 crosslinking prevents pemphigus vulgaris autoantibody-induced skin blistering. *The Journal of Clinical Investigation*, 123(2), 2013.

[60] Siu Man Tsang, Louise Brown, Hanan Gadmor, Luke Gammon, Farida Fortune, Ann Wheeler, and Hong Wan. Desmoglein 3 acting as an upstream regulator of rho gtpases, rac-1/cdc42 in the regulation of actin organisation and dynamics. *Experimental Cell Research*, 318(18):2269–2283, 2012.

[61] Martin Gliem, Wolfgang-Moritz Heupel, Volker Spindler, Gregory S Harms, and Jens Waschke. Actin reorganization contributes to loss of cell adhesion in pemphigus vulgaris. *American Journal of Physiology-Cell Physiology*, 299(3):C606–C613, 2010.

[62] Jani E Lewis, Pamela J Jensen, and Margaret J Wheelock. Cadherin function is required for human keratinocytes to assemble desmosomes and stratify in response to calcium. *Journal of Investigative Dermatology*, 102(6):870–877, 1994.

[63] Masayuki Amagai, Toshihiko Fujimori, Takuji Masunaga, Hiroshi Shimizu, Takeji Nishikawa, Nobuyoshi Shimizu, Masatoshi Takeichi, and Takashi Hashimoto. Delayed assembly of desmosomes in keratinocytes with disrupted classic-cadherin-mediated cell adhesion by a dominant negative mutant. *Journal of Investigative Dermatology*, 104(1):27–32, 1995.

[64] Siu Man Tsang, Li Liu, Muy-Teck Teh, Ann Wheeler, Richard Grose, Ian R Hart, David R Garrod, Farida Fortune, and Hong Wan. Desmoglein 3, via an interaction with e-cadherin, is associated with activation of src. *PLoS One*, 5(12):e14211, 2010.

[65] Vera Rötzer, Eva Hartlieb, Franziska Vielmuth, Martin Gliem, Volker Spindler, and Jens Waschke. E-cadherin and src associate with extradesmosomal dsg3 and modulate desmosome assembly and adhesion. *Cellular and Molecular Life Sciences*, 72(24):4885–4897, 2015.

[66] Hanna Ungewiß, Vera Rötzer, Michael Meir, Christina Fey, Markus Diefenbacher, Nicolas Schlegel, and Jens Waschke. Dsg2 via src-mediated transactivation shapes egfr signaling towards cell adhesion. *Cellular and Molecular Life Sciences*, 75(22):4251–4268, 2018.

[67] Spiro Getsios, Cory L Simpson, Shin-ichiro Kojima, Robert Harmon, Linda J Sheu, Rachel L Dusek, Mona Cornwell, and Kathleen J Green. Desmoglein 1–dependent suppression of egfr signaling promotes epidermal differentiation and morphogenesis. *Journal of Cell Biology*, 185(7):1243–1258, 2009.

[68] Donna Brennan, Sirkku Peltonen, Alicia Dowling, Walid Medhat, Kathleen J Green, James K Wahl, Francesco Del Galdo, and My G Mahoney. A role for caveolin-1 in desmoglein binding and desmosome dynamics. *Oncogene*, 31(13):1636–1648, 2012.

[69] Ansgar Schmidt and Stephanie Jäger. Plakophilins-hard work in the desmosome, recreation in the nucleus? *European Journal of Cell Biology*, 84(2-3):189–204, 2005.

[70] Stefan Bonné, Jolanda van Hengel, and Frans Van Roy. Chromosomal mapping of human armadillo genes belonging to the p120ctn/plakophilin subfamily. *Genomics*, 51(3):452–454, 1998.

[71] Amanda E Bass-Zubek, Lisa M Godsel, Mario Delmar, and Kathleen J Green. Plakophilins: multifunctional scaffolds for adhesion and signaling. *Current Opinion in Cell Biology*, 21(5):708–716, 2009.

[72] Ansgar Schmidt, Lutz Langbein, Michaela Rode, Silke Prätzel, Ralf Zimbelmann, and Werner W Franke. Plakophilins 1a and 1b: widespread nuclear proteins recruited in specific epithelial cells as desmosomal plaque components. *Cell and Tissue Research*, 290(3):481–499, 1997.

[73] Claudia Mertens, Caecilia Kuhn, and Werner W Franke. Plakophilins 2a and 2b: constitutive proteins of dual location in the karyoplasm and the desmosomal plaque. *The Journal of Cell Biology*, 135(4):1009–1025, 1996.

[74] Mechthild Hatzfeld. Plakophilins: Multifunctional proteins or just regulators of desmosomal adhesion? *Biochimica et Biophysica Acta (BBA)-Molecular Cell Research*, 1773(1):69–77, 2007.

[75] Ilse Hofmann. Plakophilins and their roles in diseased states. *Cell and Tissue Research*, 379(1):5–12, 2020.

[76] Annika Wolf and Mechthild Hatzfeld. A role of plakophilins in the regulation of translation. *Cell Cycle*, 9(15):3045–3050, 2010.

[77] Ilse Hofmann, Marialuisa Casella, Martina Schnolzer, Tanja Schlechter, Herbert Spring, and Werner W Franke. Identification of the junctional plaque protein plakophilin 3 in cytoplasmic particles containing rna-binding proteins and the recruitment of plakophilins 1 and 3 to stress granules. *Molecular Biology of the Cell*, 17(3):1388–1398, 2006.

[78] Xinyu Chen, Stefan Bonné, Mechthild Hatzfeld, Frans Van Roy, and Kathleen J Green. Protein binding and functional characterization of plakophilin 2: evidence for its diverse roles in desmosomes and $\beta$-catenin signaling. *Journal of Biological Chemistry*, 277(12):10512–10522, 2002.

[79] Mechthild Hatzfeld, Annika Wolf, and René Keil. Plakophilins in desmosomal adhesion and signaling. *Cell Communication & Adhesion*, 21(1):25–42, 2014.

[80] Brett J Roberts, Kristen E Johnson, Kathleen P McGuinn, Jintana Saowapa, Robert A Svoboda, My G Mahoney, Keith R Johnson, and James K Wahl III. Palmitoylation of plakophilin is required for desmosome assembly. *Journal of Cell Science*, 127(17):3782–3793, 2014.

[81] Annika Wolf, Katrin Rietscher, Markus Glaß, Stefan Hüttelmaier, Mike Schutkowski, Christian Ihling, Andrea Sinz, Aileen Wingenfeld, Andrej Mun, and Mechthild Hatzfeld. Insulin signaling via akt2 switches plakophilin 1 function from stabilizing cell adhesion to promoting cell proliferation. *Journal of Cell Science*, 126(8):1832–1844, 2013.

[82] Jennifer Greaves and Luke H Chamberlain. Dhhc palmitoyl transferases: substrate interactions and (patho) physiology. *Trends in Biochemical Sciences*, 36(5):245–253, 2011.

[83] Mechthild Hatzfeld, Christof Haffner, Katrin Schulze, and Ute Vinzens. The function of plakophilin 1 in desmosome assembly and actin filament organization. *The Journal of Cell Biology*, 149(1):209–222, 2000.

[84] Andrew P Kowalczyk, Mechthild Hatzfeld, Elayne A Bornslaeger, Daniel S Kopp, Jeffrey E Borgwardt, Connie M Corcoran, Aaron Settler, and Kathleen J Green. The head domain of plakophilin-1 binds to desmoplakin and enhances its recruitment to desmosomes: implications for cutaneous disease. *Journal of Biological Chemistry*, 274(26):18145–18148, 1999.

[85] James K Wahl III. A role for plakophilin-1 in the initiation of desmosome assembly. *Journal of Cellular Biochemistry*, 96(2):390–403, 2005.

[86] Katrin Rietscher, Annika Wolf, Gerd Hause, Annekatrin Rother, René Keil, Thomas M Magin, Markus Glass, Carien M Niessen, and Mechthild Hatzfeld. Growth retardation, loss of desmosomal adhesion, and impaired tight junction function identify a unique role of plakophilin 1 in vivo. *Journal of Investigative Dermatology*, 136(7):1471–1478, 2016.

[87] Lisa M Godsel, Sherry N Hsieh, Evangeline V Amargo, Amanda E Bass, Lauren T Pascoe-McGillicuddy, Arthur C Huen, Meghan E Thorne, Claire A Gaudry, Jung K Park, Kyunghee Myung, et al. Desmoplakin assembly dynamics in four dimensions multiple phases differentially regulated by intermediate filaments and actin. *Journal of Cell Biology*, 171(6):1045–1059, 2005.

[88] Werner W Franke, Carola M Borrmann, Christine Grund, and Sebastian Pieperhoff. The area composita of adhering junctions connecting heart muscle cells of vertebrates. i. molecular definition in intercalated disks of cardiomyocytes by immunoelectron microscopy of desmosomal proteins. *European Journal of Cell Biology*, 85(2):69–82, 2006.

[89] Amanda E Bass-Zubek, Ryan P Hobbs, Evangeline V Amargo, Nicholas J Garcia, Sherry N Hsieh, Xinyu Chen, James K Wahl, Mitchell F Denning, and Kathleen J Green. Plakophilin 2: a critical scaffold for pkc$\alpha$ that regulates intercellular junction assembly. *Journal of Cell Biology*, 181(4):605–613, 2008.

[90] Claudia Mertens, Ilse Hofmann, Zhengxin Wang, Martin Teichmann, Setareh Sepehri Chong, Martina Schnölzer, and Werner W Franke. Nuclear particles containing rna polymerase iii complexes associated with the junctional plaque protein plakophilin 2. *Proceedings of the National Academy of Sciences*, 98(14):7795–7800, 2001.

[91] Katja S Grossmann, Christine Grund, Joerg Huelsken, Martin Behrend, Bettina Erdmann, Werner W Franke, and Walter Birchmeier. Requirement of plakophilin 2 for heart morphogenesis and cardiac junction formation. *The Journal of Cell Biology*, 167(1):149–160, 2004.

[92] Stefan Bonné, Barbara Gilbert, Mechthild Hatzfeld, Xinyu Chen, Kathleen J Green, and Frans Van Roy. Defining desmosomal plakophilin-3 interactions. *The Journal of Cell Biology*, 161(2):403–416, 2003.

[93] Prajakta Gosavi, Samrat T Kundu, Nileema Khapare, Lalit Sehgal, Mansi S Karkhanis, and Sorab N Dalal. E-cadherin and plakoglobin recruit plakophilin3 to the cell border to initiate desmosome assembly. *Cellular and Molecular Life Sciences*, 68(8):1439–1454, 2011.

[94] Mansa Gurjar, Kumarkrishna Raychaudhuri, Snehal Mahadik, Divya Reddy, Apurva Atak, Trupti Shetty, Kruthi Rao, Mansi S Karkhanis, Prajakta Gosavi, Lalit Sehgal, et al. Plakophilin3 increases desmosome assembly, size and stability by increasing expression of desmocollin2. *Biochemical and Biophysical Research Communications*, 495(1):768–774, 2018.

[95] Tatyana Sklyarova, Stefan Bonné, Petra D'hooge, Geertrui Denecker, Steven Goossens, Riet De Rycke, Gaetan Borgonie, Michael Bösl, Frans Van Roy, and Jolanda Van Hengel. Plakophilin-3-deficient mice develop hair coat abnormalities and are prone to cutaneous inflammation. *Journal of Investigative Dermatology*, 128(6):1375–1385, 2008.

[96] Christian Michels, Thomas Buchta, Wilhelm Bloch, Thomas Krieg, and Carien M Niessen. Classical cadherins regulate desmosome formation. *Journal of Investigative Dermatology*, 129:2072–2075, 2009.

[97] Valeri Vasioukhin and Elaine Fuchs. Actin dynamics and cell–cell adhesion in epithelia. *Current Opinion in Cell Biology*, 13(1):76–84, 2001.

[98] Valeri Vasioukhin, Christoph Bauer, Mei Yin, and Elaine Fuchs. Directed actin polymerization is the driving force for epithelial cell–cell adhesion. *Cell*, 100(2):209–219, 2000.

[99] Henry Hennings and Karen A Holbrook. Calcium regulation of cell-cell contact and differentiation of epidermal cells in culture: an ultrastructural study. *Experimental Cell Research*, 143(1):127–142, 1983.

[100] Robert M Harmon and Kathleen J Green. Structural and functional diversity of desmosomes. *Cell Communication Mahoney & Adhesion*, 20(6):171–187, 2013.

[101] Ian DJ Burdett and Kate H Sullivan. Desmosome assembly in mdck cells: transport of precursors to the cell surface occurs by two phases of vesicular traffic and involves major changes in centrosome and golgi location during a ca2+ shift. *Experimental Cell Research*, 276(2):296–309, 2002.

[102] Yasushi Hanakawa, Masayuki Amagai, Yuji Shirakata, Koji Sayama, and Koji Hashimoto. Different effects of dominant negative mutants of desmocollin and desmoglein on the cell-cell adhesion of keratinocytes. *Journal of Cell Science*, 113(10):1803–1811, 2000.

[103] Oxana Nekrasova and Kathleen J Green. Desmosome assembly and dynamics. *Trends in Cell Biology*, 23(11):537–546, 2013.

[104] Lisa M Godsel, Sherry N Hsieh, Evangeline V Amargo, Amanda E Bass, Lauren T Pascoe-McGillicuddy, Arthur C Huen, Meghan E Thorne, Claire A Gaudry, Jung K Park, Kyunghee Myung, et al. Desmoplakin assembly dynamics in four dimensions: multiple phases differentially regulated by intermediate filaments and actin. *Journal of Cell Biology*, 171(6):1045–1059, 2005.

[105] Lisa M Godsel, Adi D Dubash, Amanda E Bass-Zubek, Evangeline V Amargo, Jodi L Klessner, Ryan P Hobbs, Xinyu Chen, and Kathleen J Green. Plakophilin 2 couples actomyosin remodeling to desmosomal plaque assembly via rhoa. *Molecular Biology of the Cell*, 21(16):2844–2859, 2010.

[106] Oxana E Nekrasova, Evangeline V Amargo, William O Smith, Jing Chen, Geri E Kreitzer, and Kathleen J Green. Desmosomal cadherins utilize distinct kinesins for assembly into desmosomes. *Journal of Cell Biology*, 195(7):1185–1203, 2011.

[107] Andrew P Kowalczyk, Elayne A Bornslaeger, Jeffrey E Borgwardt, Helena L Palka, Avninder S Dhaliwal, Connie M Corcoran, Mitchell F Denning, and Kathleen J Green. The amino-terminal domain of desmoplakin binds to plakoglobin and clusters desmosomal cadherin–plakoglobin complexes. *The Journal of Cell Biology*, 139(3):773–784, 1997.

[108] Miki Sato, Yumi Aoyama, and Yasuo Kitajima. Assembly pathway of desmoglein 3 to desmosomes and its perturbation by pemphigus vulgaris-IgG in cultured keratinocytes, as revealed by time-lapsed labeling immunoelectron microscopy. *Laboratory Investigation*, 80(10):1583–1592, 2000.

[109] Siu Man Tsang, Louise Brown, Hanan Gadmor, Luke Gammon, Farida Fortune, Ann Wheeler, and Hong Wan. Desmoglein 3 acting as an upstream regulator of rho gtpases, rac-1/cdc42 in the regulation of actin organisation and dynamics. *Experimental Cell Research*, 318(18):2269–2283, 2012.

[110] Reinhard Windoffer, Monika Borchert-Stuhlträger, and Rudolf E Leube. Desmosomes: interconnected calcium-dependent structures of remarkable stability with significant integral membrane protein turnover. *Journal of Cell Science*, 115(8):1717–1732, 2002.

[111] Volker Spindler and Jens Waschke. Desmosomal cadherins and signaling: lessons from autoimmune disease. *Cell Communication & Adhesion*, 21(1):77–84, 2014.

[112] Sara N Stahley, Masataka Saito, Victor Faundez, Michael Koval, Alexa L Mattheyses, and Andrew P Kowalczyk. Desmosome assembly and disassembly are membrane raft-dependent. *PloS One*, 9(1):e87809, 2014.

[113] D Oktarina, G Van Der Wier, G Diercks, M Jonkman, and H Pas. IgG-induced clustering of desmogleins 1 and 3 in skin of patients with pemphigus fits with the desmoglein nonassembly depletion hypothesis. *British Journal of Dermatology*, 165(3):552–562, 2011.

[114] Paula Berkowitz, Peiqi Hu, Zhi Liu, Luis A Diaz, Jan J Enghild, Michael P Chua, and David S Rubenstein. Desmosome signaling: inhibition of p38mapk prevents pemphigus vulgaris IgG-induced cytoskeleton reorganization. *Journal of Biological Chemistry*, 280(25):23778–23784, 2005.

[115] Sarah Wallis, Susan Lloyd, Irene Wise, Grenham Ireland, Tom P Fleming, and David R Garrod. The $\alpha$ isoform of protein kinase c is involved in signaling the response of desmosomes to wounding in cultured epithelial cells. *Molecular Biology of the Cell*, 11(3):1077–1092, 2000.

[116] Tomomi E Kimura, Anita J Merritt, Francesca R Lock, Judith J Eckert, Tom P Fleming, and David R Garrod. Desmosomal adhesiveness is developmentally regulated in the mouse embryo and modulated during trophectoderm migration. *Developmental Biology*, 369(2):286–297, 2012.

[117] Maria Shoykhet, Sebastian Trenz, Ellen Kempf, Tatjana Williams, Brenda Gerull, Camilla Schinner, Sunil Yeruva, and Jens Waschke. Cardiomyocyte adhesion and hyperadhesion differentially require erk1/2 and plakoglobin. *JCI Insight*, 5(18), 2020.

[118] Michael Fuchs, Anna Magdalena Sigmund, Jens Waschke, and Franziska Vielmuth. Desmosomal hyperadhesion is accompanied with enhanced binding strength of desmoglein 3 molecules. *Biophysical Journal*, 119(8):1489–1500, 2020.

[119] Helen A Thomason, Anthea Scothern, Selina McHarg, and David R Garrod. Desmosomes: adhesive strength and signalling in health and disease. *Biochemical Journal*, 429(3):419–433, 2010.

[120] Taofei Yin and Kathleen J Green. Regulation of desmosome assembly and adhesion. In *Seminars in Cell & Developmental Biology*, volume 15, pages 665–677. Elsevier, 2004.

[121] Kathleen J Green, Spiro Getsios, Sergey Troyanovsky, and Lisa M Godsel. Intercellular junction assembly, dynamics, and homeostasis. *Cold Spring Harbor Perspectives in Biology*, 2(2):a000125, 2010.

[122] Sabine Pokutta, Kurt Herrenknecht, Rolf Kemler, and Jürgen ENGEL. Conformational changes of the recombinant extracellular domain of e-cadherin upon calcium binding. *European Journal of Biochemistry*, 223(3):1019–1026, 1994.

[123] Titus J Boggon, John Murray, Sophie Chappuis-Flament, Ellen Wong, Barry M Gumbiner, and Lawrence Shapiro. C-cadherin ectodomain structure and implications for cell adhesion mechanisms. *Science*, 296(5571):1308–1313, 2002.

[124] Humera Tariq, Jordi Bella, Thomas A Jowitt, David F Holmes, Mansour Rouhi, Zhuxiang Nie, Clair Baldock, David R Garrod, and Lydia Tabernero. Cadherin flexibility provides a key difference between desmosomes and adherens junctions. *Proceedings of the National Academy of Sciences*, 112(17):5395–5400, 2015.

[125] Dana K Tucker, Sara N Stahley, and Andrew P Kowalczyk. Plakophilin-1 protects keratinocytes from pemphigus vulgaris IgG by forming calcium-independent desmosomes. *Journal of Investigative Dermatology*, 134(4):1033–1043, 2014.

[126] Zahurul A Bhuiyan, Jan DH Jongbloed, Jasper Van Der Smagt, Paola M Lombardi, Ans CP Wiesfeld, Marcel Nelen, Meyke Schouten, Roselie Jongbloed, Moniek GPJ Cox, Marleen Van Wolferen, et al. Desmoglein-2 and desmocollin-2 mutations in dutch arrhythmogenic right ventricular dysplasia/cardiomypathy patients: results from a multicenter study. *Circulation: Cardiovascular Genetics*, 2(5):418–427, 2009.

[127] Masayuki Amagai, Vera Klaus-Kovtun, and John R Stanley. Autoantibodies against a novel epithelial cadherin in pemphigus vulgaris, a disease of cell adhesion. *Cell*, 67(5):869–877, 1991.

[128] Masayuki Amagai. Autoimmune and infectious skin diseases that target desmogleins. *Proceedings of the Japan Academy, Series B*, 86(5):524–537, 2010.

[129] John R Stanley and Masayuki Amagai. Pemphigus, bullous impetigo, and the staphylococcal scalded-skin syndrome. *New England Journal of Medicine*, 355(17):1800–1810, 2006.

[130] Valeria Aoki, Robert C Millikan, Evandro A Rivitti, Gunter Hans-Filho, Donald P Eaton, Simon JP Warren, Ning Li, Julio Hilario-Vargas, Raymond G Hoffmann, and Luis A Diaz. Environmental risk factors in endemic pemphigus foliaceus (fogo selvagem). In *Journal of Investigative Dermatology Symposium Proceedings*, volume 9, pages 34–40. Elsevier, 2004.

[131] Andrea Kneisel and Michael Hertl. Autoimmune bullous skin diseases. part 1: clinical manifestations. *JDDG: Journal der Deutschen Dermatologischen Gesellschaft*, 9(10):844–857, 2011.

[132] Robert Pollmann, Thomas Schmidt, Rüdiger Eming, and Michael Hertl. Pemphigus: a comprehensive review on pathogenesis, clinical presentation and novel therapeutic approaches. *Clinical Reviews in Allergy & Immunology*, 54(1):1–25, 2018.

[133] Wolfgang-Moritz Heupel, Detlef Zillikens, Detlev Drenckhahn, and Jens Waschke. Pemphigus vulgaris IgG directly inhibit desmoglein 3-mediated transinteraction. *The Journal of Immunology*, 181(3):1825–1834, 2008.

[134] Franziska Vielmuth, Jens Waschke, and Volker Spindler. Loss of desmoglein binding is not sufficient for keratinocyte dissociation in pemphigus. *Journal of Investigative Dermatology*, 135(12):3068–3077, 2015.

[135] Preety Sharma, Xuming Mao, and Aimee S Payne. Beyond steric hindrance: the role of adhesion signaling pathways in the pathogenesis of pemphigus. *Journal of Dermatological Science*, 48(1):1–14, 2007.

[136] Paula Berkowitz, Peiqi Hu, Simon Warren, Zhi Liu, Luis A Diaz, and David S Rubenstein. p38mapk inhibition prevents disease in pemphigus vulgaris mice. *Proceedings of the National Academy of Sciences*, 103(34):12855–12860, 2006.

[137] Franziska Vielmuth, Marie-Therès Wanuske, Mariya Y Radeva, Matthias Hiermaier, Daniela Kugelmann, Elias Walter, Fanny Buechau, Thomas M Magin, Jens Waschke, and Volker Spindler. Keratins regulate the adhesive properties of desmosomal cadherins through signaling. *Journal of Investigative Dermatology*, 138(1):121–131, 2018.

[138] Yasuo Kitajima. New insights into desmosome regulation and pemphigus blistering as a desmosome-remodeling disease. *The Kaohsiung Journal of Medical Sciences*, 29(1):1–13, 2013.

[139] Volker Spindler, Alexander Endlich, Eva Hartlieb, Franziska Vielmuth, Enno Schmidt, and Jens Waschke. The extent of desmoglein 3 depletion in pemphigus vulgaris is dependent on ca2+-induced differentiation: a role in suprabasal epidermal skin splitting? *The American Journal of Pathology*, 179(4):1905–1916, 2011.

[140] Nicola Cirillo, Alessandro Lanza, and Stephen S Prime. Induction of hyper-adhesion attenuates autoimmune-induced keratinocyte cell–cell detachment and processing of adhesion molecules via mechanisms that involve pkc. *Experimental Cell Research*, 316(4):580–592, 2010.

[141] Alex I Chernyavsky, Juan Arredondo, Yasuo Kitajima, Miki Sato-Nagai, and Sergei A Grando. Desmoglein versus non-desmoglein signaling in pemphigus acantholysis: characterization of novel signaling pathways downstream of pemphigus vulgaris antigens. *Journal of Biological Chemistry*, 282(18):13804–13812, 2007.

[142] Paula Berkowitz, Luis A Diaz, Russel P Hall, and David S Rubenstein. Induction of p38mapk and hsp27 phosphorylation in pemphigus patient skin. *The Journal of Investigative Dermatology*, 128(3):738–740, 2007.

[143] G. Fontaine, F. Fontaliran, J.L. Hebert, D. Chemla, O. Zenati, Y. Lecarpentier, and R. Frank. Arrhythmogenic right ventricular dysplasia. *Annual Review of Medicine*, 50(1):17–35, 1999.

[144] Steffen Rickelt. Plakophilin-2: a cell-cell adhesion plaque molecule of selective and fundamental importance in cardiac functions and tumor cell growth. *Cell and Tissue Research*, 348(2):281–294, 2012.

[145] Mark M Awad, Darshan Dalal, Eunpi Cho, Nuria Amat-Alarcon, Cynthia James, Crystal Tichnell, April Tucker, Stuart D Russell, David A Bluemke, Harry C Dietz, et al. Dsg2 mutations contribute to arrhythmogenic right ventricular dysplasia/cardiomyopathy. *The American Journal of Human Genetics*, 79(1):136–142, 2006.

[146] Nicola Cirillo. Desmosome assembly, homeostasis, and desmosomal disease. *Cell Health and Cytoskeleton*, 8:9–23, 2016.

[147] John A McGrath, James R McMillan, Carrie S Shemanko, Sarah K Runswick, Irene M Leigh, E Birgitte Lane, David R Garrod, and Robin AJ Eady. Mutations in the plakophilin 1 gene result in ectodermal dysplasia/skin fragility syndrome. *Nature Genetics*, 17(2):240–244, 1997.

[148] Annamaria Zaltron, Michele Merano, Giampaolo Mistura, Cinzia Sada, and Flavio Seno. Optical tweezers in single-molecule experiments. *The European Physical Journal Plus*, 135(11):1–33, 2020.

[149] JPK Instruments AB. *NanoWizard AFM® AFM Handbook*. JPK, Berlin, Germany, 2012.

[150] Xinming Zhang, Lu Ma, and Yongli Zhang. High-resolution optical tweezers for single-molecule manipulation. *The Yale Journal of Biology and Medicine*, 86(3):367, 2013.

[151] Michael Fuchs, Marco Foresti, Mariya Y Radeva, Daniela Kugelmann, Rene Keil, Mechthild Hatzfeld, Volker Spindler, Jens Waschke, and Franziska Vielmuth. Plakophilin 1 but not plakophilin 3 regulates desmoglein clustering. *Cellular and Molecular Life Sciences*, 76(17):3465–3476, 2019.

[152] Alexander W Koch, Sabine Pokutta, Ariel Lustig, and Jürgen Engel. Calcium binding and homoassociation of e-cadherin domains. *Biochemistry*, 36(25):7697–7705, 1997.

[153] Oliver J Harrison, Xiangshu Jin, Soonjin Hong, Fabiana Bahna, Goran Ahlsen, Julia Brasch, Yinghao Wu, Jeremie Vendome, Klara Felsovalyi, Cheri M Hampton, et al. The extracellular architecture of adherens junctions revealed by crystal structures of type i cadherins. *Structure*, 19(2):244–256, 2011.

[154] Emilio Parisini, Jonathan MG Higgins, Jin-huan Liu, Michael B Brenner, and Jia-huai Wang. The crystal structure of human e-cadherin domains 1 and 2, and comparison with other cadherins in the context of adhesion mechanism. *Journal of Molecular Biology*, 373(2):401–411, 2007.

[155] Shoshana Posy, Lawrence Shapiro, and Barry Honig. Sequence and structural determinants of strand swapping in cadherin domains: do all cadherins bind through the same adhesive interface? *Journal of Molecular Biology*, 378(4):954–968, 2008.

[156] Mateusz Sikora, Utz H Ermel, Anna Seybold, Michael Kunz, Giulia Calloni, Julian Reitz, R Martin Vabulas, Gerhard Hummer, and Achilleas S Frangakis. Desmosome architecture derived from molecular dynamics simulations and cryo-electron tomography. *Proceedings of the National Academy of Sciences*, 117(44):27132–27140, 2020.

[157] Oliver J Harrison, Fabiana Bahna, Phini S Katsamba, Xiangshu Jin, Julia Brasch, Jeremie Vendome, Goran Ahlsen, Kilpatrick J Carroll, Stephen R Price, Barry Honig, et al. Two-step adhesive binding by classical cadherins. *Nature Structural & Molecular Biology*, 17(3):348, 2010.

[158] Franziska Vielmuth, Volker Spindler, and Jens Waschke. Atomic force microscopy provides new mechanistic insights into the pathogenesis of pemphigus. *Frontiers in Immunology*, 9:485, 2018.

[159] Jens Waschke, Carlos Menendez-Castro, Paola Bruggeman, Rainer Koob, Masayuki Amagai, Hermann J Gruber, Detlev Drenckhahn, and Werner Baumgartner. Imaging and force spectroscopy on desmoglein 1 using atomic force microscopy reveal multivalent ca 2+-dependent, low-affinity trans-interaction. *Journal of Membrane Biology*, 216(2):83–92, 2007.

[160] Wolfgang-Moritz Heupel, Detlev Drenckhahn, Detlef Zillikens, and Jens Waschke. Steric hindrance of desmoglein 3 transinteraction by pemphigus vulgaris IgG. In *Journal of Investigative Dermatology*, volume 127, pages S5–S5, 2007.

[161] Werner Baumgartner, Nikola Golenhofen, Niko Grundhöfer, Johannes Wiegand, and Detlev Drenckhahn. Ca2+ dependency of n-cadherin function probed by laser tweezer and atomic force microscopy. *Journal of Neuroscience*, 23(35):11008–11014, 2003.

[162] Werner Baumgartner, Peter Hinterdorfer, W Ness, Anneliese Raab, D Vestweber, Hansgeorg Schindler, and Detlev Drenckhahn. Cadherin interaction probed by atomic force microscopy. *Proceedings of the National Academy of Sciences*, 97(8):4005–4010, 2000.

[163] Zhuxiang Nie, Anita Merritt, Mansour Rouhi-Parkouhi, Lydia Tabernero, and David R Garrod. Membrane-impermeable cross-linking provides evidence for homophilic,

isoform-specific binding of desmosomal cadherins in epithelial cells. *Journal of Biological Chemistry*, 286(3):2143–2154, 2011.

[164] Volker Spindler, Wolfgang-Moritz Heupel, Athina Efthymiadis, Enno Schmidt, Rüdiger Eming, Christian Rankl, Peter Hinterdorfer, Thomas Müller, Detlev Drenckhahn, and Jens Waschke. Desmocollin 3-mediated binding is crucial for keratinocyte cohesion and is impaired in pemphigus. *Journal of Biological Chemistry*, 284(44):30556–30564, 2009.

[165] Anna M Sigmund, Letyfee S Steinert, Desalegn T Egu, Franziska C Bayerbach, Jens Waschke, and Franziska Vielmuth. Dsg2 upregulation as a rescue mechanism in pemphigus. *Frontiers in Immunology*, 11:2713, 2020.

[166] Nikolai A Chitaev and Sergey M Troyanovsky. Direct ca2+-dependent heterophilic interaction between desmosomal cadherins, desmoglein and desmocollin, contributes to cell–cell adhesion. *Journal of Cell Biology*, 138(1):193–201, 1997.

[167] Shabih-e-Hassnain Syed, Brian Trinnaman, Stephen Martin, Sarah Major, Jon Hutchinson, and Anthony I Magee. Molecular interactions between desmosomal cadherins. *Biochemical Journal*, 362(2):317–327, 2002.

[168] Omer Shafraz, Matthias Rübsam, Sara N Stahley, Amber L Caldara, Andrew P Kowalczyk, Carien M Niessen, and Sanjeevi Sivasankar. E-cadherin binds to desmoglein to facilitate desmosome assembly. *Elife*, 7:e37629, 2018.

[169] Mi Li, Dan Dang, Ning Xi, Yuechao Wang, and Lianqing Liu. Nanoscale imaging and force probing of biomolecular systems using atomic force microscopy: from single molecules to living cells. *Nanoscale*, 9(45):17643–17666, 2017.

[170] M Radmacher, RW Tillamnn, M Fritz, and HE Gaub. From molecules to cells: imaging soft samples with the atomic force microscope. *Science*, 257(5078):1900–1905, 1992.

[171] David P Allison, Ninell P Mortensen, Claretta J Sullivan, and Mitchel J Doktycz. Atomic force microscopy of biological samples. *Wiley Interdisciplinary Reviews: Nanomedicine and Nanobiotechnology*, 2(6):618–634, 2010.

[172] Andreas Ebner, Linda Wildling, ASM Kamruzzahan, Christian Rankl, Jürgen Wruss, Christoph D Hahn, Martin Hölzl, Rong Zhu, Ferry Kienberger, Dieter Blaas, et al. A new, simple method for linking of antibodies to atomic force microscopy tips. *Bioconjugate Chemistry*, 18(4):1176–1184, 2007.

[173] Julia Schmitz, Martin Benoit, and Kay-Eberhard Gottschalk. The viscoelasticity of membrane tethers and its importance for cell adhesion. *Biophysical Journal*, 95(3):1448–1459, 2008.

[174] Emily B Walton, Sunyoung Lee, and Krystyn J Van Vliet. Extending bell's model: how force transducer stiffness alters measured unbinding forces and kinetics of molecular complexes. *Biophysical Journal*, 94(7):2621–2630, 2008.

[175] Klaus D Sattler. *Handbook of Nanophysics: Nanomedicine and Nanorobotics*. CRC press, 2010.

[176] Julie A Wieland, Andrew A Gewirth, and Deborah E Leckband. Single molecule adhesion measurements reveal two homophilic neural cell adhesion molecule bonds with mechanically distinct properties. *Journal of Biological Chemistry*, 280(49):41037–41046, 2005.

[177] George I Bell. Models for the specific adhesion of cells to cells. *Science*, 200(4342):618–627, 1978.

[178] Franziska Vielmuth, Elias Walter, Michael Fuchs, Mariya Y Radeva, Fanny Buechau, Thomas M Magin, Volker Spindler, and Jens Waschke. Keratins regulate p38mapk-dependent desmoglein binding properties in pemphigus. *Frontiers in Immunology*, 9:528, 2018.

[179] René Keil, Katrin Rietscher, and Mechthild Hatzfeld. Antagonistic regulation of intercellular cohesion by plakophilins 1 and 3. *Journal of Investigative Dermatology*, 136(10):2022–2029, 2016.

[180] Srikanta Basu, Nazia Chaudhary, Sanket Shah, Carol Braggs, Aakanksha Sawant, Simone Vaz, Rahul Thorat, Sanjay Gupta, and Sorab N Dalal. Plakophilin3 loss leads to an increase in lipocalin2 expression, which is required for tumour formation. *Experimental Cell Research*, 369(2):251–265, 2018.

[181] Henry Hennings, Delores Michael, Christina Cheng, Peter Steinert, Karen Holbrook, and Stuart H Yuspa. Calcium regulation of growth and differentiation of mouse epidermal cells in culture. *Cell*, 19(1):245–254, 1980.

[182] Andrew P South, Hong Wan, Michael G Stone, Patricia JC Dopping-Hepenstal, Patricia E Purkis, John F Marshall, Irene M Leigh, Robin AJ Eady, Ian R Hart, and John A McGrath. Lack of plakophilin 1 increases keratinocyte migration and reduces desmosome stability. *Journal of Cell Science*, 116(16):3303–3314, 2003.

[183] Ediz Sariisik, Cvetan Popov, Jochen P Müller, Denitsa Docheva, Hauke Clausen-Schaumann, and Martin Benoit. Decoding cytoskeleton-anchored and non-anchored receptors from single-cell adhesion force data. *Biophysical journal*, 109(7):1330–1333, 2015.

[184] Marie-Therès Wanuske, Dominique Brantschen, Camilla Schinner, Chiara Stüdle, Elias Walter, Matthias Hiermaier, Franziska Vielmuth, Jens Waschke, and Volker Spindler. Clustering of desmosomal cadherins by desmoplakin is essential for cell-cell adhesion. *Acta Physiologica*, page e13609, 2020.

[185] Alpha S Yap, William M Brieher, Martin Pruschy, and Barry M Gumbiner. Lateral clustering of the adhesive ectodomain: a fundamental determinant of cadherin function. *Current Biology*, 7(5):308–315, 1997.

[186] Mariko Seishima, Chikako Esaki, Kazuko Osada, Shunji Mori, Takashi Hashimoto, and Yasuo Kitajima. Pemphigus IgG, but not bullous pemphigoid IgG, causes a transient increase in intracellular calcium and inositol 1, 4, 5-triphosphate in djm-1 cells, a squamous cell carcinoma line. *Journal of Investigative Dermatology*, 104(1):33–37, 1995.

[187] Kazuko Osada, Mariko Seishima, and Yasuo Kitajima. Pemphigus IgG activates and translocates protein kinase c from the cytosol to the particulate/cytoskeleton fractions in human keratinocytes. *Journal of Investigative Dermatology*, 108(4):482–487, 1997.

[188] Stefan Wöll, Reinhard Windoffer, and Rudolf E Leube. p38 mapk-dependent shaping of the keratin cytoskeleton in cultured cells. *The Journal of Cell Biology*, 177(5):795–807, 2007.

[189] Elias Walter, Franziska Vielmuth, Lukas Rotkopf, Miklós Sárdy, Orsolya N Horváth, Matthias Goebeler, Enno Schmidt, Rüdiger Eming, Michael Hertl, Volker Spindler, et al. Different signaling patterns contribute to loss of keratinocyte cohesion dependent on autoantibody profile in pemphigus. *Scientific Reports*, 7(1):1–11, 2017.

[190] Volker Spindler, Carina Dehner, Stefan Hübner, and Jens Waschke. Plakoglobin but not desmoplakin regulates keratinocyte cohesion via modulation of p38mapk signaling. *Journal of Investigative Dermatology*, 134(6):1655–1664, 2014.

[191] Akihiro Kusumi, Kenichi Suzuki, and Kotaro Koyasako. Mobility and cytoskeletal interactions of cell adhesion receptors. *Current Opinion in Cell Biology*, 11(5):582–590, 1999.

[192] Yao Wu, Pakorn Kanchanawong, and Ronen Zaidel-Bar. Actin-delimited adhesion-independent clustering of e-cadherin forms the nanoscale building blocks of adherens junctions. *Developmental Cell*, 32(2):139–154, 2015.

[193] Ashraf Al-Amoudi, Daniel Castaño-Diez, Damien P Devos, Robert B Russell, Graham T Johnson, and Achilleas S Frangakis. The three-dimensional molecular structure of the desmosomal plaque. *Proceedings of the National Academy of Sciences*, 108(16):6480–6485, 2011.

[194] Emily I Bartle, Tejeshwar C Rao, Reena R Beggs, William F Dean, Tara M Urner, Andrew P Kowalczyk, and Alexa L Mattheyses. Protein exchange is reduced in calcium-independent epithelial junctions. *Journal of Cell Biology*, 219(6), 2020.

[195] Matthias Hiermaier, Felix Kliewe, Camilla Schinner, Chiara Stüdle, I Piotr Maly, Marie-Therès Wanuske, Vera Rötzer, Nicole Endlich, Franziska Vielmuth, Jens

Waschke, et al. The actin binding protein $\alpha$-adducin modulates desmosomal turnover and plasticity. *Journal of Investigative Dermatology*, 2020.

[196] Kazuyuki Tsunoda, Takayuki Ota, Miyo Aoki, Taketo Yamada, Tetsuo Nagai, Taneaki Nakagawa, Shigeo Koyasu, Takeji Nishikawa, and Masayuki Amagai. Induction of pemphigus phenotype by a mouse monoclonal antibody against the amino-terminal adhesive interface of desmoglein 3. *The Journal of Immunology*, 170(4):2170–2178, 2003.

[197] Lawrence Shapiro, Allison M Fannon, Peter D Kwong, Andrew Thompson, Mogens S Lehmann, Gerhard Grübel, Jean-François Legrand, Jens Als-Nielsen, David R Colman, and Wayne A Hendrickson. Structural basis of cell-cell adhesion by cadherins. *Nature*, 374(6520):327–337, 1995.

[198] Alpha S Yap, William M Brieher, Martin Pruschy, and Barry M Gumbiner. Lateral clustering of the adhesive ectodomain: a fundamental determinant of cadherin function. *Current Biology*, 7(5):308–315, 1997.

[199] Soonjin Hong, Regina B Troyanovsky, and Sergey M Troyanovsky. Binding to f-actin guides cadherin cluster assembly, stability, and movement. *Journal of Cell Biology*, 201(1):131–143, 2013.

[200] David R Garrod and Tomomi E Kimura. Hyper-adhesion: a new concept in cell–cell adhesion. *Biochemical Society Transactions*, 36(2):195–201, 2008.

[201] Javier Corzo. Time, the forgotten dimension of ligand binding teaching. *Biochemistry and Molecular Biology Education*, 34(6):413–416, 2006.

[202] Sabyasachi Rakshit, Yunxiang Zhang, Kristine Manibog, Omer Shafraz, and Sanjeevi Sivasankar. Ideal, catch, and slip bonds in cadherin adhesion. *Proceedings of the National Academy of Sciences*, 109(46):18815–18820, 2012.

[203] Kristine Manibog, Chi-Fu Yen, and Sanjeevi Sivasankar. Measuring force-induced dissociation kinetics of protein complexes using single-molecule atomic force microscopy. *Methods in Enzymology*, 582:297–320, 2017.

[204] Deborah Leckband and Sanjeevi Sivasankar. Biophysics of cadherin adhesion. *Adherens Junctions: From Molecular Mechanisms to Tissue Development and Disease*, pages 63–88, 2012.

[205] Peter J Koch, M G Mahoney, Hiroyasu Ishikawa, Leena Pulkkinen, Jouni Uitto, Leonard Shultz, George F Murphy, Diana Whitaker-Menezes, and John R Stanley. Targeted disruption of the pemphigus vulgaris antigen (desmoglein 3) gene in mice causes loss of keratinocyte cell adhesion with a phenotype similar to pemphigus vulgaris. *The Journal of Cell Biology*, 137(5):1091–1102, 1997.

[206] Daniela Kugelmann, Mariya Y Radeva, Volker Spindler, and Jens Waschke. Desmoglein 1 deficiency causes lethal skin blistering. *The Journal of Investigative Dermatology*, 2019.

[207] Anita J Merritt, Mohamed Y Berika, Wenwu Zhai, Sarah E Kirk, Baijing Ji, Matthew J Hardman, and David R Garrod. Suprabasal desmoglein 3 expression in the epidermis of transgenic mice results in hyperproliferation and abnormal differentiation. *Molecular and Cellular Biology*, 22(16):5846–5858, 2002.

[208] Eva Hartlieb, Vera Rötzer, Mariya Radeva, Volker Spindler, and Jens Waschke. Desmoglein 2 compensates for desmoglein 3 but does not control cell adhesion via regulation of p38 mitogen-activated protein kinase in keratinocytes. *Journal of Biological Chemistry*, 289(24):17043–17053, 2014.

[209] Alejandra Valenzuela-Iglesias, Hope E Burks, Christopher R Arnette, Amulya Yalamanchili, Oxana Nekrasova, Lisa M Godsel, and Kathleen J Green. Desmoglein 1 regulates invadopodia by suppressing egfr/erk signaling in an erbin-dependent manner. *Molecular Cancer Research*, 17(5):1195–1206, 2019.

# Appendix

## A.1 Abbreviations

| | |
|---|---|
| **AFM** | atomic force microscopy |
| **AJs** | adherens junctions |
| **ARVC** | arrhythmogenic right ventricular cardiomyopathy |
| **cAMP** | cyclic adenosine monophosphate |
| **Cxs** | connexins |
| **DP** | desmoplakin |
| **Dsc** | desmocollin |
| **Dsg** | desmoglein |
| **E-Cad** | E-cadherin |
| **EC** | extracellular domains |
| **EGFR** | epidermal growth factor receptor |
| **EGTA** | ethylene glycol tetraacetic acid |
| **FRAP** | fluorescence recovery after photobleaching |
| **HaCaT** | human keratinocyte cells |
| **HSP** | heat shock protein |
| **IDP** | inner dense plaque |
| **IFs** | intermediate filaments |
| **JAMs** | junctional adhesion molecules |
| **KtyII k.o.** | keratin cluster II knockout |
| **MDCK** | Madin-Darby canine kidney |
| **N-Cad** | N-cadherin |
| **ODP** | outer dense plaque |
| **p38MAPK** | p38 mitogen-activated protein kinases |
| **P-Cad** | P-cadherin |
| **PF** | pemphigus foliaceus |
| **PG** | plakoglobin |
| **PKC** | protein kinase C |
| **Pkps** | plakophilins |
| **PV** | pemphigus vulgaris |
| **Src** | sarcoma-associated kinase |
| **STED** | stimulated emission depletion |
| **TJs** | tight junctions |
| **UF** | unbinding force |
| **UP** | unbinding position |
| **wt** | wild type |
| **ZO** | zona occludens |

## A.2 List of original publications

- Fuchs et al., (2020) Biophysical Journal

  **Fuchs, M.**, Sigmund, A. M., Waschke, J., & Vielmuth, F. (2020). Desmosomal Hyperadhesion Is Accompanied with Enhanced Binding Strength of Desmoglein 3 Molecules. Biophysical Journal, 119(8), 1489-1500.

- Kugelmann et al., (2019) Frontiers in immunology

  Kugelmann, D., Rötzer, V., Walter, E., Egu, D. T., **Fuchs, M. T.**, Vielmuth, F., ... & Waschke, J. (2019). Role of Src and cortactin in pemphigus skin blistering. Frontiers in immunology, 10, 626.

- Fuchs et al., (2019) Cellular and Molecular Life sciences

  **Fuchs, M.**, Foresti, M., Radeva, M. Y., Kugelmann, D., Keil, R., Hatzfeld, M., ... & Vielmuth, F. (2019). Plakophilin 1 but not plakophilin 3 regulates desmoglein clustering. Cellular and Molecular Life Sciences, 76(17), 3465-3476.

- Vielmuth et al., (2018) Frontiers in immunology

  Vielmuth, F., Walter, E., **Fuchs, M.**, Radeva, M. Y., Buechau, F., Magin, T. M., ... & Waschke, J. (2018). Keratins regulate p38MAPK-dependent desmoglein binding properties in pemphigus. Frontiers in immunology, 9, 528.

## A.3 Contributions

The data of this doctoral thesis is published in the following publications. The data was acquired from June 2017 until September 2020 in the laboratory of Prof. Dr. Jens Waschke (Institute of Anatomy and Cell Biology, Faculty of Medicine, Ludwig-Maximilians-Universität Munich).

*Declaration of contributions to "Plakophilin 1 but not plakophilin 3 regulates desmoglein clustering"*

This study was designed and planned by Jens Waschke, Franziska Vielmuth and me. I conducted this study together with Marco Foresti. I designed and performed all experiments except for Figure 1 a and c, Figure 2, Figure S1 a and Figure S2 a and b which were performed by Marco Foresti. I evaluated all data, prepared the figures, wrote and edited the manuscript. Murine keratinocyte knockout cell lines were provided by Rene Keil and Mechthild Hatzfeld.

*Declaration of contributions to "Desmosomal Hyperadhesion Is Accompanied with Enhanced Binding Strength of Desmoglein 3 Molecules"*

This study was planned and designed by Jens Waschke, Franziska Vielmuth and me. I performed all experiments. Murine keratinocyte knockout cell lines were provided by Rene Keil and Mechthild Hatzfeld. The murine desmoglein 3 knockout cell line was provided by Anna Sigmund. I evaluated all data, prepared the figures, wrote and edited the manuscript.

*Declaration of contributions to "Keratins regulate p38MAPK-dependent desmoglein binding properties in pemphigus"*

This study was planned and designed by Franziska Vielmuth and Jens Waschke. I performed fluorescence recovery after photobleaching experiments. I prepared the figure 2 E and F, wrote the corresponding figure legend and the method part and proofread the manuscript.

We hereby confirm the above statements:
Munich, 24th August 2022

| | |
|---|---|
| Marco Foresti | Dr. Franzsika Vielmuth |
| Prof. Dr. Jens Waschke | Michael Fuchs |

## A.4 Acknowledgements

First of all, I would like to express my sincere thanks to Prof. Dr. Heinrich Leonhardt for the supervision of my doctoral thesis and the preparation of the initial review. Furthermore, I would also like to thank Prof. Dr. Anja Horn-Bochtler for taking over the second review and helping me to constitute a board of committee. In addition, I would like to thank the entire doctoral thesis committee for taking their time to read my work and participate in the oral examination.

My special thanks goes to my supervisor Dr. Franziska Vielmuth for giving me the opportunity to conduct my doctoral thesis, for providing the funding, for showing and introducing me to the world of desmosomes, for many hours of discussing data, experiments and planning future strategies, and for the supervision and guidance through this time. In the same breath, I would also like to thank Prof. Dr. Jens Waschke for the many opportunities he offers in his lab, for the chance to establish new methods, for the possibility to work with state-of-art scientific instruments and for a lot of guidance during my thesis and beyond.

Next, I would especially like to thank all current and former members of the AG Waschke group for the pleasant working atmosphere. A big thank goes to Andrea for showing me all lab related stuff and helping me to master cell culture and biochemical techniques. I want to thank Sunil and Mariya who both always have an open ear and further Sunil for proofreading my thesis. A special thanks goes to the lunch crew, Kilian, Masha, Martina, Lety, Sophia and Markus. Thank you all for a lot of scientific as well as private talks during this time.

Special thanks goes to my friends outside of the lab (Stefan and Angie, Martin, Erik, Michi, AHS and my brother Andi) who always provided a change to the world of pipettes and microscopes.

Leonie, for accompanying me for more than eight years now, thank you for being there.

Last but not least, I am thankful for my parents. Without you, none of this would have been possible!